Pterin-Dependent Amino Acid Hydroxylases

T. Joseph Kappock and John P. Caradonna*

Department of Chemistry, Yale University, P.O. Box 208107 New Haven, Connecticut 06520-8107

Received May 29, 1996 (Revised Manuscript Received August 28, 1996)

Contents

I. Introduction, Scope, and Historical Background

Tetrahydrobiopterin-dependent systems occupy several interesting niches in biological chemistry, as metalloproteins that activate O_2 for highly specific oxidations, as regulators for aromatic amino acid metabolism, and as mediators for the health and proper functioning of the brain. Phenylalanine, tyrosine, and tryptophan hydroxylases perform critical and potentially rate-limiting steps in phenylalanine catabolism (PAH), epinephrine/catecholamine biosynthesis (TyrH), and serotonin biosynthesis (TrpH). This review is intended to be comprehensive with regard to the biophysical, structural, and catalytic properties of these three enzymes as reported to the end of 1995. One cannot discuss mechanistic aspects of these non-heme iron-dependent, pterin-dependent amino acid hydroxylases without an extensive consideration of the coordination chemistry of iron, the organic chemistry of pteridines, and the reactivity of each, which are duly emphasized in the current review. For the more frequently reviewed aspects of these enzymes, including the extensive work on PAH mutations and population genetics[1] and medical aspects including neurological effects, pharmacological studies, and developmental regulation,[2,3]

S0009-2665(94)00203-7 CCC: $25.00

Joe Kappock was born and raised in Honolulu, HI, where he spent his formative years hiking in the muddy mountains rather than down at the beach. After graduating from the Punahou School and Northwestern University (B.A. Chemistry, 1989) where he worked with Professor Joseph Hupp, he joined Professor John Caradonna's lab at Yale to study PAH for his Ph.D. (1996). The majority of his thesis work, which was supported by a Howard Hughes Medical Institute predoctoral fellowship, concerned the reduction of recombinant PAH by its cofactor, as well as spectroscopic and solution structure studies of the protein. Presently he is a postdoctoral fellow in Professor JoAnne Stubbe's lab at MIT, where he continues to indulge his interest in mechanistic enzymology.

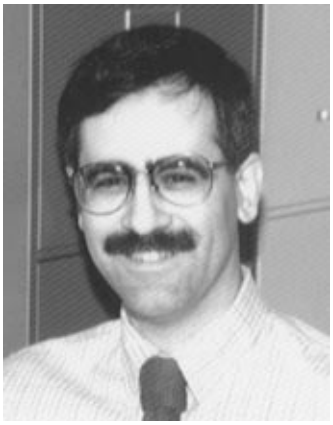

John P. Caradonna was born in Newark, NJ, in 1957 and received his B.S./M.S. degree in Inorganic Chemistry from The Johns Hopkins University in 1979 investigating metal ion binding to nucleic acids under Professor Luigi G. Marzilli. He received his Ph.D. in chemistry in 1985 working on determining the mode of binding of the anticancer drug *cis*-$Pt(NH_3)_2Cl_2$ to duplex oligonucleotides under Professor Stephen J. Lippard at Columbia University and at the Massachusetts Institute of Technology. He then moved to the Chemistry Department at Harvard University, Cambridge, where he was an NIH postdoctoral fellow with Professor Richard H. Holm. Here he studied the oxygen atom transfer chemistry of molybdenum complexes and the Mo-dependent enzyme sulfite oxidase. In 1987, he joined the faculty at Yale University in New Haven, CT, as an Assistant Professor, and was promoted to Associate Professor of Chemistry in 1993. He was a recipient of a Camille and Henry Dreyfus Award for Distinguished New Faculty in Chemistry in 1987 and received an Alfred P. Sloan Fellowship in 1993. One facet of Professor Caradonna's research lies in the area of mononuclear and binuclear non-heme Fe-dependent monooxygenases and involves examining the fundamental principles of high oxidation state iron–oxo species, non-heme iron based oxygen atom transfer catalysis, and the design of redox active and catalytic metalloproteins. A second area of work is in structural zinc centers in DNA/RNA binding proteins, where his work centers on the characterization of metal-mediated protein–DNA/RNA interactions.

not covered here, the interested reader is referred to the cited literature. Recent reviews of the catalytic chemistry,[4] regulation by phosphorylation,[5] and general behavior[6] of these hydroxylases are available,

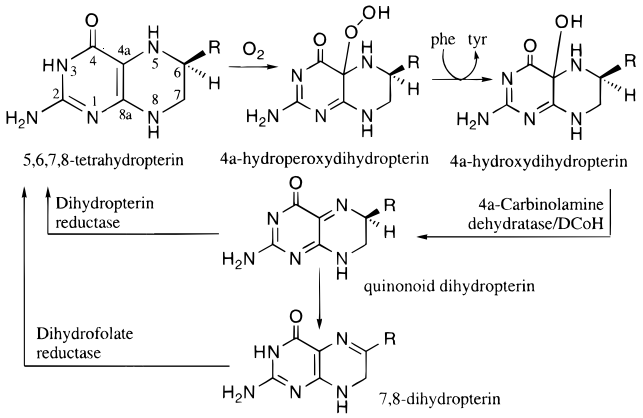

Figure 1. Cycling of the tetrahydropterin cofactor during hydroxylase catalysis.

as is a very recent, shorter review.[7] A very useful volume that covers aspects of pterin chemistry and reviews all three of the principal hydroxylases is available,[8] as is a recent book covering various aspects of pterin chemistry.[9] Conferences focusing on pteridines and folates have resulted in the appearance of two series with that emphasis.[10−12] Finally, a collection of purification and analysis methods is available.[13]

This review will concentrate on the chemical properties of the tetrahydrobiopterin-dependent hydroxylases (EC 1.14.16.*x*), and their relationship to the biophysical behavior and regulation of each enzyme. The structural and chemical analogies found in these enzymes are compelling, but can obscure important functional dissimilarities relevant to physiological chemistry, especially given the widely varying knowledge of each. The most important common mechanistic theme is the use of molecular oxygen by an active site containing a single, reduced iron atom to hydroxylate an unactivated aromatic substrate, concomitant with two-electron oxidation of a tetrahydropterin cofactor to its quinonoid dihydropterin form (Figure 1). Where $R = CH_3$, the often-used unnatural cofactor 6-methyltetrahydropterin ($6MPH_4$), the transformation is $6MPH_4 \rightarrow$ 4a-hydroxy-$6MPH_2 \rightarrow$ *q*-$6MPH_2$. (The systematic name for the intermediate 4a-carbinolamine (based on the number of double bonds) should be 4a-hydroxy-*tetra*hydropterin, but this gives a misleading indication of the oxidation state; the intermediate is the 4a,5-hydrate of *q*-$6MPH_2$.) Much of what is understood about the mechanisms of these enzymes has come from studies of the liver PAH, even though this cannot provide a full picture of the reactivity of the whole class. (For instance, the product of TyrH is a catechol, a class of compounds that strongly inhibits $\{Fe^{3+}\}$PAH.) However, the striking similarities in the nature of the transformations these enzymes can perform, including the observation that each of the aromatic amino acid hydroxylases can hydroxylate L-Phe and L-Trp, leads ineluctably to the conclusion that they generate a very similar oxygenating intermediate. These three activities were isolated within a decade of each other, and have been considered in parallel ever since, with PAH studies leading the way. This review reflects this trend in emphasizing what is known about PAH; we hope to lay plain how much

awaits detailed investigation, particularly with the related hydroxylases.

Dysfunction of PAH causes phenylketonuria (PKU), the most common clinically significant inherited disorder of amino acid metabolism. The principal clinical manifestation of PKU is severe, progressive mental retardation caused by the neurotoxicity of phenylalanine metabolites. PKU was one of the first recognized inborn errors of metabolism[14] and was the first known cause of mental retardation.[15] (McCusick's Mendelian Inheritance in Man (MIM) Catalogue Number 261600; http://gdbwww.gdb.org/omim-bin/omim/bin/omimx?261600.) The importance of catecholamine neurotransmitters has increased the scrutiny of TyrH for potential linkage to a number of psychological disorders, including schizophrenia, manic depressive illness, and Gilles de la Tourette syndrome. In these cases, no clear linkage with the TyrH locus has arisen from pedigree analysis, which is perhaps unsurprising in light of the complexity of these syndromes. Disruption of 3,4-dihydroxy-L-phenylalanine (L-Dopa) formation by TyrH is the result of the death of nigrostriatal pathway neurons in Parkinson's disease, which is typically treated by L-Dopa replacement therapy. Segawa's hereditary progressive dystonia, a motion disorder, does appear to be associated with point mutants in TyrH.[16] The function of serotonin, which is formed from the product of the TrpH reaction, is less well-understood, but is known to be low in the brains of suicides. Both serotonin and melatonin appear to be involved in circadian regulation. That clinically significant conditions may arise from altered pterin-dependent hydroxylase activity has been well-established for PAH and is suspected for the others; a major thrust in current research centers on uncovering the molecular details of hydroxylase function in hopes of future medical benefits.

Formation of tyrosine from phenylalanine was known early in the present century,[14] and the direct transformation was demonstrated, using labeled phenylalanine, in water-soluble liver extracts. Furthermore, the sensitivity of this activity to cyanide and azide suggested the involvement of a metalloenzyme.[17] The enzyme responsible for this transformation, PAH, was isolated in 1957.[18] Shortly thereafter,[19] the requirement for a tetrahydropterin was determined using the high-activity, synthetic cofactor analogues 6,7-dimethyltetrahydropterin ($DMPH_4$) and 6-methyltetrahydropterin ($6MPH_4$), the second of which remains particularly useful in this field. In 1963 the natural cofactor was identified as tetrahydrobiopterin, or (6*R*)-erythro-2,3-dihydroxypropyltetrahydropterin, isolated from rat liver extract.[20] The previous year it was reported that the tyrosine phenolic hydroxyl group derived from $^{18}O_2$ not $H_2{}^{18}O$.[21] About this time a pterin-dependent TyrH activity was observed in neural tissues,[22−24] and TrpH not long afterward.[25,26] The availability of modern molecular genetics has leveled the playing field somewhat, and it is at the beginning of the fifth decade of enzymological study of tetrahydropterin-dependent systems that we are poised to answer fundamental mechanistic questions about each of the enzymes and the family as a whole.

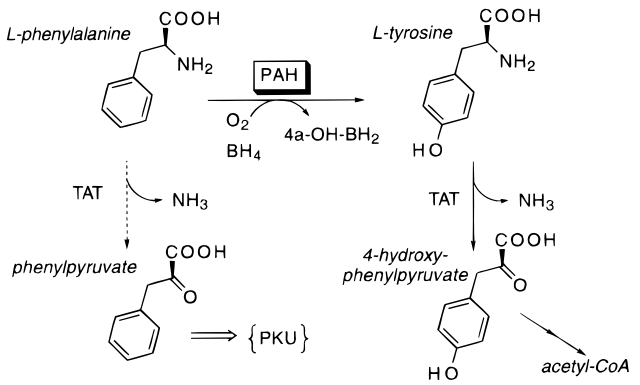

Figure 2. The PAH reaction, the first step of catabolism via tyrosine.

II. Molecular Properties

A. Phenylalanine Hydroxylase [PAH, EC 1.14.16.1]

1. Distribution and Physiological Function: Phenylketonuria

PAH from rat liver remains the exemplar of this class of enzymes, since it is highly active, soluble, and abundant (0.1−0.3% total liver protein). It has been pointed out that there is enough PAH present in liver to completely strip L-Phe from the blood in a manner of several minutes, were it all to suddenly become fully active.[27] As a result, the regulation of PAH activity has been of acute interest in the study of this enzyme. The rather limited distribution of PAH (liver, with a minor kidney enzyme) was apparent early in its study. PAH activity is controlled indirectly by glucagon, which stimulates the formation of L-Tyr as the first committed step in L-Phe catabolism, a process that results in the formation of one molecule of fumarate and one of acetoacetate (acetyl-CoA) from each amino acid (Figure 2). An investigation of the mechanism of glucagon stimulation revealed that increased phosphorylation of PAH and other enzymes occurs in liver, causing correlated stimulation of gluconeogenesis and inhibition of glycolysis.[28] This leads to rapid clearance of blood L-Phe, due to allosteric activation of PAH by its amino acid substrate (section II.A.3.2). (Throughout this review, we use the term "activation" in reference to PAH to refer solely to the allosteric activation of the enzyme by L-Phe, the well-characterized artificial activator lysolecithin, or several irreversible activating treatments.) Liver PAH, through its allosteric activation phenomena and by phosphorylation, is thought to maintain homeostatic regulation of plasma L-Phe.

Failure to remove serum L-Phe results in hyperphenylalaninemia (HPA) and an accumulation of phenylpyruvate, formed by tyrosine aminotransferase (TAT, EC 2.6.1.5), and its metabolites, which are neurotoxic. The primary neurotoxin is believed to be L-Phe.[2] L-Phe concentrations above a threshold value (>1000 μM plasma L-Phe; tolerance of <500 mg L-Phe day^{-1}) are diagnostic of clinical PKU, and the progressive mental retardation that results is slowed by restricted L-Phe intake.[2] Annually 10 million newborn infants worldwide are tested within three or four days of their birthday, and again at two weeks, for high levels of L-Phe (>150 μM plasma

L-Phe) and thereby PKU.[29] During development, high levels of L-Phe are associated with alterations in the architecture of the brain. Problems include abnormal myelination, cortical plate width, dendritic arborization, and the number of synaptic spines.[30] Behavioral disorders, especially agoraphobia,[31] are associated with PKU, and have an unknown organic origin. In addition to lower IQ scores, *treated* PKU patients have deficiencies in the performance of conceptual, visuospatial, and language-related tasks, including reading and arithmetic; they may have problems with motor coordination, attention span, response time, and problem-solving ability.[2] Even in well-treated PKU, dysmyelination occurs, which may cause some or all of the above.[32] An animal model of PKU has recently been reported, and will perhaps lead to a deeper understanding of this process.[33]

There is also a subtype of mammalian PAH found in proximal kidney tubules.[34−39] It is less abundant than liver PAH,[35] consistent with comparative activity determinations of 20% in humans[38] and 8% in rat.[40] These different tissue types appear to arise from identical mRNAs.[41] PAH isolated from rat kidney has approximately 10-fold lower specific activity than the liver form.[42,43] Although the physiological significance of this form of PAH is unknown, it appears to be a substrate for cAMP-dependent protein kinase[44] and is isolated with 0.21 ± 0.01 phosphate per subunit.[42] While glucagon treatment of rats did not cause phosphorylation of kidney PAH,[42] parathyroid hormone did increase the phosphate content.[44] With the use of rat and human sources, no difference in K_m values was identified between the liver and kidney forms, leading to an early assertion that they were identical,[37] excepting the lower specific activity and greater lability of the kidney enzyme.[38] A later study using purified, higher activity enzyme showed that the kidney enzyme had several of the characteristics of allosterically activated PAH, including increased hydrophobicity in the absence of activator and a hyperbolic, high BH_4-dependent activity (which these investigators use to quantitate the extent of L-Phe activation). However, the characteristic expanded substrate specificity of activated liver PAH was not detected for kidney PAH, nor was any stimulatory effect of phosphorylating conditions detected. The isolated kidney enzyme is a dimer in solution, which led the authors to suggest that there may be differences in the post-translational processing of kidney PAH.[42] The presence of even a minor form of PAH that was always "on" might be expected to have significant implications for L-Phe homeostasis, which are not yet known.

Recently PAH activity was identified in melanocytes, where with TyrH it participates in melanin biosynthesis.[45] Phenylketonurics are often very fair-skinned, which was attributed to L-Phe inhibition of the melanocyte TyrH. The strains of mice used as a model for PKU model are similarly hypopigmented.[46] Co-localization of the two enzymes is an attractive strategy for tissues that require appreciable amounts of L-Tyr, the least soluble of the 20 common amino acids (solubility ~1% that of L-Phe). However, TyrH has some PAH activity that may be physiologically significant,[47−49] which will be discussed in the context of that enzyme's reactivity.

The single-copy gene for PAH has been located on human chromosome 12,[50,51] consistent with the autosomal inheritance pattern of particular PKU phenotypes and linkage to other markers. As a complement to the large-scale PKU identification effort, molecular genetics has uncovered dozens of the PAH mutations that cause PKU or HPA. This has become a fascinating subfield of human genetics that is growing rapidly.[3] Particular mutations appear to move with language groups, which helps explain the uneven incidences of PKU, ranging from 0.8 to 50 per 100 000 births in Japan and Turkey, respectively.[1] Particular human PKU mutations are not discussed in the present review, except where they have been related to specific catalytic consequences.

2. Molecular Properties

Liver PAH is a homotetrameric protein with subunit weights near 50 kDa (50−53 kDa). All mammalian PAH has an absolute requirement for iron; the availability of which may even provide a limited amount of regulatory modulation.[52] No posttranslational modifications other than phosphorylation are known,[53,54] and even this causes only subtle *in vitro* kinetic changes. A procedure involving a L-Phe-mediated hydrophobic affinity step was introduced by Shiman in 1979,[55] and has proven to be a versatile method for purifying high activity PAH from a variety of other natural (human,[56] mouse, cow,[57] baboon, rabbit, and goose[58]) and recombinant (rat gene, *E. coli*, or baculovirus[59−61]) sources. (Different methods have been used to purify monkey PAH.[62,63]) This method of purification is easily scaled up and gives consistent, high activity yields of PAH;[64] as a result it is essentially the only procedure now used, although various other procedures have been employed.[54,62,65−69] Recombinant sources of PAH are as active as the enzyme isolated from hepatic tissue, contain up to one equivalent of tightly bound nonheme iron per subunit, and lack phosphate.

Two continuous assays for PAH activity are most frequently used with purified protein, in which the quinonoid dihydropterin (q-$X$$PH_2$) formed by the hydroxylation reaction is re-reduced quickly to $X$$PH_4$ by DTT[55,64,70] or NAD(P)H/DHPR.[67,71] Subsaturating amounts and continuous regeneration of $X$$PH_4$ are used because of this cofactor's high autooxidation rate.[72] This background rate is determined with an assay mixture lacking only L-Phe. Other methods include colorimetric determination of L-Tyr,[18] crystallization of (usually ^{14}C-labeled) L-Tyr,[70] continuous detection of $X$$PH_2$ formation (at 330 nm, an isosbestic point between q-$DMPH_2$ and 7,8-$DMPH_2$),[73] or direct fluorescence detection of L-Tyr separated by HPLC.[74] The assay generally used for crude samples is the conversion of L-[^{14}C]Phe to L-[^{14}C]Tyr. Additional assays are summarized in an older review.[75] Regardless of the method of detection, PAH must be thoroughly activated, either by L-Phe or lysolecithin, prior to the addition of $X$$PH_4$, in order to obtain accurate initial velocities. This is particularly important if BH_4 is used as the cofactor.[76]

All of the mammalian PAH enzymes whose sequences are known are highly homologous. To a lesser extent, the homology extends to all the mammalian pterin-dependent hydroxylases, which have

greater than 80% sequence identity after amino acid 159 (rat/human PAH numbering). Limited chymotryptic digestion of rat hepatic PAH yields three peptides: a 11 kDa N-terminal fragment, a 36 kDa catalytic core, and a 5 kDa C-terminal fragment.[77] This highly active catalytic core corresponds well to the highest sequence similarity among the hydroxylases. Like several other activating treatments, it results in a dimeric configuration of PAH.[6]

The kinetic complexity of PAH has provided the impetus for studies intended to link structural features with mechanism. While the rat liver enzyme has been crystallized,[78] further progress on the X-ray crystal structure of PAH has not been reported. It remains a challenging proposition to determine the three-dimensional crystal structure of this protein, particularly the details of the catalytically active iron site's coordination environment. Even a structure of the "inactive" PAH would be eagerly welcomed, as it would make intelligible the many mutations known to cause PKU and might illuminate how the various allosteric and active site pockets interact or overlap.

Cotton and co-workers have pioneered the use of monoclonal antibodies in mapping out the various functional regions of PAH.[79] In a study using 11 antibodies raised against monkey liver PAH, Jennings *et al.* used a competition assay to sort their specificities into five different antigen groups, representing eight different regions. The competition-sorted groups also had similar functional effects on PAH activity. Group C consisted of four antibodies able to cause an increase in BH_4-dependent PAH activity, two of which stimulated PAH to the same extent (in a 1:1 complex) as treatment with 1 mM lysolecithin. The binding of all four to PAH could be inhibited (92−97%) by preincubation with 10 mM lysolecithin. Lysolecithin and antibody binding was evident for six of the eight groups, which the authors regard as evidence supporting a large conformational change upon activation.

The binding of PH-1, an inhibitory antibody, was found to depend upon added L-Phe, with a half-maximal effect at 0.1 mM (comparable to the $K_{d,app}$ for the allosteric activation site of L-Phe[80]) and no complex formation below ~70 μM L-Phe.[79] PH-1 was found to be noncompetitive with either L-Phe or $6MPH_4$ in assays initiated by the addition of enzyme. If BH_4 was used as the cofactor, a stoichiometric amount of PH-1 could inhibit the enzyme activity 5-fold if L-Phe, PAH, and PH-1 had been preincubated together. In addition to the diminution of V_{max}, PH-1 changed the shape of the BH_4-dependent L-Phe saturation curve from sigmoidal to hyperbolic (Hill coefficient 2.0 → 1.0). The authors propose that this antibody recognizes a region involved in allosteric activation of PAH[81] but no epitope has yet been identified. PH-8, which reacts with all three aromatic amino acid hydroxylases,[82] is mapped to the same competition group as PH-1.[79] The partial or complete epitope for PH-8 was determined, by isolation of PH-8 immunoreactive tryptic and chymotryptic peptides from PAH, to fall within PAH amino acids 139−154.[83]

A different approach to the use of antibodies involves the generation of anti-idiotypic antibodies. The key concept of anti-idiotypic antibody formation is that antibodies raised against an antigen can themselves induce antibodies directed against the antigen/antibody combining sites of the primary antibody.[84] These "anti-antibodies" can in some cases mimic the original effect of the hapten, such as was demonstrated for the acetylcholine (ACh) receptor with an antibody specific for an antibody to an ACh agonist−BSA conjugate.[85] This concept was used to generate pterin-induced anti-idiotypic monoclonal antibodies from mice immunized with a $DMPH_4$-BSA conjugate, selected on the basis of their ability to bind PAH. These antibodies (NS-1, NS-6, and NS-7) bound native DHFR and DHPR from several sources, but only DHFR was inhibited by NS-6 and NS-7. Methotrexate (MTX) prevented NS-6 and NS-7 from binding DHFR.[86]

Reimmunization of mice with NS-7 elicited $DMPH_4$-binding antibodies, consistent with the combining site of NS-7 bearing some unknown chemical resemblance to $DMPH_4$. NS-7 failed to bind PAH in the presence of millimolar amounts of 7,8-$DMPH_2$ and was shown to bind to immobilized pterin-binding proteins such as all three aromatic amino acid hydroxylases, DHPR, and sepiapterin reductase.[87] Finally, the epitope for this apparent pterin mimic was located using limited, sequential proteolysis of PAH (with chymotrypsin and V8) to generate an inactive internal segment of the protein (residues 127−304). A 27 amino acid synthetic peptide (residues 263−289) was tested for its ability to bind NS-7: the peptide was competitive with immobilized PAH for NS-7, and could be prevented from binding NS-7 by 7,8-$DMPH_2$. This series of experiments does not reveal any affinity differences between NS-7 and pterin, meaning that NS-7 is a pterin "agonist" and that the peptide sequence harbors all or part of the pterin-binding specificity of PAH. The last three residues of this peptide were excluded from a pterin-binding role by limited protease treatment, and the remaining sequence was designated the putative pterin-binding sequence (PPBS).[88]

The PPBS peptide competes with PAH for a $DMPH_4$ conjugate,[88] but loses this ability following cyanogen bromide treatment, which splits the peptide nearly in half at Met275.[89] Throughout these studies, binding of PAH and PAH fragments to immobilized supports is employed, so it is difficult to assess quantitatively what fraction of the binding affinity is lost (if any) as the authors progress from full-length, native PAH to a single peptide representing ~6% of the protein sequence. Despite the convoluted and perhaps tenuous connection between pterin and NS-7, mutagenesis of the PPBS region did identify one functionally important residue, which is discussed below.

Active-site labeling with mechanism-based inactivators or photoactivated inhibitors can indicate regions of primary sequence that are important for enzymic function.[90,91] For instance, flavin-dependent enzymes have been productively studied using 8-azido-FAD.[92] Since PAH is known to tolerate various 6-substituted pterins and pyrimidines as cofactors (section III.D.1), a suitable pyrimidine analogue might be able to locate the pterin binding site. This was the strategy chosen by Gibbs and Benkovic in their study of ANBADP (5-[(3-azido-6-nitrobenzyli-

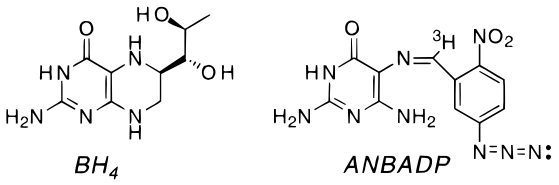

Figure 3. BH_4 and the photoactivatable pterin analogue ABANDP.

dene)amino]-2,6-diamino-4-pyrimidinone, Figure 3) labeling of PAH.[93] Upon irradiation, this class of compounds dissociates N_2, leaving a highly reactive nitrene center poised on the cofactor near the enzyme site of interest. Rat liver PAH was inactivated by irradiation with 302 nm light in the presence of ANBADP (or to a lesser extent, in its absence, since PAH is mildly photolabile).[58] This compound competitively inhibited PAH *vs* $DMPH_4$ (K_I = 9 μM); photoinactivation of PAH by ANBADP was partially blocked by $6MPH_4$ or the effective competitive inhibitor 5-deazapterin. By using [^{3}H]ANBADP, attachment of 0.9 ANBADP per subunit could be demonstrated, regardless of the allosteric state of the protein, in a concentration-dependent manner predicted by the K_I and consistent with high-efficiency modification. ANBADP did not label the atypical PAH from *Chromobacterium violaceum* (section II.A.4.5). The site of modification falls in a relatively hydrophobic region of PAH sequence, at Lys198 (and to a lesser degree at Lys194). At this position, the sequence is highly conserved among the PAH enzymes, and contains at least one Lys nearby in the aligned TyrH and TrpH sequences.[93] From modeling studies in which a pterin is docked onto unligated X-ray crystal structures of both DHPR[94] and DCoH,[95,96] Lys is thought likely to participate in mediating the interaction with the pyrimidine portion of pterin. Replacement of the "minor" Lys in TyrH had no effect on pterin binding; an Ala occupies the position analogous to Lys198 in rat TyrH.[97] Interpretation of the role played by these Lys residues is further complicated by the expectation that those residues involved in pterin recognition must interact with the region of the cofactor molecule opposite to where the reactive nitrene species was generated. Other possible functions for these Lys residues, however, such as modulating the redox properties of the reduced pterin cofactor or acting as a source of protons in coupled proton transfer/cofactor oxidation reactions, remain relatively unexplored.

The strongest evidence yet obtained for a particular residue's participation in the binding of pterin arose in a study of the PPBS sequence by combined mutagenesis/*in vitro* activity analysis.[98] A MBP-PAH chimera was employed to facilitate purifications. Of all the mutants studied, mutants at only two positions yielded protein of <1% activity. The D282N mutant rendered PAH completely inactive, while D286A and D286Q exhibited some residual activity. The other, less deleterious mutations were characterized by roughly the same K_m values for pterin and L-Phe. Notably, the purified D286A mutant had a 70-fold increase in BH_4 K_m and did not bind immobilized pterin conjugates. There was also a smaller and somewhat surprising *decrease* in the L-Phe K_m for this mutant. Proof of the structural integrity of the mutant protein is limited to (1) the identity of its CD spectrum with that of wild-type MBP-PAH and (2) the low L-Phe K_m. Since PAH is a tetramer, the effects of any single residue change will be magnified 4-fold, so it becomes essential to proceed especially carefully. In a sense, the hydrophobic affinity purification of PAH is another way of determining that the overall enzyme's structure is intact, since it is selective for those protein molecules that can reversibly undergo allosteric activation. In contrast, these constructs were purified using a different procedure selective for the introduced MBP affinity.[98]

Using *in vitro* expression and activity analysis, several groups have managed to associate particular PKU-causing mutants with catalytic impairment of PAH. Initially, these studies were performed in eukaryotic cells, so that PAH would be properly folded, phosphorylated, *etc.* The repeated demonstration that *E. coli*-expressed PAH is highly active has caused much of this work to shift to that host. (The results of various studies including *in vitro* expression studies are updated regularly by the PAH Consortium; available at http://www.mcgill.ca/pahdb.) This technique has proven to be a rapid and reliable means of screening particular sequences for detailed analysis.[99]

3. Regulatory Behavior

3.1. Gene Structure and Expression. The region 5′ to the gene for mammalian PAH lacks a proximal TATA box, which puts PAH in a class of "housekeeping" enzymes that are continually expressed in the appropriate tissue. There are consensus sequences for multiple transcription factors present in this region. The 13 exons of PAH are spread across 90 kilobases of genomic DNA (q24.1 → q24.2), and more than a dozen deleterious splicing mutations have been identified.[1,3] Figure 4 compares the structure of the aromatic amino acid hydroxylases, and illustrates the conservation of exon/intron boundaries (but not the intron sizes) among the mammalian enzymes.

3.2. Allosteric Activation by Phenylalanine. There is enough PAH present in liver to remove L-Phe from serum completely within several minutes, if all the enzyme were to become fully active. The regulation of PAH activity or inhibition in the presence of normal serum L-Phe (~0.1 mM) is of obvious importance. What might appear at first to be excess PAH capacity is probably physiologically useful; Shiman and co-workers found that 25% of a L-Phe load at 4 times normal levels was removed in a single pass through a perfused rat liver.[27] This is correlated with an increase of the specific activity of PAH, from ≤1% to ~30% full capacity, that was shown in separate experiments not to depend on protein synthesis.[52] Humans normally have similar, if lesser, L-Phe-clearance capabilities that are drastically diminished in (and diagnostic for) PKU.[2] The physiological activation largely derives from the allosteric behavior of PAH, which in the resting low-phosphate state of rat liver PAH at pH 7.4 has a maximal slope at 60 μM L-Phe.[80] Phosphorylation appears to sensitize the unactivated enzyme to L-Phe activation (*vide infra*).

Allosteric activation as formally described by Monod, Wyman, and Changeux[100] (MWC) imposes several

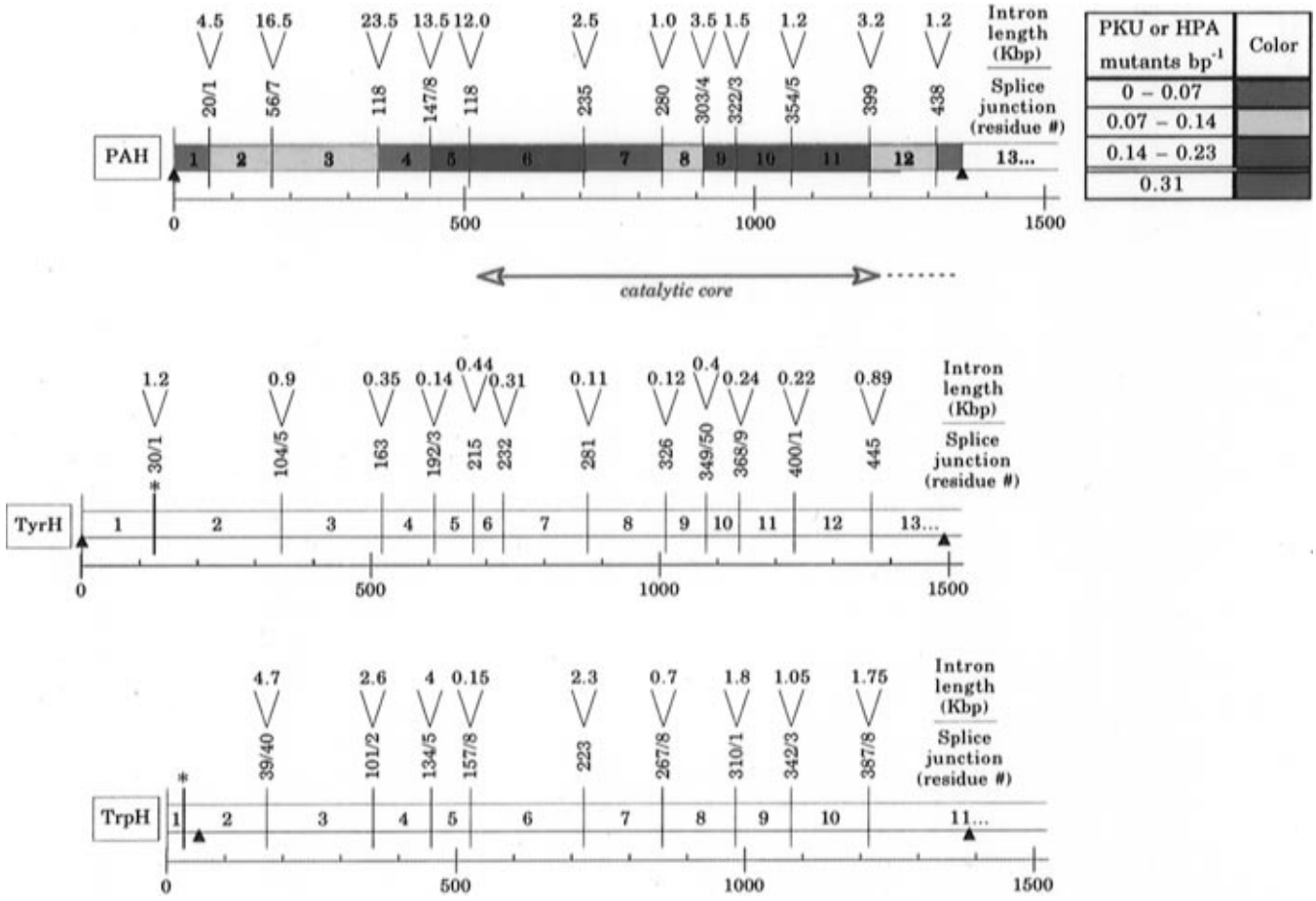

Figure 4. A comparison of the human aromatic amino acid hydroxylase genes. The boundaries shown are for the exons that comprise the coding sequence of the genes. The human PAH gene is colored according to the frequency of missense and nonsilent mutations (excluding splice site alterations) from the >220 available by Oct 25, 1995. The data were obtained from the PAH Consortium: http://www.mcgill.ca/pahdb. Note the much larger intron sizes in PAH compared to TyrH. The data are taken from refs 103−105.

theoretical restraints on an enzyme undergoing homotropic cooperative activation by substrate, both structural and kinetic, all of which are fulfilled in PAH. In order to simplify the discussion of activation, traditional allosteric nomenclature is used: the resting, inactive state of PAH is the T state, and the allosterically activated state is the R state. The choice of this nomenclature should not be taken to mean that the details of the MWC formalism have all been met for PAH, nor that other models for allosteric activation have been excluded (*e.g.*, the sequential model of Koshland *et al.*[101]). T and R refer to the two kinetically distinguishable states of PAH most commonly associated with L-Phe-dependent allosteric activation. PAH activated by its substrate or another true activator (such as lysolecithin, section II.A.3.3) has a common set of kinetic parameters associated with particular structural features (*vide infra*). Because the mechanism of activation by these other treatments is not known (and is not likely) to be the same as allosteric activation by L-Phe, we refer to lysolecithin-activated PAH as $PAH^{act}_{lysolecithin}$ rather than $PAH^{R}_{lysolecithin}$, even though there are no known functional differences between fully lysolecithin- and L-Phe-activated PAH. The simplest criterion of allostery, that the velocity response to applied substrate is sigmoidal, is met for PAH isolated from a variety of mammalian sources,[53,102] and for both un- and phosphorylated rat liver PAH.[27] Hill coefficients describing this curvature range from 2 to 2.6, placing PAH in an intermediate range of cooperativity.[59]

The next important MWC criterion is that the activator binds to a site distinct from the active site. Using a gel filtration method, Shiman demonstrated binding of 0.8 L-[^{14}C]Phe per subunit upon activation.[53] The rate of activation was shown to depend on the L-Phe concentration and pH.[80] The rate of loss of labeled amino acid from R-state subunits was further investigated in a particularly elegant study that demonstrated L-[^{14}C]Phe bound to the allosteric activation site is protected from hydroxylation.[58] Under conditions that disfavor L-Phe reactivation, the loss of PAH-bound L-[^{14}C]Phe during catalytic turnover could be described well as a slow first-order process, corresponding to the loss of a single equivalent of label per subunit. This loss of activator was concomitant with the loss of activity, as would be expected for relaxation of the R state back to the inactive (≤3%) T state. By using characteristic changes in fluorescence as an assay, L-Phe was found to inhibit this relaxation process, i.e., the R-state enzyme is "kinetically trapped" by its activator.[58] Both the forward (PAH^{T} + L-Phe → PAH^{R}_{L-Phe}[L-Phe]) and reverse reactions have the same, pronounced temperature dependence that corresponds to an Arrhenius activation barrier of ∼34 kcal (mol subunit)$^{-1}$.[58,80] This correctly predicts that the activation *equilibrium* ($K_{d,app}$ for the allosteric

L-Phe site) has a shallow temperature dependence,[58] implying the existence of a small ΔH associated with allosteric activation.

At increased pH, the rate of L-Phe activation increases, while the amount of L-Phe required to activate PAH falls (60 μM → 38 μM at pH 6.8 and 8.0, respectively). This enhancement was interpreted as being the result of an increased forward rate of activation under alkaline conditions. Since the reverse reaction has little pH dependence, increased pH favors activation as a group with pK ~8.1 is titrated.[58,80] At some pH, the activation energy barrier for the T → R conversion becomes insignificant. The possibility of this occurrence is discussed in the section on alternative activation pathways (section II.A.3.3).

A final prediction from the MWC model is that activation will increase the size of an allosterically regulated protein as the active site is formed or exposed. This structural distortion has been directly observed recently in this laboratory, both as an increase in the apparent Stokes radius (T = 55 Å, R = 56.7 Å) of the tetramer determined by gel filtration, and in preliminary low-angle X-ray scattering experiments. This ~10% increase in volume is too small to reflect a change in the oligomeric state of PAH, and is consistent with a L-Phe-induced exposure of a catalytically competent active site.[61]

Other alterations in the protein are consistent with some large distortion of the enzyme matrix. There is the large activation energy barrier mentioned above, which hints at a profound distortion in the protein's structure. Shiman's affinity purification depends upon the reversible increase in PAH hydrophobicity that is associated with conversion to the R state, which greatly increases the affinity for hydrophobic column materials by PAH.[55] Finally there is a characteristic bathochromic shift in the fluorescence emission caused by the T → R transition, and increased quencher accessibility to at least one of the three tryptophan residues of PAH.[80,106] However, there are only subtle changes in the far-UV CD spectrum, hence secondary structure, of PAH, suggesting that there is only a slight increase in the proportion of α helix found in the R-state enzyme.[61]

Using their system of MBP-human PAH fusion protein expression, Knappskog and Haavik replaced each of the three Trp residues present in human PAH (120, 187, and 326; these are also present in rat liver PAH) with the comparatively nonfluorescent Phe.[107] Several of these mutants had altered aggregation properties, which led to correspondingly low yields resulting from difficulties in cleaving soluble entities from the fusion proteins. All of the cleaved Trp → Phe mutants, including the triple mutant, had at least a third of the wild-type activity. All were cooperatively activated by L-Phe, but W120F, W120I, and the triple mutant had Hill constants below 1.7. The apparent affinity for L-Phe activation in all of the Trp → Phe mutants ranged from 50 to 470 μM. All three of the single-Trp double mutant forms of PAH were prepared and their fluorescence properties examined. The majority of the fluorescence intensity arises from Trp120, determined by the comparing quantum yields of both the T- and R-state enzymes. Trp120 is also the most solvent accessible of the three; the single Trp mutant has Stern−Volmer quenching constants nearly equal to wild-type PAH in the T (KI quenching) and R (acrylamide quenching) states. Titration of the Trp120 double mutant with BH_4 (in the presence of excess Fe^{2+} and DTT) showed appreciable fluorescence quenching nearly identical to a titration of the wild-type PAH. Addition of 3−4 equiv of Fe^{2+} to the Trp187 double mutant, a relatively buried position, caused 22% quenching, in contrast to less-pronounced effects on the other two single-Trp proteins. In sum, these results indicate that Trp120 is the primary PAH fluorophore, has the longest fluorescence lifetime, and has a limited effect on the allosteric activation process.[107] While it is likely to be a relatively small error, the tendency of these proteins to aggregate, which may reflect a tendency to denature and increased solvent accessibility of regions ordinarily buried in the wild-type protein, blunts the force of conclusions obtained from fluorescence-quenching measurements.

3.3. Other Activators. Various other stimulatory treatments have been identified in the study of PAH, the most important of which, phosphorylation, is discussed in the following section. The treatments discussed in this section have no known physiological importance.

In a series of papers, Fisher and Kaufman developed the concept of L-Phe activation and Kaufman's group discovered several treatments that appeared to give maximally active enzyme, *i.e.*, removed the necessity for L-Phe activation.[77,102,108−111] Prior to this it had been observed that propanol was able to stimulate PAH activity,[112] and butanol was even more effective.[102] Preincubation with lysolecithin or one of several other phospholipids generates fully activated PAH, despite the fact that they bear no structural resemblance to L-Phe and are not substrates. Lysolecithin appears to be a weakly cooperative activator.[61,102] The catalytic activity of PAH fully activated in this way functions like enzyme activated by L-Phe preincubation, making this technique quite useful for the separate investigation of the allosteric activator and substrate roles of L-Phe.[80] DTNB-reactive thiol increases following exposure to either lysolecithin or L-Phe, which suggests that the conformational changes resulting from activation are similar at that level.[102]

Lysolecithin activation has been employed to determine the overall kinetic mechanism of PAH across 3.5 orders of magnitude in [L-Phe]. This had not been possible with L-Phe alone because of the requirement for L-Phe activation at relatively high (>0.1 mM) concentrations.[61] Lysolecithin activation has been used to assay the alternate substrate specificities of fully active PAH (discussed in section IV.B.2), which would otherwise be complicated by L-Phe competition for the active site. In support of the structural changes caused by the formation of R state, there is an identical increase in the hydrophobicity of lysolecithin-activated enzyme.[80] An issue that awaits further investigation is the determination of the oligomeric state of lysolecithin-activated enzyme, which was reported to be the same as the native enzyme by sucrose-gradient centrifugation.[102]

Other treatments that lead to higher activity include limited chymotrypsin proteolysis, alkylation of Cys236 (rat liver numbering) by *N*-ethylmaleimide, and raising the pH. Only the last of these is potentially reversible. Interestingly, all three of these treatments result in partial or complete conversion of the PAH tetramer into dimers.[6] As was mentioned above, limited digestion with α-chymotrypsin results in the release of a dimer of the active 36 kDa catalytic core,[77] which has a solution radius of 36 Å and sediments as a 3.9 *S* particle.[102] The addition of L-Phe accelerates proteolysis slightly, while BH_4, an allosteric inhibitor (following section), blocks it.[113] A small increase in the mean residue ellipticity at 222 nm that is correlated with activation can be followed during chymotryptic proteolysis, linking activation with a conformational alteration.[110] (Larger effects are seen with lysolecithin activation, which are more pronounced than those due to L-Phe activation, indicating additional distortions caused by that process.[106])

The change in the number and reactivity of DTNB-detectable free thiol groups following activation prompted an investigation of whether NEM, which can form a stable thioether with exposed cysteine thiolates, would also cause activation. Alkylation of a single cysteine per subunit with [^{14}C]NEM correlated well with an increase in activity at 0.2 mM L-Phe. With BH_4 used as cofactor, nearly superimposable hyperbolic traces *vs* L-Phe concentration (followed by pronounced substrate inhibition) were obtained for lysolecithin- and NEM-treated PAH under conditions where a sigmoid trace was observed for unmodified PAH^T.[114]

Binding of L-[^{14}C]Phe to NEM-modified PAH, monitored by a membrane-binding assay, also showed a hyperbolic trace, where the native enzyme gave a sigmoidal response. PAH^{act}_{NEM} showed the same apparent K_d and K_m for L-Phe and bound 1.0 equiv per subunit. This was inferred to reflect active-site binding of L-Phe to PAH. Unmodified PAH showed a sharp transition at ~0.1 mM, with half-maximal L-[^{14}C]Phe binding at 0.2 mM. However, a Scatchard plot showed only 1.5 equiv of L-Phe per subunit bind to unmodified PAH under these conditions (pH 6.8, 0.1 M phosphate), which suggests that the activating L-Phe is present at 0.5 equiv per subunit.[114] If the activation equilibrium K_d is lower than the dependent-site K_d, a concave-up Scatchard plot that underestimates the true number of binding sites (by an unknown amount) will result. The binding-site number determined by this assay does not agree with the 1 site subunit^{-1} result (section II.A.3.2) obtained at pH 8.0 in 50 mM Tris-phosphate,[53] which is likely to be correct for both sets of conditions.

Neither iodoacetamide or iodoacetate, both of which react with thiols, could cause activation.[114] The modified residue was determined to be Cys236 by peptide mapping.[93] It is unclear whether the modification of this thiol traps a dynamic equilibrium between the T and R conformations in the R state, if it removes an inhibitory interaction due to the thiol, if the steric bulk of the modified residue (which is larger than a tryptophan moiety) disrupts the local structure sufficiently to cause activation, or some combination of these. A mutant of recombinant PAH in which Cys236 is replaced by Ser, shows normal purification behavior and full catalytic activity. This rules out any redox-based role for this position in allosteric activation. (T. J. Kappock and J. P. Caradonna, unpublished observations.)

Finally, whether activated by lysolecithin, chymotrypsin, or sulfhydryl modification with NEM, R-state PAH shows indistinguishable, small isotope effects with fully ring-deuterated [$^2H_5$]phenylalanine.[110]

Stimulation of PAH activity following exposure to high pH is a more unusual phenomenon, studied recently in Kaufman's group.[109] With BH_4 as cofactor, there is a large difference in the initial velocities observed at pH 7.0 when PAH is preincubated in the presence and absence of L-Phe. (A caveat about this work is that the kinetic data were obtained by monitoring NADH oxidation, which is known to be tightly coupled to phenylalanine hydroxylation near neutral pH. It is possible that the efficiency of catalytic turnover might decrease at higher pH, where the hydroxylation reaction is less favorable, which might potentially affect these conclusions.) This difference disappears as the pH is raised to 8.6, which arises from both an increase of the no-L-Phe rate and a decrease of the L-Phe-activated rate. If the pH of the 10 min preincubation is varied across this range, and the activity measured in each sample at a constant pH 7.0, there is little deviation in the initial velocity of L-Phe-preactivated enzyme but there is a marked increase in the activity of the unactivated PAH initial velocity. As a result, the optimum activity for BH_4-dependent catalysis is at pH 8.5. However, when $DMPH_4$ is used as the cofactor, the optimum pH is 7.0, and decreases to ~20% of this value by pH 8.5.[109] It is likely that this phenomenon is primarily due to increasingly inefficient allosteric inhibition by BH_4 at higher pH (following Section), but there is some evidence for structural distortions at higher pH.

The red shift and increased intensity observed in the fluorescence emission spectrum of PAH upon L-Phe activation at pH 6.8 is quite similar to the *difference* in the emission spectra of PAH^T at pH 6.8 and pH 9.5. No change in the pH 9.5 emission spectrum occurs if the enzyme is L-Phe activated. While this might indicate that the high-pH sample is in its R state, whether the fluorescence change correlates with an essential part of the activation mechanism is completely unknown. Compared to pH 7.0 assays, more NADH oxidation is observed at pH 9.3 with the partially uncoupled substrates *m*-tyrosine and tryptophan,[109] but this result is hard to explain uniquely.

Other kinetic data indicate that high-pH treatment is insufficient to activate PAH. At equimolar L-Phe and PAH subunit ratios, L-Phe-dependent activation of PAH^T is very slow at 5 °C. Under these conditions, PAH^T hydroxylates twice as much L-[^{14}C]Phe at pH 9.3 as it does at pH 6.8. When compared to $PAH^{act}_{lysolecithin}$, the amount of conversion to L-Tyr catalyzed by PAH^T at pH 9.3 or 6.8 is minimal (at 0.21 μM L-Phe, 3.0 and 1.7% conversion, respectively, compared to 22% conversion catalyzed within 30 s by $PAH^{act}_{lysolecithin}$). Under more permissive conditions, 0.1 mM L-Phe and 12 °C, the pH 9.3 assay does not show a lag in NADH oxidation that is observed

at pH 6.8. These two experiments show that if allosteric activation is impossible, the high-pH conditions do not activate PAH, but under conditions in which it can occur, PAH is rapidly activated. Because the high-pH effect seems persistent, from preincubation to assay, Parniak *et al.* suggest that a conformational change occurs in PAH during exposure to high pH that facilitates allosteric activation.[109] This is consistent with the earlier kinetic model of high- and low-pH activation pathways.[80]

The issue of L-Phe binding to PAH is complicated by the presence of multiple L-Phe-binding sites on the enzyme, the allosteric site (which is known to bind L-Phe in a positively cooperative manner) and the active site (which does not bind L-Phe cooperatively once the enzyme is activated by some means, *i.e.*, NEM alkylation[114]).

A study of L-[^{3}H]noradrenaline binding to PAH showed evidence of positively cooperative, but substoichiometric, interaction (<0.5 L-[^{3}H]noradrenaline PAH^T subunit^{-1}).[115] PAH activated by L-Phe shows only the hyperbolic (h = 1.0) interaction of L-[^{3}H]-noradrenaline with the active site, which is an even lower stoichiometry (~0.3 L-[^{3}H]noradrenaline PAH^R_{L-Phe} subunit^{-1}). On the basis of this study with L-noradrenaline (a compound not known to be an activator or substrate of PAH but which is an effective chelator of {Fe^{3+}}PAH), the claim was made for positively cooperative L-Phe binding at the *active site* of PAH (an assertion without support from kinetic observations). The binding constants obtained from this analysis are ≤0.4 μM, or ~250-fold smaller than the K_d, K_m, or K_{app} observed with L-Phe, probably because the binding is that of a simple catechol rather than an amino acid. (This would also explain the substoichiometric levels of L-noradrenaline binding, which is expected to be specific for catalytically functional active sites (active iron),[116] and appears to be consistent with the fractional specific activities of 3.6−8 U mg^{-1} Fe^{-1} reported for the enzyme preparations.[115])

Therefore, even though the cooperativity of L-[^{3}H]-noradrenaline binding is similar to that of L-Phe, the mode of binding is different; it follows that L-[^{3}H]-noradrenaline binding data cannot be used to demonstrate whether binding of L-Phe by the active site is cooperative or not. Nevertheless it remains to explain why the interaction with L-noradrenaline is cooperative, particularly since the binding of catechols to the active iron in {Fe^{3+}}PAH^T is not.[61,116]

3.4. Allosteric Inhibition by BH_4. Recently progress has been made in understanding the observations concerning the inhibitory properties of tetrahydrobiopterin.[117−119] Addition of sufficient BH_4 prior to L-Phe activation will completely block conversion to R state.[76] (This inhibition of L-Phe activation is specific for BH_4; the K_I at 5 mM L-Phe for several pterins shows that $6MPH_4$ is 1000-fold less effective than BH_4 and 50-fold less effective than 7,8-BH_2.[118]) As is discussed below, BH_4 is a potent inhibitor of phosphorylation at Ser16; conversely, phosphorylation appears to disrupt the BH_4 inhibitory site.[120] Kaufman and co-workers have used this phenomenon to develop an assay for the extent of activation, which is apparently proportional to the ratio of BH_4 to $6MPH_4$ ("full") activity, that has been used in studies of the N-terminal regulatory segment of PAH.[110,121] BH_4 is also reported to block chymotrypsin proteolysis, while L-Phe has the opposite effect.[113]

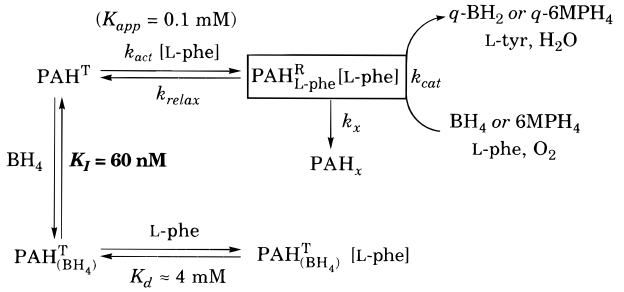

Figure 5. Relaxation of $PAH^R_{L-Phe} \rightarrow PAH^T$ during BH_4-supported L-Phe hydroxylation.

BH_4 inhibits allosteric activation of PAH (Figure 5). Whether this is due to competition for the L-Phe activation site, interference with requisite protein conformational changes, binding to a separate inhibitor site, *etc.*, is unknown. Functionally it is a MWC allosteric inhibitor, in that it prevents formation of PAH^R_{L-Phe}. BH_4 inhibits the rate of activation, most evidently at high concentrations of L-Phe,[118] and causes relaxation of PAH^R_{L-Phe} to PAH^T during catalytic turnover, probably by a common mechanism. If BH_4 and L-Phe are added together to PAH^T, there is a long lag in L-Tyr formation that is caused by L-Phe activation in competition with BH_4 inhibition. Under standard assay conditions (with $6MPH_4$ as cofactor), the activity of PAH decreases in an irreversible, first-order manner, thought to be due to inactivation of enzyme active sites (section II.A.4.1). This complicates the direct determination of BH_4-induced relaxation of PAH^R_{L-Phe}.

Shiman's first approach to this problem involved the use of substrate quantities of $6MPH_4$ and smaller quantities of BH_4, whose K_I is much smaller than its K_m (0.09 and 15 μM, respectively).[118] Three L-Tyr buildup traces were collected, to allow determination of the rate constants depicted in Figure 5. In the first, $6MPH_4$ is added to PAH^R_{L-Phe}, which allowed determination of k_{cat} and k_x. In the second, the enzyme was initially unactivated, allowing the determination of k_{act} (PAH^T + L-Phe and $6MPH_4$). Finally, varying amounts of BH_4 were included to inhibit activation (PAH^T + L-Phe, BH_4, and $6MPH_4$), and determine k_{relax}, which was defined from the extent which BH_4 inhibits k_{act} (lengthens the lag) in the varied-BH_4 buildup traces. The second approach, measuring the relaxation of PAH^R_{L-Phe} during turnover, involved using Guggenheim's method for determining the variation in velocity caused by k_x and k_{relax}. This method is sensitive enough to detect the weak relaxation of PAH^R_{L-Phe} caused by $6MPH_4$. By using the values obtained, a simulation of the combined effect of these two allosteric effectors under typical liver conditions indicates the activation response to L-Phe will be significantly sharpened when BH_4 is present.[118]

It had been observed that the intrinsic PAH activity in perfused liver is quite low (2−5% at 50 μM L-Phe) compared to the ~80% expected from this moderately cooperative enzyme's allosteric $K_{L\text{-}Phe}$.[27] Mitnaul and Shiman show that the hepatic [PAH] =

9 μM, approximately equal to the [BH_4], and that at this concentration of each 85% would be expected, from the *in vitro* K_d, to be found in a BH_4·PAH^T complex.[119] This raises the interesting possibility that the physiologically relevant state of PAH is in fact BH_4·PAH^T, which has an activity small enough to prevent loss of serum [L-Phe] caused by small amounts of PAH^R_{L-Phe} formed at the optimum concentration of this substrate. Important questions remain concerning the state of the enzyme in this inhibitory complex, particularly the mechanism of inhibition and how it is bypassed following activation. A tight complex between a protein and its natural reductant (section II.A.4.4) would be expected to cause some reduction of the protein unless some means has been devised to block a thermodynamically favorable reduction. The closely related issue of what distinguishes the PAH^T allosteric inhibition site from the reduction site remains of interest.

3.5. Phosphorylation. Rat liver PAH is regulated by specific phosphorylation of Ser16,[123] which has the overall effect of sensitizing PAH to allosteric activation by L-Phe. (Conflicting reports about whether human liver PAH is regulated by phosphorylation have appeared. Resolution of this issue should be possible now that recombinant sources of this enzyme are available.[122]) Following their observation that several phospholipids, and perhaps other anions, activate PAH, Kaufman and co-workers found that 0.7 [^{32}P]phosphate per subunit could be introduced into 90% pure PAH. The radiolabel could be dissociated from the enzyme by limited chymotrypsin proteolysis or by incubation with NaOH, consistent with an N-terminal phosphoserine or phosphothreonine.[124] These authors reported an increase in V_{max} without significant change in the L-Phe K_m. However, they used BH_4 in fixed-time assays of PAH activity without preincubating the enzyme with L-Phe to first activate it. This procedure is now known to fail to distinguish the effects of L-Phe activation, BH_4 inhibition, and the intended phenomenon, PAH phosphorylation, yielding a low velocity due to inhibition of PAH by BH_4.[76] (In retrospect, this result was one of the first to show a specific, antagonistic effect of phosphorylation on allosteric inhibition by BH_4.)

PAH phosphorylation causes a change in the distribution of peaks, arising from apparently homogeneous PAH, which elute from calcium phosphate/cellulose gels.[125] This assay was used to show that PAH isolated from glucagon-treated rats is extensively phosphorylated,[28] with most of the protein eluting in a peak that corresponds to the highest phosphate content, 1.0 phosphate per subunit.[126] PAH isolated from rat liver contains 0.2−0.3 phosphate per subunit,[124] which corresponds to a mixture of enzyme species containing predominantly 0, 1, or 2 phosphate(s) per *tetramer*.[5]

Shiman and co-workers[27] demonstrated that both un- and phosphorylated PAH require L-Phe preincubation, unambiguously showing that phosphorylation is not equivalent to allosteric activation, as it is for several other enzymes. This is generally accepted,[76,120,127] despite a contrary claim.[128] Instead, complete phosphorylation causes a shift of the allosteric L-Phe site's K_d (60 μM → 38 μM;[27] 58 μM → 30 μM[120]) and an acceleration of the *rate* of PAH activation, in 1 mM L-Phe, at pH 6.8 (2-fold) or pH 8.0 (3-fold).[27] These values are determined relative to "unphosphorylated" PAH, which as mentioned above actually contains an average of 1 phosphate per tetramer. No kinetic differences have yet been detected between "unphosphorylated" PAH and truly phosphate-free PAH, leading to the generally held suspicion that they are effectively identical.[27]

One of the first attempts to quantitate the inhibitory properties of BH_4 (section II.A.3.4) focused on its ability to inhibit the *in vitro* rate of PAH phosphorylation by cAMP-dependent protein kinase. The effect is most pronounced for the natural isomer, (6*R*)-BH_4, while (6*S*)-BH_4 was half as inhibitory; neither $6MPH_4$ nor 6,7-$DMPH_4$ inhibits.[129] This is comparable to the (6*R*) isomer's 4-fold higher V_{max} for L-Phe hydroxylation; the K_m values for these pterins are identical.[130] The BH_4-derived inhibition of phosphorylation was confirmed and extended by Døskeland *et al.*[120] who additionally reported that L-Phe has an opposite, weaker effect, and can stimulate the PAH phosphorylation rate up to 2-fold. Other amino acids that are weaker allosteric activators (L-norleucine, L-Met, β-2-thienyl-DL-alanine, and L-Trp) also show 2-fold stimulation at saturating concentrations. Unsurprisingly, L-Phe interferes with the inhibitory effects of BH_4, causing the K_{i,BH_4} to rise from 2.3 μM in the absence of L-Phe to 8.3 μM at saturating (10 mM) L-Phe, which corresponds to a ligand-coupling ΔG of 0.8 kcal mol^{-1}.[120]

The recent availability of recombinant PAH (rPAH) has allowed the substitution of Ser16 with other amino acids, in an attempt to understand how the behavior of the N-terminal regulatory domain is modulated by phosphorylation.[59,121,131] The assay chosen to investigate the effects of phosphorylation is the ratio of BH_4-dependent PAH activity to $6MPH_4$-dependent activity, using either the continuous NADH-coupled assay,[131] fixed-time (usually 30 min) colorimetric determinations,[132] or a mixture of both.[121] At 25 °C, full L-Phe activation should take place within a minute in the assays with $6MPH_4$, while no allosteric activation is observed in the presence of 0.1 mM BH_4 under these conditions (unless it is relieved by some mechanism).

It has been asserted that the activating effect of phosphorylation can only be discerned with BH_4 present and that its effects are not expressed in the presence of the synthetic cofactor $6MPH_4$.[121] This distinguishes it from allosteric activation, which can be observed with any of the common PAH cofactors. Instead, this assay measures the extent to which the high-affinity regulatory site for BH_4 is disrupted, either by Ser16 phosphorylation or a new amino acid at this position. In the limiting case, proteolytic excision of the regulatory domain, an exclusively dimeric species is formed that has no need for L-Phe activation, meaning that it is constitutively active. In this situation the phosphorylation site is lost,[110,124] and probably the BH_4-inhibition site.

The Ser16 position has been altered to Ala, Glu,[131] Asn, Asp, Gln, and Lys.[121] All of these mutants have the same $6MPH_4$-dependent activity using the fixed-time assay, consistent with a strictly regulatory role for the amino terminus. Kowlessur *et al.* show that the full $6MPH_4$ velocity can be recovered by treat-

ment of the enzyme with lysolecithin, another indication that the mutations only affect the allosteric activation phenomenon.[121] Only the Ala16 mutant has a lower BH_4 activity than the wild-type Ser16 (4.2% *vs* 8.3% of the $6MPH_4$ activity). Phosphorylated Ser16 yields 13% of the $6MPH_4$ velocity. The relative BH_4 activities of the others fall on a line when plotted against the volume of the amino acid at that position,[121] ranging up to 25% for the Glu16 protein.[131] Even though the correlation with side-chain volume includes the positively charged Lys substitution, the authors state that "activation" is mediated by a negative charge at this position. An alternative explanation not addressed would be that the mutations destabilize the regulatory domain sufficiently to prevent BH_4 inhibition of allosteric L-Phe activation. This could be the result of "overpacking" the regulatory domain, or by disrupting an interaction important for the regulatory binding of BH_4. Proteolytic removal of the N-terminus is known to change the CD spectrum of PAH, consistent with it having a defined structure.[110] Regardless of the conclusion drawn about phosphorylation *per se*, the results support the longstanding hypothesis that the regulatory domain is an "internal inhibitor" of the catalytic domain.[6,111]

As has been alluded to previously, the identity of the biophysical characteristics of PAH that underlie the correlation of increased PAH activity and phosphorylation remains a fractious issue. A quantitative appreciation of the importance and characteristics of BH_4 inhibition is required to explain how phosphorylation affects the complicated regulatory scheme PAH exploits, which appears to have no other biochemical analogue.[118,119] L-Phe is removed from blood by PAH, protein synthesis, and transamination to form phenylpyruvate; neither of the latter two is potentially regulatory. PAH phosphatase would have to be quite responsive to L-Phe levels were it to exert any dynamic regulatory behavior. While possible, this has not been demonstrated, and even if it were so it would be redundant with PAH's own capabilities.

The allosteric activation and relaxation properties of PAH are well known, and appear to be both necessary and sufficient to regulate L-Phe homeostasis.[58] The PAH contained in liver is able to respond effectively to elevated L-Phe, as evinced by the pure enzyme's ability to undergo allosteric activation within seconds.[80] Once it has restored L-Phe levels to normal, the isolated enzyme relaxes on a slightly slower time scale to basal activity, mostly T-state enzyme.[58] Regulation by phosphorylation cannot alter the fundamental behavior of this system, other than to sensitize the enzyme. If it did, there would be significantly higher basal levels of PAH activity in liver, and profoundly lower levels of serum L-Phe. Hyperphosphorylation of PAH is associated with starvation, and not with normal physiological conditions (in contrast with phosphorylase phosphorylation).

The simplest model for PAH phosphorylation is that its *sole* effect is a lowering of the activation energy barrier to allosteric activation. *In vivo* this may be a combination of (1) facilitating the T → R state protein distortion and (2) lowering the affinity

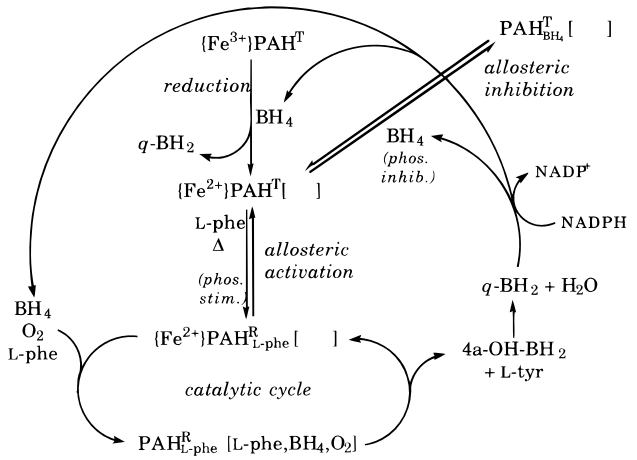

Figure 6. Regulation of PAH by BH_4, L-Phe, and phosphorylation.

of the BH_4 regulatory site for that inhibitor. If it is a true allosteric inhibitor, BH_4 stabilizes the T state, which would mean that these two phenomena have the same thermodynamic origin. This mechanism is sufficient to explain the observed increase in L-Phe sensitivity, increase in activation rate, and, *in vivo*, the decrease in effectiveness of BH_4 inhibition.

3.6. Integrated Description of PAH Regulation. A schematic view of the different interactions that occur in PAH is given in Figure 6, an adaptation of figures shown by other authors[118] updated with current nomenclature. Empty brackets represent an empty active-site substrate binding pocket. For the sake of clarity, none of the accessory enzymes involved are indicated. It is also important to emphasize that the physiological concentrations of BH_4 are equimolar with PAH, at about 9 μM each.[119]

As has been pointed out, the net effect of this complex interaction is to sharpen the response to a rise in L-Phe. BH_4 sequesters PAH, and *vice versa*, which greatly lowers the background level of activity, thus preventing L-Phe loss from the organism. It has four unique features that are important to achieving direct regulation of PAH activity by the applied [L-Phe]: the "sequestering appears to have an explicit regulatory effect, the sequestering agent is the enzyme itself, the enzyme-cofactor complex that is formed is inactive, and the agent that causes the release of cofactor and enzyme from the complex is the reaction substrate."[118]

The several different ways in which pterin can interact with PAH are depicted, including the allosteric inhibition that is exclusive to BH_4. Once this inhibited complex has formed, dead-end complexes with L-Phe form with the nonphysiological K_d 4 mM. A regulatory role for BH_4 is supported by the mutually exclusive relationship between BH_4 inhibition and phosphorylation, also depicted in the figure. Phosphorylation is only known to affect the steps indicated and cannot effect any of these transformations on its own. Although reduction is depicted as occurring from the PAH^T state, reduction of PAH^R states is even more rapid.[133] Whatever the route taken, the only catalytically active entity is reduced PAH^R.

None of the oligomeric states associated with PAH have been depicted in the figure. A consideration of the rate of activation by Shiman *et al.* led the authors

to conclude that the cooperative unit functioning in allosteric activation was the full tetramer.[58]

4. Properties of the Active Site Iron

4.1. Iron, Oxygen, and PAH. In retrospect, a requirement for an active-site transition metal might have been anticipated for PAH, given the great enhancements of $^3O_2$ reactivity possible with metal cofactors and the difficulty of the chemical transformation PAH catalyzes. The discovery of PAH and its cofactor BH_4 had both occurred by the time the cytochromes P450 were identified, as a class of enzymes capable of performing difficult transformations reminiscent of L-Phe hydroxylation (section IV.A.3).[134,135] The requirement for metals in the conversion of L-Phe to L-Tyr was first inferred by Udenfriend and Cooper, who demonstrated that this activity in liver extracts had an absolute requirement for O_2 and sensitivity to both cyanide and azide (at 8 mM, yielding 78 and 100% inhibition, respectively).[17] Using a similar preparation, Kaufman reported that Fe^{2+} (2 mM) could stimulate activity up to 30% in some situations, while Cu^{2+} was inhibitory.[18]

With the apparently reactive BH_4 cofactor in hand, the thought of an additional cofactor requirement may have seemed redundant, and it was not extensively pursued while research into the cytochromes P450 progressed (section IV.A.3). Research through the 1960s focused on the tetrahydropterin cofactor, which by its structural similarity to the well-understood flavin system, seemed sufficient to account for monooxygenase activity. Once model studies (section III.B.3) had indicated how sluggish the reaction of BH_4 with O_2 in solution really was, it became necessary to account for the acceleration accomplished by PAH. The inability of wholly organic catalysts to perform NIH shifts also demanded a reinvestigation.

The $(\pi^*)^2$ configuration of molecular oxygen's ground state is $^3\Sigma_g^-$ ("triplet oxygen"), which lies well below the $^1\Delta_g$ and $^1\Sigma_g^+$ levels ("singlet oxygen": 92 and 155 kJ mol^{-1}, 8000 and 13,000 cm^{-1}, respectively). Any reaction with either form of O_2 is thus subject to an activation energy barrier 15 kcal mol^{-1} smaller in the case of singlet oxygen. Singlet oxygen is much more reactive with ordinary organic compounds because the reactions are spin-allowed and can be generated from the ground-state diradical $^3O_2$ photochemically. Excepting the singlet route, in order for O_2 to react with organic compounds, one of two things must occur: the substrate must be converted into a singlet by radical generation, or the oxygen must be "activated" in combination with the d orbitals of a transition metal, which in biological systems is often ferrous iron, Fe^{2+}.

Ferrous ions are present in either a high-spin state ($S = 2$), in which only one of its five *d* orbitals is occupied by two electrons, or a low-spin state ($S = 0$), where the set of three t_{2g} orbitals is full. The resulting molecular orbital (MO) of a simple mononuclear $\{Fe^{2+}\text{-}O_2\}$ adduct can either be a triplet or a singlet, depending upon Δ, the energy separation between the Fe-based d_{xy} orbital and the O_2-based π^* orbital, which is determined by the geometry and ligand field of the iron's coordination environment.

Fine-tuning the reactivity of the $\{Fe^{2+}\text{-}O_2\}$ adduct in this way can explain why heme proteins are able to function both as reversible O_2 carriers (hemoglobin) and as monooxygenases (cytochromes P450). In the case of hemoglobin, the Fe^{2+} is low spin, in part because of the strong ligand field of the heme, and the bound oxygen is relatively unreactive. However, the low-lying triplet excited states of the $\{Fe^{2+}\text{-}O_2\}$ complex are accessible, leading to the formation of significant amounts of the reactive reduced oxygen species superoxide ($O_2^{\bullet-}$) in oxygenated erythrocytes. As a result, erythrocytes contain large amounts of the $O_2^{\bullet-}$- and H_2O_2-scavenging enzymes superoxide dismutase and catalase to protect the organism.

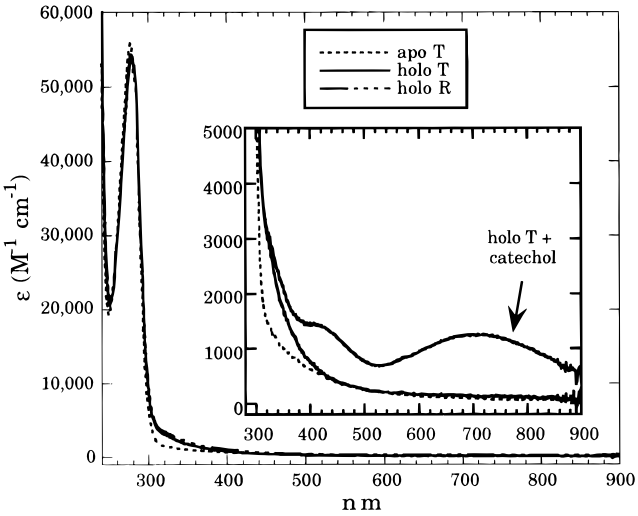

Figure 7. UV/vis spectrum of recombinant PAH states. The inset shows an adduct with catechol. Taken from ref 61.

Cytochromes P450 avoid the formation of toxic oxygen species by carefully controlling electron transfer into the substrate−O_2−enzyme complex. Non-heme iron proteins are in theory able to perform the same tasks as those with a heme prosthetic group, but the ligand set afforded by the 20 common amino acids is unsuitable for stabilizing low-spin Fe^{2+} in the presence of a labile (usually water-bound) coordination site. As a result, all non-heme iron oxygen-carrying proteins contain binuclear iron active sites, as in hemerythrin, which gives marine invertebrate blood its characteristic blue color. Other non-heme iron proteins contain high-spin iron, and must control their reactivity with O_2 carefully.

Even in its ferric state ($\{Fe^{3+}\}$PAH), the visible spectrum of PAH is notably featureless,[133] which immediately indicates that it is not a hemoprotein or a flavoprotein, nor are there thiolates, inorganic sulfides, or tyrosinates coordinated to the metal site. The modest spectral features near 350 nm are consistent with histidine and carboxylate ligation. Their intensity is diminished upon reduction of $\{Fe^{3+}\}$PAH to $\{Fe^{2+}\}$PAH,[133] or removal of iron ("apo" spectrum in Figure 7). The most easily recognizable ligands in mononuclear non-heme iron metalloproteins have strong absorptions due to a ligand (O or S) $p_\pi \rightarrow$ Fe d_π* ligand-to-metal-charge-transfer band (LMCT); these include phenolates ($\lambda_{max} = 420-530$ nm, $\epsilon \approx 4000$ M^{-1} cm^{-1}),[136] thiolates (rubredoxin-type, $\lambda_{max} = 450-560$ nm, $\epsilon = 5000-10000$ M^{-1} cm^{-1}),[137] and catecholates ($\lambda_{max} = 500-650$ nm, $\epsilon = 1000-2000$ M^{-1} cm^{-1}).[138] For instance, lactoferrin, PCD, and transferrin have pink to burgundy colors caused by

tyrosinate → Fe^{3+} LMCT bands at 460−480 nm.[139] Strong visible signals are not evident in PAH, and as a result, it is not surprising that for many years the importance of iron to PAH was overlooked.

At the beginning of the 1970s, when evidence from model studies of tetrahydropterin reactivity and the NIH shift had begun to accumulate, the role of iron in the PAH system was further delineated by Fisher *et al.*[75,140] Given its differential sensitivity to chelating inhibitors, the active form of PAH probably contained ferrous rather than ferric iron. For instance, oxalate and *o*-phenanthroline (*o*-phen) have about the same affinity for ferric and ferrous iron, respectively, but only *o*-phen inhibits PAH appreciably. EDTA is unable to inhibit PAH, an initially surprising observation best understood in context of active-site accessibility; the planar, neutral *o*-phen is an effective inhibitor because it can coordinate to the active site iron, while the anionic EDTA may not.

The optical spectrum, EPR spectrum, and colorimetric iron determination of partially purified (sucrose gradient) PAH indicated the presence of iron in the active enzyme fraction.[140] Removal of this iron by *o*-phen treatment resulted in loss of activity, which could be restored by reconstitution of the apoprotein with $FeCl_2$. Finally, the activating effects of reconstitution were found to be specific for iron, and not the dications of Co, Hg, Mn, Ca, Ni, Zn, or Cu. However, ammonium sulfate precipitation of PAH to which Fe^{2+} had been added resulted in the loss of the additional iron from the enzyme, with reversion to a low-activity state.

Shortly thereafter, the small, atypical PAH obtained from *Pseudomonas* was demonstrated to require ferrous iron, with half-maximal activation at 1.2 mM.[141] The effects appeared to be specific for iron, in contrast to an earlier report that Hg^{2+}, Cd^{2+}, and Cu^{2+} also stimulated enzyme activity.[142] Using the heterologously expressed, monomeric *P. aeruginosa* PAH, Zhao and co-workers inferred a requirement for iron based on the abolition of activity by EDTA, which could be completely restored by the addition of Fe^{2+} but not Cu^{2+}.[143] The differential sensitivity of mammalian and bacterial PAH to EDTA is consistent with greater active-site accessibility in the latter, which is also borne out by its lower affinity for iron.

The hydrophobic affinity purification developed by Shiman[55] was improved by the inclusion of an iron-reconstitution step in an early step of the purification procedure.[144] This iron remained tightly bound, in contrast to the labile iron resulting from reconstitution of purified protein.[140] No increase in activity was noted if the iron was added at a later stage, even though the PAH iron content rose ("adventitious" iron binding).[52] The differing results were hypothesized to result from the removal of a component of crude extract that facilitates iron insertion into PAH, which is removed even by "slight purification under mild conditions".[52]

This did not preclude the development of a method to strip Fe^{2+} from holoenzyme using *o*-phen in 15% glycerol, and replacing it in 2% DMF under aerobic (Fe^{2+}) or anaerobic conditions (Fe^{2+} or Fe^{3+}). In every enzyme preparation, regardless of whether an iron-addition step had been performed, the PAH activity showed a linear dependence upon iron content.[144]

The timing of iron insertion into PAH *in vivo*, which might have important regulatory consequences, has only been the subject of a single report.[52] This was investigated using rat livers perfused with a defined medium that contained bovine erythrocytes. In contrast to perfusion with rat blood, perfusion with the defined medium caused an increase in the relative PAH specific activity. Cycloheximide, an inhibitor of protein synthesis, failed to block the increase in activity. The PAH activity in extracts from unperfused livers could be stimulated by iron treatment, while extracts from the perfused livers could not. As a result, it was concluded that the stimulation of PAH activity was due to reconstitution of preexisting PAH apoprotein by increased iron levels in the cell.

This suggested that the stimulation results from an increase in the intracellular iron concentration, which might be caused by the lack of transferrin from the defined perfusion medium. Transferrin, the mammalian iron carrier, would prevent an increase of free iron in rat blood, but not in the defined medium, which would contain free iron if some of the erythrocytes were lysed. Alternately, perfusion could stimulate release of iron from ferritin or increase heme degradation in some way. The variation in the level of iron in PAH was found to follow a diurnal cycle, in both fasted and fed rats. Rats younger than 9 days had apparently full iron content in their PAH, falling to a level of 55% holoprotein in adult rats. The physiological justification for such a large content of inactive apoprotein in liver is unclear, but one can imagine mechanisms by which the iron content of PAH could be used in a regulatory sense,[52] as it is for other non-heme iron-containing liver proteins including aconitase (IRE-BP).[145]

In 1984, the reduction of "resting" PAH ($\{Fe^{3+}\}$-PAH^T) by its pterin cofactor was discovered,[133] and the site of reduction was determined to be the iron site.[146] The mechanism of how a two-electron reductant manages to reduce isolated Fe^{3+} sites by a single electron is of sufficient interest to discuss separately, in section II.A.4.4, after discussion of the active-site structure.

4.2. Structural and Spectroscopic Studies. The coordination environment of the iron in PAH controls its interaction with O_2, BH_4, and L-Phe bound in the larger active-site pocket. Assessment of the structural and electronic features is an essential component of determining how this non-heme protein is able to catalyze reactions as demanding as those performed by the cytochromes P450 (section IV.A.3).

Initial spectroscopic characterization of PAH was performed with $\{Fe^{3+}\}$PAH, which is the form of the enzyme that results from the hydrophobic affinity purification procedure. As was mentioned before, the UV−visible spectrum of PAH is not prominent, but there are distinct absorptions above 300 nm that are consistent with histidine−carboxylate coordination of a non-heme iron (Figure 7). These vanish upon reduction of the protein (section II.A.4.4). The EPR spectrum of apparently oxidized PAH was obtained by Fisher *et al.*, who observed a rhombic high-spin ($S = {}^5/_2$) signal at $g_{eff} = 4.28$, but at liquid N_2 temperature, where the EPR signals are quite

broad.[140] At lower temperatures, the signal intensity grows markedly, and new, lower field features appear. The EPR spectrum of highly active PAH was recorded in Tris buffer at 10 K, and a characteristic spectrum containing axial (g_{eff} = 6.7 and 5.4) and rhombic (g_{eff} = 4.3) components was observed.[146] Additional signals in the g_{eff} = 9.4 region arise from the lower Kramer's doublet of a component with the signal from a middle Kramer's doublet at g_{eff} = 4.3. (Fe^{3+} ($S = {}^5/_2$) is a Kramer's ion; that is, it has an odd number of unpaired electrons, and in the absence of a magnetic field, every level is at least 2-fold degenerate. The splitting of the Fe^{3+} sextet into three Kramer's doublets arises from electron−electron dipolar interactions and a second-order spin−orbit coupling interaction between the ground and excited states (^{6}A and ^{4}T, respectively). Application of a magnetic field as in the EPR experiment breaks the degeneracy of the doublet, leading to the observed transitions.) Double integration of the derivative spectrum between g_{eff} = 5 and 10 showed a linear dependence of PAH activity on the axial signal's intensity, meaning that it corresponds to "active" iron sites, while the intensity of the g_{eff} = 4.3 signal corresponds to the variable amounts of inactive and adventitious iron sites.

The EPR spectrum of oxidized PAH is sensitive to environmental conditions such as the nature of the buffer.[147,148] The EPR spectrum of $\{Fe^{3+}\}PAH^T$ in 50 mM MOPS buffer differs considerably from the spectrum of $\{Fe^{3+}\}PAH^T$ in 50 mM Tris buffer.[149] The EPR signals at g_{eff} = 6.7 and 5.4 and the less intense g_{eff} = 4.3 resonance in the Tris buffer EPR spectrum are replaced by very broad features spanning from g_{eff} = 10−5 and a prominent g_{eff} = 4.3 resonance in MOPS buffer. The Tris adduct spectrum could be regenerated by the titration of Tris into a sample of MOPS-buffered $\{Fe^{3+}\}PAH^T$.

Kinetic studies have demonstrated that Tris buffer slows the rate of reduction of $\{Fe^{3+}\}PAH^T$ by $6MPH_4$ and completely inhibits $6MPH_4$ during catalysis with a K_I of 80 mM at pH 7.8.[133] Tris most effectively inhibits reduction and catalysis at high pH (8.0−8.5) with little effect at pH 6.8, suggesting that its free base form acts as the inhibitor.[76,133] MOPS buffer has no strong affinity for transition metals and shows no influence on the initial velocity of the activity of PAH. The chemical basis of Tris buffer inhibition may arise from either the direct coordination of Tris to the catalytically active iron center, a decreased ability for either cofactor or substrate to bind in the active site pocket owing to competition with Tris, or by a buffer-induced conformational change resulting in a decreased binding affinity for either cofactor or substrate. The metal affinity of Tris is documented; Tris will bind free metal ions in a bidentate fashion through the amine group and one of the hydroxyl groups.[150−152] In addition, the crystallographic characterization of Tris coordinated to one of the three Zn^{2+} sites in phospholipase C was recently reported in which Tris displaced a water molecule originally bound to the Zn^{2+} center.[153] As observed with PAH, Tris buffer inhibits the activity of phospholipase C.

EPR spectroscopic characterization of $\{Fe^{3+}\}PAH$ was extended by examining several different preparations of rat hepatic $\{Fe^{3+}\}PAH^T$ and $\{Fe^{3+}\}PAH^R$, including a variety of adducts that are discussed in the following section. The axial signals at g_{eff} = 6.7 and 5.4 disappear if the enzyme is L-Phe-activated. A similar effect is achieved by the addition of glycerol to 10%.[146] Although the dependence of PAH activation on [L-Phe] at equilibrium is complex, owing to the cooperative involvement among all four subunits of the tetrameric form of the enzyme, it is possible to use apparent association constants obtained from the inverse concentration of L-Phe that produces one-half maximum activity to assess the loading of L-Phe in each subunit. Since the protein solutions used in these EPR experiments were quite concentrated (0.5−1.5 mM Fe), it is expected that the addition of 20 equiv of L-Phe (10 mM) is sufficient to saturate both the independent allosteric (110 μM, pH 6.8) and catalytic (180 μM, pH 6.8) sites.[149] Warming the $\{Fe^{3+}\}PAH^T$ samples in the presence of L-Phe resulted in the concomitant disappearance of the characteristic axial PAH EPR signals.[154] Titration of $\{Fe^{3+}\}PAH^T$ with L-Phe resulted in a conversion to $\{Fe^{3+}\}PAH^R_{L-Phe}$[L-Phe], (the brackets indicate occupancy of the active site, in the current case, by the substrate L-Phe), which gave rise to an EPR spectrum with a new signal at g_{eff} = 4.5 that was easily distinguishable from the g_{eff} = 4.3 transition. The intensity of the g_{eff} = 4.5 signal was shown to scale linearly with PAH activity, indicating that this signal is associated with the catalytically competent iron centers. These spectral features are similar to those reported for EPR spectra of activated PAH in the presence of the potent inhibitor, 4-fluorophenylalanine in Tris buffer.[147 148] Intriguingly, if 5-deaza-$6MPH_4$ is added to the enzyme, a new and less prominent signal at g_{eff} = 4.4 appears.[149] However, these data preclude any assessment regarding whether the observed changes in the EPR spectrum of $\{Fe^{3+}\}PAH^T$ and $\{Fe^{3+}\}PAH^R_{L-Phe}$[L-Phe] are a consequence of substrate (L-Phe) in the active site or of changes in the coordination environment of the active iron center induced by the structural reorganization accompanying PAH activation.

The effect of the allosteric activation on the EPR spectrum of PAH was qualitatively addressed by examining the various states of oxidized PAH. In addition to the $\{Fe^{3+}\}PAH^T$ and $\{Fe^{3+}\}PAH^R_{L-Phe}$[L-Phe] states, EPR spectra of lysolecithin activated ($\{Fe^{3+}\}PAH^{act}_{lysolecithin}$), α-chymotrypsin-treated PAH, ($\{Fe^{3+}\}PAH^{act}_{\alpha-chymotrypsin}$), $\{Fe^{3+}\}PAH^T$-[L-Phe] (prepared by adding L-Phe to a cold solution of $\{Fe^{3+}\}PAH^T$ and freezing it prior to allosteric activation), and $\{Fe^{3+}\}PAH^T$[L-Trp] were obtained.[149] The $\{Fe^{3+}\}PAH^{act}_{\alpha-chymotrypsin}$ and $\{Fe^{3+}\}PAH^{act}_{lysolecithin}$ samples correspond to nonphysiologically activated (catalytically competent) forms of PAH formed in the absence of substrate L-Phe. As discussed earlier (section II.A.3.3), $\{Fe^{3+}\}PAH^{act}_{lysolecithin}$ is kinetically indistinguishable from $\{Fe^{3+}\}PAH^R_{L-Phe}$[L-Phe] and represents a form of the enzyme that while active does not contain substrate in the active site. Similarly, α-chymotrypsin treatment of PAH generates a 36 kDa, iron-containing fragment that does not need to undergo an allosteric transformation in order to catalyze the 6-MPH_4-dependent oxidation of L-Phe. Interestingly, the EPR spectra of both the $\{Fe^{3+}\}$-

Table 1. EPR Simulations of Various PAH States[a]

		rPAH^T			
	λ (E/D)	(MOPS)	(phosphate)	rPAH$^R_{L-phe}$[L-Phe]	rPAH^T[deaza]
g_{eff} = 9, 5.4	0.13 ± 0.06	0.59			
	0.16 ± 0.03				0.22
	0.18 ± 0.04			0.37	
g_{eff} = 4.3, 4.1	0.31 ± 0.15	0.40	0.96		0.70
g_{eff} = 4.4, 3.9	0.29				0.07
g_{eff} = 4.5	0.315 ± 0.075			0.62	
g_{eff} = 4.3	0.33	0.01	0.04	0.01	0.01

[a] Taken from ref 156.

PAH$^{act}_{lysolecithin}$ and {Fe^{3+}}PAH$^{act}_{\alpha-chymotrypsin}$ forms are equivalent to {Fe^{3+}}PAH^T, suggesting that the immediate ligand environment of the iron center does not change significantly during the allosteric transformation.

This conclusion is consistent with additional EPR studies that show the qualitatively equivalent nature of {Fe^{3+}}PAH$^R_{L-Phe}$[L-Phe], {Fe^{3+}}PAH^T[L-Phe], and {Fe^{3+}}PAH^T[L-Trp] forms of the enzyme (g_{eff} = 4.5).[149] The addition of L-Phe to samples of {Fe^{3+}}PAH^T at low temperatures (4 °C) generates a form of the enzyme that by gel filtration chromatography and activity measurements corresponds to the resting T state of PAH.[155,156] Similarly, L-Trp will not activate PAH under the conditions employed. These data suggest that the observed change in the EPR spectrum of {Fe^{3+}}PAH^T and {Fe^{3+}}PAH$^R_{L-Phe}$[L-Phe] is caused by the interaction of substrate in the active site and not directly by the reorganization of PAH following its activation.[149]

More detailed analyses of the EPR spectra of PAH have been reported.[146−148,157] Several EPR-active species contribute to the observed spectrum and cannot be directly deconvoluted because the signals are quite broad, and because the anisotropy of the Fe^{3+} **g** tensor causes anisotropic transition probabilities, preventing quantitative comparisons between different signals. As a result, it is not adequate to perform simple double integration of the EPR spectrum. Simulation of the individual contributions within the composite signal allows the extraction of the component site parameters, and their relative contribution to the total derivative signal. Four components were simulated[156] in the spectrum of {Fe^{3+}}PAH^T in Tris buffer:

(1) The prominent axial (λ = 0.032) component with g_x = 5.4, g_y = 6.7, and g_z = 2.0, accounting for 37% of the total spins. In the sample examined, 36% was expected from the specific activity determination; therefore this is the contribution from active iron. (λ is a measure of the zero-field splitting asymmetry (λ = E/D). It ranges from 0.33, a completely rhombic environment, to 0, the axial limit.)

(2) A broad component centered on λ = 0.20, with a range of λ values. This accounted for 55% [Fe^{3+}] spins. This contribution is termed inactive iron, because it cannot be reactivated to the catalytically competent state, yet it appears to be spectroscopically distinct from the next category.

(3) Two smaller rhombic components (λ = 0.30 and 0.33; 5 and 3% of the total spins, respectively), with all transitions between g_{eff} = 3.9 and 4.4. This rhombic contribution is termed adventitious iron, because it cannot be removed from PAH and is present in variable amounts.

Using the reconstitution procedure, Bloom *et al.* were able to selectively remove the active component (no. 1), yielding an entirely rhombic residual comprising ~15% of the starting spin concentration. No interconversion between the active and adventitious component sites originating from migration of iron between sites was observed.[157]

Simulation procedures were developed, from a first-order perturbation treatment of the spin Hamiltonian, for simulating the broad, asymmetric line shapes of site no. 2 by calculation of a distribution of λ values.[147,148] This Gaussian distribution in λ values reflects the configurational heterogeneity of the Fe^{3+} sites present in the frozen solution. This is particularly important for simulation of the lower Kramer's doublet features near g_{eff} = 9.0. A second consideration, the small D value of PAH relative to the microwave $h\nu$, causes additional powder lines to appear in the spectrum at positions that do not correspond to the principal axis directions. By diagonalizing the appropriate secular determinant, one first solves for g_{eff} at various values of the polar coordinates θ and φ, which relate the laboratory to the molecular frame, the transition probability is calculated across the range of g_{eff}, and then scaled by a lineshape factor. These solutions are integrated over θ and φ, as well as over a λ distribution if necessary. This method of analysis allowed determination of the two major components of {Fe^{3+}}PAH^T and {Fe^{3+}}PAH^R[*p*-F-phe], each of which had a near-axial component (λ = 0.032 and 0.11, respectively) with spin concentrations near that expected from the activity.[147]

These observations immediately suggest a greater degree of conformational heterogeneity in the electronic environment of the {Fe^{3+}}PAH active site, which was borne out in a quantitative sense by simulation of the spectrum in the manner described above. In particular, it was necessary to apply a range of λ values and quite broad line widths in the simulations to adequately represent the broad tails of {Fe^{3+}}PAH^T in phosphate, MOPS, and Tris buffer, which required two, three, and five components respectively. In the case of the MOPS spectrum, the three components most likely represent the three subtypes of EPR-observable iron shown in Table 1: active, inactive, and adventitious. The table is grouped into three categories based on the observed λ value, and not by association of a particular

Table 2. Mössbauer Parameters of PAH[a]

	D (cm^{-1})	λ [E/D]	δ_{Fe} ($mm\ s^{-1}$)	ΔE_Q ($mm\ s^{-1}$)	FWHM ($mm\ s^{-1}$)	$-A/g_N\beta_N$ (T)
$\{Fe^{3+}\}PAH^R$ rat liver (65%)	−0.44	0.278	0.40	0.25	0.41	(22.8, 21.9, 22.0)
$\{Fe^{2+}\}PAH^R$ rat liver (35%)			1.23	2.85	0.75	
$\{Fe^{3+}\}rPAH^R$ recombinant	−0.28	0.224	0.39	-0.06	0.43	(20.4, 21.3, 22.0)
$\{Fe^{3+}\}rPAH^T$ recombinant	+0.15	0.205	0.4	0.33	0.85	(20.0, 21.8, 22.1)
Fe^{3+}(EDTAH), H_2O		0.267	0.50	0.15		22

[a] Taken from ref 156.

component with one of the iron-site designations. The phosphate-buffered sample had an activity of 5.8 U mg^{-1} and 0.6 Fe subunit^{-1}, indicating that nearly all (90−95%) of the iron present was active. All of the rest were from a single preparation (6.8 U mg^{-1}, 0.9 Fe subunit^{-1}) that should contain about 70% of the iron in the active configuration. As was mentioned above, the spectra of $rPAH^T$[5-deaza-6MPH$_4$] and $rPAH^R_{L-Phe}$[L-Phe] share some similarities, which are reflected in the electronic parameters of the simulations. In particular, the nearly rhombic component now predominates over the one that has intermediate site symmetry, which probably indicates that the similarity between the two preparations is due to a perturbation of the electronic environment of Fe^{3+} caused by binding of the substrates to the active site of the enzyme.[156] This sort of interaction is distinguishable from the formation of adducts to the iron, which results from direct coordination of a vacant site and is discussed in the following section.

The ability to selectively remove and reconstitute the catalytically active iron site in PAH with ^{57}Fe was exploited to examine the Mössbauer properties of rat hepatic PAH^R_{L-Phe}[L-Phe]. Samples for Mössbauer analysis were prepared by reduction and removal of the natural-abundance iron with βME/*o*-phen, followed by addition of $^{57}FeCl_2$, which replaces only the active iron component of PAH with this isotope of iron. This site-specific determination of Mössbauer parameters included separable contributions from both ferric and ferrous active sites, due to incomplete reoxidation of the enzyme. For recombinant enzyme, which contains little inactive or adventitious iron, the addition of ^{57}Fe to the growth medium was used to obtain isotopically enriched PAH. As can be seen from a comparison of the data in Tables 1 and 2, there is reasonable agreement between the independent EPR and Mössbauer simulations for the various states of PAH that were examined despite the two methods having distinctively different dependencies on the parameter values.[149] Mössbauer simulations are most sensitive to the sign and magnitude of the zero-field splitting term D with only a relatively weak dependence on E/D while the EPR spectra derive most of the intensity from the magnetically least anisotropic middle doublet of the Fe^{3+} spin sextet making the shape quite sensitive to the distribution of E/D values. Mössbauer spectroscopy is better than EPR for determining the value of D, which is obtained from the temperature dependence of the Mössbauer signals. The poor signal-to-noise ratio in the $g_{eff} = 9$ region of the EPR spectrum precluded a precise determination of $|D|$, which is ∼0.4 for the near-rhombic site in PAH^R_{L-Phe}[L-Phe]. Since the Mössbauer signal with $D \approx -0.4$ is due to the active iron, it follows that the near-rhombic component of the $\{Fe^{3+}\}PAH^R_{L-Phe}$[L-Phe] EPR spectrum must be the signature of the active iron site.

$\{Fe^{3+}\}PAH^R_{L-Phe}$[L-Phe] exhibits EPR and Mössbauer spin-Hamiltonian parameters different from those reported for characterized four-, five-, or six-coordinate non-heme ferric metalloproteins containing N-, O-, or S-coordination.[158] The δ_{Fe} value is representative of a high spin ferric center while the relatively large hyperfine splitting ($A/g_N\beta_N$) is consistent with a coordination environment of moderate covalency.[158] The magnitude of ΔE_Q is small for an iron enzyme, suggesting an environment in which the net ligand field strength about the iron approximates cubic symmetry (six-coordinate ligation).

A comparison of the parameters of $\{Fe^{3+}\}$-PAH^R_{L-Phe}[L-Phe] with those of structurally characterized complexes consisting of five- and six-coordinate N and/or O donor ligands showed good agreement with $[Fe^{3+}(EDTAH)(OH)]^-$ obtained at low pH where the EDTA complex adopts a six-coordinate structure with a protonated noncoordinating acetate arm and a bound water/hydroxide.[149] It was concluded that a six-coordinate oxygen−nitrogen environment is most likely present in $\{Fe^{3+}\}$-PAH^R_{L-Phe}[L-Phe]. Sulfur or phenolate coordination was definitively eliminated on the basis of the magnitude of the observed spin-Hamiltonian parameters and the lack of LMCT transitions in the electronic spectrum of the native enzyme.[149] Other oxygen atom donors, such as carboxylates and/or water, were proposed to complete the iron ligand sphere. This conclusion is consistent with mutagenesis studies that suggest Fe-His ligation in the coordination sphere of PAH, as well as with the His to Fe^{3+} LMCT transitions observed at 350 nm in its electronic spectrum.

Additional support for the presence of a N/O coordination sphere of six (or five) moderately covalent ligands came from examination of the ferrous site. The Mössbauer spectra of $\{Fe^{2+}\}$-PAH^R_{L-Phe}[L-Phe] consisted of a quadrupole doublet with $\delta_{Fe} = 1.23$ mm s^{-1} and $\Delta E_Q = 2.85$ mm s^{-1}, characteristic of high-spin Fe^{2+} in a six-coordinate N/O environment.[158] The δ_{Fe} value, which *s* electron charge density at the ferrous center, is expected to be smaller for four-coordinate centers than six-coordinate sites owing to shorter metal−ligand bond lengths that increase the s-electron density at the ^{57}Fe center.[149,159] Data obtained with model complexes indicate that $\delta_{Fe} < 1$ mm s^{-1} are expected for four-coordinate geometries while six (or five)-coordinate geometries have $\delta_{Fe} > 1.20$ mm s^{-1}.[159] Furthermore, the substitution of one nitrogen or oxygen ligand with a more covalent sulfur donor would be expected to decrease δ_{Fe} by approximately 0.1 mm s^{-1}. The parameters observed for $\{Fe^{2+}\}$-

Table 3. Comparison of the Spectroscopic Properties of $\{Fe^{n+}\}PAH^{R}_{L-phe}$[L-Phe] and $[Fe^{n+}(N\text{-}MeEDTrA)(OH)]^{-,0}$ (n = 2, 3)

technique	$\{Fe^{3+}\}PAH^{R}_{L-phe}$-[L-Phe]	$[Fe^{3+}$(N-MeEDTrA)(OH)$]^{-}$
UV/vis	350 nm ($\epsilon_M = 4500$)	205 nm ($\epsilon_M = 9000$) 255 nm ($\epsilon_M = 15000$)
redox potential	> +120 mV (*vs* NHE)	+ 31 mV (*vs* NHE)
EXAFS	2.7 O at 1.96 Å 3.1 N at 2.15 Å (six coordinate)	3.4 O at 2.10 Å 2.0 N at 2.28 Å (six coordinate)
Mössbauer	$\delta_{Fe} = 0.39$ mm s^{-1} $\Delta E_Q = -0.06$ mm s^{-1} $D = -0.28$ cm^{-1} $E/D = 0.224$ $A = -21.2$	$\delta_{Fe} = 0.44$ mm s^{-1} $\Delta E_Q = 0.27$ mm s^{-1} $D = -0.18$ cm^{-1} $E/D = 0.14$ $A = -21.3$
EPR	$g_{eff} = 4.5, 9.7$ $\|D\| = 0.35$ cm^{-1} $E/D = 0.3 \pm 0.05$	$g_{eff = 4.3}$
MCD (Fe^{2+} form)	$g = 9.4$, $\delta = 3.6$ cm^{-1} $-\Delta = 500$ cm^{-1} $\|V/2\Delta\| = 0.18$	$g_{\|\|} = 9.3$, $\delta = 4.4$ cm^{-1} $-\Delta = 400$ cm^{-1} $\|V/2\Delta\| = 0.22$

PAH^{R}_{L-Phe}[L-Phe] are consistent with a high-spin Fe^{2+} center that is exclusively coordinated to N/O ligands.

Further insights concerning the coordination sphere of $\{Fe^{3+}\}PAH^{R}_{L-Phe}$[L-Phe] came from the spectroscopic characterization of the model complex $[Fe^{3+}$-(N-MeEDTrA)(OH)$]^{-}$ and a comparison to the L-Phe activated oxidized enzyme (Table 3).[160] These data indicate that the electronic environment of $\{Fe^{3+}\}$-PAH^{R}_{L-Phe}[L-Phe] is closely approximated by a six-coordinate complex containing two N donors, three carboxylate ligands and a solvent molecule, thereby supporting previous EPR and Mössbauer spectroscopic characterization of the active site of PAH. Interestingly, both the Fe^{2+} and Fe^{3+} forms of the N-MeEDTrA complex are capable of catalyzing the heterolytic cleavage of the O−O bond of phenylperacetic acid.[160]

Most spectroscopic studies to date on PAH have focused on the resting ferric form that is more spectroscopically accessible. However, it is essential that characterization of the reduced state of the enzyme is performed since the ferrous form of PAH represents the catalytically competent oxidation level. Recently, magnetic circular dichroism (MCD) and X-ray absorption (XAS) spectroscopic methods have been used to examine the active sites of ferrous metalloenzymes in a variety of states.[161] Analysis of near infrared (near-IR) MCD spectra allow the direct observation of ligand d → d transitions whose excited state orbital energies are sensitive to the coordination number and geometry of the iron center. When coupled with variable-temperature variable field (VTVF) MCD studies, which allows the determination of the ground-state sublevel splittings and orbital energies, a complete experimentally determined d-orbital energy diagram was obtained. Complementary information regarding the oxidation and spin states, coordination number and geometry at the iron center was obtained from XAS studies. Additional insights concerning the types of ligands and the ligand distances was obtained from the extended X-ray absorption fine structure (EXAFS) portion of the XAS data.

Initial MCD and XAS studies have centered on the $\{Fe^{2+}\}PAH^{T}$, $\{Fe^{2+}\}PAH^{act}_{NEM}$, $\{Fe^{2+}\}PAH^{R}_{L-Phe}$-[L-Phe], $\{Fe^{2+}\}PAH^{T}$[L-Phe], and $\{Fe^{2+}\}PAH^{T}$[L-Trp] states.[162] The presence of two transitions near 10000 cm^{-1} split by approximately 2000 cm^{-1} is consistent with a distorted octahedral coordination site for $\{Fe^{2+}\}PAH^{T}$ and $\{Fe^{2+}\}PAH^{T}$[L-Phe]. The MCD spectra of $\{Fe^{2+}\}PAH^{T}$, and $\{Fe^{2+}\}PAH^{act}_{NEM}$ showed transitions that were nearly identical to one another, suggesting that there is no significant difference in the iron coordination environment upon activation of PAH. While these data indicate that the T/R activation state of the enzyme has little (if any) effect on the spectral properties of the reduced iron center, the presence of a substrate in the active site induces a shift to higher energy of approximately 700 cm^{-1} in the lower MCD band, indicative of a stronger ligand field at the iron and a change in geometry. Samples of $\{Fe^{2+}\}PAH^{R}_{L-Phe}$[L-Phe], $\{Fe^{2+}\}PAH^{T}$[L-Phe], and $\{Fe^{2+}\}PAH^{T}$[L-Trp] gave similar spectra. (Kinetic measurements, gel filtration chromatography, and for the L-Trp sample, low-angle solution X-ray scattering data, support the assignment of the enzyme as T-state where indicated.) These results indicate that there are two different active site forms that can be represented by $\{Fe^{2+}\}PAH^{T/R}$, which contains an empty catalytic site, and $\{Fe^{2+}\}PAH^{T/R}$-[L-Phe], in which the bound substrate alters the ferrous center's electronic environment. Complete ground-state and excited-state energy levels were obtained from VTVF MCD studies. Interestingly, the value of 10 Dq of ∼9400 cm^{-1} for $\{Fe^{2+}\}PAH^{T}$ is significantly lower than that found for $[Fe^{2+}(H_2O)_6]^{2+}$, which together with the observation that nitrogen ligation increases the ligand field strength about an iron center, suggests that the coordination sphere of the active site Fe center in $\{Fe^{2+}\}PAH^{T}$ is predominantly oxygen. Average Fe−O distances in the enzyme samples (2.18 Å) are somewhat greater than those observed in hexaaquo complexes (2.14 Å).

The complement to detailed symmetry studies is extended X-ray fine structure (EXAFS) spectroscopy, which allows precise determination of the bond lengths, the remaining component of a complete solution of the site geometry. This has been performed for the Fe^{3+} and Fe^{2+} states of PAH^{T} and PAH^{R}, so that the geometric effects of allosteric activation and iron reduction can be separately understood.[162] In XAS experiments, iron core 1s electrons are excited into the continuum states by monochromatic X-rays, in the present case at the K-edge. Pre-edge features caused by the formally electric dipole forbidden 1s → 3d transition gain intensity if a center of symmetry is present, which couples the two states via a quadrupole transition, but more significantly through 4p−3d mixing. PAH in each of the four states examined showed only small pre-edge features, which is only consistent with a six-coordinate environment. Only subtle differences were observed between PAH^{T} and PAH^{R} samples in either oxidation state, and both resembled six-coordinate model compounds with a nitrogen−oxygen primary coordination shell most closely.[162] Modulations of the extended absorption edge have a direct dependence on the distances between the primary absorber and atoms in its immediate environment,

which can be obtained by Fourier analysis of appropriately weighted and scaled EXAFS data.

From these studies and the UV/vis spectrum, one can conclude that the catalytically competent active site of PAH is a spherically symmetric one, with histidine−carboxylate ligation able to adopt a number of conformations. This flexibility causes the observed microheterogeneity in the electronic environment of its Fe^{3+} state.[156] The mutational identification of two histidines as potential iron ligands[60] is consistent with this spectroscopic characterization of intact, wild-type PAH. Geometric and electronic parameters from MCD and XAS investigations have confirmed that the iron site in $\{Fe^{2+}\}$PAH is not drastically different from that in $\{Fe^{3+}\}$PAH. This result is consistent with the observation that the redox state of the iron does not affect the affinity of PAH for L-Phe or redox-inert pterin analogues.[117] The splitting in the ligand field MCD spectrum and the shape and intensity of the pre-edge features in the XAS spectrum of $\{Fe^{2+}\}PAH^T$ are consistent with a six-coordinate distorted octahedral geometry. EPR and MCD studies show that there are characteristic differences as the result of allosteric activation that are not detectable in EXAFS; no drastic changes to the primary coordination environment occur during the T → R transition, despite the rather large (∼34 kcal mol^{-1})[80] activation energy barrier for the allosteric reorganization. "Vacant" coordination site(s) detectable by adduct formation are the subject of the next section.

4.3. Adducts. If the iron site of PAH is used for O_2 activation, at least one of its ligands must dissociate. Several good high-spin Fe^{3+} ligands have been observed to bind PAH, and in many cases, inhibit activity, usually by preventing the progression to reduced enzyme.[133] Azide was the first of these identified,[17] followed by catechols and catecholamines.[163] Incubation of catechol compounds with $\{Fe^{3+}\}$PAH results in the rapid formation of a blue-green complex (λ_{max} = 698 nm), and a highly axial EPR spectrum.[146,156,164] Catechol binds tightly, with a K_d = 0.42 μM, at a final stoichiometry of one catechol per active iron (*i.e.*, a catalytically competent, coordinately unsaturated active site iron). Referred to the concentration of active iron, the ϵ_{698} is 1900 M^{-1} cm^{-1}, with a shoulder of approximately equal intensity at 435 nm.[61]

Catechol can coordinate to Fe^{3+} by one or both of its oxygen atoms, which can be distinguished by using isotopic substitution to assign bands in the resonance Raman spectrum or in comparison to crystallographically characterized model compounds. In comparison to model compounds, the coordination of catechol to PAH is proposed to be bidentate.[164] Stronger evidence of bidentate coordination has been obtained for TyrH, in which the stretches have been assigned with the assistance of rare O and Fe isotopes.[165] *In vivo*, PAH is less likely to undergo regulation by catecholamines than TyrH, which has apparently developed a system to overcome catecholamine inhibition (section II.B.3.5).

Some of the other adducts of $\{Fe^{3+}\}$PAH that give detectable spectroscopic signatures are presented in Table 4.[156] They fall into three approximate groups: the possibly monodentate Tris and phenol, the bidentate catechol, and the weakly bound azide and glycerol. Table 4 presents results for $\{Fe^{3+}\}PAH^T$, which is an inactive form of the enzyme but clearly one containing solvent-accessible iron. Adding 10% (v/v) glycerol to $rPAH^R_{L-Phe}$[L-Phe] causes the disappearance of the g_{eff} = 4.5 signal that is characteristic of L-Phe bound to the active site of PAH, but it is not clear if this is due to an enforced, rhombic environment (as with azide binding) or by displacement of the active site-bound amino acid.[146,156]

Table 4. Adduct UV and EPR Signals

PAH adduct	UV/vis	EPR (g_{eff})
Tris base	380 nm ($\epsilon_M \approx 3000$)	6.4, 5.7
phenol	540 nm ($\epsilon_M \approx 1000$)	6.4, 5.7
catechol	435 nm ($\epsilon_M \approx 2000$) and 698 nm ($\epsilon_M = 1900$)	7.4 & 4.2 (LKD) 5.8 (MKD)
azide	450 nm ($\epsilon_M \approx 1800$)	mostly 4.3
glycerol	enhances < 500 nm	mostly 4.3, $PAH^R \approx PAH^T$

Exogenous adduct formation with $\{Fe^{2+}\}$PAH by stoichiometric *o*-phen (at concentrations far lower than what would be required to strip iron from the enzyme) indicates that two coordination sites are also accessible in the reduced state of the enzyme. This has the useful property of quenching the fluorescence due to PAH, which can be exploited as a means of measuring [$\{Fe^{2+}\}$PAH] (K_d = 0.8 μM). Binding of bathophenanthroline (K_d = 1.1 nM) is nearly diffusion controlled and causes complete quenching of the enzyme's fluorescence. Bathophenanthroline is an effective competitive inhibitor of steady-state PAH activity, with a K_I (2 nM) effectively identical to its K_d.[116]

Alternately, binding of 1,2-dihydroxynaphthalene (DHN) to $\{Fe^{3+}\}$PAH can be employed for the determination of ferric PAH levels. Binding of DHN to $\{Fe^{3+}\}$PAH also causes fluorescence quenching, is tight (K_d = 1.1 nM) but slow enough to conveniently measure binding rates, and is not reversible, meaning that it is an effective trap. Using this method, several other chelators were examined for their ability to inhibit DHN binding. Among the strongest were benzohydroxamate and acetohydroxamate (K_I = <1 and 12 μM), which are structurally similar to the tightest known Fe^{3+} chelators, the siderophores. These values compare favorably with that for glycerol, which inhibits DHN binding with a K_I of 62 mM under the same conditions (0.1 M phosphate, pH 6.8, 25 °C). All of these values correspond well with the inhibition constants determined for the reduction process (next section). As expected, acetohydroxamate was a much less effective inhibitor of steady-state PAH activity (K_I = 1.7 mM). The irreversible binding of DHN was used under hydroxylation conditions to determine that once in every ∼150 turnovers, $\{Fe^{2+}\}PAH^R$ oxidizes to $\{Fe^{3+}\}$-PAH^R. Another clear implication is that $\{Fe^{3+}\}PAH^R$ is not part of the normal catalytic cycle. Under turnover conditions, inhibition of reduced PAH by ferric chelators may be mostly attributable to aberrant oxidation of the active site.[116]

Adducts of $\{Fe^{2+}\}$PAH that are amenable to more extensive spectroscopic analysis are rarer. One that is likely to allow many new kinds of spectroscopic and kinetic investigations is the nitric oxide (•NO) adduct of $\{Fe^{2+}\}$PAH, which generates a yellow species in a

strictly anaerobic environment. Since •NO is a stable radical ($S = {}^1/_2$), it can combine with Fe^{2+} ($S = 2$) to generate one of several different coupled spin systems, which are grouped into the general designation $\{FeNO\}^7$, where the superscript represents the total number of d electrons present in the coupled system.[166] Because it binds to the ferrous state of several oxygen-activating enzymes, including PAH, it can be regarded as a probe of how O_2 might bind to the reduced iron center. The resemblance is imperfect, because of the greater reactivity of •NO and its different geometric preferences, but in any case it provides a useful EPR signal. Examination of the crossing points[167] indicates that the $\{FeNO\}^7$-PAH adduct is highly axial ($\lambda \approx 0.02$). Only a single •NO binds to PAH, at the vacant coordination site that O_2 might transiently occupy during turnover.[61]

4.4. Reduction. There should be common themes among the known tetrahydropterin−PAH interactions, listed in descending order of their apparent complexity: productive PAH catalytic turnovers, uncoupled/unproductive catalytic $6MPH_4$ oxidation by PAH, and the stoichiometric reduction reaction. First, PAH catalysis leaves the oxidation state of the iron unchanged, and results in the oxidation of two organic substrates with consumption of one equivalent of O_2. Second, uncoupled turnover causes the oxidation of at least 1 equiv of tetrahydropterin per O_2 consumed, and can cause oxidation of the ordinarily ferrous active site (section II.A.4.3). The issue of whether or not H_2O_2 is produced in this reaction remains controversial. Finally, the reduction process causes an oxidation of the tetrahydropterin and a reduction of iron, with a poorly defined and inconsistent requirement for O_2 (*vide infra*).

If there are common mechanistic themes among these three processes, one can best hope to build an understanding by starting with the simplest interaction: $6MPH_4 + n\{Fe^{3+}\}PAH \rightarrow q\text{-}6MPH_2 + n\{Fe^{2+}\}PAH$. (This excludes the allosteric inhibition of PAH caused by BH_4, which has unknown redox consequences. With $6MPH_4$, the inhibitory effect is more than 1000-fold weaker,[118] and the majority of studies of PAH reduction use this cofactor analogue to avoid this complication.) Reduction of the iron site in $\{Fe^{3+}\}PAH$ by $6MPH_4$ or BH_4 is as important for the formation of an active enzyme species as allosteric activation but has received less attention. *In vivo* it is likely that nascent or preexisting apo-PAH is reconstituted by Fe^{2+}, but the oxidation state of "resting" PAH *in situ* is unknown. By using the relatively rapid Shiman purification, which begins with a DTT/Fe^{2+} reconstitution step, most of the enzyme purified from liver or recombinant sources is found as $\{Fe^{3+}\}PAH$. $\{Fe^{3+}\}PAH$ is also the major product of analogous aerobic Fe^{2+}-reconstitution procedures *in vitro*.[144] Although the oxidation phenomenon is poorly understood, the results suggest that the enzyme readily reoxidizes under aerobic conditions during the time (minutes to hours, depending on scale of protein isolation) it requires to purify reconstituted PAH. *In vivo*, the reduction reaction may be responsible for avoiding the accumulation of the relatively stable, inactive $\{Fe^{3+}\}PAH$. In the presence of all three of its substrates, PAH oxidizes once in every 150−200 catalytic turnovers (under "tightly coupled" conditions),[116,168] which is significant relative to k_{cat}, 9−12 s^{-1}. *In vitro*, reduction is an obligate step prior to catalysis.[146]

Very little is known about the *mechanism* of reduction. In terms of enzymatic mechanisms, it is an unusual feature occurring once, in the pre-steady-state period. The initial products of coupled catalytic turnover are L-Tyr, 4a-OH-$6MPH_2$, and $\{Fe^{2+}\}PAH$ for >99.3% of the hydroxylation events, *i.e.*, $\{Fe^{3+}\}$-PAH reduction is not part of the normal catalytic cycle. In this respect it differs from flavoprotein dehydrogenases and reductases, which in their reductive half-reactions are reduced by two substrate- or NADH-derived electron equivalents stored in one or more tightly bound flavin cofactors. A separate oxidative half-reaction returns the enzyme to the initial oxidized state, which can lead to an overall pingpong catalytic mechanism. Since PAH lacks covalently bound organic cofactors, it cannot store reducing equivalents during the reduction step, unless some unidentified redox-active protein moiety participates in the reaction. The iron sites in different PAH subunits are not within 10−15 Å of each other, as determined by the lack of unusual temperature-dependent features in Mössbauer and EPR spectra. The only change known to occur in PAH during the reductive interaction is the oxidation state of the iron, and while other alterations in the enzyme have not been detected, they are certainly possible.

During catalytic turnover, $6MPH_4$ bound at the active site provides two electron equivalents as part of the reaction complex, carrying away the oxygen atom not incorporated into L-Tyr at the water oxidation level (as 4a-OH-$6MPH_2$, the hydrate of q-$6MPH_2$). As a result, the PAH catalytic mechanism is sequential. In contrast, the reductive interaction produces q-$6MPH_2$ directly.[133] While this tends to rule out mechanisms akin to an abortive catalytic turnover, there have been several reports that reduction of $\{Fe^{3+}\}PAH^T$ requires and consumes O_2.[133,157] This potential participation of O_2 is of crucial importance in the reduction mechanism.

While PAH had long been suspected to be an iron-dependent hydroxylase, Fisher and Kaufman presented the first direct evidence for a tightly bound metal cofactor, a weak Fe^{3+} EPR signal, which disappeared under catalytic conditions. The structural characteristics of the active-site iron determined by subsequent spectroscopic analyses are described in section II.B.4.2. A more direct observation of iron reduction proved elusive, probably because of the very low activity of the PAH available then.[75] Later attempts to detect a change in the visible spectrum of BH_4 or $DMPH_4$ following incubation with a stoichiometric amount or more of PAH^T failed, for unknown reasons. (It has been suggested that the reason for the failure to observe tetrahydropterin oxidation was that Tris at pH 7.4 was used in the assay. However, only a 2-fold rate inhibition would be expected at 0.1 M Tris, pH 7.8,[133] so this seems unlikely to be the cause of the discrepancy.) However, activation of the PAH with lysolecithin, in the absence of either L-Tyr or L-Phe, caused rapid oxidation of the tetrahydropterin.[169] This result was later criticized because of the possible presence of

lysolecithin hydroperoxides, which form on standing and would directly oxidize $6MPH_4$ very rapidly.[170]

The first strong evidence for an obligate prereduction process appeared in 1984. A burst of NADH oxidation was observed by fluorescence detection in the presence of O_2, DHPR, ~2 μM oxidized PAH, and a slight molar excess of $6MPH_4$.[133] When the reductions were performed under conditions that particularly stabilize the 4a-carbinolamine form of the oxidized pterin, no lag in the appearance of q-$6MPH_2$ was reported, suggesting that q-$6MPH_2$ is the first oxidized pterin product of PAH reduction.[133] Reduction of $\{Fe^{3+}\}PAH$ by $6MPH_4$ (or under anaerobic conditions, $Na_2S_2O_4$) causes characteristic intensity decreases in the visible and EPR spectra of oxidized protein.[133,146] In addition, the oxidized pterin product of reduction, q-$6MPH_2$, appeared in register with an increase in the intrinsic fluorescence of PAH (excitation at 275 or 290 nm), which was used as a convenient method of determining the kinetics and extent of reduction.[133]

Quantitation of L-[^{14}C]Tyr formation from near-equivalent amounts of $6MPH_4$ and PAH was used to determine the (maximum) stoichiometry of $6MPH_4$:PAH subunit required for reduction. Very small amounts of L-Tyr were formed when the ratio of $6MPH_4$:PAH subunit was low. This "uncoupling" was consistent with consumption of 1 (T state) and 0.5 (R state) $6MPH_4$ per PAH subunit.[133,146] An exception to this stoichiometry was observed when *o*-phenanthroline was included in the reduction assay of PAH^T as a trap for Fe^{2+}, which indicated consumption of 0.5 $6MPH_4$ per PAH subunit. This 0.5:1 stoichiometry was also observed, under anaerobic conditions in the absence of *o*-phenanthroline, if the reductant was $Na_2S_2O_4$. Dithionite-reduced PAH was kinetically indistinguishable from $6MPH_4$-prereduced PAH, determined as a constant L-Tyr:$6MPH_4$ ratio across a range of $6MPH_4$:dithionite-reduced PAH subunit ratios, i.e., no $6MPH_4$ was required to reduce PAH.[146]

The 1:1 stoichiometry for $\{Fe^{3+}\}PAH^T$ reduction implies a requirement for a minimum of four "extra" electrons per tetramer (more if the iron occupancy is lower). The fate of these reducing equivalents was not established, but the apparent O_2 requirement seemed to afford an explanation of how they might be discharged. However, no peroxide or superoxide was detected as the result of reduction.[133] When O_2 usage was quantitated, 0.5 O_2 per $6MPH_4$ was consumed during reduction of $\{Fe^{3+}\}PAH^T$ by a molar equivalent of $6MPH_4$; this dropped to 0.12 O_2 per $6MPH_4$ in the presence of catalase. Bloom *et al.* describe the processes occurring in terms of the following interactions:

$$\{Fe^{3+}\}PAH^T + 6MPH_4 + O_2 \rightarrow \{Fe^{2+}\}PAH^T + q\text{-}6MPH_2 + O_2^{\bullet-} \quad (1)$$

$$O_2^{\bullet-} \rightarrow 0.5H_2O_2 + 0.5O_2 \quad (2)$$

$$\{Fe^{3+}\}PAH^T + 6MPH_4 + 0.5O_2 \rightarrow \{Fe^{2+}\}PAH^T + q\text{-}6MPH_2 + 0.5H_2O_2 \quad (3)$$

In the presence of catalase, an additional transformation occurs, leading to a new net equation:

$$H_2O_2 \rightarrow H_2O + 0.5O_2 \quad (4)$$

$$\{Fe^{3+}\}PAH^T + 6MPH_4 + 0.25O_2 \rightarrow \{Fe^{2+}\}PAH^T + q\text{-}6MPH_2 + 0.5H_2O \quad (5)$$

None of these reactions include the contribution of tetrahydropterin autooxidation, which only raises the overall consumption of O_2, regardless of the presence of catalase (which slows this reaction):

$$O_2 + 6MPH_4 \rightarrow H_2O_2 + q\text{-}6MPH_2 \quad (6)$$

Tetrahydropterin autooxidation is thought to involve formation of $O_2^{\bullet-}$, at a relatively low rate compared to either $\{Fe^{3+}\}PAH^T$ reduction or oxidation by H_2O_2 (section III.B.3). The authors predict 0.5 O_2 per $6MPH_4$ should be consumed under the conditions of reaction 3, and state that $6MPH_4$ autooxidation is the cause of the observed low O_2 consumption (0.12 O_2 per $6MPH_4$ observed *vs* 0.25 predicted) in the +catalase experiment.[157] (H_2O_2 was not directly detected in these experiments.) Because the autooxidation process itself consumes O_2, this latter assertion is puzzling and appears to be erroneous.

The equivalent of hydrogen peroxide produced by a single reduction event (reaction 3) would be able to oxidize either the reduced PAH, or another equivalent of $6MPH_4$, both of which can occur readily:[170]

$$0.5H_2O_2 + \{Fe^{2+}\}PAH^T + H^+ \rightarrow H_2O + \{Fe^{3+}\}PAH^T \quad (7)$$

$$H_2O_2 + 6MPH_4 \rightarrow H_2O + q\text{-}6MPH_2 \quad (8)$$

If reaction 3 and reaction 7 both occur as written at a significant rate, a small amount of $\{Fe^{3+}\}PAH^T$ could catalyze the reduction of half an equivalent of O_2 by $6MPH_4$, which clearly does not occur. If reaction 3 and reaction 8 both occur, the observed consumption of O_2 and $6MPH_4$ per $\{Fe^{3+}\}PAH^T$ reduced would be 0.5 and 1.5, respectively, yielding a predicted ratio of 0.33 O_2 per $6MPH_4$.

As a result, there are unresolved imbalances in the electron accounting if one invokes an O_2 requirement for $\{Fe^{3+}\}PAH^T$ reduction. There are no such difficulties with $\{Fe^{3+}\}PAH^R$ reduction in the presence of $6MPH_4$ and L-Phe, which does not appear to require O_2 beyond what is accounted for by catalytic turnover.[157] Incubation of rat liver PAH with its substrates under turnover conditions, or reduction with sodium dithionite, results in a disappearance of the ferric EPR signals, with the exception of a small rhombic contribution. Since inactive iron sites are rhombic, this residual signal might indicate that inactive iron sites are less-reducible than competent active sites. It cannot be determined from the appearance of the EPR spectrum alone, since the active iron's middle Kramer's doublet components also contribute to the $g_{eff} = 4.3$ region.

Shiman and co-workers have investigated the rates and extent of reduction using ferric- and ferrous-PAH-specific probes.[116] Again the tetrahydropterin:subunit stoichiometry of aerobic $\{Fe^{3+}\}PAH^T$ reduction was found to be 1:1, using either $6MPH_4$ or BH_4,

determined by quantitation of either Fe^{3+} or Fe^{2+}. In their experimental procedure, enzyme reduced in 1−2 min aerobic incubations with $6MPH_4$ was quantitated by the subsequent addition of fluorescent iron chelators. Under turnover conditions, 0.53 ± 0.02 BH_4 subunit^{-1} was required for the reduction of $\{Fe^{3+}\}$-PAH^R. Extrapolating to zero BH_4, three times as much $\{Fe^{3+}\}PAH^R$ is reduced as tyrosine formed. Given the 10-fold higher k_{cat}/K_m compared to k_{red}, these authors concluded that tetrahydropterin reduction of $\{Fe^{3+}\}PAH^R$ occurs without formation of a reaction complex. Because the reduction rates are smaller for $\{Fe^{3+}\}PAH^T$ compared to $\{Fe^{3+}\}PAH^R$, these authors rule out mechanisms involving the direct reaction of each subunit with free tetrahydropterin, followed by disproportionation of the resultant trihydropterin radicals. Therefore, if trihydropterin radicals are formed, they remain bound to PAH^R and/or very quickly reduce the second iron site. This would explain why reduction of $\{Fe^{3+}\}PAH^R$ is faster. However, it is unclear why an intermediate trihydropterin radical would fail to reduce a second subunit during reductions of $\{Fe^{3+}\}PAH^T$; a different reduction mechanism must be operative in each of the allosteric states.

The reduction of $\{Fe^{3+}\}PAH^T$ was recently reexamined under both aerobic and anaerobic conditions by monitoring the fluorescence increase of PAH that occurs upon reduction of the ferric center.[171] In aerobic titrations, a 1:1 stoichiometry of $6MPH_4$:subunit $\{Fe^{3+}\}PAH^T$ was observed. Parallel experiments using NADH as titrant with a trace amount of $6MPH_4$ and excess DHPR present also yielded a 1:1 stoichiometry of NADH:subunit $\{Fe^{3+}\}PAH^T$. However, when strict anaerobic procedures were used to prepare samples for $6MPH_4$ titrations, a change in the ratio to 0.5:1 $6MPH_4$:subunit $\{Fe^{3+}\}PAH^T$ was found. Further studies analyzing the amplitude *vs* $6MPH_4$ response in the reduction progress curves gave insight into the stoichiometry of the fluorescence-detected reduction reaction under stopped-flow conditions, which are aerobic but differ from the titration experiments in that all of the $6MPH_4$ is provided at once. Given that $6MPH_4$ donates two electrons to the enzyme during reduction, it appeared that 1.2 ± 0.1 pterin-derived electrons were consumed per Fe^{3+} site.[171]

On the basis of the observation that O_2 is not required to generate the characteristic fluorescence increase of $\{Fe^{3+}\}PAH^T$ associated with iron reduction, the direct quantitation of iron reduction was determined using EPR titrations performed under anaerobic conditions. The absence of O_2 prevents catalytic turnover, which allowed a direct comparison between $\{Fe^{3+}\}PAH^T$ and $\{Fe^{3+}\}PAH^R_{L-Phe}$[L-Phe] states. The data show that the two allosteric states of PAH have the same reduction stoichiometry under anaerobic conditions, with an apparent requirement of 0.5 $6MPH_4$ per iron-containing subunit. No new radical species were observed (at $t \geq 3$ min), and the only color change reported with these concentrated samples was a bleaching of the characteristic yellow color of $\{Fe^{3+}\}PAH$.[171]

By using fluorescence-detected stopped-flow techniques, the kinetics of PAH reduction were examined for a recombinant form of the enzyme. Rates were found to have a linear dependence on $[6MPH_4]$; the second-order rate constant (18 °C, pH 6.8) was reported to be $6.58 \pm 0.08 \times 10^4$ M^{-1} s^{-1}.[171] This rate is in good agreement with previous determinations using rat liver PAH, performed using either the direct fluorescence method[133] or trapping by Fe^{2+}-specific chelators.[116] The effect of pH on the second-order rate constant was small; a decrease was observed at higher pH (18 °C, pH 8.0: $4.01 \pm 0.08 \times 10^4$ M^{-1} s^{-1}). This rate is larger than a previous determination with rat liver enzyme, performed in the inhibitory buffer Tris.[133] Finally, the reduction of L-Phe-activated $\{Fe^{3+}\}PAH^R_{L-Phe}$[L-Phe] is somwhat faster than reduction of $\{Fe^{3+}\}PAH^T$;[116] lysolecithin-activated $PAH^{act}_{lysolecithin}$ is 3-fold faster than PAH^T at 18 °C.[171]

These results indicate that the different allosteric states of rPAH require the same number of reducing equivalents, maximally 0.5 $6MPH_4$ subunit^{-1}, but the reduction reaction is several-fold faster with R-state enzyme.[133] Since the lower stoichiometry is uniformly observed with the faster reducing species, it seems reasonable that there is a competing, inefficient, O_2-consuming process that becomes kinetically insignificant relative to the efficient reduction reaction.

It remains to explain the discrepancy between the anaerobic and aerobic reduction results obtained by different investigators. Since reducing equivalents are quickly and quantitatively transferred to Fe^{3+} under strict anaerobic conditions, our results do not agree with the observations of Marota and Shiman.[133] One can explain the low O_2-consumption stoichiometry reported by Bloom *et al.* if reduction is at least partially (≥50%) efficient under their aerobic conditions.[157] (Since tetrahydropterins react directly with O_2, this fraction may be larger than half.) In turn, there is clearly some inefficient use of $6MPH_4$ under the stopped-flow assay's experimental conditions, because the observed reduction stoichiometry in this aerobic experiment is 1.2 electron Fe^{-1}, compared to 1.0 electron Fe^{-1} in the EPR titration.[171] Since the reduction reaction is ∼85% efficient under the standard reduction assay conditions, it is useful as a mechanistic probe for the efficient component of the reaction at substoichiometric $6MPH_4$ subunit^{-1} levels. Above this level, it is likely to go by the inefficient reduction mechanism, which may also consume O_2 in the manner previously reported.

Diffusible radical formation is not likely to occur on the efficient reduction pathway, because reduction reactions under kinetic control (the stopped-flow assays) show efficient reduction, even at low levels of $6MPH_4$ subunit^{-1}.[171] When a small amount of $6MPH_4$ binds to $\{Fe^{3+}\}PAH^T$, the second electron is not lost to O_2 reduction, in a process that resembles the faster reduction of PAH^R_{L-Phe}. It is reasonable to suspect that this second reducing equivalent never leaves the enzyme, *i.e.*, two $^{\bullet}6MPH_3$ radicals are unlikely to dissociate from the enzyme and disproportionate to $6MPH_4$ and q-$6MPH_2$ to give the observed 0.5:1 $6MPH_4$:PAH^R_{L-Phe} stoichiometry. This conclusion was also reached by Shiman *et al.* from the nonequivalent rates of $\{Fe^{3+}\}PAH^T$ and $\{Fe^{3+}\}PAH^R_{L-Phe}$ reduction (1.8×10^5 and 2.5×10^5 M^{-1} s^{-1}, respectively, at 25 °C).[116] If all redox

transformations are mediated by free pterins, as in a disproportionation-based mechanism, it would require the T- and R-state reduction rates to be about equivalent, or with reduction of R slower than T, the opposite of what is observed. This stems from the need for two $^{\bullet}6MPH_3$ to dissociate from the enzyme and disproportionate in the (0.5 $6MPH_4$ subunit^{-1} stoichiometry) PAH^{R}_{L-Phe} case but not in the PAH^{T} (1.0 $6MPH_4$ subunit^{-1}) case.[116] (This inference is correct for the substoichiometric case, but if excess pterin is available, as is the case for the determination of the compared reduction rates, the rate of reduction detected by a change in the properties of the iron site will not be rate-limited by the sequelae of pterin oxidation.)

For related reasons, there is value in determining the limiting behaviors of the $6MPH_4$:PAH interaction even under the conditions of inefficient reduction; however, previous investigators found no evidence for saturation of the reduction rate[133] until quite recently, with BH_4.[116]

Several intriguing issues arise from these considerations. First, it becomes uncertain what might cause the rate difference between $\{Fe^{3+}\}rPAH^{R}_{L-Phe}$ and $\{Fe^{3+}\}rPAH^{T}$ reduction, since the reduction stoichiometry is the same. The simplest explanation is that the structure of the protein matrix affects the kinetics and perhaps the mechanism of reduction. Second, the second electron transfer within the reaction complex is at least as fast as the first electron transfer from $6MPH_4$ to Fe^{3+}. If $6MPH_4$ occupies a binding pocket near the active-site iron for the reduction reaction and at least the first electron transfer, it becomes a matter of considerable interest how quantitative electron transfer to a distant, second iron site occurs. Finally, there is the lingering question of why under aerobic conditions $6MPH_4$ reacts stoichiometrically with oxidized PAH, regardless of iron content or whether the fraction of active iron present is substoichiometric. Since it is able to provide reducing equivalents in excess of what would be apparently required by the limiting stoichiometry, it must modify the enzyme in such a way that $6MPH_4$ oxidation does not continue indefinitely. Neither $\{Fe^{3+}\}PAH^{T}$ nor $\{Fe^{2+}\}PAH^{T}$ function catalytically as an O_2-dependent tetrahydropterin oxidase, even though $\{Fe^{2+}\}PAH^{R}$ does so during uncoupled turnover.

Our results are consistent with a concerted, two-electron transfer from $6MPH_4$ to two $\{Fe^{3+}\}rPAH^{T}$ subunits, in that the rate of PAH reduction is monophasic.[171] This would be expected given the instability of the trihydropterin semiquinone radical.[172] It is most likely that if O_2 is consumed during reduction, it traps an enzyme-bound intermediate rather than being a requirement for electron transfer to the protein. Perhaps PAH is altered by interaction with the pterin in a way that precludes oxidation of $6MPH_4$ beyond a single equivalent per subunit, but has no effect on the active site Fe^{2+}. Since subunits lacking iron still apparently consume one $6MPH_4$, iron is unlikely to be the (initial) acceptor of the two reducing equivalents. Even if it were, and the two electrons were accepted sequentially from the pterin, the second, extra electron would have to go elsewhere (perhaps reducing O_2).[171] This depiction is again consistent with the idea that the PAH protein matrix mediates reduction of its active site iron, a possibility of continuing interest.[171]

5. Atypical PAH

All of the mammalian PAH enzymes have very similar characteristics and a high degree of sequence similarity. Nearly all of the mechanistic work has been done on these "typical" PAH systems, with the exception of *C. violaceum*, the only atypical PAH studied extensively. In contrast to the conserved sequence and structure of mammalian PAH, the atypical PAH enzymes vary widely in their characteristics. Thus it is difficult to make comparisons among them, or with the typical forms of PAH. PAH from *Drosophila*, which is apparently a bifunctional PAH/TrpH[173] with 50 kDa subunits, shows the highest sequence homology of any atypical PAH to the mammalian enzymes. The first three exons of human PAH have little similarity to the *Drosophila* enzyme, but the sequence homology rises to 89% similarity in a segment of the C-terminal domain.[174] In principle, the determinants for selecting between the two unactivated aromatic substrates are lacking in this form of PAH, an area of inquiry that will be better understood once more is known about the catalytic characteristics of the purified *Drosophila* PAH/TrpH. There is a distinct *Drosophila* TyrH encoded by the *pale* locus (section II.B.1).[175]

Many prokaryotes, including *E. coli*, synthesize L-Phe and L-Tyr by independent pathways starting from prephenate. However, several Gram-negative microorganisms are able to subsist on L-Phe as a carbon source, forming either phenyl acetate or L-Tyr, which implies that there might be PAH activity in prokaryotes. Direct conversion of L-Phe to L-Tyr was observed in *Pseudomonas* and *Salmonicida* species.[176] The PAH activity levels in *P. acidovorans* (*P.* sp. ATCC 11299a) were shown to depend upon the identity of the inducing amino acid: L-asparagine-induced cells had low PAH activity but L-Tyr-induced cells had levels comparable to that of L-Phe-induced cells. Partially purified enzyme required Fe^{2+}, O_2, $DMPH_4$, and the L-Phe substrate for activity, which was stimulated further by NADH.[142]

In a study using more extensively purified enzyme, the stimulatory effect of added metal ions was not exclusive to iron; some doubts arise as to the relevance of this observation because of the very low activity of this preparation (SA $\sim 3 \times 10^{-6}$ U mg^{-1} at 30 °C).[142] The *P. acidovorans* cofactor was determined to be reduced L-(*threo*)-neopterin rather than BH_4,[177] which remains the only known difference in PAH cofactor preference. The four purple, non-sulfur bacteria that contain PAH (*P. facilis*, *P. acidovorans*, *Alicagenes eutrophus*, and *C. violaceum*, which also contains a TrpH activity) belong to different pseudomonad subclasses, leaving the origin of the prokaryotic PAH trait unclear.[178]

Recently, the *phhA* gene from another PAH-containing strain, *P. aeruginosa*, has been cloned and sequenced, using a strategy of tyrosine−auxotroph complementation. It encodes a 30 kDa, monomeric, iron-dependent PAH that is encoded in an

operon with 4a-carbinolamine dehydratase and an aromatic amino acid aminotransferase. Interestingly, the PAH accessory protein 4a-carbinolamine dehydratase is also a homeodomain protein transregulator in several organisms and appears to play some essential role in *P. aeruginosa* PAH expression.[143]

A more intensely studied atypical PAH is the M_r 32 000 protein from *C. violaceum*. This PAH activity was observed during a study of the TrpH activity in the same organism (section II.C.2.3), and the two activities were shown to reside in different proteins.[179] A 3000-fold purification culminating in crystallization of *C. violaceum* PAH was accomplished by Nakata *et al.* who observed normal catalytic characteristics (coupled turnover with $DMPH_4$, $V_{max} = 14$ U mg^{-1}) but could not detect iron in active preparations. $DMPH_4$ was a more effective cofactor than $6MPH_4$ or THF (1.0:0.6:0.1 relative activities).[54,180]

Pember *et al.* examined purified *C. violaceum* PAH (specific activity 10−13 U mg^{-1}), and found 0.03 Zn, <0.30 Fe, and 0.99 ± 0.05 Cu per monomer.[181] EPR spectroscopy showed a typical type II Cu^{2+} site, which up to 3 mM $DMPH_4$ could not reduce to the diamagnetic Cu^+. DTT (2 mM) caused ∼90% reduction of this signal, and complete reduction could be effected (under anaerobic conditions) by 0.88 dithionite-derived reducing equivalents per monomer.

Preincubation of *C. violaceum* PAH with excess DTT eliminated an unusual lag in the appearance of L-Tyr. The lag was not due to L-Phe activation (the lack of allostery is unsurprising in this monomeric protein, which lacks the first ∼200 residues of the normal PAH consensus), and differed in length if an NADH/DHPR or DTT-coupled reaction was employed (roughly 2 and 0.7 min, respectively). The activity was uniformly lower in the absence of DTT. Even prereduced enzyme shows a lag of ∼10 s in the NADH/DHPR-coupled system. The authors ascribed this to dehydration of 4a-hydroxy-$6MPH_2$, which like mammalian PAH is formed as the initial pterin product of *C. violaceum* PAH catalysis.[181]

On the basis of these observations, the authors associated this nonallosteric lag with Cu^{2+} reduction and fit its rate to the sum of the reduction (0.1 min^{-1} at saturating $DMPH_4$) and (re)oxidation (0.4 min^{-1}, little $DMPH_4$ dependence) rates.[181] This would explain the longer lag times in the absence of DTT as being due to inefficient reduction of *C. violaceum* PAH by $DMPH_4$ except in the presence of substrate.

However, this hypothesis yields unusual interpretations of several experiments with near-stoichiometric levels of $DMPH_4$. A plot of (L-Tyr/$DMPH_4$) *vs* ($DMPH_4$/monomer) appears to indicate 0.7 L-Tyr per $DMPH_4$ is formed as ($DMPH_4$/monomer) → 0, which is quite different from the near-zero value one would expect if prereduction of the bulk of the oxidized enzyme present was required for catalysis.

A second experiment shows a lag of L-Tyr formation, but an endpoint of 7 μM L-Tyr formed from 7.8 μM $DMPH_4$ and 3 μM *C. violaceum* PAH monomer. While these results are consistent with prereduction, they imply that the majority of L-Tyr formation is performed by a small fraction of the oxidized *C. violaceum* PAH initially present. The simulations used to determine the significant difference in $DMPH_4$ K_d values for the oxidized and reduced *C. violaceum* PAH require fixing the reduction stoichiometry at 1:1 *C. violaceum* PAH:$DMPH_4$. Most of these considerations stem from the slow reduction rate, especially given the relatively large reoxidation rate, which is unusually slow compared to other cupric proteins or to reduction of the iron site in mammalian PAH.[181]

Because $DMPH_4$ does not reduce the Cu^{2+} site by itself, the possibility of adduct formation was examined by EPR using [5-^{14}N]- and [5-^{15}N]$DMPH_4$. An analysis of the hyperfine interactions indicated a direct $Cu^{2+}-N^5$ interaction,[182] which makes the inability of $DMPH_4$ to reduce the Cu^{2+} site all the more puzzling. This system remains the only evidence supporting a direct metal−pterin interaction in any PAH.

Steady-state kinetic analysis showed that *C. violaceum* PAH operates with a partially ordered sequential mechanism, with O_2 binding first of the three substrates.[183] This was established by variation of each of the three substrates in turn, using a constant ratio or two substrates at several fixed concentrations, to generate a family of three Lineweaver−Burk plots. Replots of the slopes were parabolic, as was the intercept replot of the v^{-1} *vs* $[O_2]^{-1}$ data. The other two intercept replots were straight lines, which indicates ordered addition of O_2 as the first substrate, followed by random addition of $DMPH_4$ and L-Phe.

The kinetic mechanism also predicts that *C. violaceum* PAH (E) is in equilibrium with an E·O_2 complex. In order to test this prediction, rapid-quench experiments were performed in which enzyme and 26 mM DTT in oxygenated buffer were diluted 20-fold into an anaerobic solution containing large amounts of $DMPH_4$, L-Phe, and DTT. A burst of 0.88 turnovers per monomer was observed (determined by extrapolation to $t = 0$) if the preequilibration solution was 1.2 mM O_2 (6 K_m), which fell to 0.53 turnovers per monomer at 60 μM O_2 (0.36 K_m). The steady-state velocities following the burst were identical. A smaller burst was obtained when L-Phe was included in the preincubation, which is consistent with it functioning as a dead-end inhibitor in the overall catalytic scheme.[183]

Finally, the Evans method was used to show that *C. violaceum* PAH reduces the μ_{eff} of O_2 in a manner consistent with complex formation. Presumably, Cu^+ is the site of O_2 binding to *C. violaceum* PAH.[183] This mechanism is probably not employed in the other aromatic amino acid hydroxylases. In TyrH, where the order of addition is known, $6MPH_4$ is first to bind in the overall kinetic mechanism; inhibitor studies were used to determine that O_2 and L-Tyr bind in the following steps.[184]

C. violaceum PAH was cloned and overexpressed in *E. coli* to yield a copper-containing enzyme (1 Cu per monomer). A purification chart indicates a very high final activity of 31 U mg^{-1} but the authors state 12−18 U mg^{-1} was average. V_{max} values for both authentic *C. violaceum* PAH and recombinant enzyme (34 and 35 U mg^{-1}, respectively) were nearly twice as large as any other PAH V_{max} reported.[185]

The site characteristics and geometry of such an unusual active site metal ion were investigated using

spectroscopic techniques sensitive to the geometry and state of the copper center. EXAFS investigations of the Cu^{2+} and dithionite-generated Cu^{+} *C. violaceum* PAH (because dithionite reacts with O_2, the catalytic characteristics of enzyme reduced in this manner were not reported) show a decrease in the coordination number from ~4 to ~3 upon reduction. By using the pulsed-EPR technique ESEEM, with wild-type *C. violaceum* PAH and two site-directed mutants, histidinyl coordination of the copper was claimed, on the basis of the observation of Cu^{2+} coupling to the remote ^{14}N in coordinated imidazole.[186]

Further confirmation was obtained by the absence of this coupling in the *C. violaceum* PAH proteins lacking either His138 or His143, which were completely inactive but *did* contain tightly bound Cu^{2+}. In one of the mutants the K_d value for Cu^{2+} binding is 5-fold *lower* than wild-type.[187] The authors conclude that these two histidinyl residues ordinarily coordinate Cu^{2+} in this form of PAH,[186] which is consistent with results obtained by mutating the analogous histidinyl residues in mammalian PAH. However, replacement of these two histidines in mammalian PAH with presumably noncoordinating amino acids resulted in the isolation of a protein that was both completely inactive and completely lacked iron.[60] In the copper-PAH case, the presence of the tightly bound metal did not seem to depend upon the availability of its putative ligands, nor did it restore activity to the mutant enzymes. These data indicate that copper does not bind in the normal fashion, assuming the remainder of the protein's structure is insignificantly affected, and that the histidines are essential for activity.

These two observations would be congruent if metal binding is essential for activity, but more recent work from the Benkovic group suggests that this is not true for *C violaceum* PAH.[188] The reinvestigation was prompted in part by the observation that millimolar amounts of DTT stimulated *C. violaceum* PAH activity, rather than inhibiting it, which would be expected because of the strong bonds thiols form with late transition metals. Prolonged DTT treatment resulted in loss of copper from the enzyme, but without a decrease in activity. EDTA and bathocuproine also removed copper from *C. violaceum* PAH,[188] but these compounds inhibit activity, as do phosphate, diethyl dithiocarbamate, *o*-phenanthroline, citrate, and L-dopamine.[189]

"Copper-free" *C. violaceum* PAH, prepared by treatment with DTT followed by gel filtration, contained 1−2% Cu per monomer but retained ≥85% activity (12.2 → 11.6 ± 0.7 U mg^{-1} with DTT present). The assay mixtures contained 9% Cu per monomer. Coupled turnover using $6MPH_4$ and DTT was observed with copper-free *C. violaceum* PAH, with 0.94 ± 0.04 L-Tyr formed per 4a-OH-$6MPH_2$. If the DTT is omitted, the activity of copper-free *C. violaceum* PAH drops to 5.9 U mg^{-1} in Hepes (30 mM, pH 7.4) or 3.4 U mg^{-1} in imidazole (20 mM, pH 7.5) under conditions in which the untreated copper-containing enzyme gives 0.2 and 3.3 U mg^{-1}, respectively. Since imidazole is potentially coordinating, the equality of the treated and untreated *C. violaceum* PAH activities in that buffer suggested to the authors that the lack of activity in a noncoordinating buffer like Hepes resulted from failure to remove *inhibitory* copper from *C. violaceum* PAH. Addition of 0.5 equivalent of Cu^{2+} was sufficient to completely inhibit the activity of copper-free *C. violaceum* PAH, with Zn^{2+} nearly as effective.[188]

The surprisingly low stoichiometry of metal inhibition and the two-fold lower activity in the absence of DTT were both attributed to contamination of their assay mixtures with an "inhibitory metal", perhaps Zn^{2+}, that is presumably retained during the removal of Cu^{2+}. (Atomic absorption shows ~25 mol% Zn present in copper-free *C. violaceum* PAH.) However, DTT is initially unable to relieve inhibition of *C. violaceum* PAH by Zn^{2+}. The authors propose that the relief of Zn^{2+} inhibition during catalytic turnover proceeds by displacement of the Zn^{2+} with Cu^{2+}, followed by the removal of inhibitory Cu^{2+} by DTT to generate an active, metal-free protein. In support of this proposal, the addition of Cu^{2+} to Zn^{2+}-inhibited enzyme is reported to restore "nearly normal" activity. The inhibitory effect of both Cu^{2+} and Zn^{2+} appeared to be more extensive than what would be predicted from the near-micromolar K_d values with copper-free *C. violaceum* PAH determined by fluorescence titration.[188]

(Additional mechanistic work with copper-free *C. violaceum* PAH is described in Section IV.B, where it is most clearly compared with results from the other hydroxylases.)

The evidence for a E·O_2 complex implied from the burst of product formation[183] summarized above would be very difficult to rationalize if *C. violaceum* PAH lacks a redox-active metal cofactor. The presence of 26 mM DTT in the preincubation medium suggests that there was enough of this compound to effect whatever its activating or metal-removing effects are. Carr and Benkovic state that they were unable to directly observe a burst phase using stopped-flow techniques under conditions similar to the previous rapid-quench experiments.[188]

As for the steady-state data, which also indicates E·O_2 complex formation, the authors suggest that some other interpretation may cause the observed burst of product formation. In a metal-free mechanism, activation of O_2 must be carried out within the E·tetrahydropterin or E·L-Phe·tetrahydropterin complexes.[188] Until a mechanism consistent with all of the available data is obtained, it is prudent to withhold judgment in the case of *C. violaceum* PAH and whether it contains a metal cofactor. It is particularly critical to proceed carefully and quantitatively when considering specific activity and V_{max} values, which have the potential to identify the true active component in a particular reaction mixture. An important issue that remains unclear is the maximum specific activity of *C. violaceum* PAH, which will be required to make quantitative activity comparisons between enzyme preparations with and without added metal ions. As for the mammalian PAH enzymes, for which an iron requirement is direct and unambiguous, no structural, functional, or mechanistic inferences should be made on the basis of *C. violaceum* PAH data.

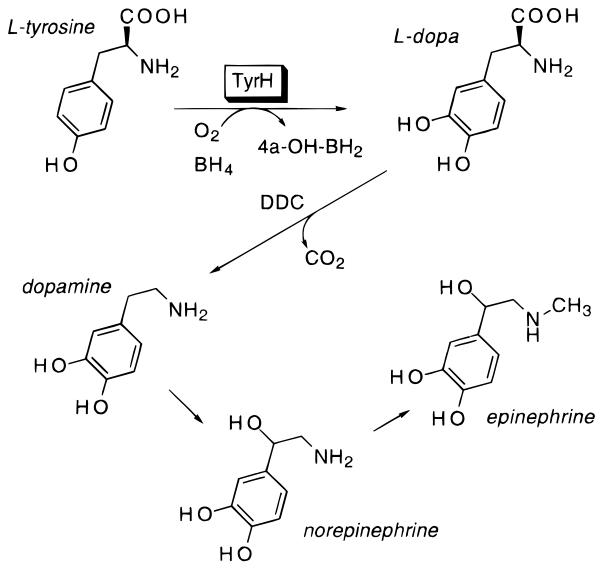

Figure 8. TyrH reaction, leading to catecholamine neurotransmitter formation.

B. Tyrosine Hydroxylase [TyrH, EC 1.14.16.2]

1. Distribution and Physiological Functions

TyrH forms the first dedicated metabolite in the biosynthesis of the catecholamine neurotransmitters (Figure 8), a clear functional distinction from the primarily catabolic PAH. In the central nervous system, TyrH is found in dopaminergic neurons (substantia nigra, ventral tegmentum, hypothalamic arcuate nucleus, superior colliculus, and the olfactory bulb), noradrenergic neurons (locus coerulus and lateral tegmental area), and in the epinephrine-containing neurons of the brainstem.

In the periphery, TyrH is found in sympathetic ganglia but the richest source is adrenal chromaffin cells.[190] The adrenal medulla secretes norepinephrine and epinephrine, which were originally proposed to arise from sequential hydroxylations of L-Phe and L-Tyr by Blaschko.[191] It was from this source that TyrH activity was first directly demonstrated, using as an assay the release of tritiated water from [3,5-^{3}H]tyrosine.[23] A related source of TyrH is from pheochromocytoma (PC12) cells, a cell line derived from a rat adrenal medullary tumor. Up to 10% of total cellular protein can be TyrH in these cells.[192] Even though enzyme from this source has not dominated work in TyrH as rat liver PAH has, many important advances have used this source of protein.

Given that TyrH and TrpH catalyze the rate-limiting steps in neurotransmitter biosyntheses, and therefore affect the normal functioning of brain, a number of investigators have expected linkages between these enzymes and psychological disorders.[193] Parkinson's disease is particularly associated with the degeneration of the dopaminergic nigrostriatial pathway,[194] and presumably TyrH capacity. The primary treatment of Parkinson's disease is by L-Dopa replacement therapy.[195]

On the basis of pharmacological observations of MPTP-treated animals, a role for TyrH function in inherited affective disorders or schizophrenia has been postulated. Microsatellite analyses have led to some positive correlations of TyrH markers with manic-depressive illness[196,197] and schizophrenia.[198] To date, linkage analyses of affected pedigrees have failed to detect a correlation of TyrH markers with manic-depressive illness, schizophrenia, autism, or Gilles de la Tourette's syndrome.[199−202] This is perhaps unsurprising, given the complicated and perhaps multifactorial origins of these disorders. A strong linkage with hereditary progressive dystonia (Segawa's disease, L-Dopa responsive dystonia) has been established for GTP cyclohydrolase I deficiency[203] and very recently with a point mutation in the TyrH catalytic core (Q381K).[16] Since GTP cyclohydrolase is the first step in the biosynthesis of BH_4, both of these linkages may reflect a linkage of the syndrome with TyrH deficiency. Interestingly, Segawa's disease patients treated with L-Dopa suffer few of the side effects associated with replacement therapy in Parkinson's disease, and the efficacy of L-Dopa therapy does not diminish over time.[195]

Several attempts have been made to abrogate TyrH in laboratory animal strains. The most recent attempts show that TyrH is required for viability. In the first system, 90% of homozygous knockout mice died *in utero* unless the pregnant females were treated with L-Dopa. Death was attributed to cardiovascular dysfunction. The newborn animals did not survive unless this treatment was continued.[204]

A second strain of TyrH-knockout mice was developed, in which exons 7 and 8 are disrupted. Most animals homozygous for the knockout allele fail to breathe after birth, but some remain alive for another day. The viable homozygous mutant mice show a marked brachycardia, which may cause death of the animal, but no gross alterations in their major organs. Animals heterozygous for the mutant allele showed an appreciable diminishment in catecholamine levels. Homozygous animals contained nearly no noradrenaline or adrenaline, and ~23% of the dopamine present in the heads of normal controls. Introduction of a human TyrH transgene rescued the phenotype.[205]

Comparable results are obtained with the *Drosophila* mutant *pale*, a null allele of TyrH which is associated with catecholamine deficiency and causes larval death.[175]

2. Molecular Structure, Isoforms, and Expression

Various purification schemes for TyrH are employed, most of which employ an affinity column: 3-iodo-L-tyrosine-linked Sepharose[49] or heparin-Sepharose.[173] The affinity of the regulatory domain of TyrH for polyanions like heparin is a unique feature of this enzyme and may have some bearing on the physiological activation of TyrH by anions (section II.B.3.4).[47] Reported subunit weights of the purified enzyme cluster around 59 kDa, and the enzyme is generally isolated as a homotetramer.[206] Isolation of rat adrenal tyrosine hydroxylase and characterization of its reaction indicated that it shared PAH's absolute requirements for iron, molecular oxygen, and a reduced pterin cofactor.[49] Assays include the tritium-release method,[23] colorimetric determination of catechols,[49] coupled L-Dopa decarboxylation using L-[1-^{14}C]Tyr,[207,208] and direct detection of L-Dopa on HPLC using fluorescence[209,210] or electrochemical detection.[211−213] Rat brain TyrH exists in either a soluble or particulate form, with the

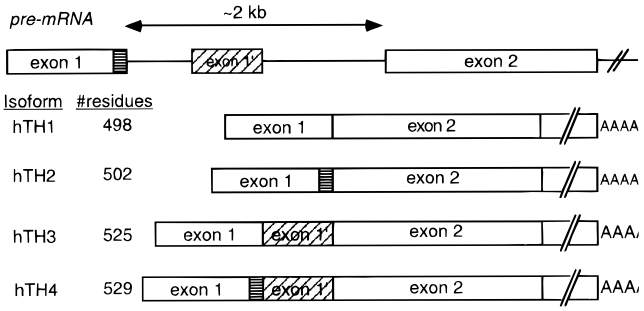

Figure 9. Human TyrH isoforms.

latter form predominant in the synaptosome fraction from catecholamine nerve terminals in midbrain and striatum. In the remainder of the midbrain, where catecholamine cell bodies are abundant, the soluble form is more common.[214]

TyrH is expressed from a single-copy gene, which is spread across 8.5 kb in 13 exons on human chromosome 11p15 (Figure 4).[215] In rat,[216] mouse,[217] and bovine TyrH[218] this gene encodes a single mRNA; in macaque, gorilla, and marmoset two mRNAs (TH1 and TH2) are formed from a single primary transcript;[219,220] in humans four mRNAs arising from alternate splicing events are known (hTH1−hTH4).[221−223] (Although tyrosine hydroxylase is referred to as "TyrH" throughout this review, in order to better distinguish it from TrpH, "TH1" *etc.* is used for the TyrH isoforms in keeping with the literature on this subject.) This occurs as a result of (1) competition between two 3′ splice sites in exon 1, and (2) insertion of another exon (1′) between exons 1 and 2 (Figure 9).[220] hTH1 has the greatest similarity to non-primate TyrH, and can be aligned to rat TyrH with only a single gap, of one amino acid.[222]

While the overall TyrH activity is lower, the *specific* activity of TyrH protein appears to be *increased* in Parkinsonian brain, perhaps in compensation for the damage to the nigrostriatal pathway.[224] The observation of multiple isoforms of TyrH has inspired several groups to determine whether there is any tissue specificity for each isoform. By using S1 nuclease protection experiments, mRNAs encoding hTH1 and hTH2 but not hTH3 were located in human dopaminergic substantia nigra and noradrenergic locus coeruleus;[222] all four isoforms were detected in human pheochromocytoma or adrenal medulla with hTH1 and hTH2 the most abundant.[222,225] Using RT-PCR, all four isoforms can be detected in human adrenal medulla and brain, although mRNAs encoding hTH3 and hTH4 are about an order of magnitude less abundant.[226] These observations have been confirmed by using isoform-specific antibodies to map the TyrH proteins in the adrenal medulla[227] and central nervous system.[228] Lewis *et al.* found that the catecholaminergic neurons of human substantia nigra and locus coeruleus contain all four isoforms of TyrH, with hTH1 and hTH2 predominant. In the caudate nucleus and putamen, all four isoforms are detectable but hTH1 predominates, particularly in the axons and dopaminergic nigrostriatal projections. hTH1 is the only detectable form of TyrH in portions of the tegmentum, including the rostral linear nucleus. Using dual-label colocalization analysis, the authors determined that any neuron containing hTH2, hTH3, or hTH4 also contained hTH1.[228]

The correct tissue specificity of human TyrH expression can be generated in transgenic mice by microinjection of an 11 kb sequence, containing 2.5 kb of 5′ sequence, the entire exon/intron region, and 0.5 kb of 3′ sequence. Primer extension detected both hTH1 and hTH2 transcripts in all regions of the brain examined, indicating that competition for the alternate 3′ splice site of exon 1 occurs in these mice. Mice normally produce a single isoform of TyrH[217] so it appears that the DNA sequence injected is sufficient to generate the observed human molecular heterogeneity. Despite a 50-fold increase in TyrH mRNA levels compared to untransformed controls, only a 3.4-fold increase in TyrH activity was observed, and there was a surprisingly small change in catecholamine content (∼9% increase).[229] Using a modified HSV vector bearing the hTH2 sequence, During *et al.* obtained persistent striatal TyrH expression in Parkinsonian rats, correlated with biochemical and behavioral recovery. The number of immunoreactive cells (mostly striatal cells) varied between animals but did not seem to correlate with the degree of behavioral recovery. While extracellular dopamine levels were elevated only 20%, the apparent TyrH activity was 60% higher in treated rats.[230]

Tissue-specific expression of TyrH in rat adrenal medulla chromaffin cells was examined using a CAT-reporter construct in PC8b cells (a subclone of the PC12 pheochromocytoma cell line). Cell-specific activation requires a sequence between −212 and −187 (relative to the start site) that contains an AP-1 recognition site. Without this sequence, CAT levels drop 90%.[190] This site, TGATTCA, differs from the AP-1 consensus sequence by a single nucleotide (the central C is a T). By using the gel mobility shift assay, specific binding of nuclear extracts from PC12 cells treated with the PKC-activating phorbol ester TPA to this sequence was demonstrated. This pathway may mediate the trans-synaptic induction of TyrH, which can be studied using the tranquilizer/vesicle storage inhibitor reserpine. In adrenal medulla cells, TyrH and c-*fos* mRNA appear in tandem following reserpine treatment, and a protein−DNA complex is detected by gel-shift assays. These results are consistent with regulation of TyrH expression by the AP-1 site.[231] Many other studies of tissue-specific expression and transcriptional activation have appeared, a subject outside the primary focus of this review.

At the molecular level, heterogeneity has been a particular problem in the study of TyrH. Even in the case of rat PC12 TyrH, which is generated from a single mRNA species, there are varying levels of phosphate and multiple phosphorylation sites.[227,232,233] Phosphorylation at various sites may have important regulatory roles[234] and is the subject of section II.B.3.2. The alternate splicing events that occur in primate TyrH result in changes of kinase specificity of the N-terminus of TyrH,[235] further complicating analysis of enzyme obtained from those sources. In either case, studies of TyrH phosphorylation performed prior to the recognition of multiple phosphorylation sites require careful reconsideration, as a result of this heterogeneity.

Table 5. TyrH Kinetic Parameters

Source	phos[a]	$K_{m,Tyr}$ (μM)[b]	K_{m,BH_4} (μM)	$K_{m,6MPH_4}$ (μM)	spec act (U mg^{-1})[c]	pH optimum
human TH1	no	37 (BH_4)	95		1.3	7.0
	yes		52 (50 μM tyr)		1.2	
human TH2[235]	no	17 (BH_4)	73		0.62	7.0
	yes		48 (50 μM tyr)		0.62	
full-length rat TyrH[243]	no	11 (100 μM BH_4)	60 (pH 6.0)		1.0 (pH 6.0)	6.3−7.0
			50 (pH 7.2)		0.9 (pH 7.2)	
	yes		40 (pH 6.0)		0.9 (pH 6.0)	7.5
			20 (pH 7.2)		1.0 (pH 7.2)	
full-length rat TyrH[244]	no	9 (BH_4)	17 (35 μM tyr)	41 (100 μM tyr)	1.8 (BH_4)	7 (br)[e]
		41 ($6MPH_4$)			3.6 ($6MPH_4$)	
	yes		8 (20 μM tyr)		2.0 (BH_4)	
C-term. domain rat TyrH[251]	n/a[f]	8.1 (BH_4)	7 (35 μM tyr)	21 (100 μM tyr)	3.9 ($6MPH_4$)	
		25 ($6MPH_4$)				

[a] Phosphorylated by cAMP-dependent protein kinase (PKA). [b] Unless indicated, at 0.5 mM tetrahydropterin. [c] One unit = 1 μmol 3,4-dihydroxyphenylalanine formed per min. Human TyrH determined at 0.2 mM BH_4. For rat TyrH, Wang *et al.* use 0.1 mM BH_4; Daubner *et al.* use 0.5 BH_4 or $6MPH_4$. [d] Reported in ref 251. [e] Determined for baculovirus-expressed enzyme by the same group.[245] [f] This construct lacks the amino-terminal phosphorylation sites and is not a substrate for cAMP-dependent protein kinase.

Recombinant sources of TyrH appear to afford the best chance of improving knowledge of that enzyme, which lags behind what is known about PAH. Any one of the human isoforms may be heterologously expressed in eukaryotic cells,[236−239] but in order to start with phosphate-free enzyme, *E. coli* expression appears to be preferred.[235,240,241] This is also the case for the single allelic form of the heavily studied rat PC12 TyrH,[242−244] which is known to be partially phosphorylated by heterologous expression in baculovirus.[244,245]

Rat PC12 TyrH, as was alluded to above, has been the most important source of this enzyme. This source of TyrH is purified from a catecholamine-rich tissue, and in some situations appears to copurify with a catecholamine, yielding a blue-green color from the Fe^{3+}−catechol complex.[164,246] This appears to be due to breakage of the catecholamine-containing secretory vesicles during tissue disruption. Others have observed colorless enzyme,[245] indicating that there is no iron-bound catecholamine, which can be easily understood if the TyrH-bound iron remains Fe^{2+} or if the enzyme's iron content is low. Since this feedback mode of regulation may be physiologically significant, it is discussed in section II.B.3.5.

The first recombinant sources of PC12 TyrH were expressed in eukaryotic cells, which allowed a demonstration that characteristic inhibitors lowered TyrH activity in cell homogenates,[236] determination of some kinetic constants,[242] and purification of highly active recombinant enzyme.[245] Fitzpatrick has carefully characterized the homogeneous TyrH from this source, which has resulted in the determination of its steady-state kinetic mechanism.[184,247] Several reports of overexpression of active, soluble TyrH in *E. coli* have appeared[243,244,248] and all are in harmony as to the general characteristics of the recombinant enzyme (Table 5). No profound changes in kinetic characteristics appear to result from phosphorylation (section II.B.3.2), which was unexpected from the older literature on this subject.[5,249]

Separate expression of each of the human TyrH isoforms in COS cells[239] or *Xenopus* oocytes[238] showed differences in the crude lysate TyrH activities, with hTH1 the most active and the other three isoforms ranging from 26 to 59% as active. Presumably phosphate-free[244] enzyme was purified from *E. coli* expression of each isoform, confirming that there are functional differences among the isoforms.[235,240,241] TyrH is often assayed in the presence of added Fe^{2+}, because the activity is higher when iron is added.[250] In support of the idea that the enzyme appears to lose this required metal cofactor easily, purified recombinant TyrH is nearly iron-free, when expressed either in *E. coli*[241] or baculovirus.[245]

Haavik and co-workers investigated the metal affinity of *E. coli*-expressed isoforms hTH1, hTH2, and hTH4, using $^{59}Fe^{2+}$ and $^{65}Zn^{2+}$.[241] For both metals, the K_d at pH 6.5 is about four times higher for hTH2 than for hTH1 and hTH4 (about 1 μM for Fe^{2+}, 0.3 μM for Zn^{2+} with ~1 binding site subunit^{-1}). The V_{max} for hTH2 is about half that of either hTH1 or hTH4 (with added Fe^{2+} at pH 6.0 and 30 °C, using $6MPH_4$ as cofactor). The basal activity, which probably arises from the 4−10% residual iron, was about the same for all three (0.013 U mg^{-1}), yielding a ratio of plus Fe/minus Fe activity of 31 for hTH1/hTH4 and 13 for hTH2.[241] The same 2-fold difference in V_{max} was observed in a comparison of hTH1 and hTH2 using BH_4 as cofactor.[235]

In contrast, Nasrin *et al.* report that the addition of Fe^{2+} to assay mixtures does not increase the activity of purified recombinant isoforms hTH1−4. The authors do not report the iron content of their purified enzyme, stating instead that the 0.1 mM $Fe(NH_4)_4(SO_4)_2$ added to the bacterial growth medium should be adequate to load the enzyme with iron.[240] The validity of this assumption may be called into question by their reported velocities, determined without added Fe^{2+}, which are 10−30 times lower (at pH 7.0 and 37 °C) than iron-treated recombinant hTH1[235,241] or recombinant rat PC12 enzyme.[244,245] With this caveat, the authors found $K_{m,app} \approx 8$ μM for L-Tyr (1 mM BH_4) and 0.1 mM for $6MPH_4$ (200 μM L-Tyr) for all four isoforms. ((6*R*)-BH_4, but not $6MPH_4$ or (6*S*)-BH_4, is observed to give biphasic Lineweaver−Burk plots with TyrH in their laboratory.[240]) In summary, for the two most prevalent human isoforms of TyrH, hTH1 and hTH2, it appears there may be a 2-fold difference in intrinsic catalytic activity (Table 5). This is somewhat surprising, given the location of this four amino acid insertion outside the catalytic core conserved among the pterin-dependent hydroxylases.[252]

Recently a study of the thermal denaturation of TyrH was reported, in which the denaturation of TyrH was examined using CD; the PC12 enzyme did not give clear or reversible melting transitions. However, the progress of the melting at 55 °C and pH 6.2 was biphasic. In the first transition, little of the enzyme activity was lost. At longer times, loss of the CD signal was correlated with appreciable inactivation. Only the second transition was observed at pH 7.2, and it had a half-life twice as long (64 min), indicating a gain in stability. Additional stability was also noted with the unphosphorylated form of the enzyme (section II.B.3.2) and at lower phosphate buffer concentrations.[253]

The catalytic core of TyrH can be separated from the N-terminus by limited trypsin proteolysis, yielding a more active, 34 kDa C-terminal fragment.[254−259] In addition, once the genes for each of the hydroxylases were found, it became clear that the trypsin site (at position 158)[259] fell near the start of the region of highest homology among the enzymes.[252] Introducing the appropriate alterations in their prokaryotic expression system, Daubner and co-workers separately expressed the N-terminal regulatory domain (158 amino acids) and the C-terminal catalytic domain (343 amino acids, lacking the first 155) of TyrH. As expected, the N-terminal domain could be purified by virtue of its affinity for heparin-Sepharose and was completely inactive. It was phosphorylated at the same rate, and to nearly the same extent, as full-length protein. The purified C-terminal, catalytic domain forms a tetramer (161 kDa), unlike the monomeric calpain-treated TyrH[260] or dimeric chymotrypsin-treated PAH,[77] and had high specific activity (2.04 U mg^{-1}, comparable to 1.43 U mg^{-1} for the full-length protein). As Table 5 shows, the C-terminal domain has slightly more favorable kinetic parameters than the full-length protein, showing that nothing essential for TyrH folding or catalysis is present in the first 155 amino acids of its sequence.[251]

Tryptic digestion of this catalytic construct caused the loss of 5 N-terminal amino acids (corresponding to a removal of TyrH amino acids 1−160), and 20 C-terminal residues, converting the tetramer of 39.2 kDa subunits to a 37 kDa monomer. This monomer has slightly smaller K_m values for its substrates and retains a quarter of the catalytic domain's activity.[261] The C-terminal deletion removes a "leucine zipper" sequence that is found in all of the pterin-dependent hydroxylases,[262] which the authors concluded is required for the formation of tetrameric TyrH.[261]

In another study, removal of the first 175 or 200 amino acids yields an inactive protein. N-terminal deletion of up to 165 amino acids yielded TyrH of equal or even higher activity (85−150% relative to full-length). C-terminal deletion of 19 amino acids from the full-length TyrH (CΔ19) causes a 70% decrease in activity,[248] in good agreement with the previously discussed result of C-terminus removal from the isolated catalytic domain. The mutant L480A, which interrupts this leucine heptad repeat, seems to cause a ~20% decrease in homogenate TyrH activity. Both the L480A and CΔ19 forms appear to give rise to multiple lower molecular weight species of TyrH, especially dimers, as determined by Western-blot detection of nondenaturing gels or activity-detected gel filtration of homogenates.[263]

Further mapping of functional regions of TyrH by genetic manipulations has allowed a reexamination of the conclusions of biochemical mapping studies of TyrH and PAH. On the basis of the observation that a photoaffinity label resembling the tetrahydropterin cofactor for PAH identified Lys194 (and Lys198) as being near to or part of this binding site,[93] the analogous Lys241 in the catalytic core of TyrH was changed to Ala. None of the kinetic constants were altered, showing that this residue is probably not involved in TyrH pterin binding.[97] From limited trypsin digestions,[258,259] a region of the N-terminal regulatory domain was associated with the ability to bind heparin, which is exploited in the standard heparin-Sepharose affinity purification of TyrH. N-terminal deletions of 32 or 68 residues bind heparin, proteins lacking the first 88 or 128 amino acids do not bind heparin, and a deletion of 76 residues gives an intermediate result. For the heparin-binding proteins, little change in kinetic parameters is observed. In addition, the constructs that do not bind heparin appeared to have a reduced solubility that requires reduced-temperature induction in *E. coli*.[264]

3. Regulation

TyrH is regulated in neural tissues at several levels, which in broad terms can be grouped into acute regulation and long-term regulation.[265] Long-term regulation will not be considered in this review, but it may underlie some of the more interesting physiological and psychological issues in the study of brain TyrH. This includes the induction of TyrH expression during development, which is especially interesting because the TyrH is expressed in sympathetically innervated tissues derived from both neural tube and neural crest.[266]

Acute regulation of the properties of TyrH activity occurs as the result of neural activity, which might include "direct" as well as second messenger-mediated responses.[234] The most intensely studied of these modes of regulation has been phosphorylation,[5,267] which has grown into a rich subfield of its own. An overview of this area is presented, placing special emphasis on characteristic *in situ* observations and the newest results with recombinant TyrH. Some of this recent evidence indicates that the stimulatory effects of at least one kind of TyrH phosphorylation may rely upon the diminishment of product feedback inhibition.

3.1. Neural Activity and Its Immediate Effects. Stimulation of catecholamine biosynthesis from radiolabeled L-Tyr (but not L-Dopa) following electrical stimulation was first demonstrated in the sympathetic nerves of vas deferens and heart.[268,269] A direct connection between TyrH activity and neural activity came from a study by Morgenroth *et al.* in which the electrical stimulation of sympathetic neurons in guinea pig vas deferens caused a stable increase in TyrH activity. Ca^{2+} was absolutely required for the electrical stimulation effect, which could be replicated *in situ* by the addition of 10 μM Ca^{2+} to unstimulated tissue.[270] These authors also noted that depolarization by K^+ could enhance the activity of TyrH in cells, an observation that has since been repeated in other TyrH-containing tissues.[234]

In addition, several types of non-catecholamine transmitters have been shown to cause upregulation of catecholamine formation *in situ*; apparently, all four well-known second-messenger systems (cAMP, Ca^{2+}, diacylglycerol, and cGMP) are partly involved in this process.[234] A common thread that can be extracted from this controversial area is that most or all of the acute regulatory effects are likely to be mediated by covalent modification of existing TyrH protein.[249] This is generally taken to mean phosphorylation, since enhancement of TyrH activity by calpain[257] or other proteases is not known to have a physiological role. In a like manner, the noncovalent interactions of TyrH with phospholipids[271] and polyanions[47] have *in vitro* stimulatory effects not known to be exploited *in vivo*.[249]

3.2. Phosphorylation. 3.2.1. Second-Messenger-Mediated, Site-Specific Phosphorylation. Stimulation of TyrH activity analogous to that obtained with electrical stimulation was observed following treatment with cAMP, leading to speculation that increased TyrH phosphorylation could be the source of activation.[272] Phosphorylation *in situ* was demonstrated by [^{32}P]phosphate incorporation into the TyrH of cultured superior cervical ganglia cells.[273,274] The phosphorylation of homogeneous PC12 TyrH by cAMP-PK was concomitant with activation mediated by an apparent conversion to a lower $K_{m,6MPH4}$ form of the enzyme.[275] An integrated study showed coordinated phosphate incorporation, catecholamine production, and TyrH stimulation following treatment of chromaffin cells with 8-bromo-cAMP and [^{32}P]phosphate.[276]

At about the same time it was recognized that at least two phosphorylation sites were present on TyrH isolated from [^{32}P]phosphate-containing cultures of bovine chromaffin cells, either untreated or treated with either 8-bromo-cAMP or ACh (the natural secretagogue). The relative amount of two tryptic phosphopeptides separable on 2D gels was different in treated cells, with 8-bromo-cAMP increasing the amount of only one phosphopeptide and ACh increasing both. Addition of the calcium antagonists EGTA or $MnCl_2$ to ACh-treated cells decreases [^{32}P]phosphate incorporation into both phosphopeptides to a similar extent.[233] Detailed mapping of the phosphoprotein sequences, in comparison with cDNA sequences, showed that there were four phosphorylation sites present in pheochromocytoma/PC12 TyrH: Ser8, Ser19, Ser31, and Ser40.[232,277,278] A secondary *in vitro* cAMP-PK phosphorylation site at Ser153 in rat PC12 cells[232] is not observed *in situ*,[278] nor is the kinase recognition site conserved among other TyrH sequences, as are the four N-terminal kinase sites.[279]

Ser40 is a canonical cAMP-PK phosphorylation site and is phosphorylated *in vitro* by cAMP-PK,[275,280,281] CaM-PK II,[282,283] cGMP-PK,[284] and Ca^{2+}/phospholipid-dependent PK (PKC).[285,286] CaM-PK primarily phosphorylates Ser19.[285] If the activation of the enzyme *in situ* is mediated by phosphorylation, these results can account for the correlation of increased TyrH activity with increased TyrH phosphorylation following treatment by cAMP, Ca^{2+}, or agents that have analogous effects. Neither of the other two phosphorylation sites falls in a recognition site for a "classical" protein kinase.

NGF and protein phosphatase inhibitors enhance Ser8 phosphorylation. Even though phorbol esters and NGF increase Ser31 phosphorylation, *in vitro* this position is not a substrate for PKC.[278,287,288] An endogenous proline-directed S/T protein kinase (E-PK) copurifies with TyrH, from which it can be separated by high-salt sucrose gradient centrifugation. E-PK phosphorylates Ser8 exclusively, recognizing sequences that contain *X*-Ser/Thr-Pro-*X*. This kinase is induced by NGF treatment of [^{32}P]phosphate-labeled PC12 suspensions.[277] However, the physiological importance of this system is not completely defined: E-PK levels are quite low in chromaffin cells and neurons and its phosphorylation of Ser8 is not known to surpass 0.25 phosphate/TyrH subunit. The E-PK site is also found at Ser31, which is not a substrate for the kinase in intact TyrH [although a peptide derived from this sequence is a substrate (P. R. Vulliet, result quoted in ref 278)], indicating that other, unrecognized kinase-specificity determinants may exist. The kinases responsible for PC12 TyrH Ser31 phosphorylation *in situ* appear to be ERK1 and ERK2, which do not phosphorylate any of the other N-terminal serines.[289]

Most of the preceding information was determined using bovine or rat adrenal TyrH, neither of which has the isoform complexity of human TyrH. TyrH from human tissues is known to be phosphorylated by cAMP-PK II and CaM-PK, although whether or not this correlates with enzyme activation in crude lysates is uncertain.[290,291]

The insertion of four amino acids between Met30 and Ser31 in hTH2 (and hTH4) introduces a new recognition site for CaM-PK.[222] Using homogeneous, *E. coli*-expressed sources of these isoforms, Le Bourdellès *et al.* demonstrated one cAMP-PK phosphorylation site per subunit for both hTH1 and hTH2, each of which yielded a peptide containing phosphorylated Ser40. [The insertion of amino acids does not change the numbering of the sequences common to all four isoforms (*i.e.*, Ser44 in hTH2 is called Ser40 for consistency's sake).] About twice as much [^{32}P]-phosphate was incorporated into hTH2 as hTH1 by CaM-PK II, consistent with phosphopeptide sequences, indicating phosphorylation at Ser19 in addition to Ser31 and Ser40.[235]

Even though it seems quite likely, it would be intriguing to know if human hTH1 is also a substrate for ERK1/ERK2. If this is the case, and if ERK1/ERK2 no longer recognize Ser31 in hTH2, it would imply that the small insertion in hTH2 causes a switch in kinase specificity. In PC12 cell cultures, ERK activity (measured with the known ERK substrate myelin basic protein[292]) and the ERK-dependent phosphorylation of Ser31 is activated by NGF, bradykinin, and various other treatments. In Swiss 3T3 cells, a fibroblast-derived cell line, EGF stimulated ERK activity. Purified ERK1 phosphorylated only Ser31, up to 0.5−0.6 [^{32}P]phosphate subunit^{-1}, but caused only a modest increase in the activity of purified TyrH.[289]

The multiple-site phosphorylation of TyrH by CaM-PK II has also been studied extensively. An unusual observation was that the kinetic activation of TyrH

following CaM-PK II treatment depends upon the presence of an "activator protein" present in micromolar concentrations in nerve cells.[282,293] Activator protein is not required for TyrH phosphorylation, nor does it have any effect on the activation of TyrH by cAMP-PK phosphorylation.[294] Interestingly, the same effects are observed with CaM-PK II-dependent phosphorylation of TrpH.[295]

Homogeneous activator protein is a member of the 14-3-3 class of brain proteins, and consists of a mixture of homologous subunits; the cloned η subunit is able to stimulate the activity of phosphorylated TrpH.[296] The mechanism for activation is unknown, but may involve direct complexation of phosphorylated TyrH by activator protein.[267]

Evidence has accumulated that the activating effects of TyrH phosphorylation are fully expressed in the absence of activator protein, which tends to discount the requirement for activator protein in TyrH function. The authors' suggestion is that activator protein may function as a means for preventing dephosphorylation of TyrH.[297]

In summary, the multiple-site phosphorylation of TyrH, which itself may be present in multiple isoforms, has become a quite complex issue. Little is known about the functional effects of phosphorylation at a single site in a single isoform, which makes it imprudent to generalize too extensively about the role of TyrH phosphorylation. One exception to this is phosphorylation of Ser40 in the monoallelic rat TyrH enzymes from brain and adrenal medulla. We turn now to this ostensibly simpler issue.

3.2.2. Phosphorylation at Ser40. Linkage *in vitro* of increased phosphorylation with perturbations in the kinetic behavior of TyrH has been easiest for cAMP-PK phosphorylation, which only phosphorylates one site in rat, bovine, and human TyrH. The activating effect of exposure of tissues or lysates to "cAMP-dependent phosphorylating conditions" (cAMP, theophylline, $MgCl_2$, ATP, EGTA, and NaF)[298,299] or purified preparations to continuous cAMP-PK activity,[275] is generally thought to be due to primarily a lowering of TyrH's K_m for BH_4 (or $6MPH_4$).[5,267,300] Some confusion over this issue may have to do with the pH of TyrH assay conditions,[5,249] which can cause large changes in K_m and V_{max} values between neutrality and pH 6.0,[301] the optimum originally reported for TyrH.[23] Assays at neutral pH and using BH_4 are now standard for determining the effects of cAMP-PK phosphorylation, and the likely physiological effects of Ser40 phosphorylation have been recognized to be less dramatic than was reported in the older literature.

Another puzzle with TyrH phosphorylation concerns the different results obtained with Ser40 phosphorylation by PKC and cAMP-PK. No apparent activation of TyrH followed PKC-dependent phosphorylation of this residue, [279,286] in contrast to the effects of cAMP-dependent phosphorylation discussed above. Both CaM-PK II and PKC phosphorylated Ser40 to the extent of 0.43 [^{32}P]phosphate subunit^{-1}, while cAMP-PK phosphorylation reached 0.78 [^{32}P]-phosphate subunit^{-1}.[302] The primary CaM-PK II phosphorylation site at Ser19 reached 0.76 [^{32}P]-phosphate subunit^{-1} in the same experiment. Even though the phosphate content of purified rat PC12 TyrH was observed to increase, only cAMP-PK addition was able to stimulate activity. The authors suggest that activation may depend upon phosphorylation, on average, of more than two subunits per tetramer. However, they obtain a linear relationship (in a narrow range best defined at 0.5 ± 0.1 phosphate per subunit) between cAMP-PK phosphorylation and enzyme activation, which rules out all-or-nothing mechanisms, *i.e.* that increased TyrH activity absolutely depends upon phosphorylation at a third or fourth site per tetramer. The linear relationship implies that activation by phosphorylation is direct and *not* cooperative. Paradoxically, the authors regard this linear relationship as evidence *supporting* cooperative interactions among all subunits undergoing cAMP-PK-dependent phosphorylation.[302]

Good evidence for a cooperative dependence of TyrH activity on phosphate content was obtained as part of the study of phosphatase activity, showing the steepest activity increase between 0.5 and 0.75 phosphate subunit^{-1}.[303] The lability of TyrH-bound phosphate in cell extracts is readily demonstrated and is the subject of the following section. Many groups assay the effect of phosphorylation under continuous exposure to phosphorylating conditions, even in purified protein samples. Exposure of minimally purified bovine striatal TyrH to increasing amounts of protein kinase under phosphorylating conditions yields a hyperbolic response of TyrH activity *vs* cAMP-PK units per mg of TyrH.[209] One might expect that if there is a direct interaction between cAMP-PK and TyrH, some of the effects mentioned in the previous paragraph might be rationalized.

As was mentioned above, the most prominent kinetic effect of phosphorylation is a lowering of the K_m value of BH_4 in homogenates. The origins of this effect were probed using a series of synthetic tetrahydropterins differing in structure at the 6-position as cofactors for minimally purified bovine striatal TyrH.[209] A large increase in V_{max}/K_m following phosphorylation was seen for all of the cofactors examined, ranging from 1700-fold ((6*R*)-BH_4) and 2000-fold (6-ethyl-PH_4) to 50-fold ($6MPH_4$), which bracketed increases with 6-hydroxymethyl-, 6-methoxymethyl-, 6-phenyl-, and 6-cyclohexyl-PH_4. With 6,6-disubstituted tetrahydropterins, the range was ~290 to 35 (6-benzyl-6-methyl-PH_4 and 6,6-dimethyl-PH_4, respectively). This effect was predominantly on K_m, which was $\geq$0.3 mM for all cofactors with unphosphorylated enzyme, and ranged from 0.8 to 14 μM (6-cyclohexyl-PH_4 and 6-benzyl-6-methyl-PH_4, respectively) for phosphorylated TyrH. V_{max} effects were inconsistent among the compounds, showing increases as well as decreases.[209] (Unlike PAH, only 7-substituted pterins have so far been shown to give uncoupled turnover with TyrH.[49])

In addition, the presence of at least one side-chain hydroxyl group was required (with either unphosphorylated or phosphorylated TyrH) in order to observe substrate inhibition caused by >80 μM L-Tyr. The authors conclude that the evidence indicates phosphorylation does not simply cause the removal of an obstructing group from the active site, but has a positive effect on the specificity of the PAH-cofactor interaction. Both the hydrophobic backbone and hydroxyl groups are recognized in the phosphoryla-

tion-induced rearrangement of the pterin binding pocket.[209]

The availability of cloned sources of various TyrH has began to resolve some of the confusion regarding TyrH phosphorylation. When expressed in eukaryotic cells, TyrH is at least partially phosphorylated.[245] Replacement of Ser40 with Tyr or Leu converted rat TyrH expressed in AtT-20 (pituitary tumor) cells to a fully active form unaffected by the addition of cAMP/ATP/cAMP-PK to TyrH-containing cell homogenates. In addition, at pH 7.2 in homogenates the Leu mutant has a 10-fold higher V_{max} than wild-type and a 7-fold smaller $K_{m,6MPH4}$.[242]

As is shown in Table 5, purified recombinant proteins show no changes in kinetic constants sufficient to account for a large phosphate-dependent activation. The activation appears to be limited to a halving of the K_m for tetrahydropterin in rat PC12 TyrH[243,244] or two isoforms of human TyrH.[235] In the same investigators' hands, 10−12-fold activation could be demonstrated following phosphorylation of crude bovine adrenal TyrH.[244] This is not an indication that there is some kind of difference between the native and recombinant source of TyrH, but is consistent with removal of an inhibitory entity, perhaps a catecholamine, during purification (section II.B.3.5).

A S40A mutant studied in highly purified protein shows no changes in the kinetic constants, except for a small but significant lowering of the K_m values for BH_4 and $6MPH_4$.[244] This initially surprising observation indicates that phosphorylation removes an inhibitory interaction due wholly or in part to Ser40 itself, a small addition to the standard model of TyrH activation by phosphorylation: release of N-terminal inhibition of the active site, caused by the introduction of a favorable phosphoserine interaction elsewhere.[209]

Replacement of Ser8, Ser19, and Ser31 with the unphosphorylatable Leu caused neither stimulation or inhibition of AtT-20-expressed TyrH. The S31L mutant could be partially stimulated in homogenates by cAMP-PK treatment.[242] Phosphorylation at Ser40 is still the only phenomenon known to cause direct, stimulatory effects on TyrH *in vitro* and *in situ*.[244]

It might appear from the studies of highly purified TyrH that the kinetic results are unable to explain the large apparent stimulation by phosphorylation, which would therefore not be the reason for the manifold activation of TyrH in catecholamine-producing cells. However, as will be discussed below, the phosphorylation of Ser40 appears to affect the ability of dopamine to inhibit TyrH.[235,244,304−306] This phenomenon, combined with the enhancement of K_m and V_{max}, may be the key to the observed large activation of TyrH by phosphorylation.[307]

3.3. Dephosphorylation. While PAH can rely on regulation by allosteric relaxation, this mechanism is not available to TyrH. Short-term regulation of TyrH would require that it be colocalized with a phosphatase activity capable of rapidly dephosphorylating the activated enzyme. Such a phosphatase activity was demonstrated by gel filtration of cAMP- and Mg^{2+}-treated bovine adrenal medulla cytosol, which removed ATP and cAMP. Within 15 min, only 20% of the starting [^{32}P]phosphate-labeled TyrH could be immunoprecipitated. Complete rephosphorylation could be achieved following the addition of ATP, cAMP, NaF, and theophylline in phosphate buffer. Complete inhibition of the phosphatase was achieved with 20 mM phosphate and 5 mM NaF.[308]

The phosphatase activity present in rat caudate nucleus could be fractionated into a Ca^{2+}-independent peak, and two minor peaks that are inhibited by Ca^{2+}. The major fraction showed a large BH_4-stimulated increase in phosphatase V_{max} (0.78 → 6.25 fmol min^{-1} mg^{-1} upon going from 0 to 30 μM BH_4) and a small increase in K_m (0.05 → 0.08 nM). The maximal effect was seen at 5−10 μM BH_4. Other stimulatory pterins included $6MPH_4$, tetrahydro-D-neopterin, and 5-methyltetrahydrofolate. GTP, the metabolic precursor of BH_4, was a strong inhibitor of TyrH phosphatase, with ATP, L-sepiapterin, and 7,8-dihydro-L-biopterin sequentially less effective inhibitors.

The "cross-reactivity" of folate is quite unusual for BH_4-responsive systems and is construed by the authors to indicate that activation is caused by a tetrahydropterin−phosphatase interaction rather than one with the hydroxylase.[309] The slight difference in phosphatase activity found between samples diluted to 1 and 10 μM BH_4 predicts that such a complex should be quite stable. However, since the "on" rate for appearance of the stimulatory effect is also slow (<1% phosphatase activation per minute of a 10 μM BH_4 incubation), there is a requirement for an exceptionally small dissociation rate of such a complex, assuming that BH_4-phosphatase complex formation directly causes activation. There is currently no data to support these assertions.

Functional classification of the TyrH phosphatases present in bovine adrenal cytosol and rabbit corpus striatum indicated that type 2A and 2C phosphatases[310] comprise 90 and 10%, respectively, of the total phosphatase activity. Similar results were obtained using TyrH phosphorylated with either cAMP-PK or CaM-PK II. In contrast to the previous study, BH_4 had no effect on the activity. Incubation of chromaffin cells with 1 μM okadaic acid, a powerful inhibitor of type 2A phosphatases, tripled the phosphate content of TyrH, indicating the importance of dephosphorylation *in situ*.[311]

This effect of okadaic acid was confirmed in a study of [^{32}P]phosphate-labeled rat striatal cells, in which the amount of TyrH-associated phosphate doubled following treatment (to ~0.5 [^{32}P]phosphate subunit^{-1}). A similar increase in TyrH phosphate content was observed by treatment of the synaptosomes with dibutyryl-cAMP/3-isobutyl-1-methylxanthine (db-cAMP/IBMX). The effects of db-cAMP/IBMX could be partially blocked by the inclusion of 0.2 mM BH_4 in the culture medium, resulting in 0.25 [^{32}P]-phosphate subunit^{-1}, about the same as untreated cells. Sepiapterin was a weak phosphatase activator if an inhibitor of sepiapterin reductase was also included in the medium, blocking conversion to BH_4. The very high levels of BH_4 treatment required (half-maximal effect at 0.1 mM) are rationalized in terms of inefficient BH_4 uptake (~0.1%). In accord with this idea, the low cellular [BH_4] was determined after 30 min incubations and found to have a linear dependence on the applied [BH_4].[312]

Table 6. Iron−Catechol Formation Constants (log *K*) at 25 °C[318]

reaction	Fe^{2+} ($\mu = 1.0$)[a]	Fe^{3+} ($\mu = 0.1$)
$Fe^{n+} + 1\ cat^{2-} = Fe(cat)^{0/+}$	7.95	20.0
$Fe^{n+} + 2\ cat^{2-} = Fe(cat)_2^{2-/-}$	13.5	34.7
$Fe^{n+} + 3\ cat^{2-} = Fe^{n+}(cat)_3^{4-/3-}$		43.8
$Fe^{n+} + cat = Fe(cat)^{0/+} + 2H^+$	−14.3 ($\mu = 0.1$)	−2.2
	−14.33	−1.36 ($\mu = 1.0$)[319]
Fe^{n+} + adrenaline = Fe^{n+}(adrenaline)$^{0/+}$ + $2H^+$		−1.16 ($\mu = 1.0$)[319]
Fe^{n+} + L-Dopa = Fe^{n+}(L-Dopa)$^{0/+}$ + $2H^+$		−1.29 ($\mu = 1.0$)[319]

[a] μ = ionic strength.

3.4. Other Activators. As was discussed above, N-terminal trypsin proteolysis of TyrH at residue 158 (or the equivalent genetic manipulation) leads to stimulation of activity.[259,313] The Ca^{2+}-activated protease calpain (also present in bovine adrenal medulla) cleaves bovine TyrH after Asp23 and Met30, causing a 20% increase in activity and dissociation of the tetramer. Like the combined genetic and tryptic removal of much more N-terminal sequence and the leucine zipper-containing C-terminus from rat TyrH,[261] calpain-treated bovine TyrH is reported to be a monomer by gel-filtration chromatography.[260] However, the more extensively modified TyrH has only ~30% activity of the full length protein.[244,261] A truncated rat TyrH lacking the final 19 amino acids shows 25% activity, which suggests that the inactivation is due to the loss of some structural feature of the C-terminus, possibly the leucine zipper.[263]

These results also imply that there is nothing essential for catalysis present in the first 165 amino acids,[248] which appears to exert a small negative regulatory effect on K_m for tetrahydropterins.[251] This effect is insignificant compared to the dramatic chymotryptic activation of PAH, consistent with the allosteric behavior of the catabolic PAH.[102] Regulation of neither enzyme is known to include a physiological role for any protease.[314]

Activation by the mucopolysaccharide heparin was first reported in TyrH preparations from dog hypothalamus[315] and has a greater stimulatory effect on the soluble form of rat brain TyrH than the membrane-associated particulate form. In a study using partially fractionated TyrH, the addition of heparin to the soluble form of TyrH converted it to a form with the same kinetic parameters as the particulate form, manifested as a 2-fold higher V_{max} and a reduced K_m for $DMPH_4$ (0.74 → 0.15 mM). In addition, both the heparin-treated soluble and particulate forms have a lower susceptibility to dopamine inhibition. This led the authors to suggest that the similarities might have a common origin in membrane-dependent activation of TyrH.[214]

Binding of TyrH to heparin is useful as an affinity step in the purification of TyrH[316] and appears to be due to specific interaction with the N-terminus.[251] Other charged activators of brain TyrH have been identified: phosphatidyl-L-serine, polyacrylic acid, polyvinyl sulfuric acid, poly-L-glutamic acid,[47] and phosphatidylinositol.[316] The last compound was also found to be an inhibitor of TyrH which gained potency as the enzyme was more extensively purified, attributed to loss of a "protective factor", probably a divalent cation.[316] Due to the lack of specificity among the polyanions, these activating effects have been attributed to electrostatic activation of TyrH. In accord with this, the addition of monovalent salts has a stimulatory effect on TyrH activity, and as would be expected, interferes with heparin-TyrH binding.[47]

The amounts of salt necessary to observe increased activity are far beyond what would be encountered *in situ*, so there is probably no linkage of these results with the stimulatory effect of increased $[K^+]$ following nerve depolarization. Polyanion activation of TyrH has been shown to be additive with cAMP-dependent stimulation and to depend upon the presence of Ca^{2+}, indicating that it is mediated, probably by CaM-PK II phosphorylation.[317]

3.5. Feedback Inhibition by Catecholamines. From the earliest studies with TyrH, it has been recognized that the catecholamine product of its reaction is a potentially strong inhibitor of the enzyme.[54] Strong evidence for the participation of a non-heme iron in the catalytic reaction is available, from this and subsequent studies that demonstrate an absolute requirement for iron and an acute sensitivity to iron chelators. The active-site iron has been presumed to be the binding site for catechols and catecholamines, although in the latter case the amino acid-like moiety may enhance the TyrH affinity.

Although catechols bind iron tightly, the large difference in catechol affinity between Fe^{2+} and Fe^{3+} is not always appreciated. As is shown in Table 6, the affinity of catechols for iron shows a pronounced dependence on pH and the oxidation state of the iron center, with both low pH and reduction to the ferrous state decreasing the overall binding affinity of catechol.[164] If air is present under low pH conditions, Fe^{3+} can be reduced by catechol (which forms a quinone) rather than directly coordinated. Since catechol's first $pK_a = 9.3$,[318] physiological conditions will mostly reflect the chemistry of protonated catechols. As long as the iron site in TyrH remains in the Fe^{2+} state, the iron's affinity for catechol or L-Dopa should be low (Table 6).

When purified from catecholamine-containing tissues, the oxidized enzyme's iron binds catecholamines, forming a colored (LMCT) complex. In a purification of TyrH from bovine adrenal[164] or rat PC12 cells,[307] Andersson *et al.* obtain a blue-green enzyme ($\lambda_{max} = 700$ nm, $\epsilon = 3100\ M^{-1}\ cm^{-1}$; $\lambda_{max} \approx 400$ nm, $\epsilon \approx 2500\ M^{-1}\ cm^{-1}$) containing 0.55 Fe subunit^{-1}. Following acid treatment, 0.49 ± 0.09 and 0.10 ± 0.03 equivalents per subunit of dopamine and noradrenaline were released from the pure enzyme.[307] These results are consistent with stoichiometric formation of a catechol-Fe^{3+} adduct on TyrH, such as is known for PAH and ferric catecholate model complexes.[138]

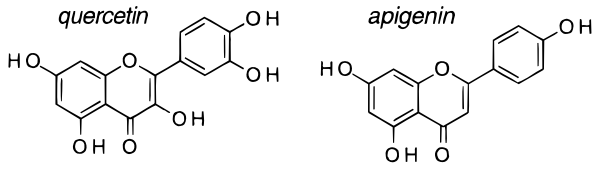

Figure 10. The flavonoids apigenin and quercetin.

Fitzpatrick *et al*. report that TyrH prepared from a recombinant source or from bovine adrenal TyrH is colorless.[245] There are slight differences in the mode of purification used by each group, the most significant of which is used by Fitzpatrick *et al*. that calls for 0.5 mM DTT during the heparin-Sepharose purification step, suggesting that what iron remains ($\sim$0.1 Fe subunit^{-1}) is probably ferrous.[245]

By reducing the endogenously catecholamine-coordinated bovine adrenal TyrH with dithionite, Haavik *et al*. demonstrated that the bulk of the catechol-iron LMCT vanishes. This indicates that the complex with catechol has been disrupted, or does not give rise to a visible chromophore in the Fe^{2+} state.[246] In those cases where a chromophore is not observed, either the iron content is low, or it is the reduced ferrous state. In addition, the recombinant enzyme will not encounter high concentrations of catecholamines in the baculovirus cells. In either case, TyrH in intact chromaffin cells may be sequestered from the highest concentrations of catecholamines in the secretory granules.

High-affinity, pH-dependent binding of catecholamines has been demonstrated with bovine and rat adrenal TyrH. The majority of the binding strength comes from the catechol moiety, with 4-methylcatechol and adrenaline having about the same affinity ($IC_{50} = 4.1$ and 1.8 μM, respectively, for recombinant hTH1 at pH 7.0).[306]

The dissociation of the endogenous catecholamines norepinephrine and adrenaline is favorable at low pH and can be accomplished with an ammonium sulfate precipitation at pH 4.4. The binding (at 4 °C) of [^{3}H]-noradrenaline to (presumably ferric) TyrH freed of catecholamines in this way requires the deprotonation of a group with p$K_a \approx 5.3$. At pH 7.0 and 30 °C, the dissociation rate of [^{3}H]noradrenaline was 0.31 h^{-1} for unphosphorylated enzyme, 1.8 h^{-1} following treatment with cAMP-PK.[320] This 6-fold increase might have some physiological importance, as a mechanism for dissociating the tightly bound catechols from ferric TyrH. TyrH may be oxidized as a side reaction of catalytic turnover, or by free peroxides (which are generated by pterins under aerobic conditions).[164]

Other catechol-containing compounds bearing no other obvious chemical resemblance to the L-Tyr substrate can reversibly inhibit TyrH. The flavonoid quercetin was found to inhibit partially purified bovine adrenal TyrH with $K_d \approx 25$ μM (determined at pH 6.0, so this would presumably be tighter at neutral pH) but the structurally similar apigenin did not inhibit <100 μM, probably because it lacks an *o*-catechol moiety (Figure 10).[321]

Note that both contain a *m*-catechol moiety as well, which is apparently not inhibitory. In support of this, a resonance Raman study of recombinant human hTH1, employing several combinations of isotope-enriched O and Fe, indicates that catechols are bound to iron by both vicinal oxygens. Fe−O stretches at 592 and 631 cm^{-1} were assigned to the *meta* and *para* oxygens, respectively, using [*m*,*p*-^{16}O]dopamine, [*m*,*p*-^{18}O]dopamine and [*m*-^{18}O,*p*-^{16}O]dopamine. A band at 528 cm^{-1} was affected by both isotopic substitutions, so it has been assigned to a chelate mode. No isotopic perturbations were detected as the result of replacing ^{54}Fe with ^{57}Fe (expected to be $\sim$4 cm^{-1} for a pure Fe−O stretch).[165]

The rate of dopamine binding has been determined for recombinant rat TyrH, by assaying aliquots from an incubation at 1:1 TyrH:dopamine (pH 7.0, 30°). The rate of loss of the initial TyrH activity was $\sim$8000 M^{-1} s^{-1},[244] which is comparable to the $\sim$2500 M^{-1} s^{-1} binding rate of various protonated catechols to Fe^{3+}.[319]

With the partially phosphorylated bovine adrenal medulla TyrH, the inhibition due to norepinephrine, dopamine, or methylcatechol is pH dependent, requiring the deprotonation of a group having a pK_a of 7.6. All three catechols were competitive inhibitors *vs* 6MPH$_4$ and noncompetitive *vs* L-Tyr. Inhibition by L-Dopa has only a mild pH dependence and was noncompetitive *vs* both L-Tyr and 6MPH$_4$ below pH 7.5, competitive above. This difference for the TyrH product L-Dopa is consistent with its dual chemical identity, being both a catechol and a L-Tyr analogue; one expects tight catechol binding to favor competitive inhibition at high pH, which is observed.[322,323]

The physiological role of catechol binding is less clear. There is evidence that the phosphorylated form of TyrH is more labile than the unphosphorylated form.[253,324] In addition, catechols are competitive with the tetrahydropterin cofactor.[323] Reduced pterins have been noted to inactivate TyrH by an unknown mechanism.[325] Potentially, catechol inhibition could serve to block TyrH lability by either of these mechanisms.

At saturating 6MPH$_4$ levels, the K_I for dopamine drops. At 0.1 mM 6MPH$_4$, the K_I is 19 μM for wild-type TyrH or 61 μM in a S40L mutant expressed in AtT-20 cells. (The phosphate content of the wild-type enzyme is not reported, so presumably the reported K_I is an upper limit.) The authors propose that the leucine mutant leads to the expression of an "activated" enzyme (lower 6MPH$_4$ K_m, higher V_{max}), which is consistent with the observations of increased homogenate velocity and reduced sensitivity to dopamine.[242]

The different observations of Wu *et al*. and Daubner *et al*. about whether or not the kinetic parameters of TyrH change in response to phosphorylation may be attributed to the state of purification. A 6-fold activity increase was seen in TyrH isolated by a different procedure, involving a pH 6.5 ammonium sulfate precipitation and HPLC isolation of fractions with the highest specific enzyme activity (but unstated purity). It is not demonstrated that this purification results in separation from endogenous catecholamines that might be present in the pituitary cell line. The activation caused by cAMP-PK-dependent phosphorylation is similar in magnitude in both homogenates and purified TyrH.[242]

Purification by Fitzpatrick's method results in protein with low apparent catechol content.[245] When studied in this highly purified, dopamine-free state, little change in kinetic constants was seen; phosphor-

ylation of dopamine-inhibited enzyme caused a 10-fold increase in V_{max} and a halving of the BH_4 K_m.[244] The likely way to reconcile these results is that Wu *et al*. studied a catecholamine-inhibited species of TyrH and that the activity enhancement derives mainly from the release of this inhibition.

In support of this idea, Bailey *et al*. observed a ~10 min lag in the activity of unphosphorylated, minimally purified bovine striatal TyrH when the assay was initiated with cofactor. This lag could be removed by phosphorylation of the enzyme or by preincubation with PH_4,[209] each of which is consistent with the disruption of the ferric−catecholamine complex: catecholamine dissociation followed by (or concomitant with) iron reduction by the pterin cofactor. Andersson *et al*. observed an increased reduction rate of ferric TyrH upon phosphorylation[326] that can be explained similarly.[320]

One would predict that the opposing effects of phosphorylation and catecholamine binding would be evident in the rate and/or extent of dopamine inhibition of TyrH phosphorylation. TyrH is a good substrate for cAMP-PK.[275] Under conditions in which the unligated enzyme is phosphorylated completely by cAMP-PK within seconds, the dopamine-treated TyrH shows a lag in the accumulation of [^{32}P]-phosphate. Both treated and untreated TyrH incorporated the same, near-stoichiometric amount of [^{32}P]phosphate within 10 min. About 30% of the dopamine-treated enzyme is phosphorylated before the first time point could be obtained, implying that 30% of TyrH is unaffected by dopamine. Since this is in rough agreement with the 0.55 [^{3}H]dopamine/TyrH subunit stoichiometry determined by a gel-filtration experiment, it appears that the dopamine-TyrH is a poor substrate for cAMP-PK. Since tight binding of dopamine should depend upon the iron content, one expects the iron content of the batch of TyrH used in this experiment to be about 0.55 Fe subunit^{-1}, but this was not reported. As would also be expected, the effects of dopamine on the S40A mutant cannot be alleviated, since no phosphorylation site is present.[244]

In summary, phosphorylation of Ser40 interferes with the binding of catecholamines to TyrH, and *vice versa*. Whether this is due to interference with the iron-binding capabilities of the catechol moiety, improved specificity for the amino acid substrates, or some other mechanism is unknown.

4. Properties of the Active-Site Iron

The optical spectrum of recombinant rat {Fe^{3+}}-TyrH is similar to the spectrum of {Fe^{3+}}PAH shown in Figure 7, indicating a primary coordination sphere of carboxylates, histidine, and water.[251] Although the nature of the primary ligands to the active site Fe center is currently unknown, the spectroscopic properties of the catechol adduct of {Fe^{3+}}TyrH allow inferences about the iron-binding site in TyrH (section II.B.3.5). Resonance Raman assignments have been made for this adduct, which lacks the 1600 and 1500 cm^{-1} bands typical of non-heme iron sites that have tyrosinate ligation. The 1500 cm^{-1} band is shifted to a 1476 cm^{-1} band, which has been assigned, together with a new 1426 cm^{-1} band, to C−C dominated stretches in the catechol moiety. In addition, thiolate-ligated metalloproteins have no bands in the region of 1100−1700 cm^{-1}. A new 527 cm^{-1} band is observed, which is only seen in the Raman spectra of bidentate-catechol ligated model compounds, which has been assigned to the chelate mode. Slight changes in the 600 cm^{-1} region are seen with the phosphorylated TyrH−catechol adduct, including a shift of the 528 cm^{-1} chelate mode to 531 cm^{-1}.[165] When compared to model compounds that contain only neutral nitrogen ligands, the catechol adduct of {Fe^{3+}}TyrH or {Fe^{3+}}PAH shows a blue-shifted absorbance, which is also observed in model compounds in which the neutral nitrogenous ligands are replaced by charged carboxylate ligands.[164]

Red phenolate adducts of TyrH can be obtained with phenol, *p*-tyramine, or *o*-octopamine, which bind with much lower affinity than the catechols (K_d for the latter two = 2.5 ± 0.5 mM,[165] compared to 1−4 μM for simple catechols[306,323]). These adducts have λ_{max} values near 500 nm, with molar extinction coefficients around 1.1 mM^{-1} cm^{-1}. Intriguingly, L-Tyr does not give visible absorptions of this kind at 3 mM (~80 K_m), indicating that it does not bind the iron site directly. Resonance Raman studies of the tyramine adduct show a Fe−OR stretch at 586 cm^{-1}, as well as the 1507 and 1605 cm^{-1} bands characteristic of tyrosinate-ligated metalloproteins.[165]

Recombinant hTH isoforms, which contain 0.02−0.01 iron subunit^{-1} when isolated, are reconstituted in a straightforward manner by the addition of Fe^{2+} to the apoprotein.[327] This can be followed by the extent of fluorescence quenching (excitation 295 nm), which for the recombinant hTH isoforms is 33−40%. Bovine adrenal enzyme, which contains 0.6−0.8 tightly bound iron subunit^{-1}, is quenched only 6% under the same conditions. The extent of quenching correlates with the final activity of the reconstituted protein, which indicates indirectly that there is a linear activity dependence upon iron content. (This is reminiscent of the reconstitution of iron-depleted PAH, which does not result in an increased population of "active" iron sites/specific activity.[144])

The rate of iron reconstitution of recombinant, apo-TyrH yields second-order rate constants of 5.9 × 10^5 M^{-1} s^{-1} for hTH1 and 3.6 × 10^5 M^{-1} s^{-1} for hTH2 at pH 7.5 and 20 °C. At pH values below 7, the apparent rate of iron binding decreases, and cannot be detected at pH 5.4 (Hepes buffer). Addition of a chelator (dipicolinic acid or EDTA) restores the increased fluorescence of apo-TyrH, in a dopamine-inhibitable manner. Other divalent metals, including Co^{2+}, are efficient quenchers, but Fe^{3+} and Ga^{3+} do not quench TyrH fluorescence > 1%. This result is unusual, since EPR evidence shows that at least part of the {Fe^{2+}}TyrH reoxidizes in the presence of dopamine (within 20 s at 20 °C) to give {Fe^{3+}-(dopamine)}TyrH (*vide infra*). The fluorescence data imply that Fe^{3+} is not efficiently bound in 20 mM Hepes, 0.15 M NaCl, pH 7.5 at 20 °C, conditions that differ from those used to generate the {Fe^{3+}-(dopamine)}TyrH EPR sample by (1) the presence of dopamine and (2) the higher concentrations needed for EPR.[327]

TyrH seems to have a lower affinity for iron than does PAH, which is isolated from natural and recombinant sources in a mostly iron-loaded form. Activity

measurements on purified, catecholamine-free TyrH generally include the addition of excess Fe^{2+} to saturate the enzyme.[328] This may be less important when TyrH is purified from a natural source and contains a bound catecholamine, if this results in slower dissociation of the iron cofactor from the enzyme (as in bovine adrenal TyrH, which is purified with 0.7 Fe subunit^{-1} bound to endogenous catecholamines[246]).

As might be expected from the previous section's discussion, there appears to be an interaction between the TyrH cAMP-PK phosphorylation site and the active site metal-binding pocket. If dopamine and Fe^{2+} are both added to TyrH, phosphorylation does not go past 0.3 phosphate subunit^{-1} under conditions in which full phosphorylation of TyrH is otherwise attainable: TyrH alone, or in the presence of *either* Fe^{2+} or dopamine. This effect appears to be most prominent at a 1:1 Fe^{2+}:TyrH subunit stoichiometry. The rate of phosphorylation by cAMP-PK is slowed in the presence of dopamine and iron, and appears to be weakly cooperative (Hill coefficients are 1.4−1.6).[306]

In order for dopamine to exert all of these effects on the holoenzyme, it most likely is bound to the {Fe^{3+}}TyrH state of the protein. While the experiments are performed under aerobic conditions, and it is certainly possible that the enzyme has reoxidized, it must be separately demonstrated that incubation of {Fe^{2+}}TyrH with a Fe^{3+} chelator results in oxidation of the metal and adduct formation. Good evidence for Fe^{2+} oxidation in the presence of catecholamines under aerobic conditions comes from an EPR study, in which Fe^{2+} was added to a solution containing equivalent amounts of apo-TyrH (hTH1) and dopamine (added 20 s before the Fe^{2+}). After the reaction was allowed to occur for 20 s at 20 °C, the sample was frozen in liquid N_2 and an apparently substantial amount of the axial catecholamine adduct was detected in the EPR spectrum.[327] This is in some sense a puzzling result, particularly given its rapidity. It would seem to force a choice between two unattractive alternatives, that the Fe^{2+} in reduced TyrH is present in some sort of equilibrium with Fe^{3+} that can be trapped in the presence of catechol, or that catechol greatly enhances the O_2 reactivity of {Fe^{2+}}TyrH by some unknown mechanism. Alternately, the Fe^{2+} reconstitution of TyrH might produce {Fe^{3+}}TyrH initially, which would ordinarily be reduced in a reconstitution experiment by excess Fe^{2+}. In the presence of catecholamines, the ferric state would be stabilized by formation of {Fe^{3+}(cat)}-TyrH. While this option would appear to be ruled out on the basis of the featureless EPR spectrum of iron-reconstituted TyrH in the absence of catecholamines, the amount of excess iron used, if any, was not given.[329] If this last alternative were the case, a single-electron acceptor should be present, one that is not evident in the EPR spectrum of the freshly reconstituted {Fe^{3+}(dopamine)}TyrH. In these multimeric enzymes, the possibility of disulfide reduction by electrons originating from different subunits remains tenable.

Since the adrenal and PC12 TyrH are isolated with tightly bound iron and (nor)adrenaline, EPR studies of various catecholamine adducts are most common. Like the catechol adduct of PAH, the signals are predominantly axial, with $g_{eff} = 7.0$, 5.9, and 5.2; small alterations occur upon phosphorylation. The axial signals diminish when the catecholamine dissociates from the iron, either following addition of L-Tyr (a new signal at $g_{eff} = 4.5$ appears) or as a result of reduction under turnover conditions.[326]

The tyrosine-bound, phosphorylated TyrH EPR spectrum closely resembles that of {Fe^{3+}}-PAH^{R}_{L-Phe}, which has been interpreted as arising from perturbation of the active site iron's environment by the binding of substrate rather than to allosteric structural alterations. In combination with the spectroscopic evidence against direct iron substrate coordination in the TyrH active site, it appears that binding of either amino acid hydroxylase by its cognate amino acid substrate causes similar electronic perturbations in the Fe^{3+} environment. TyrH can also efficiently hydroxylate L-Phe at a rate comparable to L-Tyr (section IV.C.2), which further supports the reasonable assumption that TyrH binds both amino acids in a similar fashion. Since PAH cannot hydroxylate L-Tyr, and TyrH is ~10-fold less efficient at the hydroxylation reaction than PAH, clearly differences between the two enzymes must arise elsewhere.

While the EPR spectrum of {Fe^{2+}}TyrH is basically featureless, Mössbauer spectroscopy can be used to characterize this catalytically important redox state of the enzyme. Samples of {$^{57}Fe^{2+}$}TyrH were prepared by adding anaerobic aqueous solution of $^{57}FeCl_2$ to a 4% molar excess of apo-TyrH at pH 7.5. The site parameters obtained from Mössbauer analysis are consistent with a N/O coordination sphere, with $\delta = 1.25 \pm 0.02$ mm s^{-1} and $\Delta E_q = 2.68 \pm 0.02$ mm s^{-1}.[329]

Ramsey *et al.* have recently used histidine mutagenesis in an attempt to identify iron ligands in recombinant TyrH.[330] The most deleterious alterations were caused by replacement of His331 and His336 with either Gln or Ala, which resulted in proteins with a <300-fold lower specific activity and <0.05 Fe subunit^{-1}.[330] These TyrH residues correspond to the two histidinyl ligands identified as iron ligands in PAH (His284 and His289),[60] and somewhat more directly identified, using pulsed-EPR techniques, as copper ligands in *C. violaceum* PAH (His138 and His143).[186] What remains to be addressed is whether the structure is more extensively perturbed than was intended, which can mask specific changes in metal-binding properties.

In the TyrH study, substitutions were also made at other conserved positions, and the mutant proteins were characterized kinetically and by EPR spectroscopy.[330] The alteration of His192 or His247 to Gln resulted in proteins with nearly the same iron content as wild-type enzyme, with 6- and 2-fold lower activities, and fairly similar EPR spectra. Mutations at His317 were more complex: in Ala317, the iron content remains normal but the activity is lower by a factor of 10, and Gln317 has a low iron content (but nearly the same specific activity *per iron* as Ala317). However, the decreased activity is primarily a V_{max} effect, since the K_m values for both substrates drop appreciably (K_{Tyr} 51 → 1 μM; K_{6MPH_4} 50 → 10 μM). Because the V_{max}/K_m of the mutant, and therefore the

rate-limiting step (potentially hydroxylation itself), is not significantly altered, Ramsey *et al*. suggest that His317 ordinarily functions as a general acid or base in catalysis rather than as an iron ligand. The EPR spectrum of the Ala317 mutant has a more prominent $g_{eff} = 7$ peak than any of the other wild-type or mutant EPR spectra reported, giving it a more axial appearance than the wild-type {Fe^{3+}}TyrH EPR signal.[330] Given the high concentration of glycerol (10%) in the EPR samples, this might reflect a contribution due to adduct formation. Until a crystal structure of this enzyme becomes available, it will unfortunately be impossible to ascribe particular structural characteristics from this type of functional analysis with any certainty. The relative rarity of truly conservative mutations identified in this class of enzymes confirms the general suspicion that their structures are very carefully poised to accomplish the hydroxylation reaction, with appropriate substrate specificity, avoidance of product inhibition, and a minimum of side reactions.

It has been inferred that TyrH has a requirement for prereduction analogous to that for PAH, on the basis of its acute sensitivity to several ferrous chelators including *o*-phen. Since the recombinant rat TyrH and hTH isoforms are expressed in bacteria in a low-iron state, they are often reconstituted with Fe^{2+}, which is more labile than Fe^{3+} in aqueous solutions. As a result, there is no need for a separate reduction step if most of the iron remains reduced, since the Fe^{2+} form is stable for at least several minutes under aerobic conditions (unless dopamine is present). Using enzyme obtained from natural sources, one must remove the catecholamine bound prior to reduction, which in turn would precede catalysis. While reduction by tetrahydropterins appears to be thermodynamically or kinetically unfavorable for catechol-bound {Fe^{3+}}TyrH (or PAH), it seems to be feasible in the presence of *both* L-Tyr and a tetrahydropterin or, as described in the previous section, if phosphorylation has occurred.

C. Tryptophan Hydroxylase [TrpH EC 1.14.16.4]

1. Distribution and Physiological Functions

The distribution of TrpH is the most restricted of the aromatic amino acid hydroxylases. It is found in the serotonergic neurons of the CNS, which innervate a number of disparate brain regions including midbrain, medulla, pons, and cerebellum.[266,331] TrpH produces 5-hydroxy-L-tryptophan in the rate-limiting step of serotonin synthesis (Figure 11), which is itself the precursor for melatonin biosynthesis.[332] Serotonin (5-hydroxytryptamine) and melatonin have a wide range of physiological effects, most famously as a neurotransmitter and as part of the circadian rhythm control system, respectively. TrpH is found primarily in the dorsal raphe nucleus and the pineal gland, which contains the highest TrpH activity.[26]

Serotonergic projections from the raphe nuclei, a group of nine discontiguous regions in the midline of the brainstem, heavily innervate the superchiasmatic nucleus (SCN),[333] the mammalian circadian "clock" region.[334] The SCN has a diurnal rhythm of serotonin uptake and sensitivity;[335] when serotonin is applied the firing of neurons in the SCN is decreased.[336]

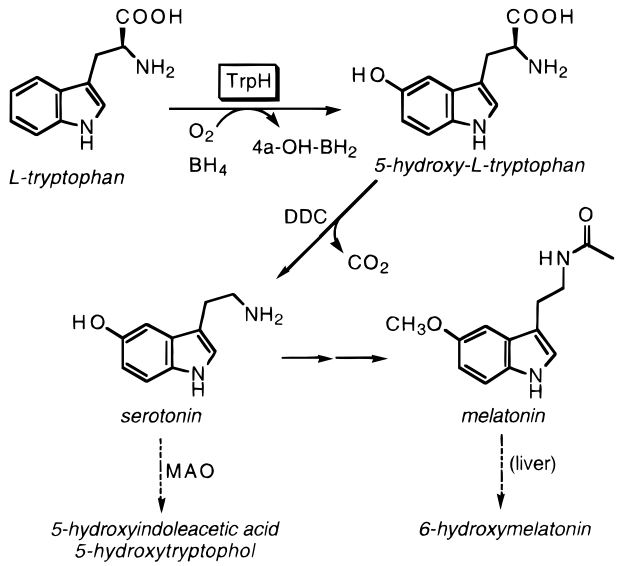

Figure 11. TrpH reaction within its biosynthetic context.

Both ascending and descending serotonergic pathways exist, with contrasting physiological effects. An increase in L-Trp or 5-hydroxytryptophan, or direct treatment with serotonin, causes a decrease in motor activity thought to be due to the *ascending* serotonergic pathway. Treatment with *p*-chlorophenylalanine, which inhibits TyrH and blocks serotonin formation in this pathway, leads to the opposite: insomnia and increased motor activity, aggressiveness, irritability, sexual activity, and social interaction.[337,338] These results represent the characteristic inhibitory effects of serotonin, which may be associated with the process of sleep.[339]

In contrast, treatment with an MAO inhibitor also increases serotonin, but causes autonomic excitatory effects, tremor, seizures, and hyperactivity, which can also be accompanied by an increased body temperature (hyperpyrexia). These effects are probably due to stimulation of the *descending* pontine and medullary serotonergic raphe nuclei. Selectivity in controlling serotonin levels in the correct region of the brain has an obvious therapeutic benefit because of these multiple effects of this powerful compound.[340] Serotonin agonists are either tranquilizers (chlorpromazine [Thorazine]) or hallucinogens (LSD and 5-methoxy-*N*,*N*-dimethyltryptamine); serotonin storage inhibitors are tranquilizers (reserpine); serotonin reuptake inhibitors are antidepressants (fluoxetine [Prozac], chlorimipramine, clomipramine, and nortryptilene) as are MAO inhibitors (iproniazid and tranylcypromine); and serotonin analogues are hallucinogens (bufotenine). The similarities between the effects of LSD and forms of mental illness were noted years ago, leading to the persistent suggestion that normal functioning of the serotonergic system is deranged in some mental disorders.[341]

In the periphery, TrpH is found in mast cells, in stem cells,[342] and in the enterochromaffin cells of pancreas and intestine.[343] Mast cells, which are descended from hematopoietic stem cells,[344] are involved in inflammatory responses, during which they produce histamines, cytokines, and heparin.[345] Overall, the intestinal mucosa contain 95% of the body's serotonin, which is involved in digestion. Increased serotonin levels are associated with starvation, and

peripheral administration can increase the sensitivity to pain (nociception).[337]

Often the serotonin content of tissues does not correspond well with the TrpH content.[346] For instance, 5-hydroxy-L-tryptophan was first isolated from platelets, which contain no TrpH activity.[347]

Nearly all of the work on TrpH performed to date has been with brain or pineal forms of the enzyme. This situation should soon be different, following the realization that mouse bone marrow-derived mast cell TrpH activity is induced in response to cytokines. Following treatment by stem cell factor/kit ligand (SCF),[348] these cells show higher TrpH activity and increased serotonin content, concomitant with induction of the BH_4-biosynthesis pathway by increased levels of GTP cyclohydrolase I.[349] This is consistent with induction of BH_4 to enhance its availability as a cofactor in a part of the immune system, distinct from and in addition to its role in nitric oxide formation in other cells (sections II.D.3 and III.A.1).

The pineal gland, which is attached to the brain but is not part of the CNS, exerts its influence on the hypothalamus using both serotonin and melatonin. It is thought that the pinealocytes transduce environmental cues, particularly ambient light levels, into chemical signals. Melatonin is produced at night and is itself a light-sensitive compound.[350] Its role in circadian rhythm generation, seasonal cycles, and sleep have been extensively reviewed.[351−357] While melatonin is produced primarily in the pineal gland, it is also found in the retina.[358−360] TrpH activity or immunoreactivity has been found in retinas from various species,[358,361−365] and its mRNA has been recently cloned from *Xenopus laevis* retina.[366]

2. Molecular Structure and Expression

2.1. Assays, Isolation, and Characteristics. Assays of the formation of 5-hydroxytryptophan include direct fluorometric determination of product[367−369] and radiometric determination of $^{14}CO_2$ from [1-^{14}C]tryptophan in a coupled assay that includes DOPA decarboxylase (aromatic L-amino acid decarboxylase, EC 4.1.1.28).[370] Total 5-hydroxyindoles can be quantitated without radioactivity by condensation with *o*-phthalaldehyde.[371]

TrpH is an unstable and relatively scarce protein, so it is not surprising that purifications of this enzyme and studies of the purified material have lagged behind PAH and TyrH. Tong and Kaufman purified a low-activity (specific activity at 37 °C = 2.1 nmol 5-hydroxytryptophan formed per minute per milligram) TrpH from rabbit hindbrain to ~90% homogeneity and demonstrated that the enzyme had a requirement for O_2, and one of $6MPH_4$, $DMPH_4$, or BH_4.[372] Using a pteridine affinity matrix, Nakata and Fujisawa purified homogeneous, high-activity TrpH from rat brainstem and mouse mastocytoma (specific activities at 30 °C = 374 and 5280 nmol min^{-1} mg^{-1}, respectively), which were apparent homotetramers with apparent subunit weights of 59 and 53 kDa, respectively.[373,374] Anaerobic conditions were not necessary to purify high activity TrpH, which had been predicted from the lability of crude TrpH-containing fractions in O_2 (section II.C.4).[375] Addition of glycerol/ethylene glycol, Tween 20, L-Trp, and EDTA greatly increased the stability of homogeneous TrpH during storage,[374] an effect not observed by a different group.[376] A purification to homogeneity of TrpH from whole rat brain yielded enzyme of specific activity 367 nmol min^{-1} mg^{-1}, or about the same as the rat brainstem preparation. This procedure includes exposure of the extract to "activating conditions" (DTT, Fe^{2+}, Ca^{2+}, and pH 8.0) prior to application to the pteridine matrix.[376]

A sense of how rare TrpH is can be conveyed by the fact that the three purifications to homogeneous protein are 5500-fold (rat brainstem[374]), 880-fold (mouse mastocytoma[373]), and 3570-fold (rat brain[376]), even though the yields are reasonable (8−47% recovery).

TrpH is generally regarded as a soluble tetrameric protein, based on the physical parameters determined for TrpH from several sources. Gel filtration indicates tetramer formation,[372] a result supported by a cross-linking study.[373] The Stokes radius determined by gel filtration is 53 Å (mouse mastocytoma [373]) or 56 Å (rat midbrain[377] or brainstem [374]). Sucrose gradient centrifugation gives $S_{20,w} = 10.9$ S[372] and 9.6 S.[377] Smaller species have also been reported, as with mouse mast cell TrpH, which appears to be a 144 kDa dimer with Stokes radius 50.3 Å and $S_{20,w} = 6.97$ S.[377] There is also a tissue-dependent distribution between soluble and particulate forms of TrpH.[346]

Mast cell TrpH and midbrain TrpH have shown differences in immunoreactivity[374] and in their kinetic and physical properties, leading to the proposal that they are "distinct molecular entities".[346] Initially, this hypothesis gained support when two mRNA species were identified from a rat pineal cDNA library,[378] but subsequent to this, only a single mRNA isoform has been found in all cloned TrpH: rabbit pineal body,[252] rat pineal,[379] human carcinoid tumor,[380] mouse mastocytoma,[381] rat dorsal raphe nucleus,[382] and human brain.[383]

The apparent implication of a single mRNA encoding biochemically distinguishable forms of TrpH is that there are as-yet unknown posttranslational modifications of TrpH. The largest sequence variation known (including intraspecies differences) is the 99 base pair difference (18 amino acid changes) between the TrpH from human carcinoid tumor and human brain (pons, cerebellum, and midbrain). Since the human brain clone was more similar to the rabbit clone, Tipper *et al.* suggest that the carcinoid tumor TrpH might have an abnormal sequence.[383] As has been mentioned, the sequence of TrpH is homologous with PAH (full human sequences, 52.3% identity; 55.6% identity in 430 residues overlap), and to a slightly lesser extent, TyrH (full human sequences, 40.7% identity; 57.8% identity in 334 residues overlap).

The human brain clone of TrpH was overexpressed using a maltose-binding protein (MBP) fusion construct, which could not be proteolytically excised from the TrpH sequence without causing precipitation of the cleaved and fused protein. The specific activity of the fused construct was low (62 nmol min^{-1} mg^{-1}).[384]

In neither of the other two reports of an overexpressed TrpH was the protein purified to homogeneity, which is critical to assessment of the relative

activity of a recombinant enzyme.[383,385] The specific activity of a recombinant mouse TrpH in cell lysates was stated to be approximately that of rat brain and rat brain stem TrpH (specific activity at 37 °C = 434 nmol min^{-1} mg^{-1}), but a detailed account of how total [TrpH] was determined was not provided.[385] By using fusions of MBP to truncated TrpH, a deletion study has been performed on the basis of similar mapping of the active site in PAH and TyrH. MBP-TrpH constructs lacking 91 N-terminal or 19 C-terminal amino acids show ~10% residual activity, which is lost if larger excisions from the C-terminus are made (≤36 amino acids).[384] These results are consistent with the delineation of regulatory and catalytic domains in the similarly sized PAH (452 *vs* 444 amino acids for TrpH) discussed in section II.A.2.

TrpH is inhibited by thiol-binding compounds (*N*-ethylmaleimide and mercurials) or agents that promote disulfide formation in proteins (DTNB and dithiodiglycolic acid). Tryptophan has a partial ability to protect crude rat brainstem homogenate TrpH activity from inactivation by these compounds. DTT is less effective at recovering activity following covalent modification of thiols than it is at re-reducing oxidatively inactivated TrpH, which is restored to full activity.[375] Thus it appears that in addition to the requirement for Fe^{2+}, at least one reduced thiol is important for TrpH activity.[386]

2.2. Gene Expression. Comparatively little is known about the expression of the *trpH* gene, which is spread across 29 kb in 11 exons[105] on human chromosome 11p15.3-p14.[387−389] Human *trpH* mRNAs are comprised of a conserved coding region, a conserved 3′ UTR, and a variable-length 5′ UTR, with the most common transcript length = 5 kb (type 1). Carcinoid tumors have a significant amount of longer transcripts, which are also present in the pineal in smaller amounts. Only the 5 kb transcript is found in the intestine. Counter to expectations, no transcripts were detected in the dorsal raphe nucleus and the pineal gland.

Shorter, ~3.6 kb transcripts (type 2) were detected in pineal mRNA that lack 1.7 kb of 5′ UTR sequence, which suggests transcript editing occurs. The shorter mRNA has an additional AUG 27 bp upstream in the 5′ UTR, which might potentially give rise to a different, slightly longer isoform of TrpH.[105] Among the aromatic amino acid hydroxylases, this potentially regulatory processing of the 5′ UTR is unique to TrpH, which contains three "introns" in the human 5′ UTR and one in the mouse 5′ UTR.[381] Multiple TrpH protein isoforms have not been reported.

cAMP levels in the pineal gland vary with a circadian rhythm;[390] when increased, cAMP increases the expression of rat pineal TrpH.[391] A 2 kb sequence of 5′ UTR was adequate to direct cAMP dependent expression, albeit not in a cell-specific manner (PC12 as well as cultured pinealocytes were tested, and both expressed a TrpH 5′ UTR-luciferase reporter construct). The region between −73 and +2 with respect to the start site confers this responsiveness, even though no CRE (cAMP-responsive element) or AP-2 site is present. Instead, an inverted CCAAT box at −71 was sufficient to give the observed cAMP regulation.[392] Intriguingly, pinealocytes lack CRE-binding protein, the usual CRE activator, but contain ICER, an inhibitory member of the CRE modulator family that has a significant circadian fluctuation.[393] The architecture and complex processing of the 5′ UTR are potentially able to account for all or part of the circadian fluctuations of TrpH and, by extension indoleamine levels. Melatonin synthesis is not rate limited by TrpH,[26] but by serotonin *N*-acetyltransferase (EC 2.3.1.87), the activity of which follows a circadian rhythm.[394]

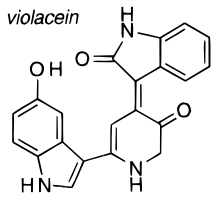

Figure 12. Violacein, the characteristic pigment of *C. violaceum*.

The half-life of [^{35}S]methionine-labeled TrpH is less than 1 h in mast cells, ranging to as low as 11−15 min in a leukemia cell line. Proteolysis depends upon ATP, but the mechanism of degradation remains unknown.[395]

2.3. Other TrpH. In addition to PAH, there is a TrpH activity in *C. violaceum*; it was in this organism that tryptophan hydroxylation was first observed.[396,397] *C. violaceum* apparently requires TrpH for the biosynthesis of violacein (Figure 12), the characteristic purple pigment of this organism, but both TrpH and PAH are induced by L-Phe to a greater extent than by L-Trp, a poor carbon source.[179] The *Drosophila* locus DTPH encodes a single protein that apparently serves as a bifunctional PAH/TrpH in that organism. The protein is present in a 45 kDa form present in early stages of development, which apparently functions only as a PAH, that is replaced in the adult by a 50 kDa bifunctional TrpH/PAH.[173] This is not chemically unusual, since PAH and TrpH readily hydroxylate each others' substrates under *in vitro* conditions, and both are inhibited *in vitro* and *in vivo* by *p*-chlorophenylalanine,[26,398] while TyrH is not.[399] A pineal "PAH" turned out to be TrpH,[400] which can catalyze the formation of L-Tyr at 39% the rate it can form 5-hydroxytryptophan; the complementary report, of a liver "TrpH", was similarly resolved as being due to a side reaction of PAH.[401] mRNA probes have confirmed that the mammalian tissue distribution of these two enzymes does not overlap.[105]

3. Regulation

The regulation of TrpH (which has been recently reviewed[402]) has several important differences from TyrH, but overall it resembles TyrH more than PAH. Neither of the two brain enzymes displays allosteric regulation by its amino acid substrate, which are present at subsaturating levels (in the case of TrpH, the concentration of L-Trp is near its K_m). As discussed above, the possibility exists that a majority of the "long-term" regulation of TyrH expression occurs on the translational level. The need for acute regulation of TrpH is harder to justify, in terms of physiological function, than it is for the TyrH/catecholamine system.

3.1. Neural Activity/Circadian Rhythms. *In vivo* electrical stimulation of the dorsal raphe nucleus in rat midbrain, which contains the cell bodies of

many serotonergic neurons, leads to an increase in the amount of TrpH activity in the resulting extracts.[403] Extracellular Ca^{2+} was required to observe this increase *in vitro*.[404−406] Depolarization of neurons, which leads to an increase of K^+ and release of Ca^{2+}, has been supposed to mediate TrpH levels, primarily by phosphorylation. Evidence that phosphorylation is a significant participant in this short-term response includes the sensitivity of the electrical stimulation-induced activation to alkaline phosphatase, a nonadditivity with phosphorylating conditions, and the similarity to potassium depolarization of brain slices, which increases the V_{max} of TrpH.[403]

In the pineal gland, the level of TrpH activity[407,408] and cAMP-dependent TrpH phosphorylation[391] cycle with a circadian rhythm. Cycloheximide, which blocks protein synthesis but not necessarily TrpH synthesis, obliterates the cAMP-dependent increase in TrpH activity.[391] The TrpH activity level in chicken retina also follows a circadian rhythm, increasing during the dark. This increase was inhibited by an injection of cycloheximide prior to the onset of darkness.[409]

Thus it appears that short-term and circadian regulation of TrpH in both brain and pineal involves phosphorylation of the enzyme, perhaps in a protein synthesis-dependent, cAMP-dependent system. Molecular details of this interaction are presented in the following section.

3.2. Phosphorylation. The addition of cAMP or its analogues to brain slice preparations causes an increase in TrpH activity,[410,411] which would superficially seem to implicate activation by TrpH phosphorylation, mediated by a cAMP-dependent protein kinase. However, the enhancement of TrpH activity required Ca^{2+},[412,413] could be blocked by antagonists of calmodulin,[414] and cAMP was found to increase the influx of L-Trp into cells (an increase in substrate levels would be expected to increase activity in this subsaturated enzyme).[415] While the first pieces of evidence clearly suggest the involvement of a Ca^{2+}/CaM-dependent protein kinase,[416] it was also found that Ca^{2+} causes proteolysis of TrpH by a neutral Ca^{2+}-activated protease.[417]

In brain cytosolic extracts, cAMP and ATP have no stimulatory effect on TrpH activity,[412−414,418] which is also the case for bovine pineal extracts.[419] Generally the exposure of extracts to CaM-PK phosphorylating conditions leads to a 2-fold stimulation of TrpH activity, except in pineal extracts.[420] Addition of phosphatase to brain sections[421] or serotonergic neurones[403] diminished the activation of TrpH, consistent with activation by phosphorylation.

The calcium-dependent activity-enhancement factors were fractionated into calmodulin, CaM-PK II, and a heat-labile activator protein.[293,294] As was mentioned in Section II.B.3.2, the activator protein is a widely distributed 14-3-3 protein required for TrpH activation, but not phosphorylation by CaM-PK II.[267,295] The level of phosphate incorporation by CaM-PK II into one or both of the two putative[379] phosphorylation sites is quite low (0.12 [^{32}P]phosphate monomer^{-1} of purified TrpH).[422] The site of phosphorylation has not been reported. In brainstem cytosolic extracts, the activation apparently mediated by phosphorylation can be reversed by the addition of EGTA, which can in turn be counteracted by the addition of more $CaCl_2$.[418] As was discussed in section II.B.3.2, dynamic phosphorylation levels are also seen in TyrH.

The predicted amino acid sequence of TrpH from all of the mammalian clones contains a canonical cAMP-PK site at Ser58, Ser260, and Ser443.[383] Recombinant, and presumably unphosphorylated, TrpH is a substrate for cAMP-PK; no change in activity is seen after phosphorylation.[423] No change in TrpH activity was observed following cAMP-PK phosphorylation of the rat brain stem TrpH unless activator protein was also included, which resulted in 2-fold activation.[424]

Recently the region in 14-3-3 responsible for interaction with TrpH has been mapped to a carboxy-terminal region, using a demonstration that only phospho-TrpH binds to a GST-14-3-3 fusion (η isoform), and that the phosphorylated TrpH will interact with smaller GST-14-3-3 fusion proteins.[425] The proposed interaction region is part of a negatively charged groove in two crystal structures of different 14-3-3 isoforms.[426,427]

Phosphorylation of TrpH by endogenous cAMP-PK and [γ-^{32}P]ATP was demonstrated in rat brain extracts by immunoprecipitation of labeled TrpH, but no change in TrpH activity was detected. In contrast to Makita *et al*. the addition of activator protein did not alter the activity of the cAMP-PK treated TrpH.[428] Since a similar demonstration has not yet been reported with purified TrpH, the site of phosphorylation, as well as the extent of phosphorylation, remain unknown.

3.3. Other Activators. In crude homogenates, TrpH activity is markedly stimulated by polyelectrolytes such as heparin, an effect that can be diminished by salt addition.[429] A report that the activity of 85% pure rabbit hindbrain TrpH is not affected by phospholipids[372] contrasts with other results that show activation of TrpH activity in rat brainstem homogenate by phosphatidylserine and inhibition by phosphatidylinositol.[430]

A later study by Imai *et al*. using crude rat brainstem TrpH at 37 °C showed initial 3- or 4-fold activation by phosphatidylserine and phosphatidylinositol, followed by inactivation. Activity was restored to the inactivated enzyme to higher-than-initial levels by the addition of Fe^{2+} and DTT. Inactivation could be blocked by preincubation with Fe^{2+} but with none of several other divalent metal salts.[431] A similar effect was noted by Lloyd using TyrH, but in that case the activity could not be restored; adding Fe^{2+} or other divalent cations prior to the phospholipid blocked inactivation of TyrH.[316]

The presumably irreversible activation of rat brainstem TrpH by Ca^{2+}-dependent protease might also account for some degree of physiological regulation, but Hamon *et al*. regard this possibility as "doubtful", given the large amounts of Ca^{2+} required.[314,432]

4. Properties of the Active-Site Iron

As was anticipated by the similarities between TrpH and the other amino acid hydroxylases, TrpH activity in different tissues was sometimes stimulated by the addition of Fe^{2+}.[26] Addition of Fe^{2+} doubles the TrpH activity of a bovine pineal homo-

genate, and can "rescue" TrpH inactivated by *o*-phenanthroline or 2,2′-bipyridine.[332] These and other metal chelators are strong inhibitors of TrpH activity, with the notable exception of EDTA, which is a relatively ineffective inhibitor.[332,375] There is a report that 10 μM EDTA is an overall activator of TrpH activity, probably because it sequesters some unidentified metal ion present in an impure mastocytoma preparation.[433] The ability of phenanthrolines but not EDTA to inhibit all three aromatic amino acid hydroxylases is regarded as a difference in the iron site's accessibility to neutral and charged chelators. Catechols strongly inhibit TrpH as well, probably by direct coordination of the oxidized ferric active site iron.[332,367]

TrpH activity in crude extracts can be raised by incubating the enzyme with Fe^{2+}/DTT under anaerobic conditions.[386,434−436] Treatment with Fe^{2+}/DTT causes a rapid, marked activation of homogenous mouse mastocytoma and rat brainstem TrpH, which is optimal at 20 μM Fe^{2+}.[373,374] Anaerobic addition of Fe^{2+}/DTT has no effect on the substrate K_m's but increases V_{max}, which is consistent with iron reconstitution of apoenzyme.[374,437]

This apparent requirement for reduction and/or reconstitution prompted Kuhn *et al.* to investigate O_2-dependent inactivation of TrpH in crude rat midbrain homogenates. Under 100% O_2 at 37 °C, the TrpH activity decreases with a half-life of 11.5 min, while under 100% N_2, TrpH activity is stable for at least 40 min. Inactivation is dependent on both temperature and P_{O_2}. Inclusion of reactive-oxygen scavengers (superoxide dismutase; catalase; the HO• scavengers mannitol, inosine, and glucose; and the $^1O_2$ scavengers histidine and dimethylfuran) did not prevent inactivation. Tryptophan has no effect on inactivation. Thiol compounds and ascorbate had some ability to slow inactivation, stabilize stored TrpH, and reactivate previously inactivated TrpH; under anaerobic conditions DTT restores 28% of the original activity. In a parallel experiment, the addition of Fe^{2+} and DTT restores 98% of the original activity, suggesting that reactivation is due to iron reconstitution of TrpH. This distinguishes the oxidative inactivation phenomenon from inactivation by thiol-oxidizing compounds, in which full restoration of activity is obtained by re-reduction and tryptophan protects active TrpH.[375]

Direct spectroscopic data sensitive to the state of the active-site iron, including optical and EPR spectra, have not been reported for pure TrpH.

D. Other Pterin-Dependent Systems

1. Glyceryl-ether Monooxygenase

The only enzyme known to cleave unsaturated glyceryl ethers is present in liver, and to a lesser extent, intestine and brain.[438] Blomstrand discovered that radiolabel in chimyl alcohol (1-*O*-hexadecylglycerol) appears in palmitic acid, providing the first evidence of direct ether cleavage, a chemically demanding transformation.[439,440] Unfortunately, the enzyme responsible for this reaction has had a variety of names: *O*-alkyl glycerol monooxygenase, glyceryl-ether hydroxylase, glyceryl etherase, alkylglyceryl-cleaving enzyme, and glyceryl-ether monooxygenase. Tietz *et al.* determined that GEM from liver microsomes has an absolute requirement for O_2 and tetrahydropterin ($6MPH_4$, $DMPH_4$, and the most active pterin tested, L-neopterin) and that the enzyme converts glyceryl ethers into glycerol and an aldehyde. Acid products were the primary product of the reaction only at long incubation times, indicating that they result from oxidation of a product aldehyde, perhaps by NAD^+. They proposed that the α-methylene group of the alkyl chain is hydroxylated to generate an unstable hemiacetal, which hydrolyzes to the observed products (Figure 13).[441]

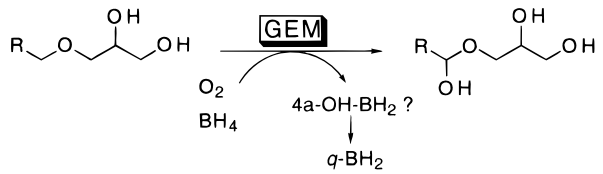

Figure 13. GEM reaction.

Despite a report to the contrary,[438] GEM is exclusively associated with the microsomal fraction in liver and cannot be removed from it by repeated aqueous washing.[442] GEM can be differentiated from microsomal cytochrome P450 by its insensitivity to CO and the inability of various reductants to replace the specific requirement for tetrahydropterin.[443] GEM can be solubilized with Triton X-100[444] or digitonin,[445] the former of which was used in purifying the enzyme to apparent homogeneity with a chimyl alcohol-affinity procedure.[446] Assays are somewhat complicated by the instability of the aldehyde product. Soodsma *et al.* established optimal conditions for cleavage of 1-*O*-hexadecyl-[1-^{14}C]glycerol (or an analogously radiolabeled substrate) by the microsomal form of the enzyme, which is stimulated by glutathione and ∼4 mM NH_4^+, and is maximal at pH 9.0.[442] A NADH-coupled continuous assay has been developed, analogous to Neilsen's PAH assay,[71] in which the rereduction of q-$6MPH_2$ is detected spectrophotometrically. This was shown to give the about the same result (plus ∼5%) as a TLC determination of total cleaved (acid + alcohol + aldehyde) product.[445] This also constitutes a demonstration that the monooxygenase activity is tightly coupled (∼1.05 NADH oxidized per ether cleavage). This was explicitly demonstrated for the microsomal *glycol* ether monooxygenase activity, which is also catalyzed by GEM (1.1 and 1.3 NADH oxidized per 2-(hexadecyloxy)ethan-1-ol cleaved, with $6MPH_4$ or $DMPH_4$ as cofactor, respectively).[443] Solubilization of the hydrophobic substrates requires the inclusion of ethanol in these assays. A modified version of the NADH-coupled assay, using ≤ 0.18% w/v of the detergent Mega-10 to solubilize substrates, can be carried out in otherwise aqueous conditions and has been used in the largest single comparison of different lipid substrates.[447] The substrates have been shown to be in micelles under these conditions.[448] Other assays include enzymatic detection of the released glycerol, detection of the aldehyde product as the *p*-nitrophenylhydrazone derivative,[441] and determination of phosphate released from cleaved *lyso*-phospholipids (*vide infra*) in a phospholipase-coupled assay.[449]

The purified rat liver enzyme migrates as a 400 kDa band on Sepharose 6B, with a monomer weight of 45 kDa.[444,446] No clones of this enzyme have been

reported. A dependence upon iron would certainly be expected by analogy to the aromatic amino acid hydroxylases and might be inferred from the sensitivity of the enzyme to KCN[444] and *o*-phenanthroline (to which it is noticeably less sensitive than PAH).[447] GEM is partially inactivated by the thiol-modifying reagents *N*-ethylmaleimide and *p*-chloromercuribenzoate.[444]

Most of the studies with this enzyme have focused on the lipid substrate specificity. As has been alluded to above, at least one free alcohol group is required on the glyceryl or glycol moiety.[443,447] The alkyl group specificity is not stringent: unbranched C14−C18 give about the same activity with microsomes.[441] The solubilized enzyme's 1-*O*-alkyl specificity is rather shallow, with C16 > C18 > C6 > C14 > (C12 ∼ C7 ∼ C8) ≫ C9, with C5 and C3 at zero. All but the last three are within a factor of 4 of the optimal activity with chimyl alcohol. The 1-*S*-octadecyl derivative is cleaved at a slightly lower rate by GEM,[450] but the enzyme is unable to hydroxylate 1,2-dihydroxyhexadecane.[447] No discrimination between the D- and L-isomers of batyl alcohol can be detected.[441] The 2-*O*-heptadecyl compound has a *higher* microsomal activity than its chimyl alcohol isomer.[438,451]

The identity of the pterin cofactor for GEM has been presumed to be BH_4, given its location in mammalian liver where high amounts of that cofactor are available to PAH. At pH 8.7 and 25 °C with Mega-10-solubilized GEM and batyl alcohol (C18) as substrate, BH_4 has $K_m = 25\ \mu M$, $V_{max} = 31$ nmol $min^{-1}\ mg^{-1}$; $6MPH_4$ has $K_m = 87\ \mu M$, $V_{max} = 22$ nmol $min^{-1}\ mg^{-1}$; and $DMPH_4$ has $K_m = 270\ \mu M$, $V_{max} = 30$ nmol $min^{-1}\ mg^{-1}$.[447] Comparable results were obtained for the glycol−ether activity, using microsomes and 2-(hexadecyloxy)ethan-1-ol as substrate. GEM was inhibited by 2,4,5-triamino-6-hydroxypyrimidine ($K_I = 0.24$ mM), a pterin analogue of considerable importance in the mechanistic study of PAH (section III.D). This pyrimidine apparently functions as a cofactor in the reaction, with low activity (0.1 nmol $min^{-1}\ mg^{-1}$) and highly uncoupled (5−18 NADH oxidized per ether cleavage) turnover.[443]

The physiological function of GEM is still unknown, partly because glyceryl−ether-containing lipids are relatively unusual. Platelet aggregation factor (PAF) is perhaps the best-known glyceryl-ether lipid. In addition to the function implied by its name, PAF also affects allergic reactions, inflammation, fertilization, fetal development, and blood pressure and may be involved in cardiovascular, renal, and pulmonary disorders. Essential features for the bioactivity of PAF include the 1-*O*-alkyl group and a 2-acetyl group. PAF is released by IgE-stimulated basophils, which mediate inflammatory responses.[452]

lyso-PAF (see Figure 14 for the structure of this compound) is generated in the penultimate step of PAF biosynthesis by deacylation of a long-chain 2-acyl neutral storage form.[453] The optimal GEM substrate contains the same alkyl group as PAF; *lyso*-PAF is a substrate for GEM.[454] GEM has been proposed to have a role in lowering the pool of *lyso*-PAF, but its limited tissue distribution would seem to preclude participation in the inflammatory response mediated by metabolism of PAF.[453]

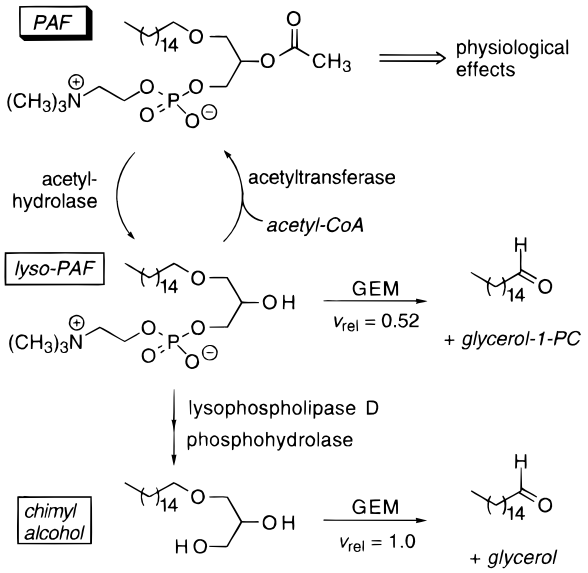

Figure 14. Platelet aggregation factor and GEM.

Tumor cells contain large amounts of glyceryl-ether lipids (1−5% total lipids are alkyl glyceryl ethers in human tumor cells, compared with <1% in normal cells; both are somewhat lower in rat).[455,456] Remarkable cytotoxic effects can be achieved (by an unknown mechanism) in these GEM-deficient cells by treatment with several lipid analogues.[457,458] Recently it has been suggested that the accumulation of ether lipids is due to increased uptake by cancer cells rather than a catabolic deficit in GEM.[459] It may also be that glyceryl-ether lipids, which are uncleavable and therefore inert if three alkyl groups are present,[458] have no metabolic role in liver and are simply prevented from accumulating there by GEM.

2. Other Hydroxylases [EC 1.14.16.3 and 1.14.16.6]

An inducible mandelate 4-monooxygenase (EC 1.14.16.6) having an absolute requirement for NADPH, Fe^{2+}, and a reduced tetrahydropterin ($DMPH_4$ was twice as active as THF) has been reported in *Pseudomonas convexa* and purified 26-fold. This enzyme differs from the other members of the 1.14.16 class in that it requires NADPH for the hydroxylation step itself, as distinguished from the recycling of the reduced pterin by DHPR.[460]

The similarly inducible, apparently Fe^{2+}- and tetrahydropterin-dependent benzoate-4-hydroxylase (from *Aspergillus niger*[461] and a soil pseudomonad[462]) and anthranilate 2,3-dioxygenase (*Aspergillus niger*) have also been reported by the same group.[463] The anthranilate-metabolizing enzyme is apparently identical to anthranilate 3-monooxygenase (EC 1.14.16.3), which is classified as forming 3-hydroxyanthranilate.

These enzymes (Figure 15) are apparently components of a degradative pathway in the organisms that contain them, a function ordinarily carried out by flavin-containing monooxygenases and the non-heme iron-dependent intra- and extradiol dioxygenases. None of the three enzymes appears to contain flavin or heme when purified, on the basis of their lack of an optical spectrum, and all are unambiguously stimulated to varying degrees by iron.

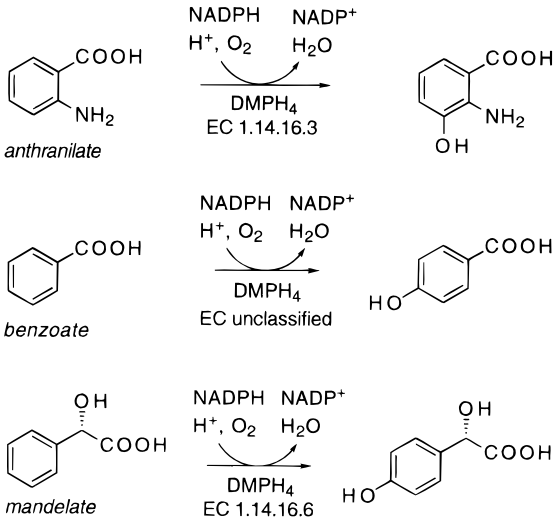

Figure 15. Other apparently pterin-dependent hydroxylases from soil organisms.

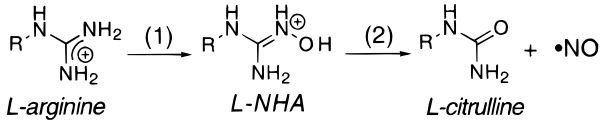

Figure 16. NOS reaction.

3. Nitric Oxide Synthase [EC 1.14.13.39]

After Tayeh and Marletta's observation of a BH_4-dependent stimulation of macrophage NOS,[464] and the recognition by Kwon *et al.* that nitrogen oxide formation by macrophages was stimulated by reduced biopterin,[465] a steady ~1% of Medline entries mentioning nitric oxide also discuss pterins. The unusual role of BH_4 in this system has revived interest in many clinical observations concerning pterin and immune responses in particular, which is discussed very briefly here and in section III.A.1. The interested reader is referred to several of the many reviews available on the topic,[466−468] some of which focus specifically on the biopterin issue.[469,470]

The tight association of BH_4 with NOS has caused quite a bit of excitement, because it appears to be necessary for maximal NOS activity (Figure 16) but does not appear to function in the manner of the aromatic amino acid hydroxylase coenzyme. The most striking difference is that the tightly associated (0.1 μM) BH_4 does not dissociate from NOS for >15 turnovers, indicating that BH_4 is not likely to be used as a source of the reducing equivalents consumed during •NO synthesis.[471] BH_4 induces tight coupling between NADPH oxidation and •NO formation,[472,473] which results from an unusual five-electron oxidation from arginine by way of N^G-hydroxy-L-arginine (L-NHA).[474] Moreover, while $6MPH_4$ can partially replace BH_4, 5-deaza-$6MPH_4$ does not lead to the same activation, indicating some role for biopterin's redox behavior.[472]

There is no indication that BH_4 dissociates during turnover, and half an equivalent of BH_4 per subunit (reported BH_4:NOS stoichiometries vary, but are ≤1 BH_4:subunit) may in fact be required for the stability of the NOS dimer.[475,476] Urea can be used to dissociate the dimer, which occurs concurrently with loss of BH_4 from NOS. (A significantly higher concentration of urea is necessary to inhibit NOS's reductase activity.) A ~30% reactivated enzyme can be reconstituted from the inactive, urea-dissociated monomers in the presence of BH_4 and NOS's other cofactors.[475]

Determining which of these cofactors (BH_4, NADPH, FMN, FAD, and protoporphyrin XI-heme iron) are involved in the two oxidations is a matter of great interest. Addition of CO inhibits both steps of the NOS reaction (*i.e.*, using either L-arginine or L-NHA as substrate), indicating the involvement of the heme in both oxidative steps.[477]

The second step, which is normally conversion of L-NHA to citrulline and •NO, can be performed anaerobically by addition of H_2O_2 to L-NHA and ferric NOS, yielding citrulline and NO^- (which binds the ferric heme). Under aerobic conditions the reaction is stimulated modestly by BH_4, and the iron−NO complex breaks down into NO_2^-/NO_3^-. The first step in Figure 16 has been envisioned to recapitulate the mechanism of cytochrome P450 hydroxylations, including the generation of a high-valent iron−oxo species (PPIX-Fe^V=O, *etc.*), which attacks the L-arginine substrate to yield L-NHA. However, L-arginine was not a substrate with *tert*-butyl peroxide, cumene hydroperoxide, H_2O_2, or iodosylbenzene as oxygen atom donor, indicating that the first step may *also* require one of the non-heme components of NOS.[478]

Recently Campos *et al.* investigated the first reaction under single-turnover conditions in the absence of NADPH, which is absolutely required for the second step.[479] Conversion of 0.16 equiv of L-[^{3}H]-arginine to L-[^{3}H]NHA by stoichiometric amounts of rat brain NOS was observed, in an O_2- and Ca^{2+}/CaM-dependent reaction. Added BH_4 stimulated the reaction 3-fold, while CO and ferricyanide inhibited the reaction. While ferricyanide is known to oxidize BH_4 rapidly (section III.B.4) the addition of more BH_4 to ferricyanide-treated NOS did not restore activity. The authors rule out heme, flavin, NADPH, and photoreduction as the unknown NOS-bound reductant, but not BH_4, which is present in these experiments at 0.3−0.4 mol per mol of NOS subunit (*i.e.*, more than the number of electron equivalents required to produce the observed amount of L-NHA).[479] A very recent report suggests that NOS reduces *q*-BH_2 (and not 7,8-BH_2) to BH_4 using its flavoprotein "diaphorase" activity, which is present within the reductase domain.[480] It will be interesting to learn if and how BH_4 participates in the early steps of •NO synthesis, particularly *when* in the sequence of NOS's chemical transformations it is most necessary.

III. Pterin Biochemistry

A. Distribution

1. Mammalian Tissues: Biosynthesis and Salvage

BH_4 is a required cofactor for the aromatic amino acid hydroxylases, glyceryl-ether monooxygenase, and for NOS. The full complement of the three BH_4-synthesizing enzymes (Figure 18), GTP cyclohydrolase I (GTPCH; EC 3.5.4.16), 6-pyruvoyltetrahydrobiopterin synthase (6-PTPS; EC 4.6.1.10), and sepiapterin reductase (SR; EC 1.1.1.153), can be found in a range of tissues that contain BH_4: liver, kidney, adrenal gland, thymus, spleen, bone marrow, small intestine, heart, lung, and testis.[481,482]

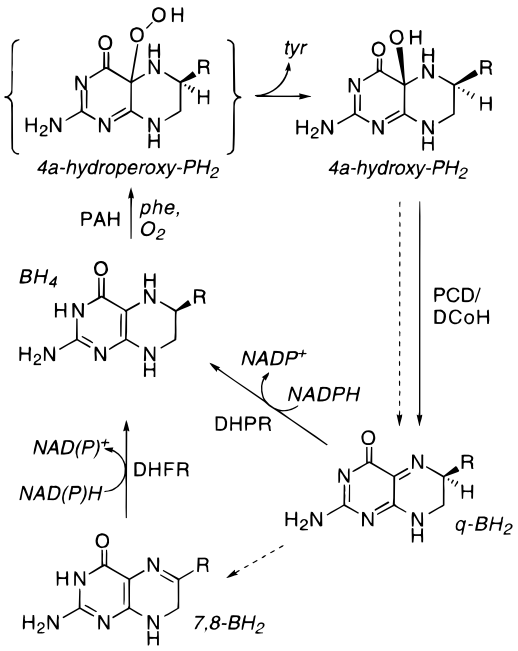

Figure 17. Salvage pathway for BH_4 that operates in hepatocytes.

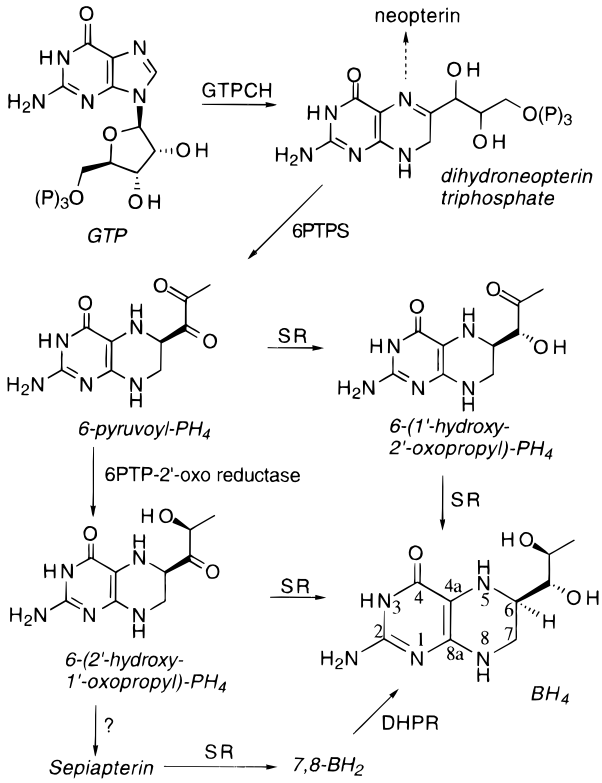

Figure 18. *De novo* biosynthesis of BH_4.

The salvage pathway (Figure 17) consists of pteridine 4a-carbinolamine dehydratase (PCD, EC 4.2.1.96), the NADH-dependent dihydropteridine reductase (DHPR, EC 1.6.99.7), and in a limited role, the NADPH-dependent dihydrofolate reductase (DHFR, EC 1.5.1.3). DHPR is not part of the normal pathway, but is capable of reducing any 7,8-BH_2 that may aberrantly form from *q*-BH_2 isomerization.[483] As can be seen in Figure 18, the BH_4 biosynthetic scheme involves only reduced forms of the pyrazine ring, which is formed from the pyrrolidine ring of GTP by GTPCH-catalyzed ring expansion. Hence DHPR (or DHFR) is not normally involved in *de novo* BH_4 biosynthesis, despite its central role in the BH_4 salvage pathway.[484,485] GTPCH, the "branchpoint" enzyme, catalyzes the first committed (and rate-limiting) step of BH_4 synthesis, which is the only step of either the *de novo* or salvage pathway known to be posttranslationally regulated.[486,487]

As would be expected, DHPR is found primarily where its hydroxylase cofactor-regeneration role is required: it is most prominent in brain stem, cerebellum, liver, kidney, adrenal gland, and small intestine, each of which is sympathetically innervated or performs L-Phe catabolism (ref 488 and refs 7−10 therein for activity correlations). The same is generally true of PCD, which is found in liver and kidney but is largely absent from brain;[489] the other role of the dehydratase is to facilitate tissue-specific transcriptional activation by hepatocyte nuclear factor 1α.[490,491] It was originally referred to as PAH-stimulating protein before the nature of its reaction was known, since it was first recognized as a nonredox stimulator of PAH activity in liver extracts.[492,493]

Many of the tissues that contain BH_4 biosynthetic enzymes, but not DHPR, are involved in cytokine-directed cell differentiation (*i.e.*, hematopoiesis and T cell proliferation),[494] some of which also express NOS when fully mature. One of the many physiological roles of •NO is cell-killing mediated by the inducible macrophage isoform of NOS. Human monocytes and macrophages produce neopterin (which has no known physiological role) after stimulation with interferon γ (INF-γ),[495] which increases GTPCH activity.[496] Neopterin appears in the urine of people with cancer, AIDS, viral or bacterial infections, arthritis, and lupus. Neopterin production appears to be primarily limited to human macrophages, which do not contain 6-PTPS.[494] Neopterin may be produced because the relatively low level of 6-PTPS is saturated by its substrate, 7,8-dihydroneopterin triphosphate, which is the product of GTPCH,[497] and is in turn converted into 7,8-neopterin by phosphatases.[496] INF-γ also induces macrophage NOS,[498] which would suggest tandem induction of the components of the BH_4•iNOS complex.

Cytokines may also affect pathways that require BH_4 in its hydroxylase cofactor capacity. As was discussed in section II.C.2, TrpH and GTPCH are induced in parallel in SCF-treated mast cells, which produce serotonin. In addition to INF-γ, GTPCH is activated in fibroblasts by tumor necrosis factor α,[499] and by INF-3.[349] The induction of GTPCH activity is slow, which suggests protein synthesis may be required. SR is induced in phytohemagglutinin-stimulated human T lymphocytes,[494] but not in macrophages, which like the lymphocytes constitutively contain large amounts of SR.[496]

In contrast to the erythroid cell lines, GTPCH appears to be constitutively expressed in liver, adrenal medulla, and brain,[500] as the first step in the *de novo* pathway for BH_4 biosynthesis (Figure 18). The GTP saturation curve of mammalian GPTCH is sigmoid, corresponding to a Hill coefficient of 2.3−2.9.[487,501] This may afford some degree of regulation, but there is ordinarily enough GTP present in PC12 cells to activate GTPCH completely.[487] A different regulatory interaction that may affect the activity of

constitutive liver GTPCH is discussed in the next section.

The next enzyme in the pathway, 6-PTPS, is found in human liver, pituitary, and erythrocytes. Again, 6-PTPS levels appear to be so low as to be rate-limiting in humans, where the chemical and metabolic instability of 6-PTP can lead to the accumulation of neopterin.[502] In human liver or cultured liver cells, the K_m of 6-PTPS for its substrate is a relatively high 10 μM.[503,504] The next enzyme, SR, is abundant in many tissues. There is also a very small amount of a 6-PTP reductase that reduces the 2′-oxo group of 6-PTP. Its scarcity is evident from the 50000-fold purification from human liver to homogeneity that has been reported.[505] SR and this aldol reductase are the only enzymes not yet associated with a form of HPA or PKU.

As had been predicted,[75,506] deficiency of one or more of the BH_4-synthesizing enzymes leads to one of a set of very rare hyperphenylalaninemias associated with grievous developmental and neurological effects ("lethal" or "malignant" PKU). These disorders do not respond to treatment with a phenylalanine-restricted diet.[2] Of these, the majority of the 263 known cases have been due to 6-PTPS deficiency (57%), followed by DHPR (33%) and GTPCH (3%) deficiencies. In addition, some 3% have PCD deficiency (primapterinuria) and 4% unclassified atypical PKUs.[507,508] Diagnostic procedures for each of these conditions have been developed, most of which are based on failure to respond to normal PKU therapy, and biochemically, on increased excretion of accumulation and degradation products of the deficient enzyme's substrate.[2]

In contrast to malignant PKU caused by GTPCH, 6-PTPS, or DHPR deficiency, deficiency of PCD causes a mild hyperphenylalaninemia associated with the excretion of elevated amounts of 7-BH_4 (section III.B.6).[509]

GTPCH and DHPR are also important in folate homeostasis, which suggests a need for additional supplementation of folinic acid when one of these enzymes is lacking.[510] No deficiency in xanthine oxidase occurs in GTPCH-deficient malignant PKU, which suggests that its essential molybdopterin cofactor is not generated, a product of *de novo* BH_4-biosynthesis pathway.[511] A deficiency of GTPCH causes L-Dopa-responsive dystonia (Segawa's disease; Section II.B.1) in heterozygotes.[203]

Recently ≤3.0 Å-resolution X-ray crystal structures of the non-cooperative[512] *E. coli* GPTCH,[513] rat liver 6-PTPS,[514] and rat PCD/DCoH[95,96] have been determined, joining the older structure of rat liver DHPR.[515]

2. BH_4 Homeostasis

BH_4 has long been known as an inhibitor of PAH activation, a role discussed particularly in section II.A.3.4. What has not been understood is the complementary relationship between cofactor levels and the fluctuating need for catabolic activity. There is plenty of PAH capacity theoretically available in a normal mammalian liver, and amounts of PCD and DHPR sufficient to prevent either from rate-limiting L-Phe hydroxylation under normal conditions. How the constitutively expressed biosynthetic enzymes manage to replenish the liver's (and perhaps brain's) need for BH_4 without accumulating a needlessly large amount of this PAH inhibitor has been unclear.

Recently a GTPCH-binding protein, p35, was identified in the 100000*g* supernatant of rat liver homogenates. In the presence of ≤7 μM BH_4, p35 inhibits GTPCH in a dose-dependent manner, with $EC_{50} = 2$ μM (0.1 mM GTP), and copurifies with GTPCH in gel filtration experiments. This level of BH_4, which gives maximal inhibition of GTPCH by p35, is close to the liver concentration, 6−9 μM.[119,500]

In the absence of BH_4, p35 does not bind to or inhibit GTPCH. If phenylalanine is added to p35/BH_4/GTPCH, GTPCH activity is restored without dissociating the p35-GTPCH complex. L-Phe has no effect on GTPCH velocity, but 10 mM L-Phe changes the shape of the GTP response curve from hyperbolic to sigmoidal (Hill coefficient 1.0 → 1.85).[516] This regulatory interaction on the rate-limiting enzyme of BH_4 synthesis has some remarkable similarities to the regulation of PAH by L-Phe and BH_4 (discussed in sections II.A.3.3−5). Mitnaul and Shiman have suggested that $PAH^T \cdot BH_4$ and PAH^R_{L-Phe} might be the negative and positive effectors, respectively, of GTPCH and/or p35 *in vivo* (*vide infra*).

In combination with the remarkably intricate regulatory system exerted on PAH by its substrates (Figure 6), these protein−protein interactions might be sufficient to explain several clinical effects of phenylalanine loading on BH_4 levels, summarized by Harada *et al.*:[516]

- An oral phenylalanine load causes an increase in BH_4 levels in normal individuals.[517]
- Hyperphenylalaninemic individuals have high BH_4 levels.[517]
- An oral phenylalanine load fails to cause an increase in BH_4 levels for individuals with partially defective BH_4 synthesis, indicating that phenylalanine might normally stimulate some component of the BH_4 biosynthetic machinery.[518]
- Plasma phenylalanine and neopterin levels are linked in cases of 6-PTPS deficiency, indicating that BH_4 biosynthesis is activated at the level of GTPCH.[519]
- An oral phenylalanine load increases plasma phenylalanine (to 1 mM) in register with neopterin.[520] This level of phenylalanine is sufficient to activate PAH directly and relieve p35-mediated inhibition of GTPCH.

The p35 regulatory system responds to a concentration of BH_4 that is near the concentration of the complex formed between BH_4 and PAH (sections II.A.3.4 and II.A.3.6). This complex is dissociated during PAH turnover, which would cause a quick rise in the amount of available BH_4, and presumably p35-dependent GTPCH inhibition, at a time one would expect *de novo* synthesis to be maximally beneficial. At other times, it is unclear if free BH_4 concentrations ever reach the amounts required to inhibit GTPCH catalysis, especially if there is rarely an excess of BH_4 over PAH available in solution. (In a related issue, it is unclear how the pterin-dependent liver enzyme GEM can function in the absence of free BH_4.) Mitnaul and Shiman's study of BH_4-dependent PAH regulation does not rule out the possibility (however

unlikely) that it is the *complex* of BH_4 and PAH that mediates p35-dependent inhibition.[119] The addition of protein−protein interactions to this already-complicated regulatory scheme is not yet required by the data, but they would certainly be available *in vivo*.

DHPR was first separated from PAH as a stable, NADPH-oxidizing activity in sheep liver extracts that lacked PAH.[18] Sheep liver DHPR was thus the first PAH accessory protein recognized and purified.[521] Later work showed that DHPR is an NAD(P)H-dependent reductase.[522] Several high-resolution crystal structures of DHPR have been solved recently, and it has been learned that the protein is structurally more similar to glutathione reductase, a flavoprotein reductase, than DHFR.[94,515] The difference between reductase structures is intriguing, because their substrate specificity does not overlap, despite the similarities of their substrates. As was mentioned above, DHPR is specific for the 5,6-dihydro, "quinonoid" isomer of dihydropterin, while DHFR recognizes 7,8-XPH_2 and dihydrofolate.[76]

Kidney contains PCD and DHPR that presumably support the activity of the PAH located there.[42] PC12 cells, and by extension the adrenal chromaffin cells, contain inducible GTPCH which appears in tandem with TyrH when the cells are stimulated.

The demands upon the BH_4-generating systems are apparently less taxing in brain, which does not contain appreciable amounts of PCD in the regions associated with TyrH and TrpH, other than in the pineal gland.[489] One would infer that the slower, nonenzymatic dehydration rate is sufficient to support maximal catalysis, but it is also reasonable that these neurons could rely upon the *de novo* BH_4 biosynthesis pathway to a greater extent. The other role of PCD, as the transcriptional activator DCoH, which participates in the HNF-1α-regulated expression of genes involved in gluconeogenesis, glycolysis, and blood clotting, probably precludes brain expression. No problems stemming from defective HNF-1α regulation that might be attributable to a malfunctioning PCD/DCoH are as yet known in the small number of primapterinuric (7-BH_4-excreting) patients.[523]

3. Other Organisms

Biopterin was first isolated as the liver factor essential for the growth of *Crithidia fasciculata*,[524] an organism that may be unique in using BH_4 in the synthesis of the pyrimidine precursor orotic acid.[525] The fully ring-oxidized biopterin was isolated at about the same time in a study of *Drosophila* eye pigments.[526] Various other pteridines are found in insect pigments, algae, *E. coli* DNA photolyase, and the ubiquitous molybdopterin enzymes.[527−529] ("Pterin" is derived from the systematic name for butterflies, which in turn is from the Greek word for wing, *pteron*: pterins are butterfly wing pigments.)[530,531]

B. Solution Studies

1. General Properties

Much of pteridine chemistry has relied upon classic structure-determination methods, principal among them UV/vis absorption spectroscopy, now supplemented by ^1H and ^{13}C NMR spectroscopic studies. Characteristic absorbances have been most important for locating the heterocyclic double bonds, which can adopt a variety of pH-dependent tautomers when the ring is partially reduced. Oxidized pterins have higher wavelength absorptions than the tetrahydropterins, which lack visible absorptions. The more extensively conjugated dihydropterins are yellow, with characteristic bathochromic shifts occurring upon isomerization of the initial pterin oxidation product, *q*-BH_2 (N^8−H tautomer of 5,6-dihydrobiopterin[532,533]), to the more stable 7,8-BH_2.[534] This dihydropterin rearrangement is buffer-catalyzed, with rate-limiting C^6−H bond cleavage (k_H/k_D values range from 10.0 to 12.0 depending on buffer and pH).[535] (A different rearrangement occurs with 6-hydroxy-PH_4 and BH_4,[536] discussed below.)

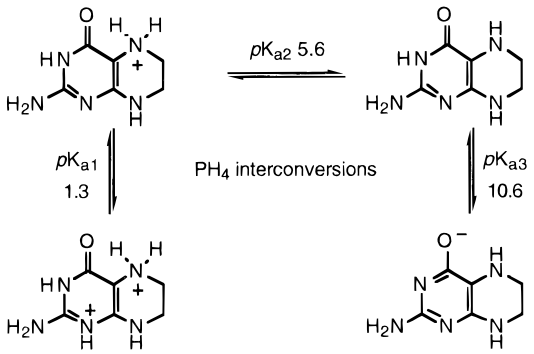

Figure 19. Ionizable groups present on the pterin ring.

An ^{15}N NMR-based absolute determination of the tautomeric form of *q*-$DMPH_2$ was possible because of the large isotope effect: *q*-[6,7-^{2}H]$DMPH_2$ is stable for >6 h at 4 °C in dilute buffer.[533]

The protonation of the nitrogens in the pterin ring follows the same general order in the dihydro- and tetrahydropterin series, only the latter of which is shown (Figure 19). In addition to the equilibria indicated in the figure, there is an additional transition at pH = −6, corresponding to protonation of the exocyclic O^4 position of PH_4. The PH_4 pK_a at 1.3 shifts to pH = −3.5 in dihydropterin but the precise structure of the protonated species is unclear.[172]

In the crystal structures of 5-formyl-$DMPH_4$,[537] 5-methyl-$DMPH_4$,[538] and the related 5,10-methylene-tetrahydrofolate,[539] N^8 and C^7 are coplanar with the flat pyrimidine ring while C^6 is above the plane of the pyrimidine ring (0.84, 0.60, and 0.08 Å, respectively), in a hemichair conformation. In 7,8-$6MPH_2$, the entire pteridine ring is flat.[540] The tetrahydropyrazine ring of tetrahydropterins has been shown by ^1H or ^{13}C NMR to adopt two interconverting half-chair conformations in solution,[541−545] a conclusion apparently at variance with the planar molecule observed crystallographically. Depending on the identity of the 6- and 7-substituents, coupling constants indicate that the 6 side chain prefers the equatorial position ($6MPH_4$) or there will be rapid interconversion between the two conformations ($DMPH_4$).[542,544,546]

A more recent ^1H NMR analysis of $6MPH_4$, $7MPH_4$, and the *cis*- and *trans*-$DMPH_4$ isomers showed unusually small *trans* $^3J_{HH}$ values for all but the *cis*-$DMPH_4$ (8.3−9.1 Hz *vs* 11.3−11.6 Hz calculated) interpreted to arise from hyperconjugation of the

axially oriented C^7-H to the π orbital formed by $N^8-C^{8a}=C^{4a}-C^4=O$. These *trans* $^3J_{HH}$ values are higher than the ~6.8 Hz that would be expected from rapid interconversion between axial- and equatorial-CH_3 conformations. From the effect of partial deuteration on the NOE data and T_1 values of $6MPH_4$, 6,7-interproton distances were calculated. By using the differential chemical shift susceptibilities of the two C^7 protons to N^5 deprotonation, an additional geometric constraint was obtained: the ratio of the distances from N^5 to *pro*-(*R*)-H^7 and to *pro*-(*S*)-H^7.

From this evidence, Williams and Storm reasoned that (1) there is a single conformer of either monomethylated tetrahydropterin with the CH_3 group preferring an equatorial position and (2) that the tetrahydropterin ring is planar except for C^6,[547] in agreement with the crystal structures.[548] In general, conformational analysis of tetrahydropterins using NMR tends to suffer from the difficulties posed by rapid exchange at N^5 and N^8. The possibility that the conformational flexibility of tetrahydropterins may be limited, and thereby able to affect its reactivity, has been raised[549,550] and discounted[551,552] in a primarily computational vein.

Pterins can self-associate in two ways, by stacking and by hydrogen-bond pairing. The first of these is evident from the difficulty of dissolving some solid pteridines in water. Dissolution generally requires that one or more of the heterocyclic nitrogens be protonated first, in order to disrupt strong intermolecular interactions. The second, and more significant, type of dimer formation was discovered in an NMR study of several folates. The concentration dependence of the p*K* and chemical shift values for dihydrofolate gave a dissociation constant of 39 mM for the neutral form, with dimerization proposed to arise from a head-to-tail aromatic stacking interaction. It appears that the dimers are in rapid equilibrium with monomers at 23 °C.[553]

The possibility that dimers can form in solution allows many additional mechanistic possibilities to enter the discussion of model pterin reactivities that follows. As a result, some of the conclusions drawn from solution studies are of uncertain relevance to the enzyme−pterin complexes, where it is unlikely that pterins can interact. Nevertheless, the studies discussed below are useful in gauging the reactivity of reduced pterins with oxidants and electrophiles and understanding the chemistry of the resulting oxidized pterins and pterin adducts.

2. Synthetic Methods

A comprehensive review of the field of pteridine synthesis is beyond the scope of the present review, especially since several extensive reviews are available.[531,554] Instead, Figure 20 presents a small but significant sample of this chemistry. The key step in the standard Gabriel−Isay methodology for synthesizing pteridines,[555,556] condensation of a 5,6-diaminopyrimidine with a 1,2-dicarbonyl compound, is indicated in Figure 20A.[557] Because of the limited substituent-directing effects of the Isay reaction used in a majority of the syntheses of pterins from pyrimidines, the early preference was for the symmetrically disubstituted $DMPH_4$ as a cofactor analogue, rather than attempting to separate $6MPH_4$ from $7MPH_4$.

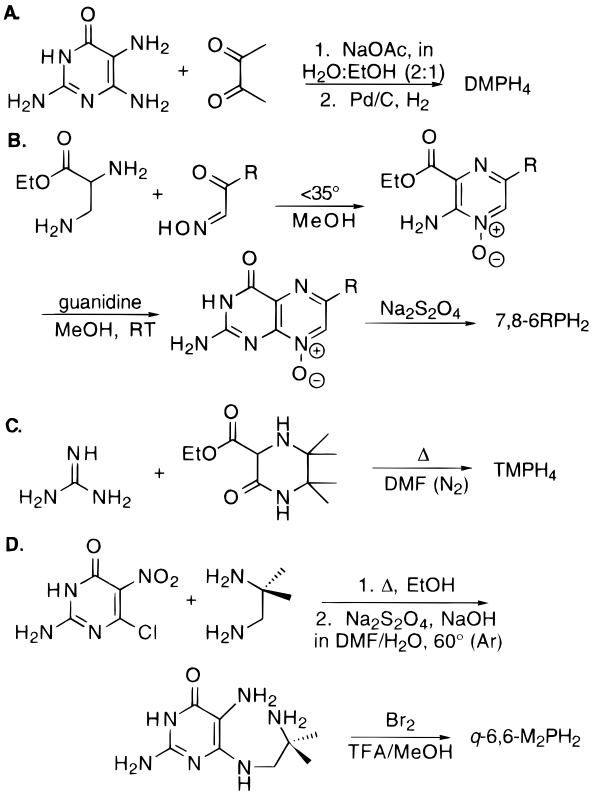

Figure 20. Synthesis of pterins.

This preference for $DMPH_4$ was largely reversed when Storm and co-workers developed a method for selective crystallization of 6-methylpterin and 7-methylpterin from the 3:1 condensation product mixture,[558] which remains the preferred synthetic approach. A slightly more elaborate, unambiguous synthesis of $6MPH_4$ (Figure 20B) was developed shortly thereafter.[559] This approach bypasses the synthetic route through a pyrimidine that is usually taken, at least with pterins of interest to the hydroxylase community. A related example of pyrazine elaboration was provided by Eberlein and co-workers (Figure 20C) in their synthesis of 6,6,7,7-tetramethyltetrahydropterin ($TMPH_4$),[172] which cannot isomerize to the 7,8-dihydropterin because it lacks a proton at the 6 position. 6,6-Disubstituted pterins cannot be synthesized using Isay chemistry. Instead they are derived from 1) methyllithium treatment of TMS-protected $7,8-6MPH_2$ followed by deprotection,[560] (2) the reaction of guanidine with an elaborated pyrazine (Figure 20C),[172] or (3) condensation of a nitropyrimidine with a substituted diamine, followed by cyclization/Schiff base formation to the quinonoid dihydropterin (Figure 20D).[561] The last of these allows direct chiral synthesis (in better than 99.5% enantiomeric purity) of the 6-alkyl-PH_4 series, making these compounds available for further study. A key step in this case is reduction by sodium dithionite immediately following cyclization, before the initial quinonoid products rearrange to the achiral 7,8-dihydropterin.[562]

3. Reaction with O_2 and H_2O_2

Tetrahydropterins autooxidize fairly quickly in aerobic neutral solutions, yielding quinonoid dihydropterin and H_2O_2. This reaction is greatly inhibited if N^5 is protonated, as in the mono- or dication.

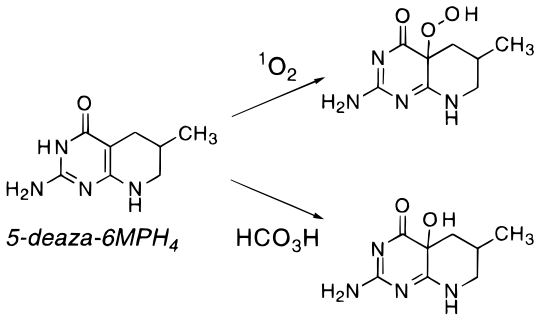

Figure 21. 5-Deaza-6MPH$_4$ and its 4a adducts.

Replacement of N^5 with a methylene (the strong competitive hydroxylase inhibitor 5-deaza-6MPH$_4$, Figure 21) renders the reduced pterin oxygen stable.[563] The large increase in reduction potential (the two-electron reduction potential *vs* NHE for 6MPH$_4$ = +0.14 V, 5-deaza-6MPH$_4$ = +0.85 V; pH 9.0, 0.1 M borate[563]) is consistent with this observation.

The electron density located at N^5 further increases the reactivity of the C^{4a} position, which even in 5-deazatetrahydropterin is attacked by electrophiles; alkylation or acetylation of the N^5 position stabilizes tetrahydropterins in oxygenated buffers. Calculations indicate that the maximum electron density in tetrahydropterins is at the C^{4a} position, which from all of the above evidence is proposed to be the site of oxygen attack during nonenzymatic autooxidation and during enzymatic hydroxylation of substrates.[564]

^{13}C NMR of relatively stable 4a-adducts of 5-deaza-6MPH$_4$ shows little change from the parent compound other than the progressive deshielding of C^{4a} in the OH, Cl, and Br adduct series.[565] Conformational analysis indicates that the major *trans* isomer is in a pseudo-chair configuration, in which the (6*S*)-methyl substituent is equatorial to avoid steric interaction with the 4a(*S*)-substituent. The (6*R*)-methyl *cis* isomer, which has the same configuration at C^6 as BH$_4$, is forced into a distorted boat conformation to avoid an unfavorable 1,3-diaxial interaction with the 4a(*S*)-substituent.[566]

Treatment of 5-deaza-6MPH$_4$ with $^1O_2$ yields the C^{4a} hydroperoxide, obtained in good yield as a white crystalline solid. This compound, a close structural analogue of the organic hydroperoxide that has been proposed to mediate enzymic hydroxylation, was sufficiently stable under PAH assay conditions ($t_{1/2}$ = 5 min) to be tested for its ability to hydroxylate substrate. Such reactivity was not observed.[563]

The initial pteridine product of the enzymatic reaction was investigated by incubation of the enzyme with [4a-^{13}C]6MPH$_4$.[567] A single adduct resonance at 72.3 ppm was observed in the ^{13}C NMR spectrum, under conditions that stabilize the 4a-carbinolamine hydrate of *q*-6MPH$_2$ (0 °C, 20 mM Tris pH 8.0; cold CD_3OD was added and the spectra acquired at −30 °C).[568] This chemical shift is close to the C^{4a} of the reduced oxygen adduct in bacterial luciferase (74 ppm)[569] and in 5-acetyl-4a-hydroxy-4a,5-dihydroflavin (71.0 ppm).[570]

The configuration of the 4a-hydroxy-6MPH$_2$ product of the hydroxylation reaction was established using CD spectroscopy, in comparison with the resolved diastereomers of chemically synthesized 5-deaza-4a-hydroxy-6MPH$_2$. Absolute structural assignments were made using ^1H NMR of the 5-deaza

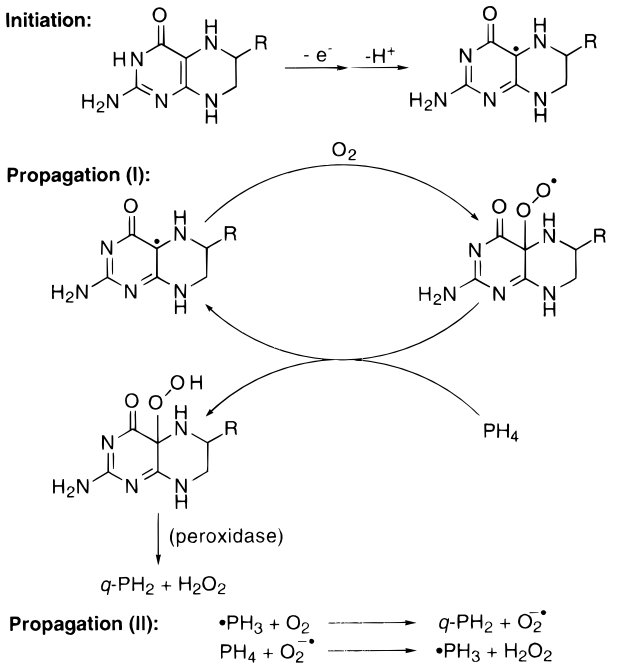

Figure 22. Autooxidation of tetrahydropterins in aerobic solutions.

diastereomers. A CD spectrum analogous to the 4a-carbinolamine product of the enzyme reaction was observed with 5-deaza-4a(*S*)-hydroxy-6(*S*)-methyl-PH$_4$, but it also closely resembled the 5-deaza-4a(*S*)-hydroxy-6(*R*)-methyl-PH$_4$ (apparently the 6-methyl group contributes little to the overall Cotton effect). Loss of the CD spectrum associated with the 4a-carbinolamine is observed in register with its dehydration (k = 0.042 min^{-1}), indicating that the majority of the signal is from the chiral alcohol. By inference, the enzyme adds the hydroxyl group stereospecifically to the *si* face. The source of the oxygen atom is O_2, demonstrated by enzymatic generation of the 4a-carbinolamine of [4a-^{13}C]6MPH$_4$ under $^{18}O_2$. A new peak, upfield-shifted by 0.023 ppm, appears in the ^{13}C NMR with a relative intensity that matches the 52:48 ^{18}O:^{16}O ratio of the phenolic hydroxyl of the tyrosine product.

Despite its formal classification as a monooxygenase, these experiments demonstrate that both L-Phe and 6MPH$_4$ are hydroxylated during PAH turnover.[571] TyrH also produces 4a-hydroxy-6MPH$_2$ as the first diffusible pteridine product of its reaction; it has been presumed that the cofactor oxidation and salvage proceeds in the same manner as with PAH.[572]

The nonenzymatic autooxidation of tetrahydropterins (dihydropterins are much less susceptible than tetrahydropterins to oxidation[16]) has been proposed to be a free-radical chain process initiated by reaction between O_2 and the electron-rich C^{4a} position, in which the O_2 is reduced by a single electron and a proton dissociates from the trihydropterin radical (Figure 22). Homolysis of the N^5−H bond was ruled out by equivalent rates in H_2O and D_2O.[72] [Determining the stability of quinonoid dihydropterins to oxidation is hampered by rearrangement to 7,8-dihydropterins, which can only occur if a proton is present at the 6-position (section III.B.5). The half-life of *q*-6,6-M$_2$PH$_2$ in 0.1 M Tris buffer, pH 7.4, at 37 °C is 1.25 h, in aerated DMSO at ambient temperatures is 48 h, in pH 6.8 phosphate buffer at

ice temperature it is >100 h.[561] This quinonoid dihydropterin is not known to be subject to the nonredox decomposition reactions shown in Figure 23. This is much slower than the autooxidation of [6,7-^{2}H]DMPH_4 in oxygenated Tris buffer, pH 7.6 at 25 °C, which has a half-life of 5.4 min (deuterated tetrahydropterin is used to minimize rearrangement of *q*-DMPH_2 to 7,8-DMPH_2, by exploiting the large isotope effect on that process; section III.B.1).[532]]

Following the initiation lag period, the autooxidation reaction is first order in O_2 and PH_4. It is not stimulated by irradiation, indicating that $^3O_2$ is sufficient for the reaction, and it is slightly faster at higher pH, which associates reactivity with increased C^{4a} electron density.[573] Oxygen is consumed during the propagation step by combining with the pterin radical, forming a C^{4a} hydroperoxyl radical that abstracts a hydrogen atom from another molecule of *X*PH_4 to regenerate the trihydropterin carrier and form a C^{4a} hydroperoxide. This hydroperoxide would then decompose into H_2O_2 and *q*-*X*PH_2.[554] Alternately, the propagation reaction could involve formation of superoxide and *q*-*X*PH_2 from electron transfer of the trihydropterin radical to O_2. The superoxide would then attack *X*PH_4 to regenerate the trihydropterin carrier, concomitant with H_2O_2 formation.[72,573] The primary difference between these proposals is the identity of the chain carrier, or whether an organic hydroperoxyl radical exists. *Neither* of the proposed hydroperoxide species has ever been directly observed, but the hydroperoxyl radical seems particularly unlikely in the light of evidence discussed in the following section.

During aerobic oxidations, a steady-state level of a red chromophore (λ_{max} = 550 nm) appears, the amount of which is not dependent on the P_{O_2} of the reaction. This species is proposed to be the intermediate trihydropterin radical,[72] which is wine-red in CF_3COOH.[574] No organic peroxides were detected by low-temperature TLC,[72] and pterin radicals generated by other oxidants (potassium ferricyanide, 2,6-dichlorophenolindophenol [DCIP]) were not scavenged by O_2,[575] ruling out an organic hydroperoxide as the chain carrier.

Both *X*PH_2 and *X*PH_4 can be oxidized by H_2O_2, but the reaction is much faster with *X*PH_4; a radical initiator may be required in each case. The product of 6MPH_4 treated with H_2O_2 in the presence of a radical initiator is *q*-6MPH_2, which was used in the recently reported first direct chemical synthesis of *q*-6MPH_2. The procedure involves a stoichiometric reaction of 6MPH_4 and H_2O_2 (in the presence of substoichiometric KI) in H_2O at 0 °C, from which crystalline *q*-6MPH_2 immediately precipitates.[576] This transformation is probably not relevant to pterin oxidations under physiological conditions.

Interestingly, whether the oxidation is by chemical or enzymatic means, the initial product of tetrahydropterin oxidation is invariably the quinonoid (or its hydrate, the 4a-carbinolamine), rather than the more stable 7,8-dihydropterin. It has been suggested that the greater resemblance of the half-chair solution conformation inferred for the quinonoid species to that of the tetrahydropterin, in comparison with the flat 7,8-dihydropterin, is the cause of this preference.[577] Direct evidence depicting the requirements for *X*PH_2 binding comes from crystal structures of DHPR, which discriminates between the two isomers. The structures of wild-type and mutant DHPR indicate that the quinonoid pterin binds at a site partially comprised of the nicotinamide portion of the NADH cofactor (which interacts with N^5), and the phenolic hydroxyl of Tyr146 (which interacts with O^2).[578] Presumably the alteration in the conformation (or basicity in the latter case, due to protonation of N^1) of these positions is sufficient to preclude binding of 7,8-*X*PH_2.

In studies of DHPR, it is necessary to oxidize tetrahydropterins cleanly to their quinonoid forms. Frequently the H_2O_2/peroxidase system is used to generate a continuous level of quinonoid dihydropterins,[522] which can also be formed by 2,6-dichlorophenolindophenol, $K_3Fe(CN)_6$, or ferricytochrome *c*. Hydroxylase-generated 4a-carbinolamine dihydropterins are not substrates for DHPR.[76]

4. Pterin Radicals

Some evidence for the formation of pterin radicals has been obtained by studying the oxidation of tetrahydropterins under conditions far removed from physiologically relevant pH and temperature values. Often the studies involve isolated pteridines, which means that the species generated are free to dimerize, *etc.*, which they are not able to do as part of the quaternary reaction complex formed during hydroxylation (section III.B.1). When exposed to radical initiators, a trihydropterin radical is generated that no longer is subject to the singlet-triplet barrier that reduces the reactivity of reduced pterins with O_2. As will be demonstrated, the loss of this barrier allows the thermodynamically favorable 2 e^- reduction of O_2 by *X*PH_4 (*vide infra*). Under such conditions, tetrahydropterin alone can cause the nonspecific hydroxylation of phenylalanine and other compounds in low yields that are not associated with an NIH shift and other features of the enzymatic reaction.[579]

Bobst generated an EPR-active organic radical by mixing either PH_4 or THF with 1−1.3 equiv of H_2O_2 at room temperature in a 6:1 mixture of CF_3COOH/CH_3OH. The EPR spectrum, acquired at liquid N_2 temperature, shows an unresolved hyperfine coupling to ^{14}N.[574] The calculated spin density was located primarily on N^5 in the cationic trihydropterin radical[577] as it was for the N^5-methyl analogue.[580] These results were confirmed and extended by H_2O_2 treatment of a range of pterins and pteridines, most of which contained *N*-methyl groups at various positions. The slow-developing yellow or red color persisted at room temperature for up to 30 min in CF_3COOH, suggesting a slow disproportionation rate for the generation of reduced and oxidized pterins under the conditions. It should be noted, however, that the authors did not identify the final pterin species present at the end of the reaction, so the occurrence of disproportionation is still an open issue. Experimental N^5 spin densities of the trihydropterin radical cations ranged from 0.31 to 0.53, somewhat more than the 0.26−0.44 observed for the monohydropterin radical cations.[581]

The relationship between the single-electron oxidation of reduced pterins and the rapid two-electron oxidation of *X*PH_4 by H_2O_2 in the synthesis of *q*-*X*PH_2

is unclear. Pterin radicals have only been studied under highly acidic conditions. At higher pH, the nearly instantaneous two-electron oxidation of XPH_4 by H_2O_2 (which may require a radical initiator) would prevail. By extension, for the enzymes to employ discrete pterin radicals, extensive protonation of the enzyme-bound XPH_4 would be required. These issues have not been confronted in mechanistic proposals for the aromatic amino acid hydroxylases that include discrete pterin radicals.[580] In large measure, the chemical resemblance between the cofactors of the unambiguously radical-based flavin-dependent hydroxylases and the pterin-dependent hydroxylases has encouraged these ideas. Of course, the presence of an additional conjugated ring in flavins greatly increases the opportunities for resonance stabilization of radicals in the central piperazine ring (especially if N^5 is also alkylated[582]). The peak-to-peak separation of the two-electron reduction of lumiflavin is 120 mV at pH 7.0, $K_{\text{comproportionation}} \approx 1 \times 10^2$, which indicates a moderately stable radical.[583] These similarities and differences are discussed in the following section.

Anaerobic treatment of $DMPH_4$ with ferricyanide, a single-electron oxidant, results in rapid formation of q-$DMPH_2$, which is 300-fold faster when a group with $pK_a \approx 5.6$ is deprotonated (at pH 8, 25 °C, the rate is 1.6×10^6 M^{-1} s^{-1}). This titrable group is probably N^5, which reemphasizes its importance in determining the redox potential and reactivity of tetrahydropterins. The second electron transfer and the loss of two protons were faster than the initial one-electron loss. Oxidation of $DMPH_4$ with the two-electron oxidant DCIP shows a 10-fold rate increase upon increasing the pH from 8.7 to 10.4. These investigators saw similar oxidations if ferric ammonium sulfate was substituted for the ferricyanide, again with a 2:1 Fe:$DMPH_4$ stoichiometry.[575]

A direct interaction of the iron site and the pterin was proposed to occur in the aromatic amino acid hydroxylases, originally envisioned as a direct Fe−N^5 interaction that leads to one-electron oxidation of the pterin ring, activating it for oxygen attack. In this early proposal, the interaction with O_2 was originally proposed to generate $HO^{\bullet}$, a very reactive species capable hydroxylating substrates.[580] Subsequent to that, it was realized (1) that the chemistry of PAH is inconsistent with $HO^{\bullet}$ formation (discussed in sections III.A.5, III.A.6, and III.B), and (2) that the hydroxylases require ferrous iron for activity and do not form ferric iron during normal turnover (once every ~150 turnovers ferric PAH is formed[116]), which vitiate the original proposal.

During the initial studies with the apparently copper-containing atypical PAH from *C. violaceum*, analogous mechanisms featuring Cu−tetrahydropterin complex formation were proposed.[182] An unsupported, isolated copper center is unlikely to generate a higher valent species than Cu^{3+} in the biological milieu, and as such is incapable of forming a multiply bonded species with oxygen atoms because of its filled π^* molecular orbitals (*i.e.*, "Cu^{IV}=O").[584] On the other hand, Cu^{2+} is known from model chemistry to coordinate the N^5 position in pterin analogues,[585−588] and $DMPH_4$ was demonstrated by multifrequency EPR to form a Cu^{2+}−N^5 adduct in *C. violaceum* PAH.[182]

A depiction of the thermodynamics of interaction of O_2 (or its reduced forms) with tetrahydropterin and its oxidized forms can be developed using electrochemistry. This can in turn be used to delimit possible outcomes of the O_2−$6MPH_4$ interaction. The instability of the initial quinonoid oxidation product to 7,8-dihydropterin formation requires that a stable quinonoid be employed in such studies. 6,6,7,7-Tetramethyl-5,6,7,8-tetrahydropterin ($TMPH_4$) was synthesized for this purpose, since it lacks a C^6 proton and should yield a stable quinonoid form. This compound is otherwise an ordinary tetrahydropterin, with familiar UV/vis features useful in determining that the pK_a values were nearly identical to the commonly used tetrahydropterins.[172]

As predicted, the quinonoid form (q-$TMPH_2$) was stable, although a slow ring contraction/decarboxylation process was observed (*vide infra*). This process did not preclude reversible electrochemistry, which was observed across a wide range of pH values. At all tested acidities, the single-wave, two-electron redox process was >98% reversible; the peak separation was 60−90 mV between pH 2.0 and −4.33. On the time scale of the cyclic voltammetry (2 mV s^{-1}), the reduction is slow under acidic conditions (pH = −6.6); oxidation is slow at neutral pH values (>5.8). Standard two-electron redox potentials were determined: $E° = +570$ mV, $E°' = +106$ mV *vs* NHE, or 35−60 mV lower than for $DMPH_4$, $6MPH_4$, and THF. From the $E°'$, the overall four-electron reduction of O_2 by $TMPH_4$ to yield q-$TMPH_2$ and H_2O is favorable, with $\Delta E = +660$ mV ($\Delta G° = -64$ kJ mol^{-1}) at pH 6.8.

While the blue semiquinone radical ($^{\bullet}TMPH_3$) was not observed electrochemically, it could be formed by mixing equimolar amounts of the fully reduced $TMPH_4$ and the electrochemically two-electron oxidized $TMPH_2$ and detected by either optical (2 mM final [$TMPH_x$], 1 M HCl) or EPR (14 mM final [$TMPH_x$], in 2:1 MeOH:CH_3COOH, or 30 mM final [$TMPH_x$] in CF_3COOH) methods. Quantitation using an approximate extinction coefficient at 475 nm or spin double integration yielded comproportionation equilibrium constants of 3.1×10^{-7} and 7.1×10^{-7}, respectively. These values indicate that the pterin radical is much less stable than the comparable flavin radical, 10^7-fold at pH 1.0 (10^2-fold at pH 7.0). The thermodynamics controlling $TMPH_4$ autooxidation and formation of reduced O_2 species can then be calculated:

reaction (2 e^-)	$\Delta E^{pH1.0}$	$\Delta G°,^{pH1.0}$
$TMPH_4 + O_2 \rightarrow q\text{-}TMPH_2 + H_2O_2$	+177 mV	−17 kJ mol^{-1}
$TMPH_4 + O_2 \rightarrow {}^{\bullet}TMPH_3 + O_2^{\bullet-}$	−765 mV	+74 kJ mol^{-1}

The observed rate for $TMPH_4 + O_2$, 5×10^{-3} M^{-1} s^{-1} at pH 1.0, yields a $\Delta G^{\ddagger} = +86$ kJ M^{-1}. Since $\Delta G° < \Delta G^{\ddagger}$ for both the one-electron and two-electron transfers, either reaction is thermodynamically feasible. The highly endergonic one-electron process predicts a diffusion-limited collapse into a semiquinone−superoxide radical pair (4a-hydroperoxy-$TMPH_2$) following the rate-limiting electron-transfer step.[172] This is thought to be analogous to the oxidation of an isolated FlH_2 by O_2; free in solution, flavins are more

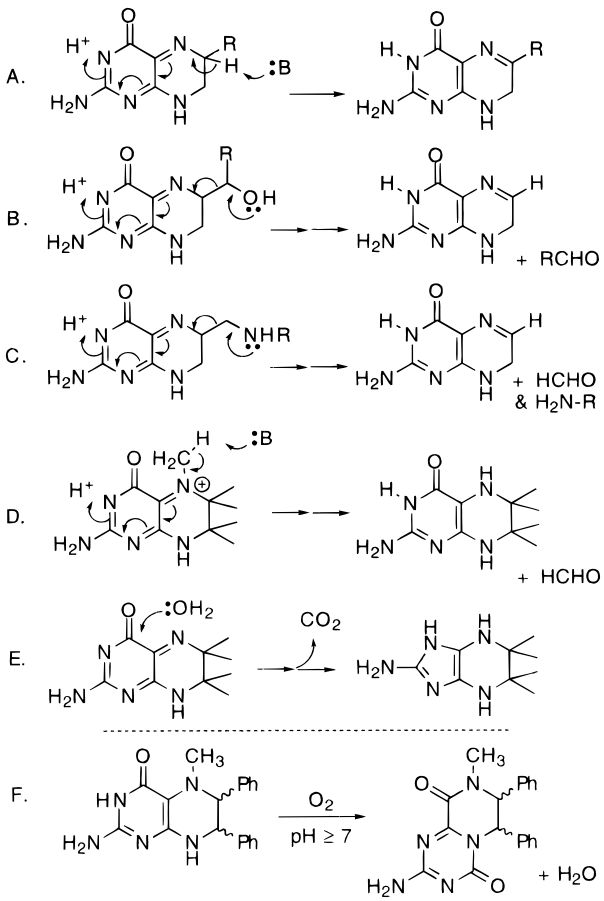

Figure 23. Decomposition of dihydropterins.

reactive with O_2 because of the greater stability of the FlH• radical (section III.C.1).[589]

The intermediacy of pterin radicals has also been invoked in the obligate prereduction of PAH by $6MPH_4$ or BH_4.[116]

5. Dihydropterin Rearrangements

The preferred tautomer of *q*-$6MPH_2$ is the *ortho* (*endo para*) tautomer, determined by absorption and reactivity studies of various $DMPH_4$ derivatives[532] and in low-temperature ^1H and ^{15}N NMR studies performed in dilute buffers, conditions that minimize rearrangement to 7,8-$6MPH_2$ (Figure 23A).[533,590] The *ortho*-quinonoid structures generated by oxidation are quite susceptible to hydrolysis or rearrangements other than the *q*-$6MPH_2 \rightarrow$ 7,8-$6MPH_2$ isomerization that is blocked by 6,6-dialkylation. Figure 23 shows several decomposition pathways available to *ortho*-quinonoid dihydropterins, which are generated by two-electron oxidation.

The first four transformations clearly arise from the same pattern of endocyclic double bond rearrangement. The reaction of Figure 23B was discovered in a study of the *q*-$BH_2 \rightarrow$ 7,8-BH_2 reaction, which was thought to be unusually rapid because of the biphasic kinetics observed with DHPR and *q*-BH_2 formed by peroxidase-catalyzed oxidation (with either H_2O_2 or O_2). Degradation of the quinonoid species does not have a large C^6-H/D isotope effect, unlike the *q*-$6MPH_2 \rightarrow$ 7,8-$6MPH_2$ conversion mentioned above. Armarego and co-workers observed that oxidized BH_4 forms 7,8-PH_2, as depicted in Figure 23B. This follows formation of 7,8-BH_2, which is in equilibrium with its 5,6-hydrate. Subsequent rearrangement of the 6-hydroxy-7,8-BH_2 to a quinonoid configuration is envisioned to precede the loss of the 6 side chain, forming 6-hydroxy-7,8-PH_2. (Side chain loss can be avoided with DTT-coupled hydroxylase assays, in which the oxidized biopterin is quickly rereduced.) This can continue to oxidize to the C^6 ketone, 7,8-dihydroxanthopterin,[536] a pteridine excreted in large amounts by patients with DHPR deficiency.[591] The reaction of Figure 23C is important in a like manner for the chemistry of oxidized folate and may be one reason that thymidylate synthase does not generate a quinonoid dihydrofolate (*vide infra*). The reaction of Figure 23E is not known for other pterins (including *q*-6,6-M_2PH_2), so it may also stem from a different aspect of the thwarted isomerization to 7,8-PH_2. It may arise from a rearrangement of the quinonoid hydrate, the 4a-carbinolamine, which would be a mechanistic complement to the formation of 7-BH_4 discussed below. Current renderings of that rearrangement require fissioning of the $C^{4a}-N^5$ bond, giving a ring-opened BH_2, which might not be possible in *q*-$TMPH_2$. The reaction of Figure 23*E* occurs with both pterin[172] and flavin[592,593] compounds and has an analogue in alloxane hydrolysis.[594] It was discovered because crystalline *q*-$TMPH_2$ stored in moist air develops a blue color, indicating formation of the semiquinone •$TMPH_3$. The authors reason that this is due to formation of $TMPH_4$ from the reduced, ring-contracted product (the tetramethylated 2-amino-1*H*-imidazo[4,5-*b*]piperazine), which reacts with *q*-$TMPH_2$ to generate •$TMPH_3$. [Whether this contaminant is present in the mixtures used to generate the EPR-detectable species was not addressed. It is worth reiterating that Eberlein *et al.* report that the pterin radical obtained by comproportionation is colored *blue* (like the flavin semiquinone radical),[172] while Bobst reports a *red* color for the peroxide-generated radical.[574]] The rate of the reaction depicted in Figure 23E depends upon deprotonation of two groups with pK_a values of 5.56 and 10.43.[595]

The reaction of Figure 23F occurs with several 5-alkyltetrahydropterins and -folates in aerobic, basic media. The incorporation of an atom of oxygen into the pyrazino-*s*-triazine product is proposed to follow an initial O_2 attack at the C^{4a} position.[596,597] The structure of the product was verified by X-Ray crystallography of the acetyl derivative.[598]

Reactions with nucleophiles have been used to probe the reactivity of several analogues of biopterin. A crystallographically characterized spiro-lactam is formed from the 4a-hydroxy-5-deaza-$6MPH_2$ after it is treated with methoxylamine or semicarbazide, but it is not clear what the mechanism of this rearrangement might be. Possibilities include (1) attack by the C^{4a}-hydroxy group on C^2 (Figure 24A), which has some mechanistic precedence, and (2) addition of the nucleophile to the C^{8a} position (Figure 24B),[563] which has a precedent in the reactions of flavins with nucleophiles.[592] Treatment of *q*-$TMPH_2$ with methoxylamine in acidic solution leads to displacement of the exocyclic amino group. The crystal structure of this adduct indicates that the presence of an exocyclic methoxylimine analogous to the disfavored *exo para* tautomer of quinonoid dihydropterin.[595]

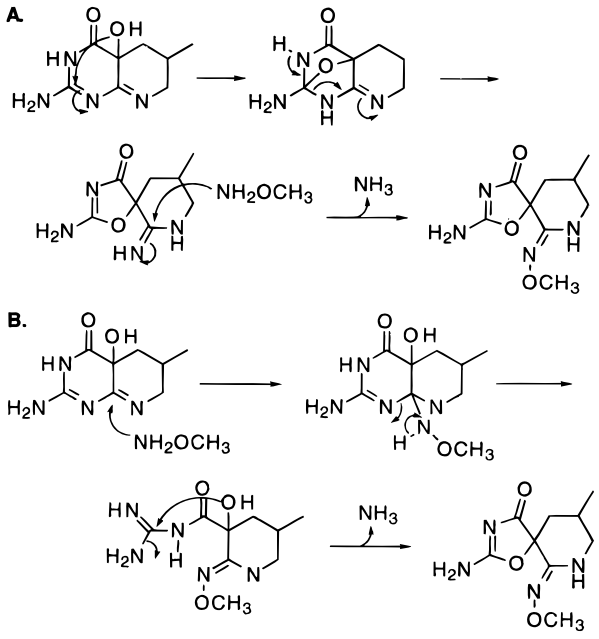

Figure 24. Rearrangements of hydroxylated pterins.

6. Formation of 7-BH4. Primapterinuria and Vitiligo

A rare form of HPA is associated with the excretion of large amounts of 7-(dihydroxypropyl)pterin, or primapterin. This is a rather benign condition detected as a result of HPA screening. Several of the rearrangements discussed above may be relevant to the formation of this metabolite.

Dhondt and co-workers identified a mild-HPA patient who excreted a blue fluorescent compound in his urine, which was also present in cerebrospinal fluid. A dose of BH_4 caused depletion of phenylalanine from his blood, indicating normal PAH was present, but the neopterin/biopterin ratio was 10 times normal.[599] Permanganate-oxidized urine from this patient contained a mixture of 6- and 7-carboxypterin, which indicated that primapterin (the oxidized form of 7-BH_4) was present in urine, a supposition confirmed by GC−MS and HPLC analyses in comparison with authentic primapterin. Primapterin was also identified in normal human urine, but it is present at 13-fold lower levels than in the affected patient.[600] Once the possibility that bacterial intestinal flora perform this conversion was ruled out, it became clear that the formation of 7-BH_4 was due to abnormal metabolism.[601] Normal GTPCH, 6-PTPS, SR, and DHPR activities were found in peripheral blood cells of the affected patient, and the 2% of 7-substituted pterins formed by GTPCH was no higher than controls. This small amount of 7-dihydroneopterin triphosphate was not metabolized by subsequent enzymes, which at a stroke indicates the *de novo* biosynthesis pathway is normal, and that the entity responsible for 7-BH_4 formation must reside in the liver.

Curtius *et al*. demonstrated that small amounts of 7-substituted pterins were formed by incubations of PAH under turnover conditions with 6-BH_4, but only in the absence of PCD.[601] Smaller amounts of anapterin, the 7-substituted homologue of neopterin that also appears in urine, were also formed *in vitro* in the absence of the dehydratase. The mechanism depicted in Figure 25 was proposed, in which formation of 7-substituted pterin can results from a prolonged lifetime of the 4a-carbinolamine hydroxylase product.[601] These results were confirmed by Davis *et al*., who found that 6MPH_4 is similarly rearranged to a 7-substituted pterin, implying that the hydroxylated sidechain does not participate in the rearrangement.[602]

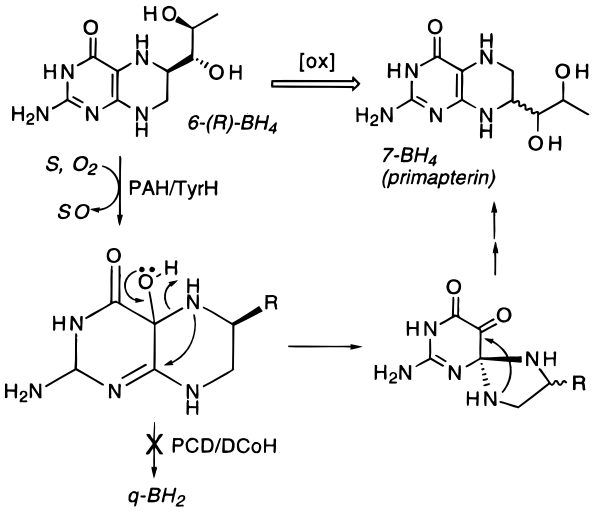

Figure 25. Proposed rearrangement of 4a-hydroxy-BH_2 to primapterin.

Chemical evidence supporting this mechanism has been found by Ayling's group using their stereospecific synthesis of 6-substituted pterins, which can be directed into producing 7-isomers during quinonoid divicine cyclization step (as in Figure 20D). Nonenzymatic dehydration proceeds with acid catalysis and has a marked buffer dependence, reaching a minimum at pH 8.25 when the buffer concentration is extrapolated to zero. Phosphate buffer is a particularly good catalyst for the dehydration reaction,[603] which may help couple PAH activity to NADH oxidation in Nielsen's DHPR-coupled PAH assay[71] by preventing accumulation of the 4a-carbinolamine intermediate.[604]

Even though the V_{max} values determined for PAH were identical (using an uncommon radioassay for tyrosine formation[605]), the K_m for 7-BH_4 was 13 and 5 times that for BH_4, with PAH and DHPR, respectively.[606] This surprising lack of a V_{max} difference probably results from the assay procedure employed; when tyrosine formation is quantitated, 85% of 7(*RS*)-BH_4-dependent PAH turnover is uncoupled (*i.e*., one tyrosine is formed per 5.9 equiv of 7-BH_4 oxidized), in stark contrast to the completely coupled reaction with (6*RS*)-BH_4.[607] This is also the case for 7MPH_4-dependent PAH turnover.[608]

A more extensive kinetic study of 7-BH_4 with all three aromatic amino acid hydroxylases showed it was a strong competitive inhibitor of BH_4-dependent PAH activity when tyrosine formation was monitored ($IC_{50} \approx 5\ \mu M$), but had a much weaker effect on TyrH or TrpH activity ($IC_{50} \geq 0.5$ mM). Monitoring NADH oxidation, the 7-BH_4-supported PAH reaction showed a K_m about 20 times that of BH_4, except with cooperativity at low [L-Phe] and substrate inhibition at high [L-Phe]. This would appear to suggest that, like BH_4, 7-BH_4 is able to inhibit the L-Phe activation of PAH.[609]

Under the conditions of the Kaufman group's "activation" assay (section II.A.3.5), previously un-

activated PAH is able to oxidize 7-BH_4 at a rate 20 times that of BH_4, under conditions where the 6MPH_4-/BH_4-dependent velocity ratio is 41. In the fully preactivated PAH controls with BH_4, the rate of NADH oxidation is 24 times higher (L-Phe activation), but is about the same with 6MPH_4 or 7-BH_4.[609] This result, which indicates that 7-BH_4 *fails* to inhibit L-Phe activation over the course of the assay, is apparently inconsistent with the observation of cooperativity in 7-BH_4-supported turnover.

It is important to remember that mostly uncoupled turnover was monitored in these experiments. One must assume that the NADH oxidation rates observed reflect a fixed uncoupling ratio, across a range of phenylalanine concentrations, in order to infer anything about the rate of tyrosine formation. In other words, the partitioning between productive and dissipative tetrahydropterin oxidation, which cannot be distinguished in the NADH-coupled assay, is inferred to be constant over a range of conditions. Particularly in the low [L-Phe] range, where PAH may only be partially activated, this is a weak assumption. For instance, exposure of the active site or stimulation of tetrahydropterin oxidase activity may occur at a phenylalanine concentration insufficient to activate PAH. [The active site of PAH is solvent accessible even when the enzyme is in its T state, as is evidenced by the rapid binding of catechols to the ferric form of the enzyme, and perhaps the binding of tetrahydropterins during reduction of the active-site iron (if the pterin binding site used for reduction overlaps the active-site pterin-binding pocket).[116] The observation of accessibility to portions of the active site's binding pocket does not indicate that the T → R state conformational changes required for catalytic competence have occurred.] This puts significant reservations on the relevance of the sigmoidal part of the velocity curve.

These considerations do not detract from the separate observation of 7-BH_4 inhibition of BH_4-supported *tyrosine* formation, which appears to occur at the same concentration of 7-BH_4 regardless of whether the enzyme was first preincubated with L-Phe or not. Competitive inhibition of PAH-dependent *tyrosine* formation by 7-BH_4 occurs under high phenylalanine conditions, but not at the more physiologically relevant 60 μM [L-Phe].[609] Among all of the data presented by Davis *et al.* there is no evidence for an interaction of 7-BH_4 with PAH^T that causes allosteric inhibition like that which is seen with the natural substrate. All of the results seem to indicate that 7-BH_4 is a particularly poor cofactor and thereby a steady-state competitive inhibitor *vs* BH_4 for PAH. In the same study, phosphorylation of TyrH was observed to lower the IC_{50} for 7-BH_4 from 2.2 mM to 0.48 mM. The IC_{50} for TrpH was 3.3 mM.[609]

Normally the liver content of PCD is about one-fourth that of PAH on the basis of milligrams per grams tissue,[67,493] which given the ~4-fold larger molecular weight of PAH means there are approximately equimolar amounts present. The V_{max} for PCD is 9.8 s^{-1} *in vitro* ((6*S*)-MPH_4, pH 7.4, 10 °C), rising to 50−90 s^{-1} at 37 °C.[604] The rate of L-Phe clearance in an intact rat treated with 25 times the normal [L-Phe] (typical dietary loads increase human [L-Phe] by 2−3 fold) is ≥5 μM s^{-1}, which requires a rate of dehydration of 50−130 s^{-1} (*i.e.*, ~10^3 higher than the spontaneous dehydration rate) if 99% of the cofactor is to be kept reduced. Thus the rate of PCD-catalyzed dehydration appears to be adequate (and necessary) to support the rate of BH_4 recycling required during L-Phe hydroxylation.[610]

Table 7. Kinetic Parameters of PCD

parameter (4 °C, pH 8.5)	wt PCD	C81S PCD	C81R PCD
V_{max} (nmol min^{-1}, 1 μM PCD)	76	52	<20
K_m (μM 4a-OH-6,6-M_2PH_2, direct)	83	80	(>200 ?)
K_m (μM PCD, PAH-coupled)	0.039	0.052	0.62

By using the cloned gene for PCD,[490] the alleles of a family with a primapterinuric-HPA-affected child (whose blood [L-Phe] = 700 μM) were probed. Two different mutations in the 104-residue PCD were identified in the heterozygous parents, each of which the affected boy had inherited: E87Ter and C82R.[509] The loss of the single Cys residue present in PCD was particularly provocative and immediately suggested the outlines of a working model for the dehydratase, which was envisioned to involve nucleophilic catalysis, perhaps in analogy to the propensity of thiol reagents to attack oxidized pterins at C^{8a}.[563]

Köster and co-workers studied the pterin affinity of wild-type and mutant recombinant human PCD, assayed by quenching of the PCD Trp fluorescence.[611] The highest affinity for a pterin is for the stable *q*-6,6-M_2PH_2 (0.9 μM), while the K_d is 20 μM for 7,8-BH_2 and BH_4. The primapterinuria-associated C81R mutant showed no difference in affinity for *q*-6,6-M_2PH_2, but C81S has a K_d = 20 μM. No evidence of product inhibition by *q*-6,6-M_2PH_2 was detected.[611]

Starting from an appropriately substituted pyrimidine quinone like the one depicted in Figure 20D, either 4a-hydroxy-6MPH_2 or 4a-hydroxy-6,6-M_2PH_2 can be prepared by forming the Schiff base at pH 9.0, which yields the C^{4a},N^5-hydrate instead of the quinonoid form in an adaptation of the synthesis developed by Bailey *et al.*[562,610] This procedure was used to prepare the substrate for the recombinant PCD enzymes, which were studied at 4 °C to minimize the background rate (about 1 min^{-1} under the conditions of the table). Assays were either direct, in which the formation of *q*-6,6-M_2PH_2 was monitored, or coupled to PAH catalysis, in which the fold stimulation of PAH is determined as V_{max}.[490] The PAH-coupled V_{max} determinations gave about the same degree of stimulation (9.5−12-fold) for all three PCD variants. As can be seen (Table 7), the usually conservative replacement of Cys81 with Ser did not perturb the dehydratase activity, but the kinetic properties of the primapterinuria mutant C81R are noticeably poorer, especially the ~10-fold higher K_m in the coupled assay.

Precise values for the direct assay of the C81R mutant cannot be determined from the k_{cat} *vs* [4a-hydroxy-6,6-M_2PH_2] plot, which is insufficiently saturated at ≤140 μM substrate. Cys81 is not involved in the tetramerization of the protein, as determined by a comparative cross-linking study. Significantly, the inclusion of either wild-type PCD or C81R in PAH mixtures obliterated the ~7% 7-substituted pterin formation that results from PAH catalysis in the

absence of PCD. Estimates of the temperature dependence suggest that at 37 °C, the wild-type V_{max} (pH 8.5, direct assay) will be ~500−600 s^{-1}. The authors conclude that while the limited catalytic capacity of the C81R mutant is sufficient to account for the rate limitation of PAH by aberrant PCD, the ability of the mutant protein to suppress 7-BH_4 formation suggests a different, unknown functional origin for primapterinuria.[611]

Ayling's group has recently determined detailed kinetic and thermodynamic parameters for the rat liver enzyme, using preparations chiral at their 6-methyl or 6-propyl groups.[603,604,610] In contrast to the findings of Köster *et al.*,[611] substrate inhibition was observed in the absence of NADH/DHPR with 4a-hydroxy-(6*S*)-*X*PH_4 as substrate (the "natural" enantiomer at C^6), which was competitive with K_I = 1.5 (*X* = methyl) or 0.7 (*X* = propyl). No inhibition was observed with 7,8-BH_2, (6*R*)-BH_4, or (6*RS*)-BH_4 below 0.2 mM.[604]

4a-Hydroxy-BH_2 can cyclize into a product tentatively identified as O2′,4a-cyclic-(6*R*)-BH_4, which contains a six-membered ring derived from condensation of the dihydroxypropyl side chain with the 4a-hydroxy group, and is dehydrated by PCD at a rate 1−2% that of the 4a-hydroxy-BH_2.[603] Appearance of this relatively stable product prevented a highly accurate assessment of the kinetic properties of 4a-hydroxy-BH_2, but they are not very different from the parameters for 4a-hydroxy-(6*S*)-MPH_2 at 10 °C: V_{max} = 9.8 s^{-1} (pH 7.4), 3.3 s^{-1} (pH 8.4); K_m = 2.5 μM (both pH values). At 37 °C, the V_{max} values rise to 53 and 18 s^{-1} for 4a-hydroxy-(6*S*)-MPH_4 at pH 7.4 and 8.4.[604] Note that these values are quite dissimilar to those determined by Köster *et al.*, who used 4a-hydroxy-6,6-M_2PH_4 as substrate.[611] No biphasic plots were observed with the chemically synthesized 4a(*RS*)-hydroxypterins, indicating that both isomers were dehydrated at the same rate, and there was only a small decrease in the dehydration efficiency of the unnatural 6(*S*)-methyl isomer. In addition, Rebrin *et al.* did not observe any effect of PAH on the K_m and V_{max} values of the dehydratase, or *vice versa*, even if large amounts (0.4 mM) of the PAH product analogue *m*-fluoro-tyrosine were added (*m*-fluorophenylalanine is a good substrate for PAH).[604] Addition of the PAH product analogue would be expected to enhance the effectiveness of product inhibition by 4a-carbinolamine, if it dissociates first from the (PAH·tyr·4a-OH-BH_2) complex. This applied for PAH assays with up to 0.4 mM 4a-hydroxy-BH_2 or 0.8 mM 4a-hydroxy-(6*RS*)-MPH_2.[604]

Another association of 7-BH_4 with human health is found in the skin depigmentation disorder vitiligo, a common condition worldwide (0.5−2% incidence) and in particular on the Indian subcontinent (incidence rates range up to 8%).[45]

Vitiligo lesions are detected by their blue, biopterin-derived fluorescence under long-wavelength UV (UVB) illumination, which is quenched in normal skin by melanin. The epidermis contains melanocytes and keratinocytes, which surround the melanocytes and produce catecholamines. While melanocytes may be present in vitiligo lesions, they do not contain the pigment melanin, produced following tyrosine oxidation by tyrosinase. Schallreuter *et al.* discovered PAH activity in human epidermis, in both melanocytes and keratinocytes, which also contain TyrH. Normal epidermal cells contain GTPCH and PCD, as well as both 6- and 7-BH_4, and it appears that both the BH_4 *de novo* and salvage pathways are present. The amounts of GTPCH, PAH, and total BH_4 are higher in darker skin, which is consistent with their importance in maintaining pigmentation.[612] Furthermore, PKU patients are often hypopigmented, as are the animal models for that condition, where there are systemic deficiencies in the supply of L-Tyr.[46] In contrast, PAH and GTPCH activities are not significantly different in affected vitiligo lesions, but the PCD activity is dramatically lower in affected epidermis, particularly in melanocytes.

The relative amounts of 7-BH_4 are higher in vitiliginous skin, which suggests inhibition of PAH by primapterin. Removal of total biopterin from vitiliginous cell extract by gel filtration resulted in a 7-fold stimulation of PAH activity, which was diminished again by the addition of 7-BH_4. As a result, the authors propose that the mechanism of depigmentation in vitiligo may be due to inhibition of PAH activity by primapterin, formed as a result of PCD deficiency in keratinocytes. This blocks the supply of L-Tyr and thereby stops melanin biosynthesis.[612]

A specific binding site for BH_4 has recently been identified on the copper oxidase tyrosinase, which is not known to depend upon pterins, that may also contribute to lowering its activity.[613] Alternatively, the formation of H_2O_2 in the uncoupled turnover reaction might mediate toxic effects; vitiligo has been associated with high concentrations of H_2O_2 and low levels of catalase.[614] A preliminary report of treatment with "pseudocatalase" (a patented, "low-molecular-weight coordination complex which is more active ... than catalase itself"), in combination with calcium and UVB irradiation, resulted in improvement in 90% of the 33 vitiligo patients examined and prevented further active depigmentation in all.[615]

High levels of primapterin are only associated with the progressive form of vitiligo and not with the stable form of the disease. The dual role of PCD as a homeobox transcriptional regulator may contribute to this form of vitiligo, since the PNMT (involved in norepinephrine synthesis) and tyrosinase genes have upstream sequences that resemble the HNF-1 consensus sequence. This leads to the interesting speculation that different defects in a single protein, which affect either its biochemical or regulatory functions, might cause different forms of a single disease by distinct mechanisms.[45]

C. Relationship to Other Cofactors and Coenzymes

1. Flavins

Flavin-dependent proteins include some electron-transfer proteins,[616] firefly luciferase,[617] oxidases, and monooxygenases.[618] Flavoprotein oxidases, which are typically dehydrogenases, produce H_2O_2 from O_2; monooxygenases form a hydroxylated product and H_2O. The monooxygenases are separable into the internal monooxygenases, in which the substrate is the source of the reducing equivalent and the product is decarboxylated, and the external monooxygenases

(hydroxylases), in which NAD(P)H is the source of electrons. The hydroxylases are ubiquitous, particularly in microorganisms, which use them in an assimilatory role.

All oxidized flavoproteins have a bright yellow color, conferred by the isoalloxazine ring, which has allowed detailed investigation of their mechanisms. The hydroxylases harness the ability of the flavin cofactor to activate O_2 for hydroxylation of an aromatic substrate, which is invariably "activated" by other functionalities (*e.g.*, *p*-hydroxybenzoate hydroxylase, PHBH, EC 1.14.13.2). In most studies of the oxidative half-reaction of these enzymes, the reduced enzyme (prepared by dithionite treatment or by photoreduction, using EDTA as an electron source[619,620]) is mixed with the aromatic substrate prior to the admission of O_2, because of the rapid reaction between oxygen and $E{\cdot}Fl_{red}$. When $E{\cdot}Fl_{red}{\cdot}$ PHB is mixed with O_2, an intermediate with λ_{max} at 385 nm appears with a rate that has a second-order dependence on pO_2. Its similarity to the absorbance spectrum of $N^{3,5}$-dimethylhydroperoxylumiflavin (λ_{max} = 374 nm in MeOH)[589] suggests that it is the 4a-hydroperoxyflavin intermediate.[621−624] No direct evidence has ever been obtained for formation of an analogous 4a-hydroperoxypterin species during pterin-dependent hydroxylations (section IV.A.2).

The flavin monooxygenases have some important differences from the pterin-dependent monooxygenases, including the lower reactivity of the hydroxylating intermediate and the lack of an NIH shift with the flavoenzymes. As will be discussed in section III.A.5, the NIH shift has been regarded as evidence for arene oxide formation, which might not be necessary for conversion of the activated aromatic substrates of flavoprotein hydroxylases.

With the lone exception of luciferase, flavins appear to be tightly associated prosthetic groups rather than diffusible cofactors like the tetrahydropterins. The most obvious and functionally significant distinction between pterins and flavins is the orders of magnitude more sluggish reaction of tetrahydropterins with O_2.[618] The reaction of XPH_4 with O_2 in neutral buffer solutions is much slower than the enzymatic utilization of O_2. At pH 7.0, 25 °C, and under saturating O_2, the turnover number for PAH is $\sim 10\ s^{-1}$, a 10^7-fold acceleration over the autooxidation of XPH_4, which occurs with a pseudo-first order rate constant of $\sim 10^{-6}\ s^{-1}$. These should be compared to the high rate of reaction of O_2 with the flavoenzyme cyclohexanone monooxygenase ($\geq 3 \times 10^7\ s^{-1}$), and FlH_2 in solution (250 $M^{-1}\ s^{-1}$;[589] $\sim 0.1\ s^{-1}$ under the above conditions). The rate of O_2 reaction with $FlH^{\bullet}$ is $\sim 10^8$ $M^{-1}\ s^{-1}$,[625] so it is unsurprising that flavodoxin, and other radical-generating flavoproteins, effectively isolate the isoalloxazine ring from contact with solution (and hence O_2).[616]

2. Folates

Folates differ in structure from pterin only in the identity of the substituent at the 6-position, and yet there is extremely little overlap in the functional identities of these two cofactors. Folate-dependent enzymes function as "one-carbon" transferring agents in a number of biosynthetic systems, using the imidazolone-containing 5,10-methylene-THF (5,10-CH_2-THF) as cofactor. Depending on the enzyme, ring opening is followed by transfer of the methylene group at the oxidation level of formaldehyde (*e.g.*, serine hydroxymethyltransferase, EC 2.1.2.1) or formate (*e.g.*, glycineamide ribonucleotide transformylase, EC 2.1.2.2).[546] Both of these activities have been proposed to involve a reactive iminium (5-CH_2^+-THF) intermediate formed by imidazolone ring opening. This exocyclic methylene then undergoes group transfer to the substrate, which in the case of the reverse reaction of serine hydroxymethyltransferase is a PLP-conjugated glycine. Neither enzyme requires a redox role for the tetrahydropteridine ring, which is generally the case for THF-dependent systems other than thymidylate synthase.

5,10-CH_2-THF is also reduced by methylenetetrahydrofolate reductase (MTHFR, EC 1.5.1.20, 1.7.99.5) to 5-CH_3-THF, which functions as a methyl group carrier. This can be envisioned to be a variant of the iminium in which it is reduced rather than acting as an electrophile. The N^5-methyl-THF formed by this reaction is employed in methionine biosynthesis, by the vitamin B12-dependent methionine synthase (EC 2.1.1.13), and in tRNA maturation but is otherwise not widely used (*vide infra*).

Methylation of dUMP by thymidylate synthase (EC 2.1.1.45) involves methylene transfer from 5,10-CH_2-THF at the oxidation level of formaldehyde, followed by oxidation of the pteridine ring to 7,8-dihydrofolate. Transfer of label from 5,10-CH_2-[6-^{3}H]THF to the methyl group of the dTMP product is quantitative, consistent with a hydride transfer mechanism.[626,627] The 7,8-dihydrofolate produced is normally reduced by DHFR in a step that can be blocked by one of several antifolate chemotherapeutics (methotrexate, 5,10-dideazafolates). Note that the unstable quinonoid form of THF is not released into solution, where the 6-methylamino group would undergo hydrolysis in the manner of Figure 23C.

Initial reports[628] of folate-dependent PAH activity were later attributed to small amounts of contaminating $6MPH_4$.[629] Hydroxylase cofactors cannot substitute for THF because they lack the N^{10} group of the 6-aminobenzoyl moiety that is required for ring formation. In turn, THF is evidently too large for, or otherwise incompatible with, the hydroxylase BH_4 binding pocket. However, there are a few points of intersection between the pterin and folate pools, the most interesting of which is the ability of MTHFR to reduce *q*-BH_2 to BH_4 with concomitant oxidation of 5-CH_3-THF to 5,10-CH_2-THF.[630] This activity provides a potential escape route from the "methyl trap" of folate metabolism, a hypothesized unproductive accumulation of folate as 5-CH_3-THF during vitamin B12, and thereby methionine synthase, deficiency.[631]

D. Cofactor Requirements

1. Biopterin Analogues and Pyrimidines

A number of different pterins are accepted by the aromatic amino acid hydroxylases as cofactors in the hydroxylation reaction. PAH was used to sort the majority of the pterins into the three classes: cofactors (Figure 26), inhibitors (Figure 27), and nonfunctional analogues (Figure 28) that neither support nor inhibit hydroxylation. Following that determination,

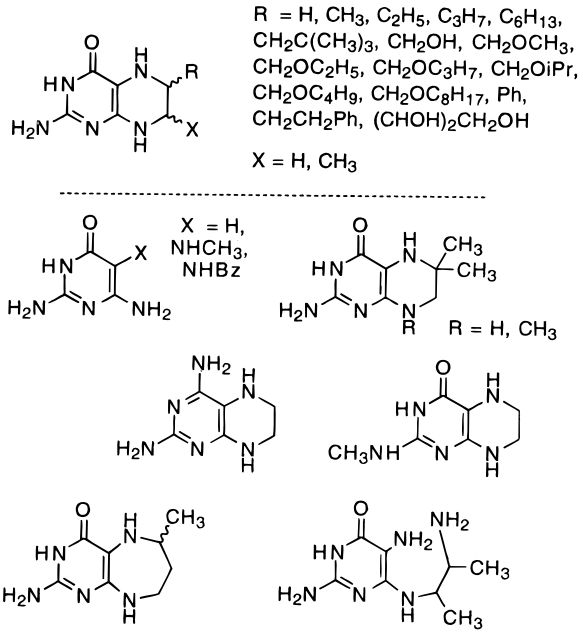

Figure 26. Pteridines and pyrimidines that function as cofactors for hydroxylase turnover. References cited in text.

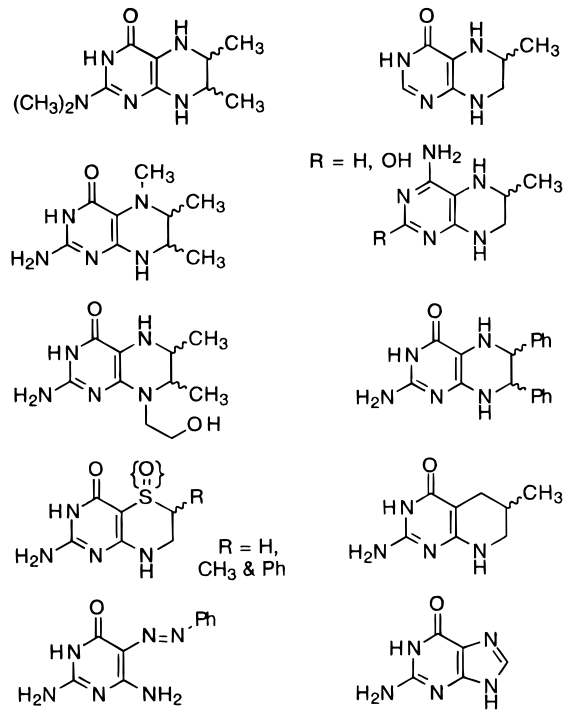

Figure 27. Inhibitors of hydroxylase turnover related to pteridines. References cited in text.

many different pterin cofactors have been screened with all three aromatic amino acid hydroxylases, usually with crude preparations as the source of enzyme, to observe the small differences among *functional* cofactors (Figure 26). Note that some of the cofactors depicted in Figure 26 will support only a single turnover (*vide infra*).

In general terms, the pyrimidine portion of the pterin ring is most essential. However, several deviations in this part of the pterin nucleus do not abrogate PAH activity, including monomethylation of the exocyclic N^2 group, replacement of the C^4 carbonyl by an amino group, and monomethylation of N^8 (6,6,8-trimethyl-PH_4 is nonfunctional with TyrH, however).[632]

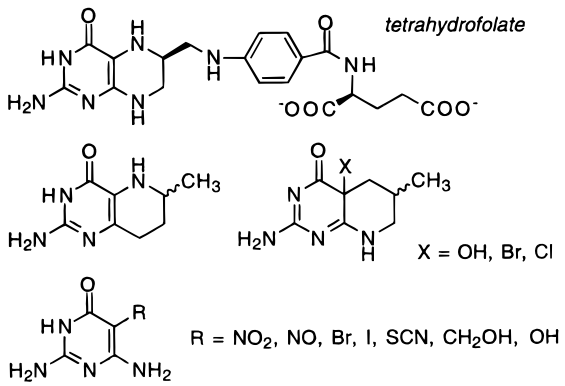

Figure 28. Ineffective pteridine compounds. References cited in text.

While the stereochemistry at C^6 is significant, both of the isomers of BH_4 or its analogues are active. The configuration of the BH_4 6-dihydroxypropyl side chain, formed by DHPR reduction, was determined to be *R*.[633−635] With PAH, the natural (6*R*)-BH_4 isomer has a V_{max} ∼4 times that of the unnatural 6(*S*)-BH_4, with no change in K_m value or any uncoupling of cofactor oxidation from tyrosine formation (*vide infra*).[130]

The dihydroxypropyl side chain allows relatively straightforward separation of the isomers of BH_4. This is not the case for $6MPH_4$ (or other alkyltetrahydropterins), which was first resolved by fractional crystallization.[636] Because of the hierarchy of stereochemical assignments, natural BH_4 has the same configuration at C^6 as 6(*S*)-MPH_4, which has a *lower* V_{max} with PAH and phosphorylated TyrH than the unnatural isomer 6(*R*)-MPH_4. However, the K_m values are such that the V_{max}/K_m values are about equal for both isomers with both enzymes. The same phenomenon is observed for the isomers of 6-propyl-PH_4, in which the unnatural isomer has a higher V_{max} (PAH, 5-fold; phosphorylated TyrH ∼10-fold) but also higher K_m values for both substrate and cofactor. The multiplier for TyrH is an upper limit, because substrate inhibition occurs with the natural 6(*S*)-propyl isomer but not the unnatural 6(*R*)-propyl-PH_4, which is the most effective cofactor known for TyrH.[637]

A range of 6-substituted tetrahydropterins can function as cofactors (Figure 26), which is consistent with the observation that the stereochemistry of the dihydroxypropyl group (the natural diastereomeric configuration is L-*erythro*, as depicted in Figure 18) of BH_4 is largely irrelevant to cofactor activity with TyrH.[48,638,639]

A vexatious fact of pterin chemistry is the intrinsic instability of the quinonoid derivative to rearrangement, except where the 6-position is dialkylated, as in 6,6-M_2PH_4.[560,561] This was mentioned above during the discussion (section III.B.4) of electrochemical studies performed with the similarly stable $TMPH_4$ (although no ring contraction has been reported with *q*-6,6-M_2PH_2). With PAH, 6,6-M_2PH_4 most closely resembles $DMPH_4$ in its kinetic properties, as both have ∼20% of the V_{max} of $6MPH_4$ with little change in the cofactor K_m values.[561]

A series of 6-alkyl-6-methyltetrahydropterins (alkyl = methyl, ethyl, propyl, phenyl, and benzyl) were all shown to be cofactors for TyrH (phosphorylated TyrH: K_m values 4−40 μM *vs* 60 μM for $6MPH_4$; V_{max}

10−24% that of $6MPH_4$). By using crude bovine striatal TyrH, a less-dramatic stimulation of activity was observed following phosphorylation in assays employing a disubstituted pterin cofactor, when compared with its monosubstituted equivalent, leading to the proposal of steric interaction between the pterin and phosphate group (section II.B.3.2). The stability of *q*-6,6-M_2PH_2 allowed the determination that "product" inhibition does not occur with PAH (using the term loosely, since the 4a-carbinolamine form is the initial product of the hydroxylase reactions).[209] Both $6MPH_4$ and 6,6-M_2PH_4 have been converted into the respective 4a-carbinolamine forms, in order to study PCD/DCoH.[604,610,611] Observing the formation of a stable quinonoid dihydropterin product from an isolable starting material in the study of this unusual, bifunctional system has an obvious advantage over previous work, which had to contend with a conversion among unstable oxidized pterins.

The oxidation of both $6MPH_4$ and $DMPH_4$ is tightly coupled to L-Tyr formation by PAH,[19,608] meaning that 1 equiv of cofactor is oxidized for each amino acid hydroxylated. 6,6-M_2PH_4 oxidation is also tightly coupled to tyrosine formation, giving a ratio of 1.00 ± 0.08.[561] This is not the case for $7MPH_4$-dependent turnover, in which 3.0 ± 0.6 equiv of tetrahydropterin cofactor are oxidized per tyrosine formed (66% uncoupled turnover).[608]

Uncoupling during hydroxylation of suboptimal amino acid substrates is also observed and will be discussed in the section on alternate substrates (section IV.A.8). In completely coupled turnover, the ternary complex of enzyme, amino acid substrate, and pterin cofactor can be imagined to be poised in a configuration that prevents side reactions. As the "fit" becomes poorer, uncoupling rises.

With particularly bad substrates, the artificially activated PAH functions as a tetrahydropterin oxidase, producing an equivalent of hydrogen peroxide for each cofactor consumed.[640] This has been regarded as good evidence for the involvement of an oxygen species at the peroxide redox level during catalysis. While it is correct to state that the hydroxylating intermediate is capable of generating hydrogen peroxide, this does not imply that the intermediate itself is a peroxide. In any case, there is disagreement about whether H_2O_2 is formed at all during uncoupled turnover, with directly contradictory results reported by the *pro*[640−642] and *con*[168,169,572] groups. It is not known what relationship the "uncoupled" pathway of unproductive tetrahydropterin oxidation bears to the normal reaction coordinate, but is of sufficient mechanistic importance to warrant full discussion in section IV.A.7 and elsewhere in section III.

In cases of pterin deficiency, TyrH and TrpH activity can be quite low because of cofactor limitation. Supplementation of the diet with tetrahydropterin has had some success in treating atypical PKU or Parkinson's disease.[508,643] As is common with other drugs, a major problem is posed by the impermeability of the blood−brain barrier to BH_4. Changing the identity of the 6-substituent offers a means of improving the pharmacological properties of tetrahydropterin without significantly compromising cofactor activity, as well as its value in enzymological studies. To that end, a collection of 6-(alkoxymethyl)-PH_4 (alkoxy = methyl, ethyl, propyl, isopropyl, and butyl) cofactors displayed activity with all three hydroxylases,[482,644] as did a series of 6-alkyl-PH_4 (alkyl = methyl, ethyl, propyl, hexyl, neopentyl, phenethyl) cofactors that were also DHPR substrates when oxidized.[645,646]

There are some differences in the effectiveness of the cofactors among the three hydroxylases reported in these papers, as with 6-$(CH_2OCH(CH_3)_2)$-PH_4 (activity relative to BH_4 = 15% for PAH, 137% for TyrH, and 44% for TrpH)[482] or 6-neopentyl-PH_4 (activity relative to BH_4 = 3% for PAH, 55% for TyrH, and ∼200−300% for TrpH below 1 mM).[646] Not much weight should be given to the differences between absolute velocities in different studies. For instance, the two groups reach drastically different conclusions about the relative activity of $6MPH_4$ in their respective tissue extracts, each of which is at variance with the values determined using purified enzymes. The alkoxymethyl series had little ability to cross the blood−brain barrier.[647] Both $6MPH_4$ and 6,6-M_2PH_4 cross the blood−brain barrier more effectively than BH_4, presumably because of their more lipophilic properties.[648,649]

As was mentioned above, many patients with atypical PKU have a deficiency of DHPR, rather than in the *de novo* synthesis pathway, and for these patients enormous amounts of BH_4 or an analogue would be required just to support the conversion of L-Phe to L-Tyr (70−120 mg BH_4 kg^{-1} day^{-1}).[650,651] However, tetrahydropterin replacement should be effective if the *de novo* pathway is blocked and the salvage pathway is intact; some beneficial effects have been noted following treatment of dystonic patients with BH_4 or $6MPH_4$.[652,653] Problems remain to be surmounted, including the hepatotoxicity of $6MPH_4$ and the widely variable response to supplementation.[654]

Another pterin analogue that is a functional cofactor is 6-methylpyrimidodiazepine ($6MPDH_4$), which has an additional methylene inserted into the pyrazine ring (Figure 26). It has about 5% of the $6MPH_4$ activity when tyrosine formation is assayed.[655] The reactivity of this cofactor is discussed extensively below.

Bailey and Ayling discovered that the pyrazine ring was not strictly required for cofactor activity in a study of the substituted pyrimidines 2,5,6-triamino-4-pyrimidinone (TP) and 5-benzyl-2,6-diamino-4-pyrimidinone (BDP), both of which function with low efficiency (Figure 29).[656] The K_m values for these compounds are quite close to their analogous pterins, 50 μM (TP) and 3 μM (BDP) *vs* 80 μM for $6MPH_4$ and 3 μM for 6-$PhPH_4$, but the velocities of tyrosine formation are 0.8% (TP) and 0.2% (BDP) that of $6MPH_4/BH_4$.[657]

Only one L-Tyr is formed for every ∼20 equiv of NADH oxidized in a coupled assay with TP (96% uncoupled).[658] However, this determination does not take into account the further oxidation of NADH by the pyrimidine product. When this is done, 2.5 TP and 1.4 BDP (1.7 BDP in Lazarus *et al.*) are oxidized for every tyrosine formed, the same degree of coupling as their respective cyclic analogues PH_4 and $6PhPH_4$.[659,660] The triaminopyrimidine cofactors are

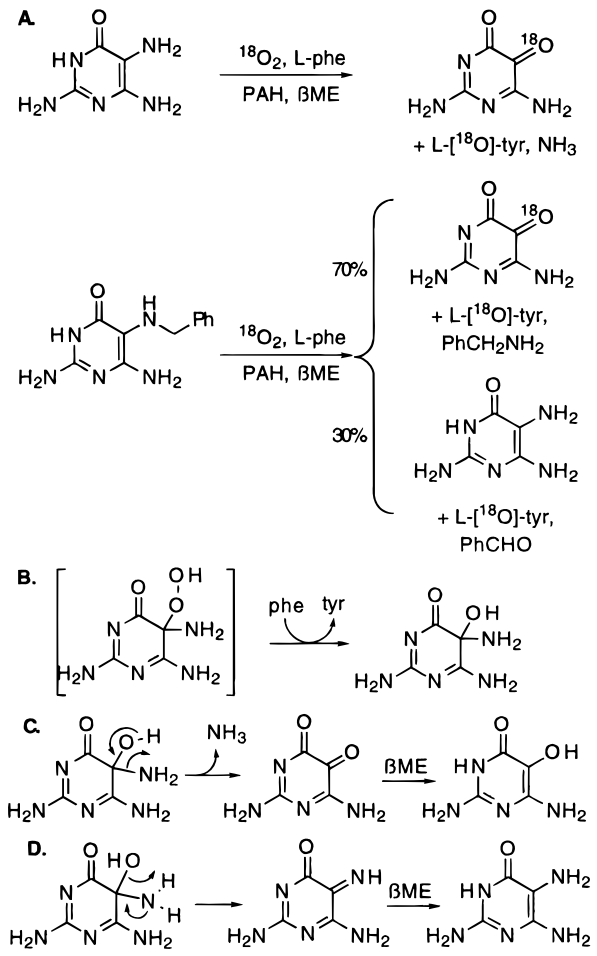

Figure 29. Pyrimidine cofactor transformations.

irreversibly modified as a result of turnover, the subject of the following section.

2. Transformations of Alternate Cofactors

The identity of the hydroxylating species remains a contentious issue. The behavior of the hydroxylating intermediate suggests that an extremely electrophilic entity is formed from molecular oxygen at the active site of these hydroxylases. A key insight that has kept the field rife with speculation is that ordinary organic peroxides cannot oxidize unactivated aromatic substrates unaided. Since one atom of oxygen is retained in the 4a-carbinolamine product, the tetrahydropterin is likely to play a role more important than as a source of two electrons. One of the more striking early proposals was that of Hamilton, who proposed the generation of a carbonyl oxide (oxenoid) at the C^{4a} carbon of the pterin ring. This necessarily involves a ring-opening step, as depicted in Figure 30, to a C^5-oxenoid pyrimidine species.[661−663]

In order to validate this mechanism, it is necessary to demonstrate that a ring-opened intermediate is on the reaction coordinate for the hydroxylases: (1) a ring-opened intermediate should be formed from a reduced pterin, and (2) such an intermediate should be recyclized by hydroxylase. Of course, the rates of both of these proposed processes must exceed the maximum turnover rate known for an aromatic amino acid hydroxylase, PAH's k_{cat} of $\sim 10\ s^{-1}$ (25 °C). As an approach to the second point, a substituted triaminopyrimidine analogue (Figure 31A) of the ring-opened quinonoid divicine (5-hydroxypyrimidine) depicted in Figure 30 was synthesized and incubated with the enzyme. Under tyrosine-forming conditions, no oxidative recyclization of the ring-opened species could be detected in excess of nonenzymatic conversion, at pH 7.4−9.0.[169] Cyclization of the pyrimidine was favored at higher pH (pH 10), which indicates that it is controlled by the charge on the terminal amino group.

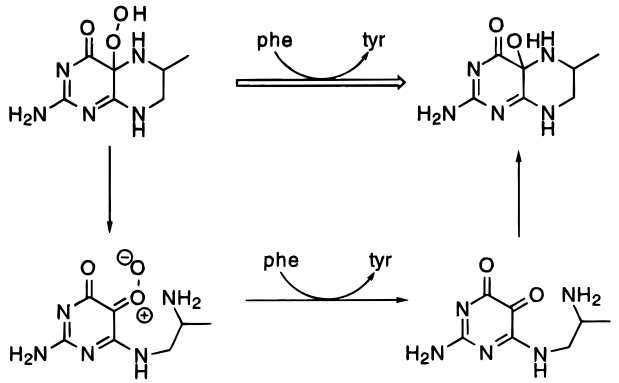

Figure 30. Hamilton proposal for the hydroxylating intermediate of pterin-dependent enzymes.

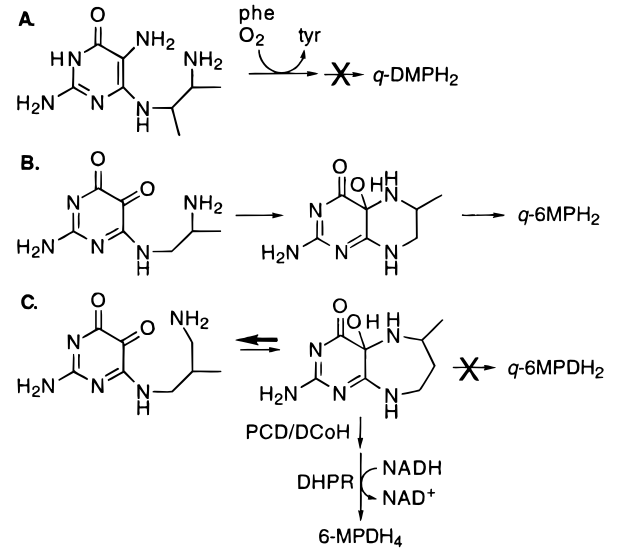

Figure 31. Inability of the diazepine cofactor to recyclize during turnover.

The exact ring-opened quinone intermediate hypothesized by Hamilton[661] was prepared by oxidation of the 5-amino compound in 0.01 N HCl, which forestalls cyclization.[655] The compound is diluted in 0.1 M Tris buffer containing a 5% excess of I_2 (pH 7.4, 27 °C), at which point it cyclizes to *q*-6MPH$_2$ rapidly, with $t_{1/2} = 7.0$ s (Figure 31B). The limiting step appeared to be dehydration of the 4a-carbinolamine. In contrast, the insertion of an additional methylene group prevents spontaneous cyclization, although ~2% can be trapped as the fully reduced, cyclic 6MPDH$_4$ if PCD, DHPR, and NADH are present (Figure 31C). The additional ring strain in this seven-membered ring containing analogue of tetrahydropterin apparently precludes spontaneous formation of *q*-6MPDH$_2$, which was estimated to be 26 times slower than its pyrazine counterpart.

Were it to occur, observation of the ring-opened oxidized intermediate (the first point mentioned above) would probably be difficult because pathway would have to support a recyclization rate in excess

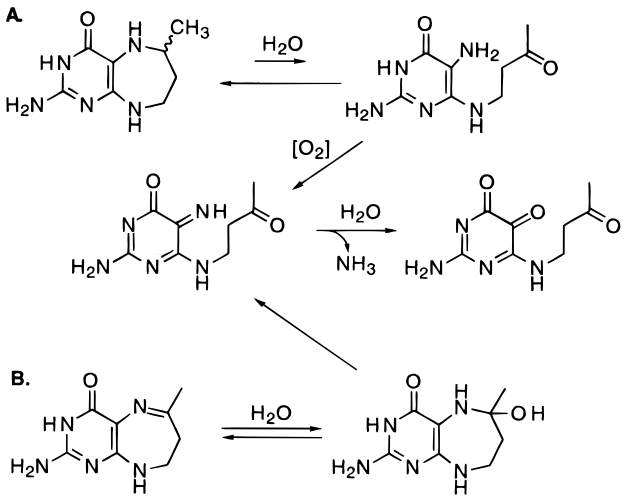

Figure 32. Opening of the diazepine cofactor during turnover.

of 10 s^{-1}. In order to slow down any recyclization occurring with the enzyme, $6MPDH_4$ was synthesized and found to be a tightly coupled cofactor for PAH (*q*-$6MPDH_2$ and 7,8-$6MPDH_2$ were efficiently reduced by DHPR and DHFR).[655] The K_m values for cofactor and phenylalanine were comparable to those with $6MPH_4$ (intriguingly, the K_m for O_2 was >10 times higher) but the rate of reaction was quite slow, about 5% of the $6MPH_4$ V_{max}. The additional methylene might also disfavor recyclization enough for a ring-opened species to be detected in reaction mixtures.

Of course, the strain also lowers the barrier to ring opening in general, which was observed as a greater susceptibility to autooxidative decomposition in aerobic solutions. While side products of nonenzymatic tetrahydropterin oxidation are well known, as was discussed in section III.B.5, they are often of minimal significance with unmodified tetrahydropterins. For instance, the eventual conversion of $6MPH_4$ to 7,8-$6MPH_2$ has a 95% yield, with the remainder forming unknown products. In contrast, $6MPDH_4$ decomposes to 53% 7,8-$6MPDH_2$ and 47% ring-opened pyrimidines (Figure 32A) at a total rate 28 times that of $6MPH_4$. Unlike the relatively stable 7,8-dihydropterin, the ring-strained 7,8-$6MPDH_2$ degrades further over the course of a day. Instead of forming an analogue of 6-methylpterin, it is converted into far-UV absorbing species proposed to arise from oxidation of the 7,8-hydrate (Figure 32B).[655]

As was alluded to above, the pyrimidine cofactors for PAH are altered as a result of oxidation, either nonenzymatic or as a result of the hydroxylation reaction. Rapid decomposition of BDP follows its anaerobic oxidation by I_2 to the quinonoid form (Figure 33), which liberates TP and benzaldehyde (≤0.5% benzylamine). Air oxidation of BDP, while much slower, gives the same products.[660]

Even if NADH/DHPR is included in PAH assay mixtures, the cofactor ability of pyrimidines ceases after 0.55 or 0.71 nmol of tyrosine is produced per equivalent of TP or BDP, respectively. In the case of BDP, there is some product partitioning (Figure 29A) that indicates the formation of a species similar to the dihydropterin 4a-carbinolamine (Figure 29B) which decomposes by one of two competing pathways (Figure 29C,D). Inclusion of βME allows the isolation of divicine (2,6-diamino-4,5-dihydroxypyrimidine), a

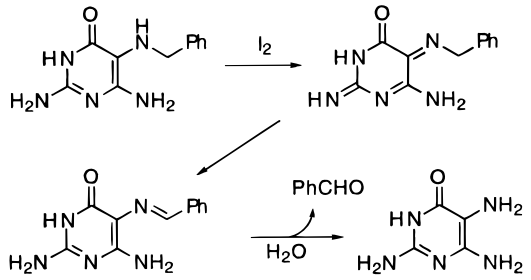

Figure 33. Oxidative degradation of a pyrimidine cofactor.

reduced form of the initial TP oxidation product, quinonoid divicine (Figure 29C,D). By using BDP with PAH, every tyrosine produced is the result of oxidation of 1.4 equiv of BDP, which forms 1.4 divicine and 1.0 benzylamine. The remainder of the cleaved BDP substituent (0.4 per tyrosine) is found as benzaldehyde, the exclusive decomposition product of nonenzymatic oxidation (and possibly of uncoupled BDP oxidation by PAH/O_2).[660]

If the reaction is performed under 72% Ar/28% $^{18}O_2$, 100.0 ± 1.4% of the divicine formed from BDP and 94% of the tyrosine formed contains an atom of ^{18}O. When TP is used as the cofactor, 97.5 ± 3.9% of the divicine and 95% of the tyrosine contains one atom of ^{18}O. (The efficiencies are corrected for label washout from synthetic [5-^{18}O]divicine, 14 ± 1.2% under the conditions of the experiment.)

PAH turnover is highly uncoupled with DL-*o*-methylphenylalanine (>10 molecules of BDP are consumed for each molecule of this substrate hydroxylated), but still the divicine product with BDP contains 90.0 ± 3.5% ^{18}O. (Intriguingly, the 90% uncoupling with BDP makes it the the most-coupled cofactor for *o*-methylphenylalanine hydroxylation. TP, $DMPH_4$, and BH_4 all give >99% uncoupled turnover.[660]) Two equivalents of ^{18}O are found in the product when [4-^{18}O]TP is used as a cofactor under $^{18}O_2$, which indicates that the keto group, equivalent to the C^4 carbonyl of a pterin, does not participate in the hydroxylating intermediate,[664] as had been suggested[665] (Figure 33).

Since $6MPDH_4$ produces tyrosine only four times faster than TP, and 20 times slower than the less-strained $6MPH_4$, it follows that ring-opening cannot be rate limiting in cofactor utilization. The extent of coupling is not relevant, since all three are utilized efficiently during hydroxylation (1.0 $6MPH_4$, 1.0 $6MPDH_4$, and 1.8 TP per tyrosine formed). Neither is ring closing a rate-limiting step, because it is extremely unfavorable with ring-opened diazepine, and for the trivial reason that it cannot occur with pyrimidines. In the Hamilton mechanism, the proposed oxenoid intermediate would be identical for all of the pyrimidine cofactors, following cleavage of the $C^{4a}-N^5$ bond. Differently substituted pyrimidines (TP, BDP, and N^5-methyl-TP) give different rates of turnover, indicating that decomposition of the proposed common oxenoid species during phenylalanine hydroxylation cannot be rate limiting. Furthermore, it indicates that the rate-limiting step in a Hamilton mechanism must occur before scission of the $C^{4a}-N^5$ bond.[655]

These results indicate that the cleavage of 5-amino group of TP results from PAH-catalyzed monooxygenation (Figure 29*B*), a result consistent with either

the Hamilton or Benkovic proposals. Evidence from the pyrimidodiazepine studies indicates that recyclization, were it to occur, would have to overwhelm completely the additional ring strain present in the larger cofactor. Under the conditions of the PAH assay, any ring opening of the diazepine causes kinetic trapping, in an inactive, open position that cannot be recyclized by PAH. If the Hamilton mechanism operates, the pyrimidodiazepine must function like a pyrimidine: oxidation of the ring-opened form is irreversible, and the cofactor would be able to perform only a single turnover. A final, decisive strike against the Hamilton proposal would be any demonstration that $6MPDH_4$ functions *catalytically* in the PAH reaction.[655] Such a result has not yet appeared, but given the weight of other evidence, the likelihood that the Hamilton mechanism will be verified is small.

The above reasoning depends upon two assumptions, the first being that hydroxylase catalysis supported by tetrahydropterin, pyrimidodiazepine, and pyrimidine cofactors functions by a common mechanism. The second is that chemical processes occurring at the pteridine ring are of central mechanistic importance in the generation of the hydroxylating intermediate.

While the first assumption is probably valid, given that all three classes of cofactor are able to support PAH catalysis, the second assumption is less sturdy. The evidence presented above strongly indicates that the pterin itself cannot support the hydroxylation reaction without a drastic enhancement of its reactivity by the enzyme and rules out most of the conceivable mechanisms that involve exotic oxygen−pterin adducts (a 4a-hydroperoxypterin intermediate and more metal-centered alternatives remain consistent with the evidence). Again, the presence of an iron in the mammalian aromatic amino acid hydroxylases appears to be an absolute prerequisite for activity. Ferrous iron is likely to be the entity that (in the two limiting extremes) either increases the reactivity of pterin with O_2 sufficiently to support catalysis, or performs oxygen activation and catalysis itself, with minimal participation of the tetrahydropterin. These possibilities, as well as others, are discussed in the next section.

IV. Mechanistic Investigations

A. Common Themes

1. Overview

The aromatic amino acid hydroxylases share a putative catalytic core, which is a functional monomer in the bacterial PAH's; within the mammalian hydroxylases, the N-terminus appears to determine functional specificity rather than contribute directly to catalysis. As a result, one would expect these hydroxylases to have similar substrate specificities and other functional resemblances that can be determined by mechanistic analysis. It also suggests that issues pertaining to reactivity ought to be considered together to emphasize functional similarities and amplify the differences, which is why this aspect is presented in a separate section. A clear conclusion from this section is that, while the familial resemblances are greater between PAH and TrpH than with TyrH, the similarities in oxygen atom transfer reactions performed by each tend to outweigh the differences among them.

We first present some common themes pertaining to oxygen atom transfer reactivity before the discussion of catalytic details for particular enzymes. The nonheme iron-dependent hydroxylases share many similarities with the protoporphyrin IX-containing cytochromes P450, regarding their ability to oxidize ordinarily unreactive aromatic and aliphatic C−H bonds. There are fewer similarities with flavin hydroperoxide-generating monooxygenases (section III.C.1), the reactivity of which is well-understood but cannot account for the observed spectrum of transformations. In this section, important observations from the vast literature on cytochrome P450 are summarized to focus on aspects of monooxygenase reactivity, before moving on to some model compounds that have reactivity reminiscent of the enzymes. Finally, some of the traits shared among the aromatic amino acid hydroxylases will be mentioned, followed by the discussion of the reactivity of each hydroxylase.

Although the taxonomic distinction between the non-heme iron-dependent monooxygenases and dioxygenases probably obscures informative functional similarities, this review does not cover the important class of dioxygenase enzymes, which includes the α-ketoglutarate-dependent dioxygenases,[666,667] catechol dioxygenases,[668] and singular catalysts like isopenicillin N-synthase[669,670] and lipoxygenase,[671] many of whose crystal structures have been recently solved.[672−674] Also excluded is discussion of the binuclear non-heme iron-containing hydroxylase domain of methane monooxygenase.[675−677] The interested reader will find the above-cited reviews and papers (as well as the other reviews in this issue) concerning the structure and reactivity of these systems informative in a larger sense of iron-dependent enzymology.

2. Hydroxylases and Oxygen-Atom Transfer

Hydroxylases (mixed-function oxidases[678]) catalyze the overall reaction by one of several potential mechanisms. An important reactivity difference between the flavin- and pterin-dependent hydroxylases is the capability of the latter to transfer oxygen atoms into unactivated aliphatic and aromatic C−H bonds. This is a specific case of the general reaction for oxygen-atom transfer,[679] $X + AO \rightarrow A + XO$, which can be adapted in the present case to (where *aa* = amino acid moiety):

$$O_2 + 2H^+ + 2e^- + aa\text{-C}-\text{H} \rightarrow H_2O + aa\text{-C}-\text{O}-\text{H} \quad (9)$$

In this depiction, the reaction catalyzed by hydroxylase-bound iron and $6MPH_4$ results in a two-electron reduction of only one of the oxygen atoms in O_2. The minimal mechanism for this transformation begins with dioxygen binding and activation (reduction). In a mechanism that involves heterolytic fissioning of the O−O bond, one of the oxygen atoms becomes the reactive *oxenoid* equivalent, and the other ends up at the oxidation level of water. Among a range of

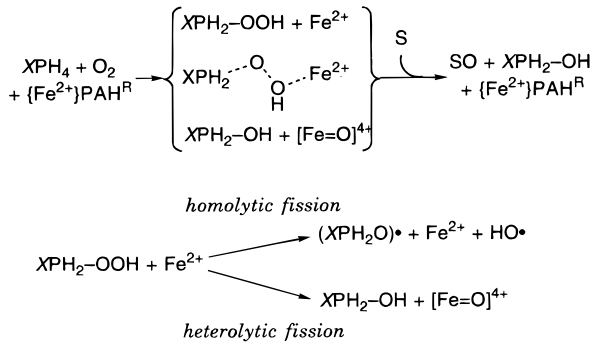

Figure 34. Various possibilities for the reactive intermediate formed during pterin-dependent hydroxylations.

possibilities, two limiting descriptions of the hydroxylating intermediate are available, one in which a tetrahydropterin peroxide species is formed, and one in which an iron-based oxoferryl species is formed (Figure 34). No direct spectroscopic evidence in support of either alternative (or any admixture of the two depictions) has ever been obtained in the non-heme iron hydroxylases. At some point following O_2 activation, insertion of an *oxo* atom (also called an *oxene* in analogy to carbene) into a substrate C−H bond takes place.

The reduced O_2 species might also fragment homolytically, which could be accomplished by symmetric O−O bond breakage, yielding at least one hydroxyl radical (HO•). The extremely reactive HO• would abstract a hydrogen atom from an organic group, which could certainly be the relevant position on the substrate amino acid. This proposal gained early attention, because it is one of the several reaction mechanisms that might explain the demanding oxidative chemistry of these hydroxylases, but several problems with this view arise.

First, the oxygen atom inserted into the product might be expected to exchange with the surrounding water (even a small extent is significant). Experiments with $^{18}O_2$ and $H_2{}^{18}O$ (described below) unambiguously demonstrate that the source of the oxygen atom in these hydroxylase reactions is O_2.

Second, there is essentially no way to control the reactivity of a hydroxyl radical once generated since no C−H bond can resist cleavage by this species. The first C−H bond encountered would be fissioned by the hydroxyl radical, which would result in organic radical formation, and likely autoinactivation of the protein and a broad product distribution. Some "model reactions" that can affect aromatic hydroxylation yield multiple products; in the case of phenylalanine-hydroxylating analogues, *o*-, *m*-, and *p*-tyrosine are all formed, often in low yield. The lack of specificity stems from the fact that the small-molecule reactive analogues cannot properly orient the substrate for oxygen atom transfer and/or because diffusible hydroxyl radicals are generated.

Hydroxyl radicals are particularly associated with Fenton's chemistry, which generally requires a reductant, O_2 or H_2O_2, and a transition metal, most often Fe^{2+}.[680] Model compounds that form hydroxyl radicals cause nonspecific hydroxylation, which can completely explain the superficially "PAH-like" reactivity. Even when such model reactions are not reported to contain metal ions, it should be remembered that even trace metal ion impurities may catalyze hydroxyl radical generation and Fenton chemistry.

A different type of "hydroxylation" follows proton abstraction and is not mechanistically associated with the current material. The prototype of this reactivity is the molybdopterin-dependent xanthine oxidase, which incorporates an atom of oxygen derived from H_2O rather than O_2 into its substrate.[529] This is the opposite of what is observed for true hydroxylases, which incorporate oxygen derived exclusively from O_2 (or under certain conditions, H_2O_2).

3. Cytochrome P450

Cytochromes P450 are ubiquitous enzymes but were first found in liver microsomes, where they are believed to perform a general detoxification function. Microsomes are easily isolable and can be used, without further purification of the membrane-bound cytochrome P450 enzymes, as a source of hydroxylase. The amounts and specificity of individual hydroxylase components in microsomes varies among animal sources and whether the animal has been exposed to an inducer of microsomal hydroxylases (typically phenobarbital). In general, cytochromes P450 perform oxygen atom transfer reactions on their substrates, with a somewhat wider substrate repertoire than is known for the pterin-dependent hydroxylases.

Our discussion is necessarily selective, as it is intended to illustrate how high-valent iron-oxygen species might function in aromatic amino acid hydroxylases. The interested reader is referred to several recent reviews and a book of monographs pertaining to cytochrome P450 biochemistry and function.[681−685] Identifying the reactive intermediate(s) formed by cytochrome P450 has been of keen interest for decades, an effort that has been greatly aided by several intense chromophores not present in non-heme iron proteins. There is a consensus that the critical intermediate is $(FeO)^{3+}$, where the oxo-bound iron is either a perferryl, $[Fe^{5+}{=}O]$, or a ferryl coupled to a porphyrin π radical, $[Fe^{4+}{=}O](P^{\bullet+})$. The latter description is supported by the similarity of the spectral properties of cytochrome P450 with those of horseradish peroxidase (HRP), for which a consistent and essentially complete set of spectroscopic evidence is available.

Cytochrome P450 forms a substrate complex that precedes binding of O_2 or an oxygen atom donor, so substrate-free oxygenated intermediates are not readily accessible. In contrast, HRP reacts with peroxides or various oxygen donors to give HRP compound I,[686] a green species that shares a number of spectral characteristics with oxidized cytochrome P450 adducts. EXAFS of HRP compound I reveals a remarkably short Fe−O distance, 1.64 ± 0.02 Å, consistent with the presence of a double bond.[687−689] Mössbauer spectroscopy[690] and higher X-ray absorption edge energies[687] support an Fe^{4+} formulation for HRP compound I. ENDOR spectroscopy indicates coupling of this $S = 1$ oxyferryl species to an $S = {}^1/_2$, 4-fold symmetric, π-cationic porphyrin radical,[691] in a manner consistent with a net $S_T = {}^3/_2$ determined by magnetic susceptibility measurements.[692]

Analogous spectroscopic observations have been made for HRP compound II, a red $[Fe^{4+}{=}O]$ inter-

mediate formed by one-electron reduction of compound I, and various reactive porphryin model compounds (section IV.A.6). Resonance Raman spectroscopy has identified a characteristic oxyferryl stretch in HRP compound II, but has been more difficult to apply in the case of the more photolabile cytochrome P450 intermediates.

The O_2 binding and rate-limiting reduction steps, as well as the need for a coupled NADPH-dependent reductase, can be skipped by adding H_2O_2 or other oxygen atom donors to ferric cytochrome P450, which generates a reactive species.[682] This "peroxide shunt" has been used to simplify mechanistic analysis considerably, although there have been occasional concerns about its exact identity with O_2-dependent turnover based on an altered substrate repertoire.[680]

We describe the various reactivities associated with the decomposition of this reactive oxygen−iron−porphyrin intermediate in section IV.A.5 in some detail, in part because its study has framed the important questions asked about all hydroxylases. The broader substrate range of the cytochromes P450 has allowed a wider range of mechanistic work than will ever be possible in the more selective aromatic amino acid hydroxylases. In particular, what can be learned from product analysis about the nature of a hydroxylating intermediate and the course of hydroxylation will be highlighted.

The similarities between the pterin-dependent, non-heme iron-dependent hydroxylases and the cytochromes P450 extend beyond normal coupled hydroxylation. In addition to reactions leading to substrate alteration, rat liver microsomes exposed to NADPH and O_2, but not a suitable substrate, produce H_2O_2 in a manner evocative of the "uncoupled" turnover of the aromatic amino acid hydroxylases.[693−695] Quantitation of the differences in partially uncoupled product formation by pure cytochrome $P450_{LM2}$ (demethylation of benzphetamine) and completely uncoupled NADPH oxidation (induced by the structurally related benzylamphetamine) confirmed that an identical amount of H_2O_2 was formed in the uncoupled component of each.[696]

4. The NIH Shift

In the course of developing assays for several aromatic hydroxylases, it was observed that the ^{3}H-release assay[23] successfully employed in assaying TyrH (section II.B.2) could not be generalized to PAH, TrpH, or several other enzymes that hydroxylate aromatic substrates.[697] Little tritiated water was released from L-[4-^{3}H]Phe or DL-[5-^{3}H]Trp, but the labeled amino acids were indeed converted into their respective hydroxylated products.[698,700] [Confirmation that the small amount of tritium-substituted phenylalanine is exclusively *para*-substituted was obtained by using a synthesis shown (by NMR) to yield only DL-[4-^{2}H]phenylalanine from *p*-Br-DL-phenylalanine.[652] An analogous determination was made with labelled hydroxyindoles, which have an additional complication of acid- or base-catalyzed washout of the label from the 5-hydroxy-L-[4-^{3}H]trp product.[698,699]] Release of label from the tritiated L-Tyr product was accomplished using TyrH (equal amounts of tritiated water and L-Dopa were obtained) or by iodination (>80% release of label, equal to that

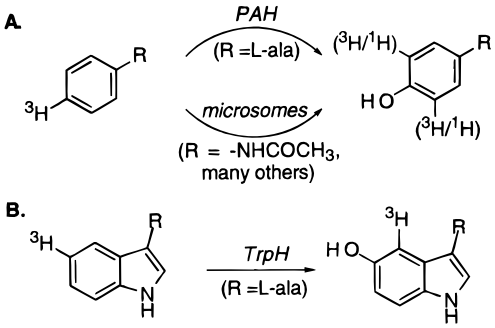

Figure 35. The NIH Shift.

from a [3,5-^{3}H]Tyr control), indicating that the *para* substituent had migrated to a *meta* position.[700]

This "NIH shift" phenomenon appears to operate in a number of aromatic *para* hydroxylations, including PAH, TrpH, and the cytochrome P450 component of liver microsomes (Figure 35). The NIH shift is not part of the normal reactivity of TyrH, which attacks the *meta* position in L-Tyr (when L-Tyr labeled with ^{18}O in the phenolic hydroxyl is used as the substrate along with $^{16}O_2$, no migration of the ^{18}O label is observed in the L-Dopa product). The availability of an *o*-quinonoid resonance structure in the initial hydroxylation product of L-Tyr appeared to explain the rapid loss of *meta* label, which is not retained in the *ortho* position of L-Dopa. There is 84% retention of tritium when TyrH hydroxylates L-[4-^{3}H]Phe.[701] In the case of the microsomal hydroxylases, which accept a wide variety of substrates, the percent retention of radiolabel in a product is higher if the substrate cannot readily rearomatize at the hydroxylated position.[697] In general terms, aromatic substrates that lack *ortho* or *para* hydroxyl or amine substituents have less leaky NIH shifts.

There is no alteration in the specific radioactivity of the L-Tyr formed from L-[4-^{3}H]Phe, indicating there is no primary isotope effect. No K_m or V_{max} differences were observed on PAH hydroxylation of L-Phe, L-[4-^{2}H]Phe, or L-[3,5-^{2}H]Phe to the corresponding L-Tyrosines.[702] However, there is no loss of label from L-[3,5-^{2}H]Phe with PAH, [4-^{3}H]Trp with TrpH, or [3,5-^{3}H]acetanilide with microsomes,[697] indicating a significant intramolecular isotope effect on the rearomatization step (Figure 36) that causes preferential *meta* proton loss. This isotope effect was measurable from the amount of tritium retention during hydroxylation of DL-[4-^{3}H]Phe and DL-[4-^{3}H][3,5-^{2}H]Phe by *Pseudomonas* cultures, yielding a k_D/k_T of 2.8 ± 0.1, which predicts $k_H/k_D \approx 10 \pm 1$.[703] Isotope effects of this type profoundly affect the interpretation of potential reaction pathways that will be discussed in the following section for cytochrome P450.

Other *para* substituents also undergo migration to a *meta* position. For PAH, these are *p*-chloro-, *p*-bromo-, and *p*-methylphenylalanines. The amount of migration varies between the substituents, in a manner that will be discussed in Section IV.B.3. For the microsomal hydroxylases, which accept a wider variety of substrates, many substituent effects have been noted,[704,705] including many that indicate accelerated label loss when a quinonoid structure is available.

Migrations of chloro and methyl substituents are known, but multiple products are common because

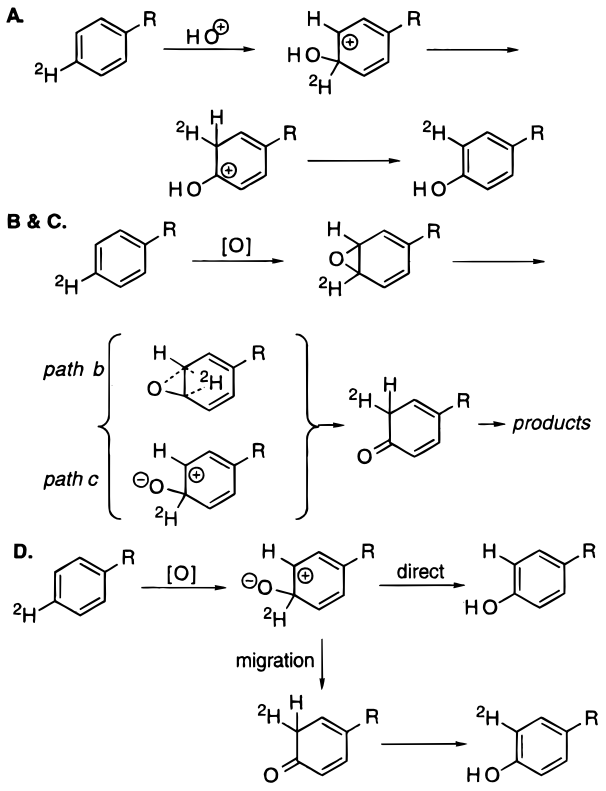

Figure 36. Mechanisms proposed for the NIH Shift.

of the ability of the relatively nonselective microsomal hydroxylases to form various initial arene oxides (*vide infra*), most of which open in one of two directions,[706−708] or because of permissive regioselectivity. (Despite the potential similarities among methyl, halogen, and hydrogen isotope migration, the term "NIH shift" refers exclusively to the 1,2-hydride migration.)

In sum, it appears that the nature of the substrate and its initial hydroxylation product determines the course of the NIH shift following hydroxylation, rather than a particular enzyme. Whether a NIH shift occurs is dependent upon the nature of the hydroxylating species. Mechanistically, the NIH shift was originally envisioned as is illustrated in Figure 36A (where *R* is appropriate to the enzyme under consideration) as an attack of the electrophilic hydroxyl cation on the *para* position, followed by 1,2-hydride migration.[697]

Considerable effort has been directed at enriching this depiction and connecting the NIH shift mechanism to oxygen atom transfer, but often the results are difficult to explain in terms of a single mechanism. In some cases, this is because more than a single mechanism is operative; in others a distinction between two possibilities has not yet been made. In the following section, results obtained with cytochrome P450 and its simple arene substrates are considered. Despite the early importance of PAH and TrpH in discovering the NIH shift, little mechanistic work has been performed since the 1960s using the pterin-dependent amino acid hydroxylases. In part this is the result of the much more stringent substrate specificity of the non-heme iron-, pterin-dependent enzymes. Since both heme-dependent and non-heme iron-dependent hydroxylases catalyze oxo atom transfers followed by a NIH shift, it is hoped that what has been learned with the simple organic substrates of microsomal hydroxylases will have useful parallels in the aromatic amino acid hydroxylases.

5. Arene Oxides and Reactive Intermediates

In the case of microsomal hydroxylases, it had been anticipated that arene oxides might be intermediates in aryl dihydroxylation,[709] which would be viewed as sequential epoxidation and hydrolysis steps. By using oxygen isotope incorporation into 1,2-dihydroxynaphthalene, it was shown that only one of the hydroxyls derived from O_2, with the other originating from H_2O.[710,711] This observation excludes endoperoxide formation and other dioxygenation mechanisms.

Following the discovery of the enzyme-mediated NIH shift, it was demonstrated that the label in [4-^{2}H]toluene 3,4-oxide migrated to the *meta* position during nonenzymatic epoxide opening, yielding only *p*-cresol. The extent of deuterium retention/migration, which ranges up to 75−85%, depended to some extent on the conditions of epoxide ring opening. Most important, this experiment indicated that the "later" stages of aromatic hydroxylation with an NIH shift did not require the intervention of an enzyme at all.[712] This started a series of investigations focused on microsomal hydroxylation and solution studies of epoxide decomposition pathways.

Naphthalene 1,2-oxide was found to be an isolable intermediate in the formation of 1-naphthol, and other naphthalene metabolites formed by epoxide ring opening, by rabbit liver microsomes from naphthalene.[713] Nonenzymatic opening of the arene oxide could also account for the small amount of 2-naphthol produced by microsomes. Thiol compounds, including glutathione, form ring-opened adducts following nucleophilic attack on the epoxide. Thus it was concluded that the initial product of naphthalene metabolism was an arene oxide, an obligatory intermediate in naphthol formation, formed by direct epoxidation. The absence of an intermolecular isotope effect in hydroxylation of an equimolar mixture of normal and perdeuterated naphthalene is consistent with rate-limiting arene oxide formation. Furthermore, proton abstraction and concerted C−H insertion mechanisms leading to an NIH shift were excluded by this observation.[714]

Because the nonenzymatic formation and breakdown of arene oxides appeared sufficient to account for the behavior of the NIH shift in the naphthalene → 1-naphthol conversion, a tendency to regard arene oxides as invariable participants in aromatic hydroxylations arose at this point. While evidence has accumulated in support of other plausible mechanisms participating in the hydroxylation of different substrates, the arene oxide mechanism remains important in the understanding of NIH shifts.

The synthetic availability of various arene oxides (reviewed in ref 715), the presumptive initial products of aromatic hydroxylation, allowed investigations of the later steps in the NIH shift reaction, which are ordinarily obscured by the initial rate-limiting oxygen transfer. From the pH dependence of the ring opening, it was realized that nonenzymatic epoxide opening was the sum of two processes: a spontaneous process and a distinct acid-catalyzed

process associated with less-efficient substituent migration.[714,716]

Decompositions of [1-^{2}H]- and [2-^{2}H]naphthalene 1,2-oxides, whether microsome-mediated or nonenzymatic, yield the same levels of deuterium in their respective 1-naphthol products. This indicates that a common [3-^{2}H,3-H]cyclohexadienone intermediate is formed, which undergoes keto−enol tautomerization to form the aromatic product. An intramolecular $k_H/k_D = 4$ for enolization is implied by the observed ~80% deuterium retention.[714]

Irradiation of naphthalene 1,2-oxide allowed direct detection of the keto tautomer of 1-naphthol at 77 K (but not 153 K), which decomposed to the 1-naphthol product upon warming to 173 K.[717] Formation of this cyclohexadienone intermediate would follow either a concerted (Figure 36, path b) or stepwise mechanism (Figure 36, path c). Concerted hydride/epoxide migration was ruled out on the basis of (1) the lack of an isotope effect on naphthalene and benzene oxide disappearance (the perdeuterated and perprotiated arene oxides yield $k_H/k_D = 1.00-1.05$ for both spontaneous and acid-catalyzed decomposition) and (2) a large negative value for the Hammett parameter ρ determined with various substituted arene oxides, both of which argue against a triangular transition state. It follows that a C−H bond does not participate in the isomerization and that a discrete positive charge is developed during the transition state. Therefore the cyclohexadienone intermediate is probably formed by a *meta* carbonium intermediate, depicted in Figure 36, path c.[718]

A different situation arises in the formation of *p*-chloro[3-^{2}H]phenol from [3-^{2}H]- or [4-^{2}H]chlorobenzene, which gives 93 and 54% deuterium retention, respectively. This suggests partitioning between at least two pathways for breakdown of the chlorobenzene 3,4-oxide, an NIH shift leading to *meta* migration of the *para* substituent, and a simple direct loss mechanism, in which the *para* substituent is released following hydroxylation. If arene oxide formation has to precede the NIH shift, the difference in the levels of deuterium retention at the *meta* position of chlorobenzene implies an isotope effect on enolization of $8 - 9$ (k_H/k_D).[714] (When more than one mechanism to a product is operative, the isotope effects observed are averages.)

Other evidence does not favor the hypothesis that partitioning into either pathway results from decomposition of a directly formed arene oxide. While *meta*-hydroxylated chlorobenzene is a minor metabolic product in rat or of rat liver microsomes, it is *not* observed following nonenzymatic opening of chlorobenzene 3,4-oxide or 2,3-oxide, which yield exclusively *para* and *ortho* products. Since arene oxides are incapable of forming this product, one of several mechanisms for direct hydroxylation not involving arene oxide formation must prevail.[719,720] Figure 36D depicts this earlier partitioning of intermediates. The issue of chlorobenzene will be returned to later, after mentioning some other evidence supporting nonarene oxide-dependent, direct hydroxylation pathways.

Intermolecular isotope effects larger than unity, and therefore inconsistent with exclusive initial arene oxide formation, were observed for methyl phenyl sulfone and nitrobenzene *meta* hydroxylation (1.75 and 1.40, respectively). For *para* and *ortho* hydroxylation of these compounds, or of a group of other monosubstituted benzenes, no isotope effect larger than 1.2 was observed.[721] These values are close to what is observed for direct carbene insertions into aliphatic C−H bonds (1.6−1.8, cited work in ref 721) but higher than carbene additions to aromatic systems, which have intermolecular isotope effects ≤1.1. On this basis, the authors conclude that direct oxygen atom insertion into an aromatic C−H bond is unlikely to explain the observed isotope effects.[721] Perhaps the clearest example of a primarily nonarene oxide-dependent (>90%) aromatic hydroxylation is the direct 3-hydroxylation of 2,2′,5,5′-tetrachlorobiphenyl (TCB) by phenobarbital-induced rat liver microsomes. In contrast, microsomal conversion of TCB 3,4-oxide (TCBO) to 3-hydroxylated TCB was at least 8-fold less efficient, and even that reactivity seemed to result from TCBO *reduction* to TCB, followed by hydroxylation.[722]

Cytochrome P450-mediated hydroxylations are known for olefinic and acetylenic substrates as well. While non-arene compounds cannot undergo the typical NIH shift, 1,2-subunit migrations can occur. Quantitative migration of an acetylenic proton to the vicinal carbon occurs during hydroxylation of aryl acetylenes and is associated with a large isotope effect whether the oxidant is *m*CPBA (*m*-chloroperbenzoic acid, an oxo-transferring reagent) or cytochrome P450.[723−725]

A comparable situation also occurs during the microsomal metabolism of trichloroethylene ($CHCl{=}CCl_2$, TCE), which is degraded *in vivo* to chloral (Cl_3CCHO), trichloroethanol, trichloroacetic acid, and covalent TCE-derived adducts. Using liver microsomes + NADPH, cytochrome P450 + iodosylbenzene (OIPh, an oxygen atom donor capable of supporting enzymatic hydroxylation), or cytochrome P450 + its NADPH-coupled reductase, TCE oxide formation was detected with a specific trapping reagent. The amount of TCE oxide formed was 5−28 times too small to account for the observed product formation (chloral and glyoxylate), so it cannot be an obligatory intermediate.[726] TCE oxide decomposes to CO, dichloroacetic acid, and formic acid, but not chloral or glyoxylate.[727]

In order to account for the observed reactivity, including the 1,2-chloride migration in chloral formation, Miller *et al*. propose the formation of a substrate adduct, resulting from interaction of TCE and a high-valent heme iron−oxo intermediate (Figure 37).[726] A similar intermediate in olefinic hydroxylation having a distal radical rather than a carbonium ion had been proposed by Groves *et al.* on the basis of studies with manganese porphyrin catalysts.[728]

An analogous situation obtains for arene substrates, which would form radical or cationic adducts (Figure 37), each of which might also form an arene oxide, *meta* carbonium, or cyclohexadienone intermediate prior to rearomatization. A key difference between these alternatives is the timing of electron transfers. This is an experimentally challenging distinction, in part because it follows the typically rate-limiting step of hydroxylating intermediate generation. One intriguing observation stems from the

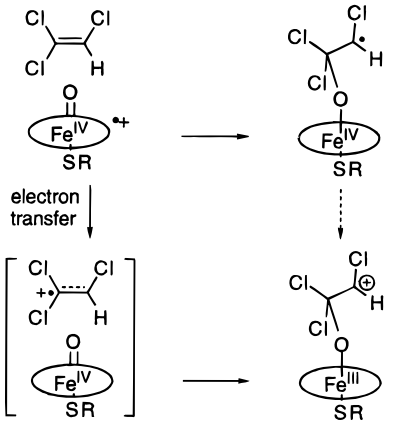

Figure 37. Potential substrate adducts in the cytochrome P450 reaction with TCE.

fact that during their oxidation, the distal carbon of TCE or an aryl alkene alkylates a pyrrole nitrogen in the porphyrin, perhaps by a radical-trapping process. In the case of aryl acetylenes, the heme modification reaction has no isotope effect, unlike the metabolite-forming reaction, which suggests that it occurs before oxygen transfer is complete, and that both reactions proceed along separate stepwise pathways.[729]

The important insight is that regardless of its structure, adduct formation is strongly suggested for a range of cytochrome P450 products. As several authors point out, the substrate affects the preference for cationic or radical intermediates, and thereby how the electron distribution should be rendered in the adduct. The identity of the oxidant (catalyst) is equally important in determining product distribution. In the case of cytochrome P450, the iron participates in modulating intermediate partitioning and reactivity. It is reasonable to expect that the non-heme iron-dependent monooxygenases are capable of a similar feat.

Since there are at least two pathways (NIH shift and direct hydroxylation) observed with cytochrome P450-mediated aromatic hydroxylations, a useful strategy for sorting out their relative contributions has been to hydroxylate specifically deuterated arene substrates, examine product distributions, and thereby separately calculate the contributions due to mechanistic partitioning and isotope effects.

A sophisticated approach of this type was employed by Hanzlik *et al.* for monosubstituted benzene hydroxylation by rat liver microsomes, using an analytical approach, based on the product distributions from 1-*X* substituted [3,5-^{2}H]- and [2,4,6-^{2}H]-benzenes, that allowed the calculation of individual enolization isotope effects and mechanistic partitioning factors F_i (where $F_i = 1$ indicates complete substituent migration, and $F_i = 0$ indicates complete direct hydroxylation) for *each* of the *o*-, *m*-, and *p*-phenolic products. For all of the monosubstituted compounds examined (X = Br, CN, NO_2, OCH_3, CH_3, and Ph), the k_H/k_D for enolization was 4.05 ± 0.2 at each ring position, which indicates the generality of cyclohexadienone formation following 1,2-hydride migration. These isotope effects are "pure", because the mechanistic branching has been factored out, and are therefore more reliable than those derived from simple deuterium retentions. However, the value of

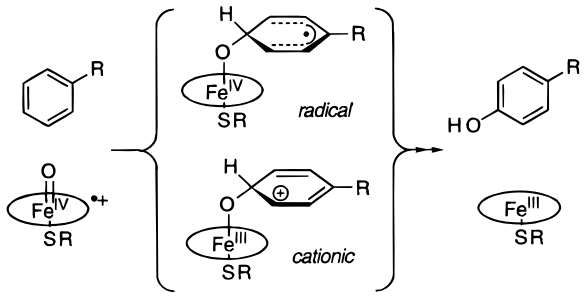

Figure 38. Plausible radical and cationic substrate adducts of cytochrome P450.

F_i varied widely, from 0.975 for *para* hydroxylation of bromobenzene to 0.203 for *para* hydroxylation of nitrobenzene, indicating that substituents do affect mechanistic partitioning.[697]

An analogous approach was used with chlorobenzene, which as was mentioned above is *meta* hydroxylated by microsomes to a product unavailable from nonenzymatic arene oxide opening. Two general descriptions of the oxygen transfer apply: a "singlet" mechanism leading to concerted epoxide formation without intermediates, or one of several "triplet" mechanisms involving formation of a tetrahedral intermediate as depicted in Figure 38. Pathways in which the oxygen is triplet-like include (1) addition of the oxygen to form a (bi)radical species that rearranges to the final phenolic product, the "radical" pathway of Figure 38, or (2) initial single-electron oxidation of the substrate to a cation radical, followed by recombination of the substrate radical and iron-bound oxygen, the "cationic" pathway. (The biradical state used for computations has a ring-based radical and an oxygen-based radical. This is a third limiting case of the $(FeO)^{3+}$ depiction, [Fe^{IV}–O•]. Since the oxygen-bound iron would facilitate triplet → singlet conversion, only the singlet state was considered important.)

Theoretical considerations suggest that the cationic pathway will show marked substituent effects and favor direct phenol or ketone formation, while the (bi)radical pathway will not show substituent effects and will favor epoxide formation.[730] Isotope effects were determined for [3,5-^{2}H]-, [2,4,6-^{2}H]-, and [2,3,4,5,6-^{2}H]chlorobenzene in order to distinguish between these possibilities. Small, normal isotope effects were measured for both [3,5-^{2}H]- and [2,4,6-^{2}H]chlorobenzene on *meta* hydroxylation (1.09−1.17), which rules out singlet mechanisms of direct epoxide formation. This follows from the fact that a normal isotope effect on the site of hydroxylation, indicating reversible epoxide formation, would also require an inverse isotope effect on the adjacent position that is not observed. Direct ketone formation during *meta* hydroxylation is also inconsistent with the observations. Initial electron abstraction is disfavored by the observation of an inverse isotope effect for *ortho* and *para* hydroxylation; however, electron transfer from the substrate *after* the formation of the tetrahedral intermediate appears to explain the observed *meta* hydroxylation isotope effects.

The mechanism most consistent with all of the observations is an attack of the activated, triplet-like oxygen species on the aromatic substrate's π system, followed by addition and rearrangement.[731] In a later

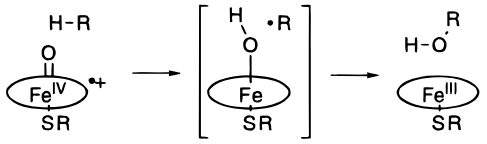

Figure 39. The "oxygen rebound" mechanism of hydroxylation by cytochrome P450.

^{19}F NMR study of the regioselectivity of hydroxylation for various fluorine-substituted benzenes, a similar conclusion excluding an epoxide intermediate was reached. Fluorobenzenes confer several advantages, including the absence of dehalogenation and that >95% of the metabolites are phenolic. Most important, the smaller van der Waals radius of a fluorine substituent argues against steric or substrate-orientation effects.[732] Thus it appears that whether the substrate is an olefin or an arene, cytochrome P450 can generate an electrophilic oxygen species capable of forming an enzyme-bound radical or cationic intermediate, as depicted in Figure 37 and Figure 38.

One of the more remarkable properties of cytochrome P450 is an ability to catalyze aliphatic hydroxylation with retention of stereochemistry, as in the hydroxylation of camphor, which gives primarily the 5-*exo* product. Previously, only carbenes (*i.e.*, :CH_2) were known to insert into C−H bonds with retention of stereochemistry.[733]

In Groves' classic experiment, partial epimerization during hydroxylation of *all-exo*-[2,3,5,6-^{2}H]norbornane was detected by observing a small amount of the *tetra*deuterated *exo*-alcohol product. Stereochemical scrambling during hydroxylation is best explained by a stepwise, radical mechanism, and would not be observed during a concerted oxygen insertion. The small amount of inversion induced in this cytochrome P450 hydroxylation by a sizable isotope effect ($k_H/k_D = 11.5$) pointed at proton abstraction as a rate-limiting step in catalysis.[734] Proton abstraction indicates that the highly reactive, activated oxygen species probably has significant radical character.[735] If discrete substrate radical intermediates are formed, they have extremely brief lifetimes prior to recombination with an iron-bound OH species. This abstraction−recombination proposal, the so-called "oxygen rebound" mechanism (Figure 39), has been examined using radical-sensitive cyclopropane-containing substrates. The product distribution from methylcyclopropane hydroxylation included 15% ring-opened products, a signature of radical processes.[736]

Following this result, a series of more sensitive radical clock substrates have been synthesized, in order to put an upper limit on the radical intermediate in the oxygen-rebound mechanism from a comparison of the ring-opening rate and the fraction of ring-opened products. A potential problem with timing radical intermediates in this way is the potential for ring opening during a parallel, cationic process.

In a recent report, Newcomb *et al.* were able to distinguish ring-opened products formed by either cationic or radical pathways, using a hypersensitive probe substrate (Figure 40). Three stable products are obtained, which allow a simultaneous determination of the branching between cationic and radical pathways and the amount of ring opening that occurs

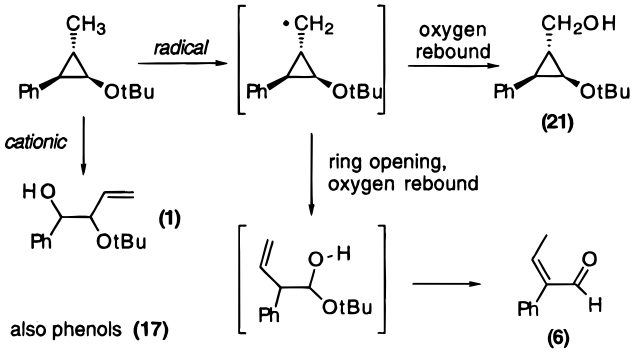

Figure 40. A radical clock with different "cationic" and "radical" product distributions.

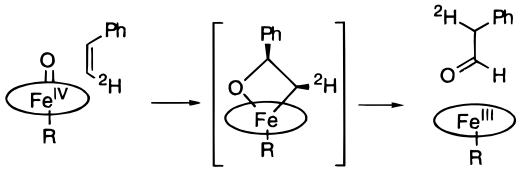

Figure 41. Putative metallaoxetane intermediate in *cis*-[2-^{2}H]styrene hydroxylation.

during the time it takes for the oxygen to rebound. The relative amounts (parentheses in Figure 40) of specifically radical-derived ring-opened products indicate a 70 fs lifetime for the radical, too short for it to be considered a discrete intermediate. In this concerted, nonsynchronous process, the carbon is near enough to the oxygen atom at the time of proton abstraction to undergo hydroxylation as part of the reacting ensemble. Newcomb *et al.* suggest that this is indicative of a "side-on" approach of the oxygen to the C−H bond,[737] which has some support from crystal structures of cytochrome P450cam bound to its camphor substrate or its *exo*-5-hydroxycamphor product. A comparison of the two complexes shows only slight differences in the position of the bound camphor with respect to the enzyme.[738,739]

Alternate attacking geometries have also been proposed by Ostović and Bruice,[740] and by Breslow *et al.*[741] on the basis of model studies.

Another proposal, formation of a metallaoxetane intermediate after side-on approach of the substrate's C−H to the oxyferryl (Figure 41), has been receiving renewed attention since it was first proposed for cytochrome P450 on the basis of model studies.[742−744] Perhaps the strongest evidence for an enzyme-bound metallaoxetane is the quantitative migration of deuterium in the *cis*-[2-^{2}H]styrene → phenyl[1-^{2}H]-acetaldehyde conversion, studied with iron and manganese porphyrin catalysts.[743] Again, something other than the arene oxide-dependent NIH shift must account for this transfer.

Metallaoxetane formation might also account for the unusual observations (*complete* acetylenic hydrogen transfer, heme alkylation without an isotope effect, and apparently direct aldehyde formation) during phenylacetylene oxidation.[745]

As yet, there is no direct evidence for metallaoxetane formation. Many of the objections to metallaoxetane formation come from steric considerations, particularly since catalytically active but very crowded porphyrin model compounds would tend to exclude metallaoxetane formation.[740,741] The potential for metallaoxetane formation in various systems

has been recently reviewed.[746] While an absolute determination that a metallaoxetane forms is at present unavailable, it is potentially consistent with the isotopically substituted chlorobenzene analysis of Korzekwa *et al*. if adduct formation is reversible ("substrate debinding").[731] Some evidence supporting reversible adduct formation, consistent with either an olefin π-complex or metallaoxetane formation, was obtained by Groves and Watanabe in their detection of a dark green (porphryin radical), catalytically competent intermediate.[747]

In a general sense, the evidence indicates that arene oxide formation is sufficient, but not necessary, to give an NIH shift. As a result there is a tendency to include an arene oxide unless there is direct evidence against its intermediacy. In contrast, the observation of an NIH shift with heavy hydrogen isotopes is good evidence for a normal isotope effect on cyclohexadienone enolization, and transitively, for invocation of an initial oxidized species (either epoxide or a tetrahedral adduct). It is difficult to imagine how a hydroxyl radical would be consistent with an NIH shift, which in turn is regarded as good evidence for oxygen atom transfer.

Partitioning of this reactive intermediate between aromatic and aliphatic hydroxylations has been examined in the case of toluene, which gives phenolic products and benzyl alcohol in a 1:2.2 ratio. Since aromatic hydroxylations have no significant isotope effects, hydroxylation of ring-deuterated toluene shows about the same aromatic:aliphatic partitioning (1:2.1). Increasing the number of deuteriums in the methyl group from 0 to 3 causes a reversal of this preference (1:0.32), which was about the same in perdeuterated toluene (1:0.24). When the partially rate-limiting, slow dissociation of benzyl alcohol is accounted for, an isotope effect of 7.4 is obtained for benzylic hydroxylation of toluene.

Despite a high commitment to catalysis (small intermolecular isotope effects), the $^{D}(V/K)$ of the observed aliphatic:aromatic ratio is substantial, 6.3.[748] This indicates that the partitioning is due to isotopically sensitive branching ("metabolic switching" [749]) that results from a reversible interaction of toluene with the activated, enzyme bound-oxygen species, and that product formation from this interaction is faster than substrate release.[748]

There are some parallels between these observations and the small number of aromatic amino acid hydroxylase reactions known to produce multiple products (*e.g.*, *p*-methyl-L-Phe hydroxylation by PAH, L-Phe hydroxylation by TyrH) that will be discussed below, in the context of each enzyme's reactivity.

6. Reactivity Models Relevant to Monooxygenase Chemistry

One of the cornerstones of bioinorganic chemistry has been finding compounds that model metalloprotein active sites. An important distinction between *structural/spectroscopic* modeling and *functional* modeling is that the former are sometimes inert, in which case any inferences made about catalytically active entities are necessarily indirect. Of course, the perfect model of an enzyme's active site is both structurally and functionally identical; this ideal has been nearly realized for models of iron−sulfur clusters and for hemoprotein monooxygenases.[750−752]

The general strategy for heme monooxygenase modeling has been to react a soluble iron porphyrin with near-stoichiometric amounts of an oxygen atom donor, usually OIPh or *m*CPBA, thereby avoiding complications associated with O_2 reduction followed by homolytic *vs* heterolytic cleavage of the peroxo O−O bond. Sequestering the reactive oxyferryl adducts of these heme compounds proved to be the key to obtaining structural analogues of HRP intermediates, which were also reactive compounds themselves. Tetraarylporphryins have sufficient steric bulk to preclude formation of the inert μ-oxo-bridged dimer. Using [Fe^{2+}(TPP)Cl] with OIPh as the source of oxygen (TPP = tetraphenylporphyrin), Groves *et al*. first demonstrated catalytic cyclohexene epoxidation and allylic hydroxylation (55 and 15% yields, respectively, *vs* starting material). The stereochemical integrity of *cis*-decalin (5:1 *cis*:*trans* decalol product) and *cis*-stilbene (*cis*-stilbene oxide) were maintained during oxidation, but *trans*-stilbene was not epoxidized. These results require direct participation of the porphyrin catalyst in the oxygen-transfer step, since they are inconsistent with oxidation due to free radical formation or any small oxidant (*i.e.*, HO$^{\bullet}$ and OIPh).[753]

The first structurally characterized, catalytically competent oxyferrylporphyrin was formed by reaction of [Fe^{3+}(TMP)Cl] (where TMP = tetramesitylporphyrin) with OIPh or *m*CPBA, which yielded a green adduct. A π-cation radical was indicated by ^{1}H NMR and visible absorption spectroscopy, Fe^{4+} by Mössbauer spectroscopy, and $S_T = {}^3/_2$ by magnetic susceptibility, consistent with a [Fe^{4+}═O (TMP$^{\bullet+}$)(L)] formulation. Most important, norbornene oxide was generated in 78% yield (*vs m*CPBA) with incorporation of label exclusively from $H_2{}^{18}O$, which would not occur were the oxidation mediated by *m*CPBA itself.[754] EXAFS of this species in comparison with HRP compounds I and II showed short Fe−O distances (1.60−1.65 Å), and therefore is consistent with Fe^{4+}═O being present in each. The spectral similarity between HRP intermediates and the reactive [Fe^{4+}═O (TMP$^{\bullet+}$)(L)], which functions like cytochrome P450, reinforces the previously inferred chemical similarity between the two enzymes' active sites and intermediates, despite their overall functional differences. [Fe^{4+}═O](P$^{\bullet+}$) is now generally accepted to be an intermediate in all three pathways.

From this point, work with models has expanded to include O_2 binding and asymmetric catalysis by increasingly elaborate porphryin-based molecules.[755] A parallel modeling approach, using manganese porphyrins, continues to provide information about the effects of the metal's oxidation state on complex formation and catalysis.[735] A current area of interest is in improving the selectivity of the useful manganese and iron porphyrins by alteration of ligands and the reaction conditions.[685] The longstanding synthetic challenge of creating a model porphyrin with an axial thiolate ligand has recently been achieved and should be useful in broadening our understanding of electron transfer into the iron site.[756] Protein-centered catalytic studies have evolved in two directions: toward understanding the mechanistic details of (and partitioning between) alkane hydroxylation, N- and O-demethylation, and the other en-

zyme activities of cytochromes P450, and toward "protein engineering," an approach to determining reactivity and specificity that employs various cytochrome P450 mutants and remodeling other hemoproteins that are not ordinarily monooxygenases.[757]

Although the success with hemoproteins and porphryin compounds has been remarkable, it remains unknown which aspects of the enzymes and model compounds are essential to the generation of reactive intermediates. In part, slight modifications of heme-containing compounds and biomolecules can illuminate this issue, but it is quite clear that neither heme nor iron is essential for oxygen-atom transfer. In order to encompass and understand the chemistry of selective oxygen atom transfers, it is important to step away from heme compounds. For the rest of this section, various methods of oxygen atom transfer that do not include a heme moiety are discussed, in order to generalize oxygen transfer itself and understand how the aromatic amino acid hydroxylases might be able to perform chemistry reminiscent of cytochrome P450 without the presence of its versatile prosthetic group.

As expected from the term "oxygen atom transfer", atomic oxygen is capable of oxidizing a number of organic substrates. The ground-state triplet species $O(^3P)$ can be generated by mercury-photosensitized decomposition of N_2O in the gas phase, or by γ-irradiation of liquid CO_2. In the latter case, the reactivity properties of $O(^3P)$ are most easily examined. Retention of configuration in the hydroxylation of *cis*- and *trans*-decalin (83% and 93%, respectively) confirms that the abstraction of a proton is followed very quickly by radical recombination, perhaps because the radical pair is confined to a "solvent cage".[758] When toluene is exposed to $O(^3P)$, *o*- and *p*-cresols are the primary products, formed with no significant isotope effect ($k_H/k_D = 1.1$ for benzene). However, deuterium is retained in the products, indicating an NIH shift occurs: with [2,4,6-^{2}H]-toluene the retention of label is 52% with $O(^3P)$ compared to 54% with microsomes. An isotope effect of 2.1 is obtained for cyclohexadienone rearomatization, and the rates of phenol formation from various substituted benzenes yield a negative value for the Hammett parameter ρ, both of which are similar to results with cytochrome P450 itself.[759] Thus it appears that this simplest electrophilic oxidant has all of the mechanistic hallmarks of enzyme-mediated aromatic hydroxylation, with the obvious exception of positional specificity.

In a preparative sense, perhaps the simplest solution method of aromatic hydroxylation is the Fenton reaction, in which Fe^{2+}/H_2O_2 mixtures generate highly reactive hydroxyl radicals.[760] Incubation of [4-^{3}H]acetanilide (a substrate of microsomal hydroxylases that undergoes an NIH shift) with Fenton's reagent causes formation of the three isomeric hydroxyacetanilide products. Only the *m*- and *o*-hydroxyacetanilide products retain full ^{3}H levels, while >98% of the label is lost in the *p*-hydroxyacetanilide product. This demonstrates the incompatibility of the hydroxylation mechanisms that lead to an NIH shift and the HO•-mediated Fenton's chemistry.[761]

While this may be true for HO•, later studies of Fe^{2+}/H_2O_2 in *dry* acetonitrile have uncovered reactivities that are inconsistent with HO• formation. This appears to be due to the 1.2 V increase in the Fe^{3+}/Fe^{2+} redox couple, to +1.4 V (*vs* NHE).[762] When aromatics are oxidized by this system, an NIH shift occurs, to about the same extent as microsomes.[763] However, the extent of NIH shift for toluene is only slightly reduced when the reaction is run in the presence of H_2O, in a reaction inhibited by O_2. Under $^{18}O_2$, preferential incorporation of label into the *meta*-position was observed (toluene in 90% CH_3CN gives 6% phenolic products, containing 4.0% (*ortho*), 29.3% (*meta*), and 5.0% (*para*) ^{18}O). Methoxylation also gave an NIH shift, indicating a non-arene oxide mechanism.[764]

Some directing effects were observed with cyclohexanol hydroxylation, which produced mostly *cis*-1,3-cyclohexanediol. Only a small isotope effect was observed ($k_H/k_D = 1.18$) on initial hydrogen abstraction, which was proposed to lead to carbonium ion formation by Fe^{3+}. In specifically deuterium-labeled 7-hydroxynorbornanes, the overhanging hydroxyl directs stereoselective collapse of the carbonium following 2,6-hydride transfer. The net conservation of stereochemistry is proposed to result from two sequential stereoselective processes.[765]

Thus it appears that this "simplest" oxidation mechanism has both alternate pathways and can form some sort of oriented, perhaps oxyferryl-containing, intermediate complexes. While Sugimoto and Sawyer claim to have excluded high-valent iron species,[766] alternate proposals for the mechanism of this reaction remain speculative.

The observation of an NIH shift in any case strongly suggests oxygen atom transfer. Related systems, such as the Udenfriend reagent Fe^{2+}/O_2/ascorbate/EDTA, give product distributions inconsistent with HO• formation but which are still relatively unselective and do not yield an NIH shift.[579]

Only a limited number of entirely organic compounds are capable of hydroxylating unactivated aromatics by themselves, most notably dioxiranes, iodosylbenzenes, and peracids (CF_3CO_3H, phenylperacetic acid, and *m*CPBA). All of these are capable of catalyzing oxo atom transfer, but homolytic fragmentation also occurs, especially with peracids. This is due to the competition between oxo atom transfer and fissioning of the weak O−O bond (~50 kcal mol^{-1} for H_2O_2 homolysis compared to 120 kcal mol^{-1} for HO• formation by proton abstraction). When these oxygen-atom donors are used with metal complexes, either method of decomposition can occur.

An important tool in distinguishing these two alternatives was developed by Coon *et al.* for phenylperacetic acid-dependent oxidations. When the O−O bond is fissioned homolytically, the phenylacetoxyl radical is formed and decarboxylation occurs extremely rapidly, on the order of the time required for bond motions. The resulting benzylic radical then forms toluene or one of several radical-reaction products. If heterolytic fission occurs, the product is phenylacetic acid, which cannot be produced by the radical pathway. Quantitative analysis of the decomposition products of the oxygen atom donor can thereby reveal the underlying mechanism of oxygenation with phenylperacetic acid,[767] which is often related to the mechanism with related oxidants.

Efficient NIH shifts occur with peracids, to an extent that depends on the aromatic substituents, but *not* the Hammett σ^+ values, and is different from that with microsomes (perhaps because of the acidic conditions used). No primary isotope effect is detected with CF_3CO_3H-mediated conversion of benzene to phenol. When chloro- and bromobenzenes are treated with CF_3CO_3H in $CHCl_3$ or CH_2Cl_2, appreciable amounts of di- and trihalogenated phenolic products are also obtained. This strongly suggests that radical formation occurs at least some of the time. However, the CF_3CO_3H results are consistent with direct formation of a short-lived arene oxide, which is almost certainly what leads to the observed NIH shift.[768]

Methyl group and chloride migrations are known,[769,770] as in the conversion of prehnitene (1,2,3,4-tetramethylbenzene) to 2,3,4,6-tetramethylphenol by CF_3CO_3H.[771]

While iodosylbenzenes are most often used as oxygen sources in metal-mediated hydroxylation, it should be remembered that they are capable of epoxidizing substrates directly or by nonredox adduct formation, particularly the very reactive OIC_6F_5.[743,772]

One of the most reactive organic oxidants available is dimethyldioxirane, a cyclic peroxide formed from acetone by monoperoxysulfuric acid (caroate, $KHSO_5$), commercially available as a stable mixture of $2KHSO_5 \cdot KHSO_4 \cdot K_2SO_4$ (Oxone, DuPont). Dimethyldioxirane performs clean oxygen atom transfers to alkanes, alkenes, aromatics, and heteroatom-containing substrates.[773,774] Arene oxides (many are "multiple hits", containing more than one epoxide moiety) are formed in moderate yield by Oxone from polycyclic aromatic hydroxycarbons but not benzene.[775] Dioxiranes pass several important tests for nonradical oxo transfer, including retention of stereochemistry upon hydroxylation of *cis*-1,2-dimethylcyclohexane, and for the *cis* and *trans* isomers of decalin,[776] styrene,[777] and stilbene.[778] A negative value of the Hammett parameter ρ is obtained for *para*-substituted styrene epoxidation,[777] and cyclododecane yields $k_H/k_D = 4.97$.[776]

In addition to these three common oxidants, an NIH shift is also observed with HOF[779] and irradiated pyridine *N*-oxides,[780] perhaps in analogy to the $O(^3P)$ reactivity described above. No NIH shift results from incubation of substrates with reduced flavin/O_2,[781] or Fe^{2+}/O_2/reduced pteridine.[579] In the former case, this appears to be a matter of requiring a phenolic or similarly "activated" aromatic substrate for flavin hydroxylases, which would be expected to exchange deuterium because of a stabilized carbonium ion; the latter case appears to be an instance of reduced pteridine functioning as a simple reductant in a Fenton-like, $HO^{\bullet}$-producing system.

The few organic compounds that perform oxygen atom transfer are all oxides of a sort and have already overcome the key barrier, the conversion of triplet O_2 to a reactive $S = 0$ or $^1/_2$ species. Only metal compounds and organic radicals are known to react with triplet O_2 directly, forming oxides, peroxides, and superoxides. Many metal oxides are able to transfer oxygen atoms, including the extremely reactive ferrate ion (FeO_4^{2-}) and the more conveniently handled permanganate (MnO_4^-) and chromyl (CrO_2^{2-}) ions. In addition to their invaluable role in organic synthesis, their study[782] laid the foundation for later mechanistic work with organic and coordination compounds, including much of what was discussed above. In a biomimetic vein, Sharpless and Flood discovered that chromate-mediated arene epoxidations are associated with NIH shifts.[742]

Given the wide distribution of porphyrins in nature, it is perhaps initially surprising that in the short history of non-heme iron model chemistry, a number of systems have been found to have reactivity analogous to that described for heme compounds. Chemically, there is nothing peculiar about heme compounds; they happen to function well in their biological niche and so have been maintained. Using comparatively simple principles from standard coordination chemistry, one can design a broad range of functional non-heme compounds having desired solubility, reactivity, and stereoselective properties.

Since progress in this area has been recently reviewed,[783] the current discussion is restricted to mononuclear iron complexes that catalyze oxidations. In the wake of the crystal structure of the binuclear non-heme iron hydroxylase component of methane monooxygenase, which has a carboxylate-rich primary coordination sphere, the coordination chemistry of anionic ligands has returned to prominence in the modeling field. Bruice's group has shown how the reactivity of $[Fe^{3+}(EDTA)(Sol)]^-$ can be modulated by the identity of the "leaving group" of the oxygen atom donor.[784] A related phenomenon has also been observed with heme compounds, which catalyze oxygen transfer from OIC_6F_5 faster than from OIPh.[772]

Recently, the ability of a carboxylate-rich environment to support oxygen atom transfer chemistry in model systems was demonstrated.[160] Reactivity studies performed with $[Fe^{2+}(MeEDTrA)(Sol)]^-$ and $Fe^{3+}(MeEDTrA)(Sol)$ show that both model systems are capable of catalyzing the decomposition of phenylperacetic acid by heterolytic cleavage of the peracyl O−O bond. Furthermore, isostructural Zn^{2+} and Ga^{3+} complexes did not catalyze this reaction, indicating that a metal-based redox process is necessary for the peracid decomposition reaction. Using dimethylanaline *N*-oxide (DMANO) as the oxygen atom donor molecule, $Fe^{3+}(MeEDTrA)(Sol)$ catalyzed oxygen atom transfer reactions to a variety of substrates; simple olefins (cyclohexene, cis-, trans-stilbene, styrene) gave either allylic oxidation products (cyclohexenol, cyclohexenone) or epoxides with loss of the original stereochemistry of the olefin. Oxidation of sulfides and sulfoxides gave the corresponding sulfoxides and sulfones, indicating the capability of this system to perform $2e^-$ oxidation reactions. In all cases, the Zn^{2+} and Ga^{3+} complexes were inactive as oxygen atom transfer catalysts. The chemistry of $[Fe^{2+}(MeEDTrA)(Sol)]^-$ was dominated by the rapid formation of the μ-oxo$(Fe^{3+}(MeEDTrA)_2$ complex by either DMANO or O_2 (4:1 Fe^{2+} per O_2), thereby precluding any investigation of its catalytic chemistry.[160]

Reactivity studies have a disproportionate importance in the absence of enzyme crystal structures, which is unfortunately the situation in the pterin-dependent monooxygenases. Non-heme iron-dependent hydroxylases must position metal-binding resi-

dues, the ligands that determine the geometry and behavior of reactive metal-centered intermediates, using only the structure of the protein matrix and an armamentarium of the common amino acids. The geometric parameters of the PAH active site are being determined in our laboratory, with the eventual goal of depicting the structure of the quaternary reaction complex. When combined with the development of reactive compounds that recapitulate the catalytic details of aromatic hydroxylation, a good foundation for understanding how the iron site functions in the context of the surrounding protein and substrates can be developed.

7. Uncoupling of 6MPH$_4$ Oxidation

In the case of both PAH and TyrH, the coupling of reduced *X*PH$_4$ oxidation to substrate hydroxylation is imperfect for several alternate substrates and cofactor analogues. At least some H_2O_2 is formed by uncoupled turnover of 6MPH$_4$ by PAH. Since it is capable of oxidizing both the reduced enzyme and additional 6MPH$_4$, the buildup of substoichiometric levels of H_2O_2 may indicate that it is rapidly reacting elsewhere. Peroxide formation is either the result of partitioning of the normal hydroxylating intermediate into a nonproductive release of H_2O_2 (which may not be direct), or it is evidence of a different oxygen-activation reaction.

Since uncoupling generally increases (the reaction efficiency decreases) when the suitability of the substrate or cofactor available to the hydroxylase is poor, some form of partitioning is likely to occur prior to peroxide formation. A completely coupled reaction is obtained with PAH or TyrH using 6MPH$_4$ or BH$_4$ as cofactor, and the appropriate enzyme substrate. Lysolecithin-activated PAH gives mostly uncoupled 6MPH$_4$ oxidation when L-Tyr or *o*-methylphenylalanine are presented as substrates, but the reactions with the two amino acids are mechanistically distinct. In the former case, no L-Dopa is formed, and L-Tyr labeled with ^{18}O in the phenolic hydroxyl position suffers no washout following exposure to uncoupled PAH turnover in normal air and water, indicating that there is no exchange of the hydroxyl group.[641] Less than 1% conversion to phenolic products is observed in the latter case, with 6MPH$_4$, BH$_4$, or pyrimidine cofactor.[664] However, even this small amount of conversion indicates that the enzyme is capable of performing the reaction, albeit ineffectively. The complete inability of PAH to oxidize L-Tyr is likewise significant, even though the net results are nearly the same.

TyrH is able to hydroxylate L-Phe but with significant uncoupling (the reaction is roughly as efficient as *p*-fluorophenylalanine hydroxylation by PAH). Each 6MPH$_4$ oxidized by TyrH in the presence of L-Phe generates 0.7% *m*-tyrosine and 16.8% *p*-tyrosine, with 82.5% of the 6MPH$_4$ oxidation uncoupled to hydroxylation.[785] Both PAH and TyrH are able to hydroxylate L-Trp at the same 5-position as TrpH. TrpH is also able to hydroxylate L-Phe.[332,372]

As was mentioned above (section IV.A.3), uncoupling also occurs with cytochrome P450 when the substrate pocket is not occupied by a suitable substrate. Uncoupling is not unique to iron-containing hydroxylases. A structural rationale involving incorrect positioning of the isoalloxazine during turnover has recently been suggested for *p*-hydroxybenzoate hydroxylase uncoupling.[786]

8. Substrate Specificity and the Hydroxylating Intermediate

The different amino acid hydroxylases are well suited to their catabolic and biosynthetic tasks, which unlike the detoxifying or biosynthetic tasks allotted to the cytochromes P450, requires both high selectivity and high conversion rates. As with cytochromes P450, toxic reduced oxygen species are not released into the cytoplasm as a result of the non-heme enzyme catalysis. The heme-dependent hydroxylases accomplish this by careful control of electron transfer. The non-heme iron-dependent hydroxylases appear to increase efficiency by tightly sequestering their reactive intermediates and avoid release of reduced oxygen species, with the possible exception of the relatively unreactive H_2O_2. This may be because of internal trapping/autoinactivation, or the abortive uncoupled turnover, which may serve to safely discharge the hydroxylating species in the absence of an appropriate substrate without enzyme autoinactivation.

One might expect enzymes of this type to distinguish carefully among their closely related substrates. However, it appears that the K_m (or K_I) values of each hydroxylase for the three aromatic amino acids are relatively similar, as is the rate of 6MPH$_4$ consumption. Substrate selectivity may be achieved for the cognate substrate by optimizing the geometry of the transition state within the context of the conserved catalytic core. TyrH has a unique ability to overcome catecholamine inhibition (section II.B.3.5), which is the single physiologically significant regulatory phenomenon that has been shown to affect the active site iron configuration directly, by bidentate coordination. Since PAH does not have this ability, the potential for product inhibition is minimized if L-Tyr is never accepted as a substrate. Perhaps TyrH would be similarly overwhelmed by catecholamines were they not continually removed from the neuronal cytosol into storage vesicles.

PAH does not form *m*-tyrosine, a product that might accumulate unproductively in liver, nor is it able to modify L-Tyr. When TyrH is presented with L-Phe, it forms mostly *p*-tyrosine rather than the "expected" *m*-tyrosine product. These reactions are only partially coupled to cofactor oxidation (Table 11, section IV.C.2). Despite the inefficient oxidation of 6MPH$_4$ in this reaction, the V_{max} of TyrH (NADH oxidation) with L-Phe is 44% higher than with the fully coupled hydroxylation of L-Tyr.[787] This partially compensates for the uncoupling with L-Phe, yielding a hydroxylated phenylalanine formation rate that is ~30% of the L-Dopa formation rate. If one considers the possibility that the hydroxylation of an unactivated aromatic substrate, which is more difficult than the hydroxylation of a phenolic substrate, is intrinsically slower, then the difference between consumption of the two different substrates would be even more subtle.

On the other hand, the maximum coupled velocity of L-Tyr hydroxylation by TyrH is 5- to 7-fold smaller than the maximum coupled velocity of L-Phe hy-

droxylation by PAH. This suggests that TyrH pays for its selectivity with a slowing of the rate-limiting step (an irreversible step, thought to be generation of the hydroxylating intermediate or perhaps hydroxylation itself). In redirecting the tendency of the hydroxylase catalytic core to attack the *para* position of the amino acid substrate, TyrH avoids uncoupled turnover with its cognate substrate, the opposite of what occurs in the PAH/L-Tyr pairing. TyrH is likely to have unique structural or functional features that allow L-Tyr hydroxylation that are missing in PAH and TrpH.

A possibly related issue is the irreversible, first-order inactivation of PAH that occurs during coupled L-Phe hydroxylation,[53] with a half-life of 4−6 min under standard assay conditions (25 °C).[53,61] Whether such inactivation occurs in TyrH catalysis is apparently dependent upon the preparation of enzyme and/or assay conditions.[788] In an older report using a lower activity, partially purified preparation, product accumulates linearly over 20 min (assay method unstated).[49] Catalase is near-ubiquitous in assays of these hydroxylases, whether included intentionally or as an impurity, because it protects the enzymes from some form of inactivation, which might be mediated by a tetrahydropterin/O_2 interaction that forms peroxides or superoxide.[71]

A simple link between the uncoupled turnover and inactivation processes might be that both arise from creation of a reactive intermediate at an inappropriate time, followed by wasteful or damaging discharge of the electrophilic oxygen species.[168] Perhaps the more-rapid catalytic turnover of PAH is related to its more rapid rate of autoinactivation during turnover, relative to TyrH, and by extension, to the control of the hydroxylating intermediate. TyrH is expressed in a developmentally regulated manner in neurons and builds up a pool of recycled neurotransmitters, while PAH is expressed constitutively at high levels in liver, where it is responsible for a detoxifying, bulk catalytic conversion. It may be reasonable to accept rapid PAH degradation if greater catalytic power is gained. (The physiological half-life of PAH in a normally fed rat has been reported to be 48 h[789] but this value has been challenged.[76])

It seems that the bound iron is more easily removed/exchanged in TyrH and some forms of PAH (the human and *P. acidovorans* forms) when compared to the rat liver PAH. The potential hydroxylase-regulatory role of iron availability has not been extensively explored *in vivo* or *in situ* beyond one report with PAH.[52]

B. PAH

1. Kinetic Mechanism

The overall steady-state kinetic mechanism of PAH is terbisequential, with some degree of randomness in the order of substrate addition. Several early reports of the kinetic mechanism using crude fractions indicated other mechanisms might apply, on the basis of the appearance of parallel lines in the double-reciprocal plots. The only full set of steady-state experiments with all three substrates was performed using $DMPH_4$, L-Phe, and O_2 using low-activity PAH, which yielded the assignment of the mechanism.[790]

An examination of the $6MPH_4$ and L-Phe saturation behavior at ambient O_2 was reported using L-Phe- and lysolecithin-activated highly active, recombinant PAH.[61] An advantage in using the unnatural activator is that one is not limited to a narrow L-Phe substrate range when it is used as the activator; the K_m for L-Phe (0.18 mM) is within a factor of 2 of the $K_{d,app}$ (0.11 mM) for the allosteric activator site.[76] While the L-Phe activated data were best fit by parallel lines, the lysolecithin-activated data clearly showed a sequential mechanism is operative in a wide range of substrate concentrations. There is no indication in the lysolecithin-activated data for a preferred order of substrate addition.[61] This result rules out release of any product prior to the binding of all substrates and with it all substituted-enzyme mechanisms (like $\{Fe^{4+}{=}O\}PAH^R$ + L-Phe → products *after* dissociation of *q*-$6MPH_2$). The K_m for $6MPH_4$ is essentially the same for L-Phe activated (45 μM) and lysolecithin-activated PAH (60 μM).[61,76]

The K_m for BH_4 is lower than for $6MPH_4$, with values of 3−21 μM.[102,117,637] The K_d for BH_4 binding to $\{Fe^{2+}\}PAH^R_{L-Phe}$ (performed in the presence of saturating acetohydroxamate to inhibit catalysis) is 14 μM, close to the K_{m,BH_4} determined under the same conditions (15 μM, no inhibitor present), and the K_d obtained by direct titration of $\{Fe^{2+}\}PAH^T$ with $6MPH_4$ (14 ± 1.5 μM).[117] Rat liver PAH has a V_{max} = 22 s^{-1} (per subunit for fully iron-loaded enzyme).[170]

Inhibitor studies that might indicate the order of substrate addition or product release have not been informative. Phenylalanine is a weak inhibitor using $6MPH_4$ (>4 mM),[76] and O_2 has been reported to inhibit the enzyme at high levels with BH_4 as cofactor.[791] The K_m (NADPH oxidation) for L-Tyr has been estimated to be eight times that of L-Phe under comparable conditions, yielding a rate of ∼2% that of coupled L-Phe hydroxylation.[102] Since the PAH-catalyzed oxidation of $6MPH_4$ in the presence of L-Tyr is completely uncoupled, this indicates an approximate K_d of 2 mM, which approaches the solubility of L-Tyr under assay conditions.

While the oxidized pterin products of the PAH reaction are ordinarily unstable, the stable analogue *q*-6,6-M_2PH_2 does not inhibit PAH catalysis, up to 0.4 mM.[561] A comparable determination has not been reported with 4a-OH-$6MPH_2$, the initial hydrated pterin reaction product, but the recent synthesis of this compound (section III.B.6) should allow that experiment to be performed. 5-Deaza-$6MPH_4$ is a competitive inhibitor *vs* $6MPH_4$ during hydroxylation and is noncompetitive with L-Phe binding to $\{Fe^{3+}\}$-PAH^R,[117,566] as are most inhibitory tetrahydropterin analogues (Figure 27). The only mechanistic conclusion arising from the use of this completely unreactive inhibitor is that it can bind PAH prior to L-Phe.

A tight- and reversibly-binding L-Phe antagonist has not been discovered, although many inhibitors show some limited degree of competition *vs* that substrate. The classic PAH inhibitors *p*-chloro- and *p*-fluorophenylalanine are actually poor hydroxylation substrates that cause significant uncoupling. In principle, one might monitor the specific rate of hydroxylation of a poor alternate substrate (*i.e.*, appearance of *m*-chlorotyrosine or F^- release, and *not* tetrahydropterin oxidation) in an attempt to deter-

Table 8. Alternate PAH Substrates

alternate substrate	product (assay)	comments	ref(s)
L-methionine	L-methionine sulfoxide	activates at 28 mM	795
L-tryptophan	5-hydroxy-L-tryptophan	activates at 28 mM	80, 401, 795
L-norleucine	ϵ-hydroxy-L-norleucine	activates at 28 mM	795
D-methionine	(NADPH)		795
D-phenylalanine	D-tyrosine (85%)	activates at 28 mM	795
DL-β−2-thienylalanine	(NADPH)	activates at 28 mM	80, 795, 796
DL-β−3-thienylalanine	(NADPH)		795
S-methyl-L-cysteine	(NADPH)	$I_{55\%} = 6$ mM	795
DL-*m*-tyrosine	(NADH)		42
L-[2,5-H]phenylalanine	3,4-epoxide	<50% activating at 20 mM	797
L-cyclohexylalanine	7-hydroxy-L-cyclohexylalanine ("*para*")	*Cv* PAH[a] gives 9:1 axial:equatorial products	798
p-methylphenylalanine	4-(hydroxymethyl)-L-phenylalanine and 3-methyl-L-tyrosine (3.9:1, $6MPH_4$)[b]	also hydroxylated by *Pa* and *Cv* PAH's to both products	798−800
p-(hydroxymethyl)phenylalanine	(NADH)		800
p-methyl-*m*-tyrosine	(NADH)		800
m-tyrosine	Dopa	reaction is completely coupled to NADPH oxidation	102, 801
o-methylphenylalanine	(2-methyltyrosine)	reaction is <1% coupled	664
o-fluorophenylalanine	(NADPH)		796
m-fluorophenylalanine	(NADPH)	unpublished claim in ref 604 that this is a good substrate	604, 796
p-fluorophenylalanine	tyrosine	reaction is ~20% coupled; no NIH shift	608, 802
p-chlorophenylalanine	3-chlorotyrosine	reaction is partially coupled; also hydroxylated by *Pa* PAH	802
p-bromophenylalanine	3-bromotyrosine	also hydroxylated by *Pa* PAH	802

[a] *Cv* = *Chromobacterium violaceum*; *Pa* = *Pseudomonas aeruginosa*. [b] An early report[799] of 4-methyl-m-tyrosine formation from 4-methylphenylalanine or 4-chlorophenylalanine by Pa PAH has not been observed with other sources of PAH.

mine the preferred order of substrate addition, if any, but this has not been reported.

Haavik, Martínez, Mildvan, and co-workers have studied the enhancement of the longitudinal relaxation rates (T_1^{-1}) of HDO or L-Phe protons in the presence of either PAH or TyrH containing paramagnetic Fe^{3+} or Co^{2+}.[327,792,793] Paramagnetic ions decrease T_1 because of the availability of relaxation mechanisms due to nuclear coupling with the unpaired electron, which has a rapid spin−lattice relaxation rate. Broadening of L-Phe aromatic resonances results from incubation of 3 mM L-Phe with $\{Fe^{3+}\}PAH^{R}_{L-Phe}$, in a manner that can be diminished by addition of 1 mM L-noradrenaline.[793] Relaxation enhancement is not seen with Fe^{2+}-containing PAH.[327] The paramagnetic relaxation pathway dominates the effective dipolar correlation time, which was found not to depend upon the rotational correlation lifetime or exchange lifetime. Enhancement of the HDO relaxation (T_{1P}^{-1}) is caused by $\{Fe^{3+}\}PAH^{T}$ in phosphate buffer, a rate that is approximately halved if the buffer is Tris (pH 7.25) or if $\{Fe^{3+}\}PAH^{R}_{L-Phe}$[L-Phe] is used in either buffer. Because T_{1P}^{-1} is temperature dependent but frequency independent, the exchange of water appears to limit the relaxation rate. This evidence is consistent with direct coordination of water to the Fe^{3+} site. The decrease in the relaxation rate is not the result of allosteric activation *per se*, since lysolecithin concentrations to 5 mM do not significantly decrease T_{1P}^{-1}, but addition of L-Phe causes a progressive decrease (K_{app} ~0.5 mM) consistent with its perturbation of the active site environment. In contrast, titration of $\{Fe^{3+}\}PAH^{T}$ with L-Phe or L-noradrenaline gives a multiphasic relaxation response.[792] It is highly likely that a weakly coordinated site is present in PAH^{R}_{L-Phe}[L-Phe] that is used for interaction with O_2 or the putative tetrahydropterin hydroperoxide. The displacement of water evident from the lengthening of the relaxation lifetime has an unknown structural correlate; independent iron spectroscopic work rules out the possibility of a change (*i.e.*, 6 → 5) in the iron coordination number upon allosteric activation.[162]

The suggested displacement of a labile water molecule upon substrate binding resulting in a five-coordinate active site iron center[792] is not supported by recent MCD and XAS studies.[162] A detailed examination of $\{Fe^{2+}\}PAH^{T}$, $\{Fe^{2+}\}PAH^{R}$, and $\{Fe^{2+}\}PAH^{R}_{L-Phe}$[L-Phe] was consistent only with a six-coordinate site. NMR studies using Co^{2+}-substituted TyrH (section IV.C.2) suggest that the aromatic ring of the alternative substrate L-Phe is located in the second sphere of the Co^{2+} ion with no other group of the substrate near enough to bind directly to the metal center.[794] The data from the MCD and XAS studies indicate that substrate binding causes a rearrangement of the existing active site coordination environment and does not alter the nature of those ligands.[162]

2. Alternate Substrates

PAH will hydroxylate several aromatic and aliphatic amino acids when activated, usually by lysolecithin. Other amino acids, notably L-Met and L-Trp, are PAH activators and substrates at high levels (28 mM). Subtle catalytic effects resulting from different activators have been reported,[795] but in the main, PAH activated by whatever means will hydroxylate the range of substrates indicated in Table 8. Included on the list are examples of oxygen atom insertion into alkane and aromatic C−H bonds, and the somewhat less energetically demanding oxygen atom transfers to form an epoxide or sulfoxide.

Few alternate substrates are hydroxylated in a completely coupled manner. Even minor conversion to a hydroxylated product indicates that the PAH-bound hydroxylating intermediate is sufficiently reactive to effect the conversion. Whether this hydroxylating intermediate is the "same" as with coupled hydroxylation of L-Phe is unknown, since each substrate necessarily follows a formally different mechanism. However, it is reasonable to infer a common intermediate(s) formed among the iron, oxygen, and tetrahydropterin, that is discharged with concomitant substrate oxidation. If the aromatic C−H bond strength at the *para* position in L-Phe can be approximated by the known C−H bond strength in benzene (111 kcal mol^{-1}), even the natural substrate clearly requires formation of an extremely reactive species; this intermediate is also capable of breaking a C−F bond in *p*-fluorophenylalanine.

Many amino acids and amino acid analogues are not substrates for lysolecithin-activated PAH, including L-glutamine, L-proline, L-glutamate, L-isoleucine, L-valine, phenylglycine, phenyllactate, phenylproprionate, phenylacrylate, phenylpyruvate, *n*-caproate, or phenethylamine at 6 mM.[795] These compounds do not stimulate the rate of tetrahydropterin oxidation (detected by coupling to NADPH oxidation), so it is reasonable to conclude that they either bind insignificantly to the amino acid binding site or (if they do bind) they are incapable of inducing the quaternary complex to commit to generation of the hydroxylating intermediate.

Several substrates are poorly utilized by PAH but nevertheless are oxidized to a limited extent. Each of these slowly utilized substrates also yields uncoupled tetrahydropterin oxidation. In general terms, the degree to which V_{max} is lowered (hydroxylated product formation) correlates well with the increase in uncoupling. The remainder of the substrates in Table 8 fit this description, ranging from the tightly coupled L-[2,5-H]Phe (98% coupled at 0.1 μM [797]) to *o*-methylphenylalanine, which yields detectable phenolic products in <1% yield.[664]

As the similarity to the natural amino acid substrate decreases, so does the reaction efficiency: for example, L-norleucine hydroxylation is 47 ± 2% coupled while *p*-methylphenylalanine hydroxylation (to several products, *vide infra*) is 91 ± 1% coupled.[795,800] A *para*-substituted phenylalanine (F or OH) leads to more significant uncoupling than if the same moiety were located in the *meta* or *ortho* positions. While there may be some Hammett-type substituent effects contributing to this observation, it is more likely that the *para* substituent may cause some steric crowding and thereby inhibit catalysis. Other substrates give entirely uncoupled tetrahydropterin oxidation, including L-Tyr, L-leucine, and L-norvaline.[795,803] These compounds evidently activate the catalytic commitment "trigger" within the quaternary complex, but their side chains are not correctly presented to the hydroxylating intermediate, perhaps because they are too small to extend from the glycine-binding region to the vicinity of the reduced oxygen species. (Were this not the case, a methyl C−H bond in the latter two would be expected to show at least some conversion.)

The rather finicky nature of PAH with respect to its amino acid substrate is probably the main reason no unambiguous stereochemical probes of the hydroxylation reaction have been developed. With L-cyclohexylalanine hydroxylation by *C. violaceum* PAH, a 9:1 axial:equatorial (relative to the presumably equatorial alanine substituent) product ratio has been observed. Since the cyclohexyl group is conformationally nonrigid, it is impossible to determine if this result indicates a stereospecific hydroxylation or a statistical distribution between two conformations within the enzyme active site, but the incomplete stereochemical scrambling does rule out substrate radical formation. Cyclohexylalanine is a superior substrate for *C. violaceum* PAH, which hydroxylates it at twice the rate supported by rat liver PAH, in a reaction that is 110 ± 10% coupled to $DMPH_4$ oxidation.[798]

Occasionally there can be unexpected effects with different substrates. The most carefully studied of these is the discrepancy between *p*-chlorophenylalanine inhibition *in vitro*, where it is a mild competitive inhibitor *vs* L-Phe and an ordinary alternate substrate, and *in vivo*, where it causes a profound inhibition and leads to temporary PKU.

p-Chlorophenylalanine is also a mild TrpH inhibitor *in vitro* and a severe one *in vivo*,[398] which probably accounts for many of the physiological and psychological effects, including insomnia and increased aggressiveness (section II.C.1). The 80−95% inactivation of PAH and TrpH activity is not reversible by dialysis,[804,805] which is evocative of irreversible modification of the enzymes, possibly by *p*-chlorophenylalanine incorporation.[806] This possibility was ruled out by Miller *et al.* who observed no inactivation of rat liver extract at 0 °C nor substrate protection during inactivation at 37 °C.[70] Inhibition was unlike cycloheximide and seemed to cause an increase in the amount of inactive enzyme, even in low-density cultured cells.[807]

Chang *et al.* were able to exclude *p*-chlorophenylalanine-initiated proteolysis as the cause of inhibition in rats, and reported that no *p*-chloro[^{3}H]phenylalanine was incorporated into PAH. A similar conclusion was reached by Gál and Whitacre using *p*-[4-^{36}Cl]chloro[2-^{14}C]phenylalanine, the label from which was found incorporated as L-[2-^{14}C]Tyr into PAH, which contained no labeled chlorine.[808] This would seem to suggest that the uncoupled component of *p*-chlorophenylalanine turnover would be deleterious to PAH *in vivo* for reasons not expressed *in vitro*. If that is the case, it is curious that *p*-fluorophenylalanine, which is a similarly uncoupled substrate, does not inactivate PAH *in vivo*.[70] (However, *m*-fluorophenylalanine is an *in vivo* inhibitor.[809]) It remains possible that some aspect of *coupled p*-chlorophenylalanine turnover is inhibitory.

3. NIH Shifts and Substituent Migration

PAH exhibits no isotope effect during hydroxylation of [4-^{2}H]- or [2,3,4,5,6-^{2}H]Phe,[110] a remarkable result for an enzyme that inserts an oxygen atom into a C−H bond. However, it is a familiar-enough observation from the work with cytochrome P450 and model compounds discussed in the first part of this section. The lack of an isotope effect is highly

evocative of oxygen atom transfer, as is the observation of an NIH shift.

Hydroxylation of [4-^{3}H]Phe by PAH results in >90% retention of label in the amino acid, which was a pivotal discovery regarding the mechanism of aromatic hydroxylation, as discussed in section IV.A.4. While this is consistent with oxygen atom transfer, choosing among the several alternatives (arene oxide, radical or cation adducts, metallaoxetane) for the course of the NIH shift is significantly more difficult because of the limited substrate tolerance of PAH. While it is formally true to say that for enzymes there are no alternate substrates, only alternate mechanisms, in the case of PAH this is a tangible, practical guideline. Coupled turnover with an alternate substrate is the best evidence of an interaction with PAH akin to its interaction with L-Phe.

One of the most efficiently oxidized alternate substrates is L-[2,5-H]Phe, which is also a moderate activator. Miller and Benkovic determined that PAH epoxides this substrate, with the same K_m and V_{max} ($6MPH_4$ oxidation) as its natural substrate. No allyl oxidation or rearomatization is detected, which would lend support to adduct formation of the type depicted in Figure 38. Adding glutathione/glutathione *S*-transferase to the PAH reaction mixtures did not lead to epoxide opening, which was effected by heating the product to 50 °C with DTT. The same relatively stable 3,4-epoxide is formed by *m*CPBA. This constitutes the first direct evidence that PAH can form an epoxide, but because the cyclohexenyl 3,4-epoxide is so resistant to ring opening, it is not possible to conclude whether a facile opening of the corresponding arene oxide might be enzyme catalyzed. The lack of PAH inactivation by the dihydrophenylalanine argues against the presence of strong nucleophiles in the PAH active site.[797] A hypothesis of direct oxygen addition to the isolated π-bond seems most likely to account for this result, but it would be desirable to have direct isotope evidence (for instance, a small k_H/k_D for the [$^2H_7$]-ring analogue) to that effect. The most significant result of this work is that there is no allylic rearrangement detected, which rules out formation of an allylic radical and thereby one electron transfer. It follows that, at least for this substrate, a two-electron process occurs.

Recently, Carr *et al.* have examined the "metal free" *C. violaceum* PAH in parallel with rat liver PAH.[798] No kinetic isotope effects (on *V* or *V*/*K*) significantly different from 1.0 were detected using L-[4-^{2}H]Phe or L-[2,3,4,5,6-^{2}H]Phe. Hydroxylation of either L-[4-^{2}H]Phe or L-[2,3,5,6-^{2}H]Phe by PAH from either source leads to indistinguishable levels of deuterium retention (84 ± 2%) in the product. This indicates a common cyclohexadienone intermediate is formed by both enzymes, with an isotope effect on enolization of 5.5 ± 0.8. By analogy to other systems, in which Hammett analysis indicates that cyclohexadienone is formed by 1,2-hydride transfer within a *meta* carbonium intermediate, the sequence of intermediates in L-Phe hydroxylation probably includes a *meta* carbonium ion, which is likely to be formed during ring opening of an arene oxide intermediate.

Stronger evidence for a *meta* carbonium is found in hydroxylations of *p*-methylphenylalanine, which is converted by PAH into *p*-(hydroxymethyl)phenylalanine and *m*-methyltyrosine, but not *p*-methyl-*m*-tyrosine. Siegmund and Kaufman reported that the distribution between aromatic and aliphatic hydroxylation products is significantly affected by deuteration of the methyl group but not of the ring protons (Figure 42).[800] Less than 2.5% ^{18}O incorporation was observed in either product when the hydroxylations were run in $H_2{}^{18}O$; under $^{18}O_2$, 89−108% ^{18}O incorporation was observed. The isotope effect on aliphatic hydroxylation is 8.0,[800] a value in good agreement with that determined for the benzylic hydroxylation of toluene, 7.4 ± 0.7.[748] As expected, the appreciable isotope effect on methyl hydroxylation combined with a small ring hydroxylation isotope effect favors the latter. However, a *larger* amount of *m*-methyltyrosine is produced from deuterated methyl substrates, indicating an inverse isotope effect of 0.5 for [$^2H_5$]methylphenylalanine. [[$^2H_5$]Phenylalanine is 1-(4-[1,1,1-^{2}H]methylphenyl)-[3,3-^{2}H]alanine; [$^2H_9$]phenylalanine is 1-(4-[1,1,1-^{2}H]methyl-[2,3,5,6-^{2}H]phenyl)-[3,3-^{2}H]alanine.] A comparable result is obtained for [$^2H_9$]methylphenylalanine. Acceleration of ring hydroxylation/methyl migration as aliphatic hydroxylation is slowed indicates that inversion of the product distribution results from an isotope-sensitive branching step, such as was observed with *all-exo*-[2,3,5,6-^{2}H]norbornane hydroxylation by cytochrome P450 (section IV.A.5). For both [$^2H_5$] and [$^2H_9$] substrates, the $^D(V)$ for total product formation is small (0.96 and 1.17, respectively), indicating that the rate-determining step is not isotope sensitive.[800] A similar, non-rate-limiting, isotope-sensitive alteration in *p*-methylphenylalanine product ratios is observed with *C. violaceum* PAH.[798] High commitment to catalysis is also observed for cytochrome P450, where it has been associated with irreversible generation of a hydroxylating species.

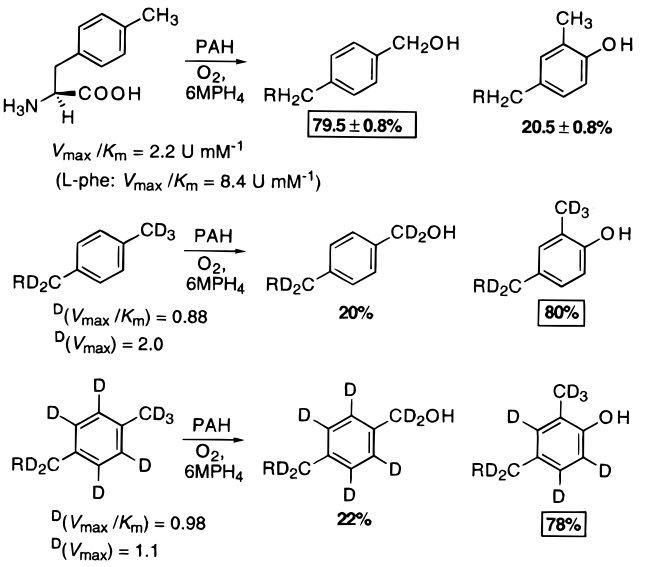

Figure 42. *p*-Methylphenylalanine transformations by PAH.

Formation of *m*-methyltyrosine requires a 1,2-methyl migration that is almost certainly dependent upon carbonium ion formation. Because there is a rearrangement of the carbon skeleton, the methyl shift is formally a Wagner−Meerwein rearrangement, despite the obvious mechanistic resemblance to a 1,2-hydride migration in the NIH shift. A large and coherent chemical literature is available on

carbonium-dependent rearrangements, and an abundance of relevant transformations are known, among them the trifluoroperacetic acid-induced methyl migration observed with prehnitene (section IV.A.6). A scale of "relative migratory aptitude" developed using a variety of compounds indicates that methyl groups are among the slowest migrators (Ph > *t*Bu > Et > Me), because the carbonium gains the least stabilization from primary alkyls. (An interesting prediction following from this is that more substituted *para* substituents, for instance *p*-ethyl- or *p*-isopropylphenylalanine, should undergo increasingly facile 1,2-migration in the coupled component of the hydroxylation reaction.) The lack of crossover during rearrangements of mixed, differently substituted pinacol analogues indicates that the migrating group does not dissociate from the reacting ensemble,[810] in much the same way that heavy hydrogen isotopes are not dissociated from opened arene oxides during their 1,2-shift.[712]

One underexplored area of carbonium chemistry is the stereochemical configuration of the migrating group following migration. An excellent test of this would be *p*-methylphenylalanine, because the PAH hydroxylation reaction is highly specific, is favored by isotopic substitution of the methyl group, and occurs in a controlled environment on the enzyme. In one instance where the stereochemical integrity of an enzyme-mediated alkyl group migration has been examined, Leinberger *et al.* investigated the retention of stereochemistry during the 4-hydroxyphenylpyruvate dioxygenase (EC 1.13.11.27) catalyzed 1,2-migration. Using deuterium-substituted substrates chiral at the migrating methylene, a mixture of retention, inversion, and label loss was observed, some of which occurred during derivatization. A minimum 3-fold (*R*) or 4-fold (*S*) excess of products having the substrate's methylene configuration was observed, indicating that the 1,2-migration generally goes with retention of stereochemistry.[811]

Halogen migration during the coupled component of *p*-chloro- or *p*-bromophenylalanine hydroxylation falls somewhere between the migration of hydride and methyl groups. Chloride is transferred to the *meta* position of L-Tyr in 85% of the coupled PAH turnovers.[802] In contrast, the halogen in *p*-fluorophenylalanine is unable to undergo migration.[608,812] Hydroxylation of the halophenylalanines is deceptively complicated, because it is not as clean a reaction as with the completely organic substrates: there is both uncoupling of tetrahydropterin oxidation and partitioning between tyrosine + halide and halotyrosine formation. (To the best of our knowledge, *p*-iodophenylalanine has not been examined in this regard with PAH; *m*-iodotyrosine is a strong TyrH inhibitor, section IV.C.1.) This was recognized in Storm and Kaufman's early work with this substrate, in which the authors note that an extra reducing equivalent is required in the production of F^- and L-Tyr from *p*-fluorophenylalanine, compared to the normal two-electron process.[608] The source of that reducing equivalent is completely obscure, but it is worth recalling that *p*-chlorophenylalanine causes depletion of PAH *in vivo* in a manner not sufficiently consistent with it being merely a poor substrate or reversible inhibitor (section IV.A.2). Ferrous PAH is oxidized *in vitro* during halophenylalanine hydroxylation, and part of the "uncoupled turnover" with *p*-chlorophenylalanine is due to rereduction of the active site by excess tetrahydropterin.[116,157] In any case, the metabolism of *p*-chlorophenylalanine is not a closed issue.

C. violaceum PAH is unable to support even uncoupled turnover with *p*-chlorophenylalanine, despite its ability to hydroxylate the nearly isosteric *p*-methylphenylalanine.[798]

4. Tetrahydropterin Oxidation, with and without Hydroxylation

The metabolism of oxygen by mammalian PAH is linked to the chemistry of both iron and pterin, and its incorrect disposition during uncoupled turnover is a rich source of information about the normal, productive interaction.

Occasional hints arise elsewhere about the interrelationship of the pterin−PAH interaction and the efficiency of O_2 fixation; for instance, the exchange of a pterin cofactor for the pyrimidodiazepine analogue (section III.D.2) increases the K_m for O_2 by a factor of 10.[655] However, this kind of information is difficult to understand without more information on the rate-limiting step, the formation of the hydroxylating intermediate. In turn, this intermediate is more comprehensible when one understands how it is formed, and what causes it to misfire once constituted on PAH.

Two methods of causing rapid tetrahydropterin oxidation without hydroxylation by PAH have been discovered. The first is uncoupled turnover, best exemplified by PAH's failure to modify L-Tyr while oxidizing appreciable amounts of tetrahydropterin. The second is the "tetrahydropterin oxidase" activity of PAH, which is supported by oxidants other than molecular oxygen.

As is mentioned in sections II.B.2.6, II.B.4, IV.A.8, and elsewhere, PAH will reduce O_2 and oxidize the tetrahydropterin cofactor unproductively if the arrangement of the quaternary reaction complex is not optimal. There is some disagreement over whether the presence of an amino acid, generally meaning L-Tyr, the only known inhibitor that is not even a marginal substrate, is required to initiate uncoupled turnover. There is also controversy over the oxidation products, in particular, whether H_2O_2 is released in appreciable amounts from PAH undergoing uncoupled turnover.

These related issues are both critical, as they determine the requirements for, and timing of, the generation of an oxidizing species on PAH. While it has been generally assumed that this would be the same intermediate as the hydroxylating species, the fact that uncoupled turnover does not cause the hydroxylation of substrate makes this a natural but potentially misleading assumption. Furthermore, it is important to recall that in oxygenated solutions, tetrahydropterins spontaneously produce H_2O_2 (section III.B.2). PAH's inability to oxidize L-Tyr was first reported by Fisher and Kaufman, using a lysolecithin-activated rat liver preparation.[803]

Evidence for a C^{4a} hydroxyl adduct as the first pterin product of the PAH reaction, initially based

Table 9. Products of Coupled and Uncoupled PAH Turnover[a]

	substrate (1 mM init)	cofactor (20 μM init)	hydroxylation (μM)	4a-carbinolamine (μM)	O_2 consumed (μM)	maximum [H_2O_2] (μM)
1	L-Phe	$6MPH_4$	18.0	18.2	18.5	0.7
2	*p*-Cl-DL-Phe	$6MPH_4$	6.4	6.7	12.6	1.5
3	L-Phe	PH_4	10.5	10.5	14.3	1.0

[a] Coupled and uncoupled turnover under pterin-limiting conditions at pH 8.2, 25 °C. Data taken from and other conditions given in ref 168.

on the resemblance of transient enzyme intermediate spectra to that of the stable 4a-hydroxy-5-deazadihydropterin,[169] immediately suggested that the terminal oxygen of a pterin hydroperoxide is incorporated into the amino acid substrate with the participation of the active site Fe^{2+}.[564] (Again, the pterin hydroperoxide intermediate remains entirely hypothetical.)

The distinctive 244 nm intermediate corresponding to the 4a-carbinolamine was not detected during the mostly uncoupled turnover of *p*-fluorophenylalanine.[169] In order to investigate the participation of the 4a-carbinolamine in uncoupled turnover, Dix and Benkovic developed conditions in which uncoupled turnover is particularly favorable and the 4a-carbinolamine is relatively stable, pH 8.4 in dilute borate buffer, with 1.0 mM *p*-chlorophenylalanine as substrate or PH_4 as cofactor. It can be seen in Table 9 that in all three cases, equal amounts of hydroxylated product and 4a-carbinolamine are formed from 3 μM of $\{Fe^{3+}\}PAH^R$ and limiting tetrahydropterin (some of which is consumed by enzyme reduction). In addition, the identical rates of hydroxylated product and 4a-carbinolamine formation indicate they are formed concurrently in the 35% coupled *p*-chloro-DL-Phe/$6MPH_4$ reaction (entry 2 in Table 9). The extent of coupling did not depend on [$6MPH_4$] during *p*-chloro-DL-Phe hydroxylation. Little H_2O_2 was detected by two different assays under conditions that allowed quantitative detection of added H_2O_2. When the contributions due to reduction, H_2O_2 formation, and coupled turnover are subtracted, the uncoupled component of entries 2 and 3 consumed 2.1 and 2.0 XPH_4 per O_2, respectively. This implies a "complete" reduction of O_2 to H_2O during uncoupled turnover and is consistent with the small amount of H_2O_2 found.

As the *p*-chloro-DL-Phe is not modified during uncoupled turnover, the authors examined what happens when it is omitted. Incubation of $6MPH_4$ with PAH results in a slow autooxidation of the pterin without 4a-carbinolamine formation. Addition of H_2O_2 accelerates this conversion to within a factor of ~20 of the coupled reaction rate, again without formation of 4a-hydroxy-*q*-$6MPH_2$. Peroxide irreversibly inactivates PAH at high levels. Even under "optimal conditions" for this amino acid-free reaction, 1:1 H_2O_2:$6MPH_4$, one in every 50 oxidations results in PAH inactivation. (The issue of peroxides, PAH, and $6MPH_4$ will be discussed later in this section.)

Uncoupled turnover also causes $\{Fe^{3+}\}PAH$ formation, detectable with catechol trapping. Dix and Benkovic propose formation of a common [$\{Fe^{2+}\}$-$PAH^R{\cdot}O_2{\cdot}XPH_4$] intermediate in both coupled and uncoupled turnover, that is discharged by productive amino acid hydroxylation, liberating *q*-XPH_2 and leaving a [$\{Fe^{2+}$-OOH$\}PAH^R$] species. This Fe^{2+}-O_2 species (with the oxygen at the peroxide oxidation level) would decompose with O−O bond homolysis to yield $HO^{\bullet}$, which either inactivates PAH or oxidizes 0.5 mol of XPH_4, and $\{Fe^{3+}\}PAH^R$, which consumes another 0.5 equiv of XPH_4 in rereduction to yield the observed 2:1 XPH_4:O_2 stoichiometry. The other oxygen is presumably released as HO^-. (Some superoxide was also reported to be released during catalysis, but it is possible that this arises from pterin autooxidation.) The proposal of hydroxy radical formation during uncoupled turnover is based on the observation that no *additional* H_2O_2 is formed during uncoupled turnover compared to coupled turnover, and therefore the damaging oxygen species destroyed by catalase during uncoupled turnover must have a different origin.[168]

Fisher and Kaufman's 1973 report of L-Tyr stimulated uncoupled turnover with H_2O_2 formation followed a determination that the hydroxylation of *p*-chloro- and *p*-fluorophenylalanine was partially uncoupled with respect to NADH oxidation. Addition of HRP, which catalyzes the H_2O_2-dependent oxidation of $6MPH_4$, increased the fraction of uncoupling, which provided indirect evidence supporting H_2O_2 formation during this reaction.[608]

When Dix and Benkovic reexamined this, they found HRP increased the rate of NADH-coupled $6MPH_4$ oxidation, but the reaction was not dependent on the presence of PAH and could be inhibited 90% by the addition of catalase or BHT.[168] Citing evidence[536] that only a trace of H_2O_2 can support HRP-catalyzed XPH_4 oxidation (section III.B.3), the authors conclude that formation of appreciable H_2O_2 during uncoupled turnover does not occur.[168]

Since there is some productive turnover, the partially uncoupled turnover reaction is potentially different from the fully uncoupled reaction observed with L-Tyr. Davis and Kaufman found that at ≥0.1 mM lysolecithin, the addition of 0.81 mM L-Tyr to a mixture of PAH, BH_4, lysolecithin, catalase, NADH, and DHPR in phosphate buffer causes a notable acceleration in the oxidation of BH_4.[640] At this concentration of L-Tyr and pH 8.2, variation of [BH_4] resulted in a normal hyperbolic response of oxidation velocity, but at pH 6.8 the pattern was nonsaturating.

Addition of superoxide dismutase (SOD) limited the pH 6.8 oxidation to a saturating velocity half that obtained in its absence at 0.4 mM BH_4. [The authors cite this as evidence that superoxide is produced during uncoupled turnover and in the absence of SOD will oxidize additional BH_4, which may be enzyme catalyzed or not. It seems highly unlikely that any additional BH_4 oxidation by superoxide is PAH catalyzed. Perhaps SOD inhibits initiation of a radical BH_4 autooxidation process that has a pterin radical carrier (section III.B.3).] Under these conditions, the NADH-coupled assay gave $V_{max} = 2.2$ μmol

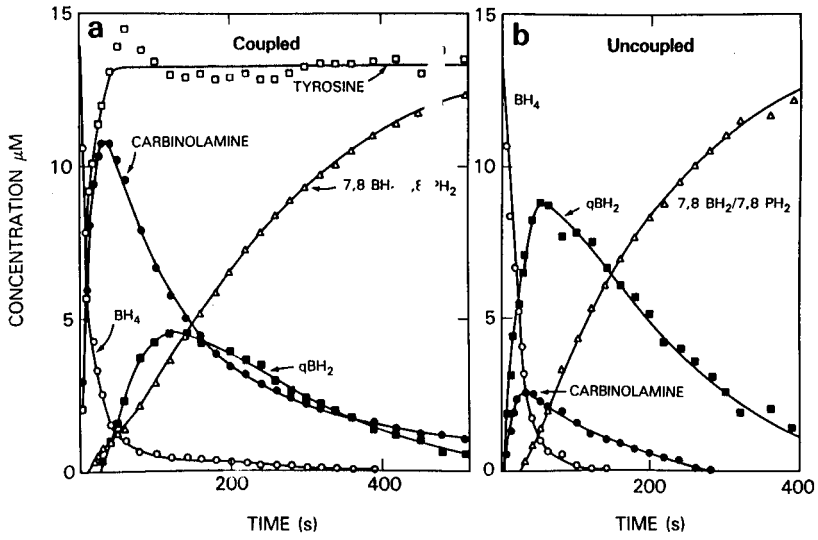

Figure 43. Transformations of the pterin cofactor during coupled and uncoupled PAH turnover. This figure is reproduced from ref 813. Copyright 1993 Academic Press. Results of the simulations performed on these data are given in Table 10.

Table 10. Parameters of Coupled/Uncoupled PAH Turnover[a]

		k, ($\times 10^{-3}$ s^{-1})			
	species	formation	decay	conc (μM)	rel
coupled (L-Phe)	BH_4		58	14.4	1.00
	L-tyrosine	63		13.4	0.93
	4a-OH-q-BH_2	80	8	14.8	1.03
	q-BH_2	14	5	14.5	1.01
	7,8-BH_2 and 7,8-PH_2	5		12.3	0.85
uncoupled (L-Tyr)	BH_4		46	13.7	1.00
	4a-OH-q-BH_2	69	10	4.4	0.32
	q-BH_2	36	5	14.1	1.03
	7,8-BH_2 and 7,8-PH_2	7		12.2	0.89

[a] Lysolecithin-activated PAH preincubated 10 min at 25 °C with 20 mM phosphate, L-phe or L-tyr, and catalase. Initial concentrations: 0.3 mM L-phe or 0.74 mM L-tyr, 14 μM (6*R*)-BH_4, 50 μM lysolecithin, 50 μg mL^{-1} catalase, and 0.12 μM (coupled) or 2.9 μM (uncoupled) PAH at specific activity 7 U mg^{-1}. Data adapted from ref 641.

min^{-1} mg^{-1} of the active PAH component (preparations are stated to range from 30−50% active, which means the velocity is 2.2/14 = 16% that of the L-Phe-dependent specific activity), with $K_{m,BH_4} = 24$ μM and $K_{m,Tyr} = 0.32$ mM. At pH 8.2 all three values are slightly lower. Using 6MPH_4, saturation kinetics were obtained with SOD at both pH values, and both V_{max} and $K_{m,6MPH_4}$ were about 3-fold higher, while $K_{m,Tyr}$ was 9-fold higher (3.2 mM at pH 6.8). The L-Tyr-dependent increase in the background 6MPH_4 oxidation rate (at 1.0 mM lysolecithin) was 6.7-fold, smaller than the 14-fold observed with BH_4, a difference that may be due to the different [L-Tyr]/$K_{m,Tyr}$ ratios used (0.4 for 6MPH_4, 2.4 for BH_4). Supporting a role for amino acid binding during uncoupled turnover, the rate of uncoupled XPH_4 oxidation depends directly on [L-Tyr].[640]

A distinction between uncoupling due to abortive hydroxylation or due to inappropriate electron transfer can be made by examining the pterin product distribution of uncoupled turnover. Dix and Benkovic showed that hydroxylated product and 4a-carbinolamine were formed simultaneously and to the same extent in a partially coupled reaction, implying that uncoupled turnover does not generate 4a-carbinolamine.[168]

Davis and Kaufman reexamined this question with completely uncoupled turnover, reaching a different conclusion.[813] Using a rather complicated spectral-deconvolution procedure to estimate the concentrations of multiple pterin species during turnover, these authors detected formation of 4a-hydroxy-q-BH_2 using repetitive scanning of completely coupled (L-Phe-dependent) and completely uncoupled (L-Tyr-dependent) reactions. As expected, the addition of PCD obliterated the 4a-carbinolamine intermediate. No tetrahydropterin-regenerating system was present and the reactions were run in 20 mM phosphate, pH 8.2, to stabilize the 4a-carbinolamine. A timecourse of the conversion BH_4 → 4a-carbinolamine → q-BH_2 → (7,8-BH_2 and 7,8-PH_2) is shown (Figure 43), with kinetic constants from this model shown in Table 10. In the absence of a pterin-regenerating system, some q-BH_2 loses its 6-substituent upon rearrangement (section III.B.5).

The coupled reaction shows simultaneous buildup of L-Tyr and 4a-carbinolamine as BH_4 is oxidized. This is followed by nonenzymatic dehydration of the 4a-carbinolamine, which is somewhat slower than would be expected from the rate of appearance of q-BH_2. Finally, q-BH_2 rearranges at the rate of 7,8-dihydropterin formation. In the uncoupled reaction, using 24 times more PAH to maintain a similar rate of BH_4 oxidation, BH_4 is again rapidly oxidized, but it appears that it is converted directly to both q-BH_2 and the 4a-carbinolamine.

The steady-state amount of 4a-carbinolamine formed is reported to depend upon the amount of tyrosine present, in a manner consisted with the previously determined K_m for L-Tyr in uncoupled turnover. This

is an extremely interesting observation, because it indicates that there is an amino acid-dependent partitioning of the uncoupled turnover reaction into *two* reaction pathways. Davis and Kaufman propose that the uncoupled interaction of BH_4 and PAH results in the formation of the 4a-carbinolamine and a modified enzyme (the putative iron−oxo group) able to oxidize another equivalent of BH_4 directly to *q*-BH_2.[813] This would result in the eventual reduction of O_2 to H_2O, in agreement with the Benkovic group's observations.[168] To account for the production of H_2O_2, which Kaufman's group claims accounts for 30−40% of O_2 consumption, Davis and Kaufman propose that the enzyme-bound intermediate (they suggest a pterin hydroperoxide) decomposes into H_2O_2 and *q*-BH_2.[641] It would also be consistent with Davis and Kaufman's partitioning model to invoke participation of a $(Fe^{3+}-O_2^{\bullet-})/(Fe^{2+}-O_2)$ complex on PAH. This is supported by the observation of superoxide release and $\{Fe^{3+}\}$PAH formation during partially uncoupled turnover.[168]

Davis and Kaufman directly observe (electrochemical detection) significant H_2O_2 formation by PAH undergoing partially or fully uncoupled turnover: with $6MPH_4$ and *p*-chloro-DL-Phe, *p*-fluoro-DL-Phe, or L-Tyr/lysolecithin, and with PH_4 and L-Phe. In the last pairing, the 4a-carbinolamine was detected by HPLC. The most H_2O_2 was produced during *p*-fluoro-DL-Phe hydroxylation, which is probably a reflection of the higher V_{max} (*vs* *X*PH_4 oxidation) for partially uncoupled turnover compared to fully uncoupled turnover.[642] The reason for the quantitative discrepancy between the amount of H_2O_2 formation observed in the two different groups remains unknown.

There are definitely common themes among partially uncoupled turnover, fully uncoupled turnover, and substrate-free uncoupled turnover. The uncoupled component of turnover with a very poor substrate can generate the 4a-carbinolamine. Apparently this does not depend on the full pterin ring, as the analogous transformation occurs during the mostly uncoupled oxidation of *o*-methylphenylalanine by pyrimidines, which are oxidatively deaminated.[664] However, the primary oxidation product is *q*-*X*PH_2 in both fully and partially uncoupled turnover, which may mean that formation of the 4a-carbinolamine is substrate dependent. Certainly 4a-carbinolamine formation occurs exclusively in an enzyme-catalyzed manner, which is *not* the case for *q*-*X*PH_2 formation. In the limiting case, where substrate is absent, exclusive *q*-*X*PH_2 formation results.

Without the (intentional) addition of peroxide, this slow oxidation appears to be most closely associated with the radical tetrahydropterin autooxidation processes discussed in section III.B.3. When peroxide or peroxyacetic acids are added ("tetrahydropterin oxidase" activity of PAH), the possibility for heterolytic or homolytic processes is reintroduced.

A direct test of this was made by Benkovic *et al.*, who used phenylperacetic acid as the oxygen donor in a substrate-free reaction (section IV.A.6).[814] When phenylperacetic acid is reacted with $\{Fe^{2+}\}$PAH, toluene is formed, indicating exclusive homolytic fragmentation of the peracid. Inclusion of *N*,*N*-dimethyl-*p*-nitrosoaniline causes its bleaching, indicating trapping of $HO^{\bullet}$, under similar conditions (H_2O_2 + $\{Fe^{2+}\}$PAH). The situation is reversed when $6MPH_4$, phenylperacetic acid, and $\{Fe^{2+}\}$PAH are reacted, which produces phenylacetate, indicating exclusive heterolytic peracid decomposition. No bleaching of *N*,*N*-dimethyl-*p*-nitrosoaniline occurs when $6MPH_4$, H_2O_2, and $\{Fe^{2+}\}$PAH are mixed.[814]

This suggests that the tetrahydropterin oxidase activity is not a radical process and therefore differs substantively from the slow autooxidation process. However, Benkovic *et al.* also show a good inverse linear correlation between the $\ln(k_{ox})$, where k_{ox} is the rate of the tetrahydropterin oxidase reaction, and ΔH for the peroxide/peroxyacetic acid RO−OH bond strength, which they regard as evidence for homolytic peracid decomposition during this reaction.[814]

This interpretation is not more persuasive than direct evidence for heterolytic phenylperacetic acid decomposition in the presence of $6MPH_4$. The correlation of reactivity (*m*CPBA > phenylperacetic acid ≫ *t*Bu hydroperoxide > H_2O_2) is in fact consistent with other mechanisms, including one where formation of the tetrahydropterin-oxidizing species is rate limiting or otherwise affected by the stability of the leaving group. An analogy from the cytochrome P450 modeling field is the more-rapid utilization of OIC_6F_5 as an oxygen atom donor, compared to OIPh.[772] Nonetheless, there is good evidence for heterolytic O_2 fissioning in uncoupled turnover, as evidenced by the formation of 4a-carbinolamine and *q*-*X*PH_2 during completely uncoupled L-Tyr turnover, and heterolytic peroxide fissioning during tetrahydropterin oxidase activity (discussed below). The possibility for a substituted-enzyme species, possibly an oxyferryl, exists in both: in the first case it would follow 4a-carbinolamine formation, in the second, it might be formed by oxygen atom transfer from the peroxide.

The tetrahydropterin oxidase activity has been examined in both single- and multiple-turnover regimes, as an extension of the initial characterization of PAH's redox behavior. $\{Fe^{3+}\}$PAH is reduced by $6MPH_4$ to $\{Fe^{2+}\}$PAH, which in turn can be reoxidized by H_2O_2 or another peroxide (section II.A.4).[133]

Hill *et al.* examined this oxidative interaction using 13-hydroperoxylinoleic acid (LOOH, 13-*S*-hydroperoxy-9(*cis*),11(*trans*)-octadecadienoic acid), and found that the stoichiometry was 0.52 ± 0.04 LOOH per PAH subunit oxidized.[170] If the iron content is near-stoichiometric, this immediately suggests that two electrons from two $\{Fe^{2+}\}$PAH subunits are used to reduce LOOH. Since under the experimental conditions, 1.02 ± 0.02 $6MPH_4$ is oxidized to reduce each subunit, the "extra" electron is not recovered from the redox cycle. When the amounts of LOOH and $6MPH_4$ are increased relative to the level of PAH, multiple cycles of enzyme reduction/oxidation occur, with comparatively little inactivation. This PAH-catalyzed, LOOH-supported $6MPH_4$ oxidation to *q*-$6MPH_2$ is the tetrahydropterin oxidase activity referred to earlier. The overall stoichiometry for this reaction is

$$1.0\ 6MPH_4 + 1.0\ O_2 + 0.61\ LOOH \rightarrow 1.0\ q\text{-}6MPH_2 + 0.35\ H_2O_2 + L' \quad (10)$$

where L′ indicates a mixture of fatty acid products, most prominently 13-hydroxy-9,11-octadecadienoic

acid and 9-hydroxy-10,12-octadecadienoic acid. The 13-keto analogue of the first product is also observed, as are 11-hydroxy-12,13-epoxy-9-octadecadecenoate and the related 11,12,13-trihydroxy-10-octadecenoate. (These are the same products observed for the one-electron oxidation of LOOH by hematin.[815]) This conversion can be completely stopped by preincubation of PAH with DHN prior to the addition of LOOH and XPH$_4$ (BH$_4$ is less effective than 6MPH$_4$ in supporting turnover), which indicates that the iron site is essential.

Neither L-Phe nor 5-deaza-6MPH$_4$ interferes with the binding of LOOH, which is consistent with the site of interaction being the iron center. Overall, the oxidation of LOOH occurs with a V_{max} of 30 s^{-1}, which is faster than L-Phe hydroxylation (22 s^{-1}). If the order of addition is changed so that PAH is added after LOOH and XPH$_4$, BH$_4$ is completely ineffective while 6MPH$_4$ is oxidized at 87% of the normal rate. This is probably not due to BH$_4$-dependent inhibition of the allosteric transformation, which is not required for the tetrahydropterin oxidase activity.[170]

Whether PAH is present in either stoichiometric or catalytic amounts, the reaction stoichiometry is the same, which indicates that the reaction mechanism is pingpong: LOOH oxidizes two subunits to {Fe^{3+}}PAH, which are then reduced by two 6MPH$_4$ equivalents in a separate step to {Fe^{2+}}PAH with formation of q-6MPH$_2$. This would leave two "extra" electrons, which may be consumed in the formation of H$_2$O$_2$ from O$_2$. (O$_2$ consumption has only been directly demonstrated in the catalytic reaction.) The stoichiometry indicates that LOOH oxidizes two {Fe^{2+}}PAH subunits but is itself decomposed into products derived from an alkoxy radical; presumably two distinct active sites are oxidized, followed by disproportionation of, or hydrogen abstraction by, the organic radicals. However, it appears from the nonintegral stoichiometry of reactants and products that several integral stoichiometry processes are occurring, which Hill *et al.* suggest are[170]

$$0.35\ 6MPH_4 + 0.35\ O_2 \rightarrow 0.35\ H_2O_2 + 0.35\ q\text{-}6MPH_2 \quad (11)$$

$$0.65\ 6MPH_4 + 0.65\ O_2 + 0.61\ LOOH \rightarrow 0.65\ q\text{-}6MPH_2 + L' \quad (12)$$

These reactions are envisioned to occur upon formation of a ferrous-reduced O$_2$ species from an interaction of 6MPH$_4$ and O$_2$ with presumably ferrous PAH. The first reaction would be the result of LOOH inducing, without its own consumption, aberrant formation of H$_2$O$_2$. In the second reaction, LOOH would react with this enzyme-bound species to give the observed fatty acid products L' with concomitant oxidation of 6MPH$_4$.[170] It is unclear where the consumed O$_2$ is disposed in the second of these reactions. If LOOH removes an electron from the [{Fe^{2+}}PAH·O$_2$·6MPH$_4$] complex, the observed L′ products will be formed and perhaps q-6MPH$_2$ is released, leaving a {Fe^{2+}·O$_2^{\bullet-}$}PAH species. The total H$_2$O$_2$ formation in the overall reaction is insufficient to account for discharge of this ferrous superoxide by H$_2$O$_2$ release, and it is unclear how this undoubtedly reactive species is eliminated. If it dissociates into water and {Fe^{4+}=O}PAH, further oxidation of some component in solution (including oxidative inactivation) would be expected but is not observed.

Perhaps this intriguing reactivity should be reinvestigated under anaerobic conditions. If LOOH (or a different compound) can serve as an oxygen atom donor to {Fe^{2+}}PAH, rather than as a single-electron oxidant, an oxyferryl might be formed, and perhaps the 13-keto L′ product. If a burst of tetrahydropterin oxidation (or a different substrate) can be observed, it would constitute the strongest direct evidence yet for participation of an iron-bound species in PAH-catalyzed oxidations. In a mechanistic vein, these results do not allow more than confirmation that PAH can catalyze a two-electron oxidation of its cofactor by peroxides.

Different uncoupling phenomena are observed with PAH isolated from sources other than liver. The kidney form of rat PAH, a form that is apparently a constitutively active enzyme (section II.A.1), does not oxidize BH$_4$ in the presence of either L-norleucine or L-methionine, both of which are substrates for liver PAH, while DL-*m*-tyrosine induces BH$_4$ oxidation (and perhaps hydroxylation) to the same extent as native (T state) rat liver PAH.[42] The "metal-free" *C. violaceum* PAH yields no uncoupled DMPH$_4$ oxidation (or H$_2$O$_2$ formation) with either *p*-chloro-L-Phe or L-Tyr, while L-norleucine gives *completely* uncoupled turnover. *p*-Chloro-L-Phe is a reasonable competitive inhibitor *vs* L-Phe, with IC$_{50}$ = 0.2 mM. In the case of L-Tyr, which is not an inhibitor *vs* L-Phe hydroxylation at ≤ 1.5 mM, the lack of DMPH$_4$ oxidation is simply due to its failure to associate with the enzyme. Uncoupled DMPH$_4$ oxidation indicates that L-norleucine is activating the "trigger" for catalysis, presumably within the standard quaternary complex.

The inability of *C. violaceum* PAH to hydroxylate L-norleucine is very interesting, because one would not expect a mononuclear copper-dependent or metal-free enzyme to perform primary C−H activation. (Recall, however, that *C. violaceum* PAH is able to hydroxylate the secondary carbon in L-cyclohexylalanine and the primary carbon in *p*-methylphenylalanine.) PH$_4$, which is poorly coupled to hydroxylations in the other forms of PAH, is a tightly coupled cofactor for the *C. violaceum* PAH reaction, with 1.0 ± 0.1 PH$_4$ oxidized per L-Tyr formed. As would be expected if the enzyme lacked an iron active site, alternative oxygen atom donors are unable to support tetrahydropterin oxidase activity with *C. violaceum* PAH.[798] It is perplexing to envision a mechanism by which *C. violaceum* PAH can manage its relatively wide spectrum of reactivity, an efficient NIH shift, and tightly coupled turnover (which is in some ways more discriminating than rat liver PAH itself) in the absence of a metal cofactor. The number of small differences in the uncoupled turnover mentioned here are indicative that different mechanisms function in the atypical prokaryotic and mammalian PAH's, but it cannot yet be determined whether the differences are a consequence of subtle alterations of a delicate balance among the components of the PAH reaction, or whether they are of more fundamental import.

C. TyrH

1. Kinetic Mechanism

Mechanistic studies require pure enzymes. Since effective procedures for TyrH purification (specific activity around 0.4 U mg^{-1}) were developed within a few years of the first overexpression systems (section II.B.2) , the majority of mechanistic work with pure TyrH has been done with recombinant sources of the enzyme. Specific activities have continued to improve throughout the 1990s, in recent work to 2−3 U mg^{-1} or better.[330] In terms of mechanism, the focus on activity is particularly important because the other pterin-dependent hydroxylases cannot oxidize L-Tyr, which means that there may be a unique mechanism functioning with TyrH's cognate substrate. In general, TyrH is a less efficient enzyme than PAH: when forming L-Dopa, it has been reported to be up to 10% uncoupled with $6MPH_4$ or 40% uncoupled with $DMPH_4$.[49] As with PAH, the initial oxidized pterin product is the 4a-carbinolamine, formed quantitatively and concurrently with L-Dopa.[572,816] Both 5-deaza-$6MPH_4$ and *m*-iodotyrosine are tight competitive inhibitors *vs* their substrate analogues.[817] A large and useful, if dated, list of TyrH inhibitors is available.[818] Other kinetic constants are given in Table 5.

Recent evidence indicates that pure TyrH inactivates during catalysis,[328,572] in contrast with reports, using partially purified or low activity preparations, that show linear product accumulation over 20 min.[49,819] With higher activity enzyme, the velocity of L-Dopa formation is linear over only a few minutes at 30−37 °C, in a process that may involve tetrahydropterin inhibition.[325,328,788] Preincubation with other reductants, included in assays to recycle the oxidized pterin cofactor,[71,375,820] has been observed to inhibit PAH or TyrH activity, including ascorbate and DTT.[819,821] In the case of TyrH and ascorbate, inhibition occurs under phosphorylating conditions, but not under turnover conditions (±phosphorylation).[819] The mechanism of this phenomenon is unclear but it seems reasonable to expect that metal chelation or aberrant O_2 reduction is responsible.

Inhibition of TyrH by pterins has been reported; contrary to what might be expected, it does not appear to be limited to reduced or redox-active pterins or to those with the 6-dihydroxypropyl side chain. This tends to rule out several routine mechanisms for this observation, which remains unexplained.[325]

Another complicating factor in studying TyrH is substrate inhibition by L-Tyr, which is observed when BH_4, but not $6MPH_4$ or $DMPH_4$, is used as the cofactor.[49] This characteristic is shared by recombinant sources of TyrH, including phosphorylated, unphosphorylated, and mutant enzymes that lack Ser40.[243−245] If the inhibitory amino acid/TyrH interaction resembles that with catecholamines, one might have expected phosphorylation or removal of Ser40 to alleviate substrate inhibition (sections II.B.3.2 and II.B.3.5), because of the resemblance between catecholamines and L-Tyr, and the relatively lower affinity of the catechol moiety for iron at the lower pH values (*vide infra*) used to assay TyrH. Since a Ser40-based effect is not observed, one might expect inhibition to be due to amino acid binding out of sequence in an ordered mechanism. However, L-Phe is as efficiently hydroxylated by TyrH as L-Tyr with BH_4 as cofactor, and shows no substrate inhibition below ~0.3 mM.[49,243,822] (One report indicates that L-Phe inhibition is detectable at "high levels", apparently >2 mM, with baculovirus-expressed rat TyrH.[247])

In a chemical sense this is easily rationalized as resulting from the presence of a phenolic group in L-Tyr, which might interact directly with the iron site; in a mechanistic sense the inference is that TyrH can bind L-Tyr differently than L-Phe, which is a potentially important observation.

Lineweaver−Burk plots *vs* the reciprocal of L-Tyr, O_2, or $6MPH_4$ concentration show intersecting lines with pure recombinant TyrH, indicating a sequential terbi mechanism.[184] Previously, both intersecting and parallel lines were observed, using impure bovine adrenal medulla TyrH and the 6-isomers of BH_4. Using the natural (6*R*)-BH_4 cofactor, Oka *et al.* observed two different K_m values for each of the three substrates, and both L-Tyr and O_2 inhibition. A simple intersecting pattern was observed with (6*S*)-BH_4, corresponding to the higher K_m values determined with the natural cofactor. With this unnatural isomer, no substrate inhibition was observed with O_2 or ≤ 0.1 mM L-Tyr.[823]

A single K_m, corresponding to the lower K_m value of adrenal medulla TyrH, was observed by the same group for bovine brain (caudate nucleus) TyrH with (6*R*)-BH_4 cofactor. Bovine caudate nucleus TyrH did not show L-Tyr inhibition at ≤ 0.1 mM. This means that the adrenal medulla enzyme contained at least two kinetically distinguishable forms,[824] and highlights the importance of examining pure TyrH in kinetic studies. These ambiguities were avoided by Bullard and Capson in a study of partially purified bovine brain (striatal) TyrH, in which each of the three substrates were pairwise varied under conditions that give pure saturation kinetics (linear Lineweaver−Burk plots).[825] In all cases, intersecting lines were observed, indicating a sequential mechanism. The two organic substrates have an antagonistic relationship, since raising the concentration of either BH_4 or L-Tyr raises the K_m of the other; in contrast, BH_4 and O_2 favor the other's binding; and O_2 and L-Tyr do not interact.

The deadend inhibitors *m*-iodotyrosine and 5-deazapterin were competitive against L-Tyr and BH_4, respectively, and noncompetitive against the other two substrates.[825] If it is assumed that the inhibitors bind TyrH like the substrates they resemble, this result indicates that L-Tyr and BH_4 can bind in either order, followed by O_2 binding (which may be in rapid equilibrium). Alternately, there is random addition of either BH_4 or L-Tyr, but O_2 binding follows BH_4 binding. Dopamine was competitive *vs* BH_4 and noncompetitive *vs* L-Tyr; the product L-Dopa was noncompetitive *vs* all three substrates, which implies that it is released from the enzyme complex before *q*-BH_2. The two catecholamines therefore bind different forms of the enzyme, and dopamine binds the same form of the enzyme bound by BH_4. While substrate inhibition was not directly addressed, it was suggested that when L-Tyr inhibits the enzyme it might bind the (*E* 4a-OH-BH_2) form. Presumably

it would not bind (*E* 4a-OH-6MPH$_2$), or other TyrH complexes of quinonoid pterins that fail to give substrate inhibition.[825]

The mechanism of inhibition was examined further by Fitzpatrick, using purified bovine adrenal medulla TyrH.[323] The catechols norepinephrine, methylcatechol, and dopamine were competitive inhibitors *vs* tetrahydropterins and noncompetitive *vs* L-Tyr, confirming and extending the original result. Furthermore, inhibition was stronger at high pH (pK_a 7.6), as would be expected if inhibition is due to a direct catecholate−iron interaction (section II.B.3.5).[323]

Comparable results were obtained by Haavik *et al.* for [^{3}H]noradrenaline release from ferric bovine adrenal TyrH, but the pK_a was much lower, 5.2.[320] In contrast, Ribiero *et al.* found a sharp maximum (at 0.08 subunit^{-1}) in the amount of [^{3}H]dopamine bound to apparently ferric, recombinant (*E. coli*) rat TyrH at pH ~6.8.[305]

m-Iodotyrosine was competitive with respect to L-Tyr (K_I = 0.11 μM with BH$_4$, 0.24 μM with 6MPH$_4$) and uncompetitive *vs* tetrahydropterin (K_I = 0.24 μM with BH$_4$, 0.34 μM with 6MPH$_4$), which indicates that it binds to (*E* BH$_4$); pH studies indicated that maximal inhibition requires two groups, one of which is deprotonated (pK_a ~ 5.5) and the other protonated (pK_a 7.5).[323] This differs from the previously reported results, where noncompetitive *m*-iodotyrosine inhibition of tetrahydropterin indicates random binding of the two organic substrates.[825] Further evidence that L-Tyr adds after tetrahydropterin, supporting the order of addition determined with *m*-iodotyrosine, lies in the greater susceptibility of BH$_4$-coupled turnover to *m*-iodotyrosine inhibition (lower K_I values *vs* L-Tyr and tetrahydropterin), relative to 6MPH$_4$- or DMPH$_4$-coupled turnover.[323]

Because of the counteracting effects of decreasing amino acid affinity and increasing catechol affinity at higher pHs, L-Dopa has a relatively pH-insensitive inhibition profile. However, as the affinity of L-Dopa for TyrH becomes more dependent upon the catechol moiety, it undergoes a transition at pH 7.6 from a noncompetitive pattern *vs* 6MPH$_4$ (like *m*-iodotyrosine) to a competitive pattern, as is observed with other catechols.[323] The functional difference between L-Dopa and dopamine inhibition depends on the protonation of a group with pK_a ≤7.6. It is reasonable to associate this with the group responsible for high-affinity *m*-iodotyrosine binding.

Unlike other investigators who observe competitive inhibition *vs* BH$_4$,[825] Fitzpatrick reports that 5-deaza-6MPH$_4$ is a noncompetitive inhibitor *vs* both L-Tyr and tetrahydropterins.[323] Using the expression

$$v = VS/\left[K_m\left(1 + \frac{I}{K_{is}}\right) + S\left(1 + \frac{I}{K_{ii}}\right)\right] \qquad (13)$$

the 5-deaza-6MPH$_4$ interactions with at least two different enzyme forms that contribute to the net inhibition can be separately examined. The "competitive" K_{is} value is independent of L-Tyr and the particular tetrahydropterin used, when tetrahydropterin is the variable substrate, S. In contrast, K_{ii} is dependent on L-Tyr concentration, and is an apparent binding constant to the second form of the enzyme. When L-Tyr is the variable substrate, all of the inhibition constants are apparent and depend upon the tetrahydropterin concentration. Fitzpatrick concludes that the data are most consistent with formation of a deadend complex of TyrH, L-Dopa, and 6-methyl-5-deazatetrahydropterin, which in turn indicates that the 4a-carbinolamine product is the first product to dissociate, leaving an enzyme−L-Dopa complex to which inhibitors can bind.[323]

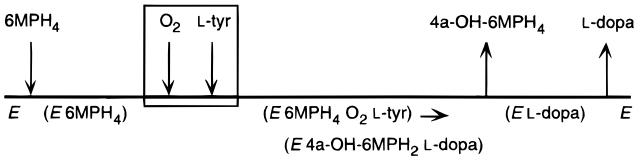

Figure 44. Cleland diagram for TyrH.

The conclusion that L-Dopa is the last product to dissociate is the opposite of that reached by Bullard and Capson, who based their reasoning on the noncompetitive inhibition of all three substrates by L-Dopa (observed by both groups), which remains noncompetitive under "infinite BH$_4$" conditions.[825] In a later, full kinetic analysis (*vide infra*), Fitzpatrick concludes that noncompetitive inhibition patterns seen with L-Dopa are more consistent with L-Dopa being the first product released.[184] This seems to leave the puzzling observation of noncompetitive 5-deaza-6MPH$_4$ inhibition *vs* tetrahydropterin an open issue; perhaps there is some randomness in the order of L-Tyr and tetrahydropterin addition to TyrH.

At this stage, the inhibition and available double reciprocal data were consistent with the Cleland diagram given in Figure 44, where the order of addition required for L-Tyr and O_2 binding (box) is unknown. Since L-Tyr inhibition occurs, it is reasonable to expect that it might be the result of deadend inhibition. Fitzpatrick *et al.* observed no alleviation of substrate inhibition as [BH$_4$] was increased, which is inconsistent with substrate inhibition being due to the formation of an (*E* L-Tyr) complex.[245] However, at high levels of L-Tyr (0.2−0.6 mM), exclusive competitive inhibition *vs* 6MPH$_4$ occurs, which is consistent with deadend inhibition.[826] Thus it appears that the greater susceptibility of BH$_4$-coupled TyrH turnover to L-Tyr inhibition may be mechanistically misleading. In the full-scale kinetic analysis of recombinant TyrH that is discussed next, 6MPH$_4$ was used to minimize this effect.

When any two of 6MPH$_4$, L-Tyr, and O_2 are varied at a nonsaturating constant level of the third, an intersecting, sequential pattern is observed, except when L-Tyr and O_2 are varied at fixed 6MPH$_4$, which gives an equilibrium ordered pattern. This is again consistent with a sequential terbi mechanism and quaternary complex formation. No O_2 inhibition was observed, other than what can be inferred indirectly from the shorter linear period in L-Dopa formation at 1.2 mM O_2.[184]

The denominator of the general expression for the forward velocity for a sequential ter mechanism (p 706 in ref 827) contains three cross-terms involving two substrates (*e.g.*, K_{O_2}[L-Tyr][6MPH$_4$]) and three single-concentration terms (*e.g.*, C_{Tyr}[L-Tyr], where the three *C* terms are coefficients comprised of various kinetic constants) in addition to two invariant terms, the product of the three substrate concentrations and a kinetic constant term C_{all}. A standard approach for determining these values involves satu-

rating the concentration of each of the three substrates in turn while varying the other two. The standard approach is not feasible in the case of TyrH, in part because of L-Tyr inhibition, but a modified procedure in which two substrates are varied at a fixed ratio *vs* the third was successfully employed for TyrH. Replots of the slopes and v^{-1} axis intercepts from the double-reciprocal plots reveal nonzero coefficients as finite intercepts and nonlinear curves, respectively. This information can be used to determine the ordered addition steps, and whether there are rapid equilibrium steps involved (pp 712−713 in ref 827).

As can be seen in the inset to Figure 45A, the intercept replot is linear, which implies that $C_{O_2} = 0$. The slope replot in Figure 45A has a zero intercept, which means that $K_{O_2} = 0$, and is nonlinear, which means the kinetic constant term C_{all} is nonzero. All of the replots in Figure 45B and C are nonlinear, and the intercept replots have finite intercepts. This allows a velocity expression to be constructed:

$$\frac{v}{V} = [\text{Tyr}][O_2][6\text{MPH}_4]/([\text{Tyr}][O_2][6\text{MPH}_4] + K_{6\text{MPH}_4}[\text{Tyr}][O_2] + K_{\text{Tyr}}[O_2][6\text{MPH}_4] + C_{6\text{MPH}_4}[6\text{MPH}_4] + C_{\text{Tyr}}[\text{Tyr}] + C_{\text{all}}) \quad (14)$$

The actual values for V_{max} (1.5 ± 0.2 s^{-1}), K_{Tyr} (22 ± 4 μM), and K_{6MPH_4} (30 ± 8 μM) are extracted from this analysis; no isotope effects different than 1.0 were observed on these parameters. This velocity equation indicates that O_2 binds after both organic substrates, whose order of binding is not specified. Inhibition analysis from previous work, and using 7,8-$6MPH_2$, suggests that tetrahydropterin binds first. The rapid equilibrium, ordered pattern from the subsaturating fixed-$6MPH_4$ experiment (which indicates that O_2 binds *before* L-Tyr) and the determination that $K_{O_2} = 0$ from the constant-ratio experiment both indicate that O_2 binding is in rapid equilibrium. Since this would ordinarily make $C_{Tyr} = 0$ in an ordered addition process (a linear intercept replot in Figure 45*B*), Fitzpatrick suggests that deadend inhibition due to L-Tyr reintroduces the term.[184] The resulting kinetic mechanism for baculovirus-expressed rat TyrH is presented in Figure 46.

It is worth recalling the failure to observe significant substrate inhibition by L-Phe[49] in the light of this mechanism. The ability of L-Tyr to cause inhibition of $6MPH_4$- or BH_4-dependent TyrH catalysis below 0.15 mM (≥10-fold lower than with L-Phe), seems to imply a specific inhibitory interaction between L-Tyr and TyrH.

As is observed with cytochrome P450 and the other aromatic amino acid hydroxylases, TyrH displays no *V* or *V*/*K* isotope effects different than unity with [3,5-^{2}H]tyrosine. A burst of L-Dopa formation was not detected at 2 °C during the first few turnovers of TyrH at high L-Tyr concentration, with saturating $6MPH_4$ and O_2. (Therefore product release is not rate-limiting, an important point underlying the preceding discussion.) These observations are consistent with rate-limiting and irreversible formation of the hydroxylating intermediate during TyrH catalysis.[184,826]

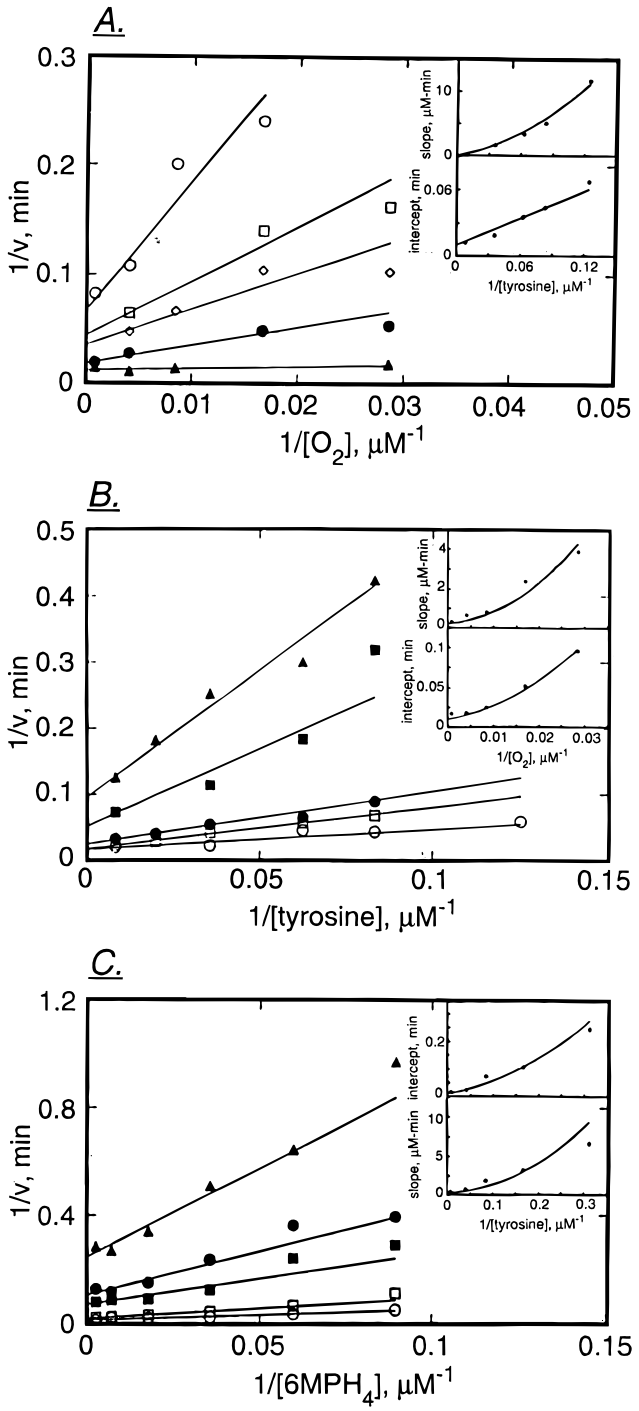

Figure 45. Double-reciprocal plots for TyrH. In each of A−C, two of the substrates are varied in a fixed ratio while the third is held constant. Insets show replots of slopes and intercepts from the individual figures. Reproduced from ref 184 with permission. Copyright 1991 American Chemical Society.

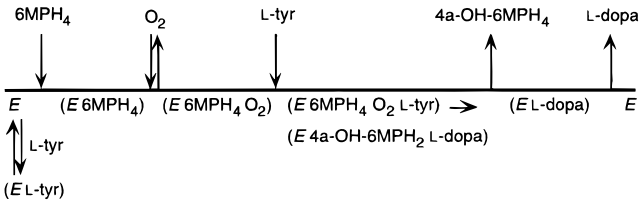

Figure 46. Revised kinetic mechanism for TyrH.

The presence of a nearby and relatively acidic proton in the L-Tyr substrate has been recognized to be a major potential difference between this enzyme and PAH or TrpH and has been proposed to require

Table 11. TyrH Amino Acid Substrates

alternate substrate	product (assay)	rel V/K_m (Tyr = 100%)	comments	ref
Phe	*p*- and *m*-tyrosine (26:1); Dopa	24%	K_I = 0.13 mM. Hydroxylation is 21% coupled to 6MPH_4 oxidation	247, 785, 787, 828
p-aminophenylalanine	(NADH)	6.8%		247, 787
p-methoxyphenylalanine	(NADH)	0.81%		247, 787
p-fluorophenylalanine	(NADH)		K_I = 0.34 mM	247
m-tyrosine	Dopa	1.6%	K_I = 2.5 mM	247, 787, 801, 829
m-fluorophenylalanine	(NADH)			247
L-Trp	(NADH)	0.85%	K_I = 2.1 mM	247, 787
4-pyridylalanine	(NADH)	0.21%	K_I = 8 mM	247, 787

the action of a basic enzyme moiety in some of the proposed mechanisms for this enzyme (section IV.C.3). Exchange of water for D_2O causes only ordinary shifts in TyrH pK_a values. No solvent isotope effect on V or $V/K > 1.1$ was detected at the optimal pH (pD), indicating that the rate-limiting formation of the hydroxylating intermediate does not involve proton transfers.[247] In section IV.C.3, the discussion focuses on results with compounds intended to resemble potential intermediates in the hydroxylation pathway, which follows a discussion of the substrate specificity and product distribution of TyrH.

2. Substrate Specificity; NIH Shift

TyrH will hydroxylate several other amino acids, shown in Table 11. In some of these and other cases V_{max} information has been obtained, generally as the rate of substrate-dependent, q-BH_2-coupled NADH oxidation. Intriguingly, the V_{max} values of q-BH_2 formation by bovine adrenal TyrH with several potential and known substrates (phenylalanine, *p*-methoxyphenylalanine, *p*-aminophenylalanine, and 4-pyridylalanine) are indistinguishable from that with L-Tyr, even though some of these amino acids are not hydroxylated (the last two in the previous list).[787] Recombinant (baculovirus) rat TyrH has about the same V_{max} (q-BH_2 formation) with *p*- and *m*-tyrosine (product = L-Dopa) and *p*- and *m*-fluorophenylalanine (products unknown); relative V/K values are given in Table 11. For both sources of TyrH, L-Trp has a lower V_{max} and is at least partially hydroxylated. Whereas the other amino acids, regardless of whether they are hydroxylated, are mostly competitive inhibitors, the recombinant rat enzyme shows noncompetitive inhibition with L-Trp, which means that it binds multiple forms of the enzyme.[247] L-Phe is an apparently ordinary TyrH substrate, hydroxylated in a ratio of ~26:1 at the *para* and *meta* positions,[777,820] and from either on to L-Dopa,[801] but the majority of tetrahydropterin oxidation with L-Phe is uncoupled to hydroxylation. L-Phe hydroxylation by TyrH is usually but not ubiquitously observed. Using rat PC12 TyrH, Dix *et al.* found that L-Phe was a competitive inhibitor *vs* L-Tyr but was not hydroxylated itself (section IV.C.3). Neither did L-Phe induce uncoupled BH_4 oxidation by TyrH.[572] This singular report contradicts many others that show L-Phe is a good alternate substrate for TyrH isolated from either adrenal or pheochromocytoma cells.[49,822] This is not the case for *m*-tyrosine, which is converted to L-Dopa in a reaction completely coupled to q-BH_2 formation.[247]

These results emphasize the difference between total turnover and substrate oxidation. While an amino acid moiety is required to trigger generation of the hydroxylating intermediate, it is not necessarily sufficient. This is the case for the classic TyrH inhibitor *m*-iodotyrosine, which does not induce tetrahydropterin oxidation even though it binds with submicromolar K_I values. In addition, 3-pyridylalanine (and some amino acids intended to resemble the TyrH transition state, *vide infra*) do not induce q-BH_2 oxidation with recombinant rat TyrH, even though it is a reasonable competitive inhibitor (K_I = 0.8 mM, 1.7 mM with bovine adrenal TyrH).[247,787]

Because the velocity of q-BH_2 formation is not dependent upon the nature of the amino acid, it follows that the decision to commit to catalysis is also partly independent of the amino acid sidechain. While this has been claimed to indicate "the total rate of formation of a hydroxylating species",[787] this is only indirectly inferred from the rate of tetrahydropterin oxidation, as was mentioned in the case of PAH (section IV.B). Even when 4a-hydroxydihydropterins are detected directly,[816] indicating O_2 fissioning, it is still taken on faith that iron, O_2, and tetrahydropterin interact in the same fashion as during productive hydroxylations. A reckoning[247] that the rate of electrophilic hydroxylation must be many times faster than the generation of the hydroxylating intermediate, based on the range in σ^+ (but not V_{max}) represented by the extremes of L-Phe and *p*-aminophenylalanine, is less convincing because the latter substrate is not hydroxylated. More data on the products and rates of formation using the other compounds is needed, which should reveal any trends in the uncoupling behavior. Fortunately, TyrH appears to be tolerant of a number of substituents that PAH would not accept, even as middling competitive inhibitors. Since TyrH is able to hydroxylate (either) *meta* position and the *para* position of L-Phe, a fuller range of substrate studies is possible (*vide infra*). Until the coupling issue is clearer, the efficiency of productive TyrH turnover seems to be only incidentally related to the ability to activate its "trigger" for irreversible O_2 reduction.

Despite the fact that it is a mostly uncoupled reaction, L-Phe hydroxylation by TyrH is another example of a multiple-product-forming reaction and so is a source of information about the nature and partitioning of the reactive intermediate(s). The *p*-/*m*-tyrosine product ratio, reported as ~6 with an impure bovine adrenal preparation[829] and 26 with highly purified recombinant (*E. coli*) rat TyrH, is also apparently temperature dependent.[785]

At higher temperatures, the ratio is smaller, revealing a 2.2 kcal mol^{-1} difference in activation energy for hydroxylation at the two positions. Using

Table 12. Labeled L-Phe Hydroxylation by TyrH[a]

ring-deuterated phenylalanine	$^{D}V_{p-Tyr}$	$^{D}V_{m-Tyr}$	$^{D}p/m$	^{D}coupling
4-^{2}H	**1.22 ± 0.01**	1.01 ± 0.09	**1.22 ± 0.02**	**1.21 ± 0.07**
3,5-$^{2}H_2$	1.04 ± 0.07	**1.72 ± 0.28**	**0.55 ± 0.03**	1.05 ± 0.05
$^{2}H_5$	**1.21 ± 0.09**	**1.52 ± 0.21**	**0.77 ± 0.13**	**1.29 ± 0.12**

[a] Table adapted from ref 785.

specifically deuterated phenylalanines, the individual reactions were investigated; as expected the primary isotope effects are small but are significantly different from unity (bold entries in Table 12). No secondary isotope effects were detected (nonbold ^{D}V entries in Table 12), but the data are not precise enough to show the predicted small inverse isotope effect (0.996 on *m*-tyrosine formation) expected for initial electrophilic oxygen attack on a nondeuterated position. It follows that the isotope-dependent alteration in the product distribution ($^{D}p/m$) is sensitive only to the hydrogen isotope present at the point of hydroxylation, a result inconsistent with obligatory arene oxide formation.[785]

Were an arene oxide formed, there would be a 5-fold increase in the amount of *m*-tyrosine formed from [4-^{2}H]Phe corresponding to the observed 17% decrease in *p*-tyrosine formation. Since there is no such increase, there cannot be a common amino acid intermediate responsible for the partitioning, which rules out initial arene oxide formation. Partitioning between the two products probably "occurs upon initial attack of the activated oxygen species on the substrate", and the relative ratio of product formation depends upon the relative rates of oxygen addition.[785] The evidence against an obligatory arene oxide intermediate during cytochrome P450-mediated hydroxylation of chlorobenzene and other substrates (section IV.A.5) suggests direct oxygen attack occurs. Analysis of that possibility predicts an inverse secondary isotope effect on V_{max} as small as 0.8. In order to account for the observed normal isotope effects, oxygen attack is coupled to C−H bond breaking, which would have a primary isotope effect sufficient to mask the predicted inverse effect. Alternately, attack of the activated oxygen species is reversible; this seems most likely in the context of metallaoxetane formation, which is compatible with the TyrH evidence presented.[785]

The extent of coupling corresponds well to the isotope effect on the velocity of *p*-tyr formation ($^{D}V_{p-Tyr}$) for all three labeled L-phenylalanines because nearly all productive turnovers generate *p*-tyrosine, leaving the isotope effect on coupling (^{D}coupling) undetectably different from this value.[785] Thus it appears that the rate of $6MPH_4$ oxidation remains constant for all of the isotopically substituted phenylalanines, which would be predicted from the constant V_{max} of tetrahydropterin oxidation by TyrH in the presence of suitable amino acids.

As was mentioned in the introduction to the NIH shift (section IV.A.4), the majority of L-[4-^{3}H]Phe hydroxylations by TyrH involve a 1,2-hydride transfer.[701] It would be interesting to learn if label is retained to a similar extent in [3,5-^{2}H]Phe, both during *para* hydroxylation (to determine the isotope effect on cyclohexadienone rearomatization) and *meta*-hydroxylation (efficiency of the NIH shift at a *meta* position, which is generally less effective in the case of cytochrome P450 substrates). Relatively few other substrates expected to show an NIH shift have been examined with TyrH. While its alternate substrates show that TyrH can catalyze oxygen atom transfer reactions, the peculiar characteristics of the reaction with L-Tyr itself open the possibility of other mechanisms for oxygen transfer. These are discussed in the following section.

Cobalt-substituted TyrH, an inactive form of the enzyme, has been used to attempt to "triangulate" the position of L-Phe bound at the active site. Both Co^{2+} and Zn^{2+} compete with Fe^{2+} ($K_I = \sim 1$ and ~ 0.1 μM, respectively) for binding to TyrH, at a final stoichiometry of one metal ion per subunit.[327] Normalized values were obtained for the paramagnetically broadened nonexchangeable protons in L-Phe bound to Co^{2+}-substituted TyrH and Co−H distances were derived from them. No significant differences among the metal−proton distances were obtained for the L-Phe·{Co^{2+}}TyrH complex, or this complex with added 7,8-BH_2. Interproton NOESY data were also collected on L-Phe bound to Zn^{2+}-substituted TyrH in the presence of 7,8-BH_2, which is supposed to bind in a manner analogous to the natural cofactor. A model of the interaction of L-Phe with TyrH was then proposed using these distance constraints, which has a relatively extended conformation of L-Phe ~7 Å from the metal center, *i.e.*, L-Phe is near, but not in, the primary coordination sphere of the metal.[794]

We are only beginning to understand the molecular components of pterin-dependent hydroxylases responsible for particular functional behaviors. One early bit of evidence is that the Segawa's dystonia-causing TyrH mutant Q381K raises the K_m for L-Tyr by about half an order of magnitude and lowers but does not abolish activity.[16]

3. Transition-State Analogues, Alternate Oxidants

Alone among the pterin-dependent amino acid hydroxylases, TyrH normally hydroxylates an "activated" aromatic substrate. This allows for mechanisms akin to those proposed for flavin hydroperoxide-dependent hydroxylations, where an electron-withdrawing substituent participates in oxygen atom insertion.[826] TyrH might function by attacking the phenoxide form of its substrate (Figure 47, in which the active oxidant is depicted as the hypothetical 4a-hydroperoxypterin), which appears to be the case with *p*-hydroxybenzoate and phenol hydroxylases.[624]

Since *p*-methoxyphenylalanine is apparently oxidized by TyrH (Table 11), phenoxide formation may not be obligatory. However, since the products formed and extent of coupling are unknown with this substrate, it is uncertain whether the methyl group is a serious impediment to *meta* hydroxylation. Several compounds intended to function as transition

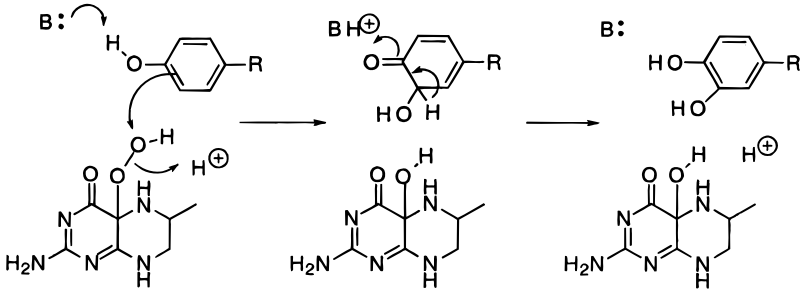

Figure 47. Phenoxide-dependent mechanism for TyrH.

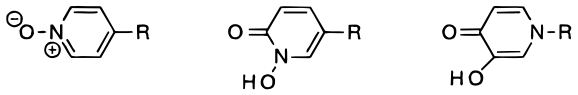

Figure 48. Compounds intended to be transition-state analogues for TyrH.

state analogues for different species in the phenoxide mechanism were prepared (Figure 48). The first of these was intended to resemble the phenoxide intermediate, and the other two were expected to mimic the semiquinone intermediate. All three were weak or ineffectual inhibitors *vs* L-Tyr ($K_I = \gg 4$, 3, and 0.4 mM, respectively), and the last gave a noncompetitive instead of the anticipated competitive pattern, which is reminiscent of inhibition by L-Dopa.[247] While a mechanism of hydroxylation fundamentally different from that with the other pterin-dependent hydroxylases is not supported by these observations, it seems quite likely that TyrH will employ a somewhat altered hydroxylation strategy for achieving coupled turnover with its cognate substrate.

A powerful technique for examining the cytochrome P450 intermediates has been to use alternate oxygen atom sources, most famously the "peroxide shunt" mechanism, by which hydroxylation is supported even though O_2 reduction steps are bypassed (section IV.A.3). Attempts to use peroxides as oxygen atom donors for the PAH reaction have failed, but there has been some success in this vein with TyrH.[572]

Just as the uncoupled reactions of PAH are more favorable at high pH, TyrH gives uncoupled BH_4 oxidation with L-Tyr at pH 8.2 (40−50% coupled turnover) using a rat PC12 preparation that gives 95% coupled turnover at pH 7.2. Significant amounts of BH_4 oxidation occurred in the absence of L-Tyr (20 μM BH_4 oxidation occurs at 4×10^{-3} s^{-1} with 2 μM TyrH, *vs* coupled hydroxylation at 5×10^{-3} s^{-1} with L-Tyr/1 μM TyrH). These results suggested that formation of a hydroxylating species might be possible in the absence of substrate.[572]

Dix *et al.* discovered that L-Tyr hydroxylation could proceed in the absence of tetrahydropterin: when 0.5 μM TyrH was incubated with a 20-fold excess of H_2O_2, 0.61 μM L-Dopa (1.2 turnovers) was formed, as determined by the ^{3}H-release assay.[572] If a 200-fold excess of H_2O_2 was added, only 0.09 μM hydroxylation occurred, indicating that oxidation of the enzyme was occurring faster than hydroxylation. Indirect evidence for H_2O_2 formation by TyrH and BH_4 was obtained by adding L-Tyr at different times after mixing (no reduced BH_4 remained after 30 s). From 1 μM BH_4 and 1 μM TyrH, a maximum of 0.5 μM product was obtained as $t \rightarrow 0$, an ability to form product that diminished very slowly ($t_{1/2} \approx 10$ min). Addition of catalase did not disrupt the catalytic ability of this presumably enzyme-bound intermediate by more than 10%.

These remarkable observations have no analogue in either of the other aromatic amino acid hydroxylases, so it seems they are particularly dependent on the "activated" nature of L-Tyr as a substrate. In agreement with this, *m*CPBA (but not *tert*-butyl hydroperoxide) was able to support L-Tyr hydroxylation but the reaction is completely nonenzymatic, owing to the rapid destruction of TyrH by both *m*CPBA and *t*BuOOH. In contrast, *m*CPBA is completely unable to hydroxylate L-Phe (neither is the particular rat PC12 TyrH employed in this study). Thus there is considerable doubt that the hydroxylating species examined here has any necessary resemblance to the natural enzyme-bound intermediate of TyrH. The authors use these data to support a Fenton-like intermediate on PAH, in order to explain the greater rate of autoinactivation by that enzyme relative to TyrH and suggest there is a higher reduction potential for the active-site iron TyrH that allows that enzyme to "exhibit alternative modes of peroxide reactivity in competition with Fenton's chemistry".[572] There is no direct evidence to support these ideas, which are in conflict with much of the mechanistic work done with PAH. There is no need to invoke a different structure for the hydroxylating intermediate generated by the two enzymes if TyrH can hydroxylate unactivated aromatic substrates. This criterion is met by the observation of L-Phe hydroxylation by other forms of TyrH, including rat pheochromocytoma (PC12 and PC18) TyrH.[814]

Furthermore, Ribiero *et al.* were unable to reproduce the BH_4-independent, H_2O_2-dependent hydroxylation of L-Tyr under the conditions of Dix *et al.* using the same source of enzyme. By a number of criteria, the PC12 enzyme appeared to function as a "normal" TyrH.[814] The reasons for the discrepancies between the unique observations of Dix *et al.* and those of other investigators remain unknown.

D. TrpH

Very little mechanistic work has been done with TrpH. A preliminary study of the velocity patterns of mouse mastocytoma TrpH by Hosoda indicates a sequential mechanism with $DMPH_4$ as cofactor.[830] Gál has reached a similar conclusion with BH_4 as cofactor.[831] Using a partially purified rabbit hindbrain TrpH, Tong and Kaufman determined the tetrahydropterin:L-Trp stoichiometry of the TrpH reaction, which is tightly coupled: 0.96 ± 0.01 $6MPH_4$ or 0.90 ± 0.05 $DMPH_4$ consumed per 5-hydroxytryptophan formed.[372] Working with a less-pure preparation from the same source, Friedman *et*

al. determined a stoichiometry of 0.95 BH_4 consumed per 5-hydroxytryptophan formed.[369]

A pH optimum for TrpH between 7.0 and 7.6 is generally observed.[332,373,374] The kinetic constants for pure mouse mastocytoma TrpH, which at specific activity 5.3 μmol min^{-1} mg^{-1} is the most active TrpH yet reported, are 45 μM (K_m, L-Trp) and 55 μM (K_m, $6MPH_4$).[373] Various BH_4 K_m values have been reported,[346] typical among them the value of 22 μM for impure rabbit hindbrain TrpH.[369]

Most of the strong TrpH inhibitors known are potential iron chelators, consistent with an essential role for the iron, as was discussed in section II.C.4. Generally, the inhibitors of this type that are of physiological interest are catechols, like the L-Dopa-derived TyrH catecholamine products or other compounds, such as benserazide, a catechol used in combination with L-Dopa as a Parkinson's treatment (Medopar).[332,373,818,832,833] Benserazide is competitive *vs* BH_4 ($K_I = 80 \pm 10$ μM) and uncompetitive *vs* L-Trp ($K_I = 176 \pm 13$ μM);[367] similar results were obtained with TyrH.[834] This result implies that this catechol and L-Trp do not bind the same form of TrpH; if benserazide binds to the free enzyme only, this could indicate some degree of order in the sequential mechanism.

Several catechol-containing tetrahydroisoquinolines and related compounds inhibit TrpH with submicromolar K_I values.[833] Noncompetitive inhibition was observed *vs* BH_4 and L-Trp for both L-Dopa and dopamine,[832] as is observed for dopamine but not L-Dopa inhibition of TyrH. (In turn, the TrpH product 5-hydroxy-L-Trp is a moderate inhibitor of TyrH, with $IC_{50} \approx 0.1$ mM.[835]) Further studies with simple catechols will be required to interpret these observations in mechanistic terms, just as they were necessary in the TyrH case (section IV.C.1).

MAO inhibitors cause accumulation of both serotonin and 5-hydroxytryptophan. *In vitro*, serotonin is a weak inhibitor of TrpH,[332,373,385] but *in vivo* there is a negative feedback mechanism operating that diminishes the apparent TrpH activity in brain slices.[836] More effective inhibition was observed with 5-hydroxytryptophan, the product of TrpH. This compound does not ordinarily accumulate because of the action of AAADC; there is some variability in the concentration required to cause inhibition.[332,373] At 0.1 mM, 5-hydroxytryptophan inhibits pure mastocytoma TrpH by 80%.[373]

TrpH is subject to substrate inhibition when assayed with BH_4.[369] This effect is diminished or absent when $6MPH_4$ (or $DMPH_4$) is the cofactor or if L-Phe is the substrate (either $6MPH_4$ or BH_4), for a variety of natural and recombinant sources of TrpH.[343,369,372,383,384] Inhibition of TrpH due to *p*-chlorophenylalanine is also stronger when BH_4 is the cofactor.[383]

It is perhaps surprising that *p*-chloro-DL-Phe ($K_I = 26$ μM for mastocytoma TrpH) is as strong a TrpH inhibitor *vs* L-Trp as 4- or 5-fluoro-DL-Trp, and that 6-fluoro-DL-Trp is stronger than either.[319,360,809] As was discussed above, *p*-chlorophenylalanine causes depletion of TrpH (section IV.B.2), which is followed by an increase in TrpH transcription in dorsal raphe.[837] No information about any of these compounds as TrpH substrates is available.

One of the consequences of TrpH's low activity and its rarity is that its 5-hydroxyindole products are nearly always assayed directly, using sensitive radiochemical or fluorometric methods. As a result little is known about the coupling of tetrahydropterin oxidation to product formation, because only productive product turnover is detected. In the only case where the extent of coupling has been reported, TrpH oxidation of $6MPH_4$, $DMPH_4$, or BH_4 is tightly coupled to 5-hydroxytryptophan formation.[369,372] The same preparation hydroxylates L-Phe at 44% ($6MPH_4$), 29% ($DMPH_4$), and 86% (BH_4) the velocity of L-Trp hydroxylation, yielding exclusively *p*-tyrosine.[372] L-Phe is both a competitive inhibitor *vs* L-Trp ($K_I = 0.2$ mM; rabbit hindbrain with BH_4) and a very efficiently used alternate substrate (*vide infra*).

This ability to cross-hydroxylate the two amino acids has occasionally led to confusion about the tissue distribution of each protein (sections II.C.2 and IV.A.8). The potential that TrpH might be inhibited in cases of PKU has been raised, on the basis of the low levels of brain hydroxyindoles associated with that condition.[342] It seems that direct inhibition of TrpH by elevated [L-Phe] provides a reasonable explanation for this phenomenon.[372]

L-Tyr is a poor TrpH substrate, being converted by the partially purified rabbit brain enzyme to L-Dopa at 1−5% the rate of L-Trp hydroxylation. Thus it is unsurprising that *m*-iodotyrosine is unable to inhibit TrpH.[372] L-Tyr is neither an effective inhibitor nor a substrate of pure TrpH (≤1% of L-Trp activity). Any ability to hydroxylate L-Tyr is significant, given the complete inability of PAH to alter L-Tyr. Pure mouse mastocytoma TrpH hydroxylates L-Tyr at 1% of the L-Trp rate, while L-Phe is hydroxylated 32% *faster* than L-Trp.[373] Pure rat brainstem TrpH (which has a specific activity 14-fold lower than the mastocytoma enzyme) shows no L-Tyr hydroxylation, and hydroxylates L-Phe at 39% of the L-Trp rate.[374] This is one important example of the differences between brain and peripheral TrpH, which are more significant than those between brain and adrenal TyrH, or between liver and kidney PAH.

The streptomycete-produced antibiotic L-[2,5-H]Phe is a good competitive inhibitor of TrpH *vs* L-Trp ($K_I = 44$ μM).[838] Since this compound is an excellent PAH substrate, there is a very good chance that it is also a TrpH substrate. It would be interesting to learn if it is epoxidized by TrpH in analogy to the PAH transformation (section IV.B.2). One would predict that this would be the case, since the NIH shift functions very effectively in TrpH. As was mentioned in section IV.A.4, L-[5-^{3}H]Trp forms 5-hydroxy-L-[4-^{3}H]Trp with at least 85% retention of label.

This differs from the PAH transformation in that the migration is directed exclusively to the 4-position and the label in this position is easily exchanged with acidic water. The first difference seems to be due to the greater stability of the carbonium ion at the 4-position compared to the 6-position. The second may be enhanced by *p*-quinonoid resonance structures due to the heterocyclic nitrogen. If the effective TrpH inhibitor 6-fluorotryptophan is also a substrate, one might examine the effect of "*meta*" substitution by this strong electron-withdrawing group, or the tendency to redirect the 1,2-hydride migration if

4-fluorotryptophan is a substrate. If several substituted-indole compounds are substrates, it would seem that TrpH would afford the best opportunity to examine the detailed mechanism of the NIH shift in the aromatic amino acid hydroxylase enzymes.

V. Future Directions

Despite the great advances that have been made in characterizing the pterin-dependent hydroxylases over the past three decades, our understanding of the nature of the active-site environment, regulatory behavior, nature of the reactive intermediate, and mechanism of oxygen atom transfer, are far from complete. This state of affairs is clearly reflected in the contradictory results that have been included to demonstrate the current status of the field.

However, recent successes in using molecular biological techniques to overexpress proteins will allowed the isolation of pure enzyme with nearly complete activity, a necessary first step for any detailed investigation. Identification and analysis of the structural changes induced by the allosteric effectors will be essential to understand the fundamental aspects of how the reactivity properties of the active site are controlled and what steps are responsible for the commitment to catalysis. Undoubtedly, significant insights into this problem will arise from comparative crystallographic studies of the resting and activated forms of these enzymes. The ability to systematically generate a variety of enzymatic states at concentrations appropriate for spectroscopic investigation will greatly facilitate a more detailed understanding of the role played by the active iron center in these enzymes.

Several significant issues are still poorly understood, including such fundamental questions as to the basis for the differential reactivity of PAH and TyrH with respect to L-Tyr. Detailed chemical explanations for the phenomenon of uncoupled turnover readily observed in these pterin-dependent hydroxylases also promises to be a major challenge. Furthermore, investigating the identity of the active hydroxylating species, its formation pathway, and its similarities and differences with other non-heme- and heme-centered hydroxylating intermediates promises to yield insights into iron-based oxidation chemistry.

Likewise, much is still to be learned about the thermodynamics and kinetics of the interconversion of the different states of these enzymes. Such a level of understanding will be of equal, if not greater, significance to the medical community. For instance, comparison of the state-dependent properties of wild-type PAH with those of missense mutants that give rise to PKU in the human population offers the real opportunity to uncover the chemical basis of this common inborn metabolic disorder. Equally intriguing is the possibility of understanding the effects of specific mutations in TyrH and TrpH and their possible links to neurochemical (behavioral) disorders. Building on the foundations formed during the past 30 years, research on the pterin-dependent hydroxylases is poised to answer many fundamental and exciting questions during the next decade of effort.

VI. Glossary of Symbols and Abbreviations

14-3-3	TrpH activator protein
5-HT	5-hydroxytryptamine, serotonin
$^{\bullet}6MPH_3$	trihydropterin radical form of 6-methylpterin
$6MPDH_4$	6-methylpyrimidodiazepine
$6MPH_4$	6-methyl-5,6,7,8-tetrahydropterin
$6,6\text{-}M_2PH_4$	6,6'-dimethyl-5,6,7,8-tetrahydropterin
6-PTPS	6-pyruvoyl-tetrahydropterin synthase, EC 4.6.1.10
$7\text{-}BH_4$	isomer of BH_4; reduced form of primapterin
$7,8\text{-}6MPH_2$	6-methyl-7,8-dihydropterin
$7,8\text{-}BH_2$	6-methyl-7,8-dihydropterin
$7,8\text{-}DMPH_2$	6,7-dimethyl-7,8-dihydropterin
$7,8\text{-}XPH_2$	6-substituted 7,8-dihydropterin
AaT-20	neuroendocrine (anterior pituitary) cell line
ACh	acetylcholine
ANBADP	5-[(3-azido-6-nitrobenzylidene)amino]-2,6-diamino-4-pyrimidinone
BH_4	tetrahydrobiopterin, (6*R*)-erythro-2,3-dihydroxypropyl-5,6,7,8-tetrahydropterin
CaM	calmodulin
cAMP-PK	cyclic AMP-dependent protein kinase; protein kinase A
CaM-PK II	CaM-dependent protein kinase II
cGMP-PK	cyclic GMP-dependent protein kinase
CNS	central nervous system
COS	monkey cell line
CRE	cAMP-responsive element
DCoH	dimerization cofactor of homeoboxes; PCD
DEAE	(diethylamino)ethane
DHFR	dihydrofolate reductase, EC 1.5.1.3
DHPR	dihydropteridine reductase, EC 1.6.99.7
$DMPH_4$	6,7-dimethyl-5,6,7,8-tetrahydropterin
L-Dopa	3,4-dihydroxy-L-phenylalanine
DTNB	5,5′-dithiobis(2-nitrobenzoic acid); Ellman's reagent
DTT	dithiothreitol, Cleland's reagent
EDTA	ethylenediaminetetraacetic acid
EGTA	ethylenebis(oxyethylenenitrilo)tetraacetic acid
E-PK	endogenous proline-directed serine/threonine protein kinase
EPR	electron paramagnetic resonance
EXAFS	extended X-ray fine structure
Fl	isoalloxazine portion of FMN or FAD
$FlH^{\bullet}$	flavin semiquinone radical
FlH_2	reduced flavin
g_{eff}	effective *g* factor
GC−MS	gas chromatography detected by mass spectra
GEM	glyceryl-ether monooxygenase, EC 1.14.16.5
GOD	hydroxyl-deuterated glycerol, $CH(OD)(CH_2\text{-}OD)_2$
GTPCH	GTP cyclohydrolase I, EC 3.5.4.16
HEPES	*N*-(2-hydroxyethyl)piperazine-*N*′-2-ethanesulfonic acid
HNF-1	hepatocyte nuclear factor-1, a tissue-specific transcription factor
HRP	horseradish peroxidase, EC 1.11.1.7
HPA	hyperphenylalaninemia
HPLC	high-pressure liquid chromatography
HSV	herpes simplex virus
hTH1−4	human TyrH isoforms 1−4
IBMX	3-isobutyl-1-methylxanthine
IC_{50}	50% inhibitory concentration
ICER	inducible cyclic AMP early repressor
K_{6MPH_4}	Michaelis constant for $6MPH_4$
K_{app}	apparent dissociation constant
K_{av}	gel filtration partition coefficient
K_d	dissociation equilibrium constant
K_I	inhibition equilibrium constant

K_{ia}	binding constant in sequential mechanism
K_{ii}	"uncompetive" inhibition constant in non-competitive inhibition expression
K_{is}	"competitive" inhibition constant in non-competitive inhibition expression
K_m	Michaelis constant
K_{O_2}	Michaelis constant for O_2
K_{phe}	Michaelis constant for L-Phe
K_{tyr}	Michaelis constant for L-Tyr
k_{cat}	catalytic rate constant
k_H/k_D	intermolecular deuterium isotope effect
LOOH	linoleic hydroperoxide; (13*S*)-hydroperoxy-9-*cis*,11-*trans*-octadecadienoic acid
lyso-PAF	dealkylated form of PAF
MBP	maltose-binding protein
MCD	magnetic circular dichroism
*m*CPBA	*meta*-chloroperbenzoic acid
MOPS	3-(*N*-morpholino)propanesulfonic acid
MTHFR	methylenetetrahydrofolate reductase, EC 1.5.1.20 and 1.7.99.5
MTX	methotrexate, amethopterin
MWC	Monod, Wyman, and Changeux
NCDC	2-nitro-4-carboxyphenyl *N*,*N*-diphenylcarbamate, an α-chymotrypsin inhibitor
NEM	*N*-ethylmaleimide
NGF	nerve growth factor
NHE	normal hydrogen electrode
L-NHA	N^G-hydroxy-L-arginine
Nle	norleucine
NMR	nuclear magnetic resonance
NOS	nitric oxide synthase, EC 1.14.13.39
NS-1, 6, and 7	antibodies that bind pterin-binding proteins
o-phen	*o*-phenanthroline; 1,10-phenanthroline
$P^{\bullet+}$	porphyrin cation radical
p35	GTPCH inhibiting protein
PAF	platelet aggregation factor
PAH	phenylalanine hydroxylase, EC 1.14.16.1
PAH^R_{L-Phe}	R-state allosteric configuration of PAH; active state of PAH
PAH^R_{L-Phe}-[L-Phe]	PAH^R_{L-Phe} with substrate present at the active site L-Phe binding site
$PAH^{act}_{\alpha-chymotrypsin}$	PAH activated by limited α-chymotrypsin cleavage
$PAH^{act}_{lysolecithin}$	PAH activated with lysolecithin
PAH^{act}_{NEM}	PAH activated with NEM
PAH^T	T-state allosteric configuration of PAH; resting state of PAH
PAH^T[L-Phe]	T-state PAH with substrate present at the active site L-Phe binding site
PC12, PC18	pheochromocytoma-derived cell lines
PCD	pterin 4a-carbinolamine dehydratase, EC 4.2.1.−
PCD/DCoH	PCD
PH-1, PH-8	aromatic amino acid reactive antibodies
PHBH	*p*-hydroxybenzoate hydroxylase, EC 1.14.13.2
PKC	protein kinase C; Ca^{2+}/phospholipid-dependent protein kinase
PKU	phenylketonuria
$^Dp/m$	isotope effect on *para vs meta* hydroxylation of L-Phe by TyrH
PNMT	phenethanolamine *N*-methyltransferase, EC 2.1.1.28
PPBS	putative pterin binding site
q-6,6-M_2PH_2	*ortho*-quinonoid 6,6'-dimethyldihydropterin; 6,6′-dimethyl-5,6-dihydropterin
q-6MPH_2	*ortho*-quinonoid 6-methyldihydropterin; 6-methyl-5,6-dihydropterin
q-BH_2	*ortho*-quinonoid dihydrobiopterin; 6-methyl-5,6-dihydrobiopterin
q-DMPH_2	*ortho*-quinonoid 6,7-dimethyldihydropterin; 6,7-dimethyl-5,6-dihydropterin
q-6MPDH_2	*ortho*-quinonoid dihydropyrimidodiazepine
q-TMPH_2	*ortho*-quinonoid 6,6′,7,7′-tetramethyldihydropterin; 6,6′,7,7′-tetramethyl-5,6-dihydropterin
q-*X*PH_2	6-*X*-substituted quinonoid dihydropterin
R	PAH^R state, catalytically active state
rPAH	recombinant PAH
S236-rPAH	Cys236 → Ser mutant of rPAH
SCN	superchiasmatic nucleus
Sol	solvento ligand
SR	sepiapterin reductase, EC 1.1.1.153
T	PAH^T state, resting state
TCB, TCBO	2,2′,5,5′-tetrachlorobiphenyl, TCB oxide
TCE	trichloroethylene
Ter	termolecular
TH1, TH2	non-human primate TyrH isoforms
THF	tetrahydrofolate
5,10-CH_2-THF	5,10-methylene-THF
$^\bullet$TMPH_3	trihydropterin radical form of 6,6′,7,7′-tetramethylpterin
TMPH_4	6,6′,7,7′-tetramethyl-5,6,7,8-tetrahydropterin
TMS	trimethylsilyl
TPP	tetraphenylporphyrin
TrpH	tryptophan hydroxylase, EC 1.14.16.4
TyrH	tyrosine hydroxylase, EC 1.14.16.2
U	units of PAH, TyrH, or TrpH; μmol L-Tyr (or appropriate product) min^{-1}
UTR	untranslated region
v	enzyme velocity
VTVF	variable-temperature, variable-field
V_{max}	maximum enzymic velocity
w.t.	wild-type
XANES	X-ray absorption near-edge spectroscopy
XAS	X-ray absorption spectroscopy
*X*PH_4	6-substituted tetrahydropterin
φ-Sepharose	Phenyl Sepharose CL-4B

VII. Acknowledgments

J.P.C. expresses his sincere appreciation to all of his students and collaborators listed as co-authors in the cited literature for their contributions to this work. The authors also gratefully acknowledge the contributions which our colleagues in the field of pterin-dependent hydroxylases have made to our thoughts in this area. We also acknowledge helpful suggestions from Professor Ross Shiman (Dept. of Biol. Chem., M.S. Hershey Medical Center, Hershey, PA) whose careful reading of this manuscript is greatly appreciated. This research has been supported by an Alfred P. Sloan Foundation fellowship (J.P.C.) and by grants from the National Institutes of Health. T.J.K. thanks the Howard Hughes Medical Institute for a predoctoral fellowship.

Note Added In Proof

Heterologously expressed human PAH has been purified to homogeneity and shown to have kinetic constants similar to native human and rat liver PAH, but with a specific activity 5 times smaller than rat liver PAH. The recombinant human PAH is partially activated and is less responsive to phosphorylation.[839] Phosphorylation has also been recently shown to increase the activity of a MBP−human PAH fusion and improve proteolytic excision of the MBP domain.[840] Radiation target analysis has been used to support a minimally dimeric configuration for the active PAH species.[841]

Recent reviews of TyrH focused on regulation have appeared.[842,843] Alternate TyrH mRNA splicing, involving skipping of exon 3 or use of an alternate splice donor in exon 2, has been detected in human pheochromocytoma cells and rat adrenal medulla.[844,845] These minor species are present at ~5% abundance, and in the human case are particularly associated with a neurodegenerative disorder.[845] Co-induction of GTPCH and TyrH activity has been detected in stimulated PC12 cells, suggesting coordinate regulation of BH_4 and TyrH in these cells.[846] Reduced levels of immunoreactive PAH and TyrH protein were found in the GTPCH-deficient *hph*-1 mouse, suggesting that deficiencies in aromatic amino acid hydroxylase levels in this strain may be due to a combination of low hydroxylase and BH_4 levels.[847] The helical content and thermal stability of pure, phosphorylated TyrH has been shown to be increased upon addition of Fe(II).[848] Theoretical support for a metal chelate origin in the catecholate iron 520 cm^{-1} Raman band has been reported.[849] An expanded study of the alternate substrate reactivity of TyrH has lent support to the proposal of a highly electrophilic oxygenating species and a cationic intermediate during catalysis.[850] Interestingly, hydroxylation of *p*-F-Phe yields only L-Tyr (35% coupled to BH_4 oxidation), in contrast to the mixture of *para*- and *meta*-halogenated tyrosines formed from other *para*-halogenated phenylalanines (11% coupled for *p*-Cl, 2.1% coupled for *p*-Br). The direct-elimination mechanism occurring with *p*-F-Phe appears to be less sensitive to substituent electronegativity than the NIH shift-generating pathway.[850] Studies examining the iron site in catecholamine-free TyrH show that the *in vitro* resting state Fe^{3+} enzyme is readily reduced by 0.5 equiv of $6MPH_4$, with *q*-$6MPH_2$ as the only detectable pterin product.[851] The presence of O_2 readily causes oxidation to the ferric state. During catalytic turnover, the iron site remains reduced although slow oxidation of the ferrous center to the ferric level is observed by catechol trapping.[851]

TrpH levels have been shown to vary in a "clock-dependent" circadian rhythm, as opposed to a melatonin-dependent manner, peaking in early night.[852] Heterologous expression of rat TrpH in human fibroblasts or as GST fusions has been reported; in both cases enzyme activity is greatly stimulated by the presence of ferrous iron.[853,854] Purified GST fusions to full-length or truncated TrpH (amino acids 99−444) have identical, iron-dependent specific activity, which is an order of magnitude higher than has been reported for native brain enzyme.[854] The demonstration of •NO inhibition of TrpH activity provides additional evidence that it is a non-heme iron-dependent enzyme.[855]

VIII. References

(1) Eisensmith, R. C.; Woo, S. L. C. *Adv. Genet.* **1995**, *32*, 199−271.
(2) Scriver, C. R.; Kaufman, S.; Eisensmith, R. C.; Woo, S. L. C. In *The Metabolic and Molecular Bases of Inherited Disease*, 7th ed.; Scriver, C. R., Beaudet, A. L., Sly, W. S., Valle, D., Eds.; McGraw-Hill: New York, 1995; Vol. I.
(3) Scriver, C. R.; Eisensmith; Woo, S. L. C.; Kaufman, S. *Annu. Rev. Genet.* **1994**, *28*, 141−165.
(4) Dix, T. A.; Benkovic, S. J. *Acc. Chem. Res.* **1988**, *21*, 101−107.
(5) Kaufman, S. In *The Enzymes*, 3rd ed.; Boyer, P. D., Krebs, E. G., Eds.; Academic Press: Orlando, FL, 1987; Vol. 18.
(6) Kaufman, S. *Adv. Enzymol. Relat. Areas Mol. Biol.* **1993**, *67*, 77−264.
(7) Hufton, S. E.; Jennings, I. G.; Cotton, R. G. H. *Biochem. J.* **1995**, *311*, 353−366.
(8) Blakely, R. L.; Benkovic, S. J. *Chemistry and Biochemistry of Pterins*; Wiley and Sons: New York, 1985.
(9) Lovenberg, W.; Levine, R. A. *Unconjugated pterins in neurobiology*; Taylor & Francis, Ltd.: Philadelphia, 1987.
(10) Ayling, J. E.; Nair, M. G.; Baugh, C. M. *Chemistry and Biology of Pteridines and Folates*; Plenum: New York, 1993.
(11) Curtius, H.-C.; Pfleiderer, W.; Wachter, H. *Biochemical and Clinical Aspects of Pteridines*; W. de Gruyter: Berlin, 1983.
(12) Kisliuk, R. L.; Brown, G. M. *Chemistry and Biology of Pteridines*; Elsevier and North-Holland: Amsterdam, 1979.
(13) Kaufman, S. *Metabolism of Aromatic Amino Acids and Amines*; Academic Press: New York, 1987.
(14) Garrod, A. E. *Inborn Errors of Metabolism*, 2nd ed.; Henry Frowde and Hodder & Stoughton: London, 1923.
(15) Fölling, A. *Z. Physiol. Chem.* **1934**, *277*, 169−176.
(16) Knappskog, P. M.; Flatmark, T.; Mallet, J.; Lüdecke, B.; Bartholomé, K. *Hum. Mol. Genet.* **1995**, *4*, 1209−1212.
(17) Udenfriend, S.; Cooper, J. R. *J. Biol. Chem.* **1952**, *194*, 503−511.
(18) Kaufman, S. *J. Biol. Chem.* **1957**, *226*, 511−524.
(19) Kaufman, S. *J. Biol. Chem.* **1959**, *234*, 2677−2682.
(20) Kaufman, S. *Proc. Natl. Acad. Sci. U.S.A.* **1963**, *50*, 1085−1093.
(21) Kaufman, S.; Bridgers, W. F.; Eisenberg, G. *Biochem. Biophys. Res. Commun.* **1962**, *9*, 497−502.
(22) Brenneman, A. R.; Kaufman, S. *Biochem. Biophys. Res. Commun.* **1964**, *17*, 177−183.
(23) Nagatsu, T.; Levitt, M.; Udenfriend, S. *J. Biol. Chem.* **1964**, *239*, 2910−2917.
(24) Kaufman, S. *Trans. N. Y. Acad. Sci.* **1964**, *26*, 977−983.
(25) Grahame-Smith, D. G. *Biochem. Biophys. Res. Commun.* **1964**, *16*, 586−592.
(26) Lovenberg, W.; Jequier, E.; Sjoerdsma, A. *Science* **1967**, *155*, 217−219.
(27) Shiman, R.; Mortimore, G. E.; Schworer, C. M.; Gray, D. W. *J. Biol. Chem.* **1982**, 11213−11216.
(28) Donlon, J.; Kaufman, S. *J. Biol. Chem.* **1978**, *253*, 6657−6659.
(29) American Academy of Pediatrics *Pediatrics* **1989**, *83*, 461−462.
(30) Bauman, M. L.; Kemper, T. L. *Acta Neuropathol. (Berl.)* **1982**, *58*, 55−63.
(31) Waisbren, S. E.; Levy, H. L. *J. Inherited Metab. Dis.* **1991**, *14*, 755−764.
(32) Hommes, F. A. *Biochem. Med. Metab. Biol.* **1991**, *46*, 277−287.
(33) Shedlovsky, A.; McDonald, J. D.; Symula, D.; Dove, W. F. *Genetics* **1993**, *134*, 1205−1210.
(34) Tourian, A.; Goddard, J.; Puck, T. T. *J. Cell. Physiol.* **1969**, *73*, 159−170.
(35) Mercer, J. F.; Grimes, A.; Jennings, I.; Cotton, R. G. H. *Biochem. J.* **1984**, *219*, 891−898.
(36) McGee, M. M.; Greengard, O.; Knox, W. E. *Biochem. J.* **1972**, *127*, 669−674.
(37) Ayling, J. E.; Pirson, W. D.; al-Janabi, J. M.; Helfand, G. D. *Biochemistry* **1974**, *13*, 78−85.
(38) Ayling, J. E.; Helfand, G. D.; Pirson, W. D. *Enzyme* **1975**, *20*, 6−19.
(39) Berry, H. K.; Cripps, R.; Nicholls, K.; McCandless, D.; Harper, C. *Biochim. Biophys. Acta* **1971**, *261*, 315−320.
(40) Murthy, L. I.; Berry, H. K. *Arch. Biochem. Biophys.* **1974**, *163*, 225−230.
(41) Robson, K. J.; Chandra, T.; MacGillivray, R. T.; Woo, S. L. C. *Proc. Natl. Acad. Sci. U.S.A.* **1982**, *79*, 4701−4705.
(42) Rao, D. N.; Kaufman, S. *J. Biol. Chem.* **1986**, *261*, 8866−8876.
(43) Richardson, S. C.; Fisher, M. J. *Int. J. Biochem.* **1993**, *25*, 581−588.
(44) Richardson, S. C.; Aspbury, R. A.; Fisher, M. J. *Biochem. J.* **1993**, *292*, 419−424.
(45) Schallreuter, K. U.; Wood, J. M.; Ziegler, I.; Lemke, K. R.; Pittelkow, M. R.; Lindsey, N. J.; Gütlich, M. *Biochim. Biophys. Acta* **1994**, *1226*, 181−192.
(46) McDonald, J. D. *Acta Paediatr. Suppl.* **1994**, *407*, 122−123.
(47) Katz, I. R.; Yamauchi, T.; Kaufman, S. *Biochim. Biophys. Acta* **1976**, *429*, 84−95.
(48) Kato, T.; Oka, K.; Nagatsu, T.; Sugimoto, T.; Matsuura, S. *Biochim. Biophys. Acta* **1980**, *612*, 226−232.
(49) Shiman, R.; Akino, M.; Kaufman, S. *J. Biol. Chem.* **1971**, *246*, 1330−1340.
(50) Lidsky, A. S.; Law, M. L.; Morse, H. G.; Kao, F.-T.; Rabin, M.; Ruddle, F. H.; Woo, S. L. C. *Proc. Natl. Acad. Sci. U.S.A.* **1985**, *82*, 6221−6225.
(51) Lidksy, A. S.; Robson, K. J. H.; Thirumalachary, C.; Barker, P. E.; Ruddle, F. H.; Woo, S. L. C. *Am. J. Hum. Genet.* **1984**, *36*, 527−533.
(52) Shiman, R.; Jefferson, L. S. *J. Biol. Chem.* **1982**, *257*, 839−844.
(53) Shiman, R. *J. Biol. Chem.* **1980**, *255*, 10029−10032.
(54) Nakata, H.; Fujisawa, H. *Biochim. Biophys. Acta* **1980**, *614*, 313−327.
(55) Shiman, R.; Gray, D. W.; Pater, A. *J. Biol. Chem.* **1979**, *254*, 11300−11306.
(56) Abita, J. P.; Blandin-Savoja, F.; Rey, F. *Methods Enzymol.* **1987**, *142*, 27−35.

(57) Døskeland, A.; Ljones, T.; Skotland, T.; Flatmark, T. *Neurochem. Res.* **1982**, *7*, 407−421.
(58) Shiman, R.; Jones, S. H.; Gray, D. W. *J. Biol. Chem.* **1990**, *265*, 11633−11642.
(59) Citron, B. A.; Davis, M. D.; Kaufman, S. *Protein Expression Purif.* **1992**, *3*, 93−100.
(60) Gibbs, B. S.; Wojchowski, D.; Benkovic, S. J. *J. Biol. Chem.* **1993**, *268*, 8046−8052.
(61) Kappock, T. J.; Harkins, P. C.; Friedenberg, S.; Caradonna, J. P. *J. Biol. Chem.* **1995**, 30532−30544.
(62) Choo, K. H.; Jennings, I. G.; Cotton, R. G. H. *Biochem. J.* **1981**, *199*, 527−535.
(63) Cotton, R. G. H.; Grattan, P. J. *Eur. J. Biochem.* **1975**, *60*, 427−30.
(64) Shiman, R. *Methods Enzymol.* **1987**, *142*, 17−27.
(65) Kaufman, S.; Fisher, D. B. *J. Biol. Chem.* **1970**, *245*, 4745−4750.
(66) Cotton, R. G. H. *FEBS Lett.* **1974**, *44*, 290−292.
(67) Kaufman, S. *Methods Enzymol.* **1987**, *142*, 3−17.
(68) Yamashita, M.; Minato, S.; Arai, M.; Kishida, Y.; Nagatsu, T.; Umezawa, H. *Biochem. Biophys. Res. Commun.* **1985**, *133*, 202−207.
(69) Al-Janabi, J. M. *Arch. Biochem. Biophys.* **1980**, *200*, 603−608.
(70) Miller, M. R.; McClure, D.; Shiman, R. *J. Biol. Chem.* **1975**, *250*, 1132−1140.
(71) Nielsen, K. H. *Eur. J. Biochem.* **1969**, *7*, 360−369.
(72) Blair, J. A.; Pearson, A. J. *J. Chem. Soc., Perkin Trans. 2* **1974**, 80−88.
(73) Ayling, J.; Pirson, R.; Pirson, W.; Boehm, G. *Anal. Biochem.* **1973**, *51*, 80−90.
(74) Bailey, S. W.; Ayling, J. E. *Anal. Biochem.* **1980**, *107*, 156−164.
(75) Kaufman, S. *Adv. Enzymol. Relat. Areas Mol. Biol.* **1971**, *35*, 245−319.
(76) Shiman, R. In *Chemistry and Biochemistry of Pterins*; Blakely, R. L., Benkovic, S. J., Eds.; Wiley and Sons: New York, 1985; Vol. 2.
(77) Iwaki, M.; Phillips, R. S.; Kaufman, S. *J. Biol. Chem.* **1986**, *261*, 2051−2056.
(78) Celikel, R.; Davis, M. D.; Dai, X. P.; Kaufman, S.; Xuong, N. H. *J. Mol. Biol.* **1991**, *218*, 495−498.
(79) Jennings, I. G.; Russell, R. G.; Armarego, W. L.; Cotton, R. G. H. *Biochem. J.* **1986**, *235*, 133−138.
(80) Shiman, R.; Gray, D. W. *J. Biol. Chem.* **1980**, *255*, 4793−4800.
(81) Parniak, M. A.; Jennings, I. G.; Cotton, R. G. H. *Biochem. J.* **1989**, *257*, 383−388.
(82) Haan, E. A.; Jennings, I. G.; Cuello, A. C.; Nakata, H.; Fujisawa, H.; Chow, C. W.; Kushinsky, R.; Brittingham, J.; Cotton, R. G. H. *Brain Res.* **1987**, *426*, 19−27.
(83) Cotton, R. G. H.; McAdam, W.; Jennings, I.; Morgan, F. J. *Biochem. J.* **1988**, *255*, 193−196.
(84) Jerne, N. K. *Ann. Immunol.* **1974**, 373−389.
(85) Cleveland, W. L.; Wassermann, N. H.; Sarangarajan, R.; Penn, A. S.; Erlanger, B. F. *Nature* **1983**, *305*, 56−57.
(86) Ratnam, S.; Ratnam, M.; Cotton, R. G. H.; Jennings, I. G.; Freisheim, J. H. *Arch. Biochem. Biophys.* **1989**, *275*, 344−353.
(87) Jennings, I.; Cotton, R. *J. Biol. Chem.* **1990**, *265*, 1885−1889.
(88) Jennings, I. G.; Kemp, B. E.; Cotton, R. G. H. *Proc. Natl. Acad. Sci. U.S.A.* **1991**, *88*, 5734−5738.
(89) Cotton, R. G. H.; Howells, D. W.; Saleeba, J. A.; Dianzani, I.; Smooker, P. M.; Jennings, I. G. *Adv. Exp. Med. Biol.* **1993**, *338*, 55−57.
(90) Silverman, R. B. *Methods Enzymol.* **1995**, *249*, 240−283.
(91) Brunner, J. *Annu. Rev. Biochem.* **1993**, *62*, 483−514.
(92) Fitzpatrick, P. F.; Ghisla, S.; Massey, V. *J. Biol. Chem.* **1985**, *260*, 8483−8491.
(93) Gibbs, B. S.; Benkovic, S. J. *Biochemistry* **1991**, *30*, 6795−6802.
(94) Varughese, K. I.; Xuong, N. H.; Kiefer, P. M.; Matthews, D. A.; Whiteley, J. M. *Proc. Natl. Acad. Sci. U.S.A.* **1994**, *91*, 5582−5586.
(95) Endrizzi, J. A.; Cronk, J. D.; Wang, W.; Crabtree, G. R.; Alber, T. *Science* **1995**, *268*, 1421.
(96) Ficner, R.; Sauer, U. H.; Siter, C.; Suck, D. *EMBO J.* **1995**, *14*, 2034−2042.
(97) Daubner, S. C.; Fitzpatrick, P. F. *Arch. Biochem. Biophys.* **1993**, *302*, 455−460.
(98) Dickson, P. W.; Jennings, I. G.; Cotton, R. G. H. *J. Biol. Chem.* **1994**, *269*, 20369−20375.
(99) Okano, Y.; Eisensmith, R. C.; Guttler, F.; Lichter-Konecki, U.; Konecki, D. S.; Trefz, F. K.; Dasovich, M.; Wang, T.; Henriksen, K.; Lou, H.; Woo, S. L. C. *N. Engl. J. Med.* **1991**, *324*, 1232−1238.
(100) Monod, J.; Wyman, J.; Changeux, J.-P. *J. Mol. Biol.* **1965**, *12*, 88−118.
(101) Koshland, D. E., Jr.; Némethy, G.; Filmer, D. *Biochemistry* **1965**, *5*, 365−385.
(102) Fisher, D. B.; Kaufman, S. *J. Biol. Chem.* **1973**, *248*, 4345−4353.
(103) DiLella, A. G.; Kwok, S. C.; Ledley, F. D.; Marvit, J.; Woo, S. L. *Biochemistry* **1986**, *25*, 743−749.
(104) O'Malley, K. L.; Anhalt, M. J.; Martin, B. M.; Kelsoe, J. R.; Winfield, S. L.; Ginns, E. I. *Biochemistry* **1987**, *26*, 2910−2914.
(105) Boularand, S.; Darmon, M. C.; Mallet, J. *J. Biol. Chem.* **1995**, *270*, 3748−3756.
(106) Phillips, R. S.; Parniak, M. A.; Kaufman, S. *Biochemistry* **1984**, *23*, 3836−3842.
(107) Knappskog, P. M.; Haavik, J. *Biochemistry* **1995**, *34*, 11790−11799.
(108) Parniak, M.; Hasegawa, H.; Wilgus, H.; Kaufman, S. *Biochem. Biophys. Res. Commun.* **1981**, *99*, 707−714.
(109) Parniak, M. A.; Davis, M. D.; Kaufman, S. *J. Biol. Chem.* **1988**, *263*, 1223−1230.
(110) Abita, J. P.; Parniak, M.; Kaufman, S. *J. Biol. Chem.* **1984**, *259*, 14560−14566.
(111) Fisher, D. B.; Kaufman, S. *J. Biol. Chem.* **1972**, *247*, 2250−2252.
(112) Sullivan, P. T.; Kester, M.; Norton, S. J. *Fed. Proc.* **1971**, 1067.
(113) Phillips, R. S.; Iwaki, M.; Kaufman, S. *Biochem. Biophys. Res. Commun.* **1983**, *110*, 919−925.
(114) Parniak, M. A.; Kaufman, S. *J. Biol. Chem.* **1981**, *256*, 6876−6882.
(115) Martínez, A.; Haavik, J.; Flatmark, T. *Eur. J. Biochem.* **1990**, *193*, 211−219.
(116) Shiman, R.; Gray, D. W.; Hill, M. A. *J. Biol. Chem.* **1994**, *269*, 24637−24646.
(117) Shiman, R.; Xia, T.; Hill, M. A.; Gray, D. W. *J. Biol. Chem.* **1994**, *269*, 24647−24656.
(118) Xia, T.; Gray, D. W.; Shiman, R. *J. Biol. Chem.* **1994**, *269*, 24657−24665.
(119) Mitnaul, L. J.; Shiman, R. *Proc. Natl. Acad. Sci. U.S.A.* **1995**, *92*, 885−889.
(120) Døskeland, A. P.; Døskeland, S. O.; Øgreid, D.; Flatmark, T. *J. Biol. Chem.* **1984**, *259*, 11242−11248.
(121) Kowlessur, D.; Yang, X. J.; Kaufman, S. *Proc. Natl. Acad. Sci. U.S.A.* **1995**, *92*, 4743−4747.
(122) Knappskog, M.; Eiken, H. G.; Martinez, A.; Olafsdottir, S.; Haavik, J.; Flatmark, T.; Apold, J. *Adv. Expr. Med. Biol.* **1993**, *338*, 59−62.
(123) Wretborn, M.; Humble, E.; Ragnarsson, U.; Engström, L. *Biochem. Biophys. Res. Commun.* **1980**, *93*, 403−408.
(124) Abita, J. P.; Milstien, S.; Chang, N.; Kaufman, S. *J. Biol. Chem.* **1976**, *251*, 5310−5314.
(125) Barranger, J. A.; Geiger, P. J.; Huzino, A.; Bessman, S. P. *Science* **1972**, *175*, 903−905.
(126) Donlon, J.; Kaufman, S. *J. Biol. Chem.* **1980**, *255*, 2146−2152.
(127) Kaufman, S. *Enzyme* **1987**, *38*, 286−295.
(128) Fisher, M. J.; Pogson, C. I. *Biochem. J.* **1984**, *219*, 79−85.
(129) Phillips, R. S.; Kaufman, S. *J. Biol. Chem.* **1984**, *259*, 2474−2479.
(130) Bailey, S. W.; Ayling, J. E. *J. Biol. Chem.* **1978**, *253*, 1598−1605.
(131) Citron, B. A.; Davis, M. D.; Kaufman, S. *Biochem. Biophys. Res. Commun.* **1994**, *198*, 174−180.
(132) Tipper, J.; Kaufman, S. *J. Biol. Chem.* **1992**, *267*, 889−896.
(133) Marota, J. J.; Shiman, R. *Biochemistry* **1984**, *23*, 1303−1311.
(134) Omura, T.; Sato, R. *J. Biol. Chem.* **1964**, *239*, 2370−2378.
(135) Omura, T.; Sato, R. *J. Biol. Chem.* **1964**, *239*, 2379−2385.
(136) Ainscough, E. W.; Brodie, A. M.; Plowman, J. E.; Brown, K. L.; Addison, A. W.; Gainsford, A. R. *Inorg. Chem.* **1980**, *19*, 3655−3663.
(137) Maelia, L. E.; Millar, M. M.; Koch, S. A. *Inorg. Chem.* **1992**, *31*, 4594−4600.
(138) Cox, D. D.; Benkovic, S. J.; Bloom, L. M.; Bradley, F. C.; Nelson, M. J.; Que, L. J.; Wallick, D. E. *J. Am. Chem. Soc.* **1988**, *110*, 2026−2032.
(139) Que, L., Jr. *Coord. Chem. Rev.* **1983**, *50*, 73−108.
(140) Fisher, D. B.; Kirkwood, R.; Kaufman, S. *J. Biol. Chem.* **1972**, *247*, 5161−5167.
(141) Letendre, C. H.; Dickens, G.; Guroff, G. *J. Biol. Chem.* **1975**, *250*, 6672−6678.
(142) Guroff, G.; Rhoads, C. A. *J. Biol. Chem.* **1967**, *242*, 3641−3645.
(143) Zhao, G.; Xia, T.; Song, J.; Jensen, R. A. *Proc. Natl. Acad. Sci. U.S.A.* **1994**, *91*, 1366−1370.
(144) Gottschall, D. W.; Dietrich, R. F.; Benkovic, S. J.; Shiman, R. *J. Biol. Chem.* **1982**, *257*, 845−849.
(145) Klausner, R. D.; Rouault, T. A.; Harford, J. B. *Cell* **1993**, *72*, 19−28.
(146) Wallick, D. E.; Bloom, L. M.; Gaffney, B. J.; Benkovic, S. J. *Biochemistry* **1984**, *23*, 1295−1302.
(147) Yang, A.-S.; Gaffney, B. J. *Biophys. J.* **1987**, *51*, 55−67.
(148) Gaffney, B. J.; Mavrophilipos, D. V.; Doctor, K. S. *Biophys. J.* **1993**, *64*, 773−783.
(149) Glasfeld, E.; Xia, Y. M.; Debrunner, P. G.; Caradonna, J. P. *Eur. J. Biochem.* **1996**, submitted for publication.
(150) Good, N. E.; Izawa, S. *Methods Enzymol.* **1972**, *24*, 53−68.
(151) Fisher, B. E.; Häring, U. K.; Tribolet, R.; Sigel, H. *Eur. J. Biochem.* **1979**, *94*, 523−530.
(152) Hanlon, D. P.; Watt, D. S.; Westhead, E. W. *Anal. Biochem.* **1966**, *16*, 225−233.
(153) Hansen, S.; Hansen, L. K.; Hough, E. *J. Mol. Biol.* **1993**, *231*, 870−876.
(154) Benkovic, S.; Wallick, D.; Bloom, L.; Gaffney, B. J.; Domanico, P.; Dix, T.; Pember, S. *Biochem. Soc. Trans.* **1985**, *13*, 436−438.
(155) Kappock, T. J. Ph.D. Thesis, Yale University, 1996.
(156) Glasfeld, E. Ph.D. Thesis, Yale University, 1994.
(157) Bloom, L. M.; Benkovic, S. J.; Gaffney, B. J. *Biochemistry* **1986**, *25*, 4204−4210.

(158) Debrunner, P. G. In *EMR of Paramagnetic Molecules*; Berliner, L. J., Ruben, J., Eds.; Plenum Press: New York, 1993; Vol. 13.
(159) Trautwein, A. X.; Bill, E.; Bominaar, E. L.; Winkler, H. In *Structure and Bonding*; Springer Verlag: Berlin, 1991; Vol. 78.
(160) Kasibhatla, B. T. S.; Loeb, K.; Westre, T. E.; Hedman, B.; Hodgson, K. O.; Solomon, E. I.; Debrunner, P. G.; Caradonna, J. P. *J. Am. Chem. Soc.* **1996**, manuscript in preparation.
(161) Solomon, E. I.; Pavel, E. G.; Loeb, K. E.; Campochiaro, C. *Coord. Chem. Rev.* **1995**, *144*, 369−460.
(162) Loeb, K. E.; Westre, T. E.; Kappock, T. J.; Mitic, N.; Glasfeld, E.; Caradonna, J. P.; Hedman, B.; Hodgson, K. O.; Solomon, E. I. *J. Am. Chem. Soc.* **1996**, submitted for publication.
(163) Burkard, W. P.; Gey, K. F.; Pletscher, A. *Life Sci.* **1964**, *3*, 27−33.
(164) Andersson, K. K.; Cox, D. D.; Que, L., Jr.; Flatmark, T.; Haavik, J. *J. Biol. Chem.* **1988**, *263*, 18621−18626.
(165) Michaud-Soret, I.; Andersson, K. K.; Que, L., Jr. *Biochemistry* **1995**, *34*, 5504−5510.
(166) Enemark, J. H.; Feltham, R. D. *Coord. Chem. Rev.* **1974**, *13*, 339−406.
(167) Petrouleas, V.; Diner, B. *Biochim. Biophys. Acta* **1990**, *1015*, 131−140.
(168) Dix, T. A.; Benkovic, S. J. *Biochemistry* **1985**, *24*, 5839−5846.
(169) Lazarus, R. A.; Dietrich, R. F.; Wallick, D. E.; Benkovic, S. J. *Biochemistry* **1981**, *20*, 6834−6841.
(170) Hill, M. A.; Marota, J. J. A.; Shiman, R. *J. Biol. Chem.* **1988**, *263*, 5646−5655.
(171) Kappock, T. J.; Caradonna, J. P. *Biochemistry* **1996**, submitted for publication.
(172) Eberlein, G.; Bruice, T. C.; Lazarus, R. A.; Henrie, R.; Benkovic, S. J. *J. Am. Chem. Soc.* **1984**, *106*, 7916−7924.
(173) Neckameyer, W. S.; White, K. *J. Biol. Chem.* **1992**, *267*, 4199−4206.
(174) Morales, G.; Requena, J. M.; Jimenez-Ruiz, A.; Lopez, M. C.; Ugarte, M.; Alonso, C. *Gene* **1990**, *93*, 213−219.
(175) Neckameyer, W. S.; White, K. *J. Neurogenet.* **1993**, *8*, 189−199.
(176) Mitoma, C.; Leeper, L. C. *Fed. Proc.* **1954**, *13*, 266.
(177) Guroff, G.; Rhoads, C. A. *J. Biol. Chem.* **1969**, *244*, 142−146.
(178) Berry, A.; Johnson, J. L.; Jensen, R. A. *Arch. Microbiol.* **1985**, *141*, 32−39.
(179) Letendre, C. H.; Dickens, G.; Guroff, G. *J. Biol. Chem.* **1974**, *249*, 7186−7191.
(180) Fujisawa, H.; Nakata, H. *Methods Enzymol.* **1987**, *142*, 44−49.
(181) Pember, S. O.; Villafranca, J. J.; Benkovic, S. J. *Biochemistry* **1986**, *25*, 6611−6619.
(182) Pember, S. O.; Benkovic, S. J.; Villafranca, J. J.; Pasenkiewicz-Gierula, M.; Antholine, W. E. *Biochemistry* **1987**, *26*, 4477−4483.
(183) Pember, S. O.; Johnson, K. A.; Villafranca, J. J.; Benkovic, S. J. *Biochemistry* **1989**, *28*, 2124−2130.
(184) Fitzpatrick, P. F. *Biochemistry* **1991**, *30*, 3658−3662.
(185) Onishi, A.; Liotta, L. J.; Benkovic, S. J. *J. Biol. Chem.* **1991**, *266*, 18454−18459.
(186) Balasubramanian, S.; Carr, R. T.; Bender, C. J.; Peisach, J.; Benkovic, S. J. *Biochemistry* **1994**, *33*, 8532−8537.
(187) Balasubramanian, S.; Carr, R. T.; Bender, C. J.; Peisach, J.; Benkovic, S. J. *Adv. Exp. Med. Biol.* **1993**, *338*, 67−70.
(188) Carr, R. T.; Benkovic, S. J. *Biochemistry* **1993**, *32*, 14132−14138.
(189) Pember, S. O.; Villafranca, J. J.; Benkovic, S. J. *Methods Enzymol.* **1987**, *142*, 50−56.
(190) Cambi, F.; Fung, B.; Chikaraishi, D. *J. Neurochem.* **1989**, *53*, 1656−1659.
(191) Blaschko, H. J. *J. Physiol.* **1939**, *96*, 50P−51P.
(192) Greene, L. A.; Tischler, A. S. *Proc. Natl. Acad. Sci. U.S.A.* **1976**, *73*, 2424−2428.
(193) Bartholomé, K. *Acta Paediatr. Scand.* **1983**, *72*, 921−922.
(194) Hirsch, E.; Graybiel, A. M.; Agid, Y. A. *Nature* **1988**, *334*, 345−348.
(195) Yahr, M. D.; Duvoisin, R. C.; Schear, M. J.; Barrett, R. E.; Hoehn, M. M. *Arch. Neurol.* **1969**, *21*, 343−354.
(196) Leboyer, M.; Malafosse, A.; Boularand, S.; Campion, D.; Gheysen, F.; Samolyk, D.; Henriksson, B.; Denise, E.; des Lauriers, A.; Lepine, J. P.; Zarifian, E.; Clerget-Darpoux, F.; Mallet, J. *Lancet* **1990**, *335*, 1219.
(197) Meloni, R.; Leboyer, M.; Bellivier, F.; Barbe, B.; Samolyk, D.; Allilaire, J. F.; Mallet, J. *Lancet* **1995**, *345*, 932.
(198) Meloni, R.; Laurent, C.; Campion, D.; Benhadjali, B.; Thibaut, F.; Dollfus, S.; Petit, M.; Samolyk, D.; Martinez, M.; Poirier, M. F.; Mallet, J. *C. R. Acad. Sci. Paris, Sciences de la Vie/Life Sciences* **1995**, *318*, 803−809.
(199) Korner, J.; Fritze, J.; Propping, P. *Psychiatry Res.* **1990**, *32*, 275−280.
(200) Inayama, Y.; Yoneda, H.; Sakai, T.; Ishida, T.; Kobayashi, S.; Nonomura, Y.; Kono, Y.; Koh, J.; Asaba, H. *Am. J. Med. Genet.* **1993**, *48*, 87−89.
(201) Byerley, W.; Plaetke, R.; Hoff, M.; Jensen, S.; Holik, J.; Reimherr, F.; Mellon, C.; Wender, P.; O'Connell, P.; Leppert, M. *Hum. Hered.* **1992**, *42*, 259−263.
(202) Comings, D. E.; Gade, R.; Muhleman, D.; Sverd, J. *Biol. Psychiat.* **1995**, *37*, 484−486.
(203) Ichinose, H.; Ohye, T.; Takahashi, E.; Seki, N.; Hori, T.; Segawa, M.; Nomura, Y.; Endo, K.; Tanaka, H.; Tsuji, S.; Fujita, K.; Nagatsu, T. *Nature Genet.* **1994**, *8*, 236−242.
(204) Zhou, Q. Y.; Quaife, C. J.; Palmiter, R. D. *Nature* **1995**, *374*, 640−643.
(205) Kobayashi, K.; Morita, S.; Sawada, H.; Mizuguchi, T.; Yamada, K.; Nagatsu, I.; Hata, T.; Watanabe, Y.; Fujita, K.; Nagatsu, T. *J. Biol. Chem.* **1995**, *270*, 27235−27243.
(206) Okuno, S.; Fujisawa, H. *Eur. J. Biochem.* **1982**, *122*, 49−55.
(207) Waymire, J. C.; Bjur, R.; Weiner, N. *Anal. Biochem.* **1971**, *43*, 588−600.
(208) Okuno, S.; Fujisawa, H. *Anal. Biochem.* **1983**, *129*, 405−411.
(209) Bailey, S. W.; Dillard, S. B.; Thomas, K. B.; Ayling, J. E. *Biochemistry* **1989**, *28*, 494−504.
(210) Haavik, J.; Flatmark, T. *J. Chromatogr.* **1980**, *198*, 511−515.
(211) Nagatsu, T.; Oka, K.; Kato, T. *J. Chromatogr.* **1979**, *163*, 247−252.
(212) Philipp, E. *J. Chromatogr.* **1987**, *419*, 27−36.
(213) Naoi, M.; Takahashi, T.; Nagatsu, T. *J. Chromatogr.* **1988**, *427*, 229−238.
(214) Kuczenski, R. T.; Mandell, A. J. *J. Biol. Chem.* **1972**, *247*, 3114−3122.
(215) Craig, S. P.; Buckle, V. J.; Lamouroux, A.; Mallet, J.; Craig, I. *Cytogenet. Cell Genet.* **1986**, *42*, 29−32.
(216) Grima, B.; Lamouroux, A.; Blanot, F.; Biguet, N. F.; Mallet, J. *Proc. Natl. Acad. Sci. U.S.A.* **1985**, *82*, 617−621.
(217) Ichikawa, S.; Sasaoka, T.; Nagatsu, T. *Biochem. Biophys. Res. Commun.* **1991**, *176*, 1610−1616.
(218) D'Mello, S. R.; Weisberg, E. P.; Stachowiak, M. K.; Turzai, L. M.; Gioio, A. E.; Kaplan, B. B. *J. Neurosci. Res.* **1988**, *19*, 440−449.
(219) Ichikawa, S.; Ichinose, H.; Nagatsu, T. *Biochem. Biophys. Res. Commun.* **1990**, *173*, 1331−1336.
(220) Ichinose, H.; Ohye, T.; Fujita, K.; Yoshida, M.; Ueda, S.; Nagatsu, T. *Biochem. Biophys. Res. Commun.* **1993**, *195*, 158−165.
(221) Kaneda, N.; Kobayashi, K.; Ichinose, H.; Kishi, F.; Nakazawa, A.; Kurosawa, Y.; Fujita, K.; Nagatsu, T. *Biochem. Biophys. Res. Commun.* **1987**, *146*, 971−975.
(222) Grima, B.; Lamouroux, A.; Boni, C.; Julien, J. F.; Javoy-Agid, F.; Mallet, J. *Nature* **1987**, *326*, 707−711.
(223) Kobayashi, K.; Kaneda, N.; Ichinose, H.; Kishi, F.; Nakazawa, A.; Kurosawa, Y.; Fujita, K.; Nagatsu, T. *Nucleic Acids Res.* **1987**, *15*, 6733.
(224) Mogi, M.; Harada, M.; Kiuchi, K.; Kojima, K.; Kondo, T.; Narabayashi, H.; Rausch, D.; Riederer, P.; Jellinger, K.; Nagatsu, T. *J. Neural Transm.* **1988**, *72*, 77−82.
(225) Le Bourdellès, B.; Boularand, S.; Boni, C.; Horellou, P.; Dumas, S.; Grima, B.; Mallet, J. *J. Neurochem.* **1988**, *50*, 988−991.
(226) Coker, G. T., III; Studelska, D.; Harmon, S.; Burke, W.; O'Malley, K. L. *Mol. Brain Res.* **1990**, *8*, 93−98.
(227) Haycock, J. W. *J. Neurochem.* **1991**, *56*, 2139−2142.
(228) Lewis, D. A.; Melchitzky, D. S.; Haycock, J. W. *Neuroscience* **1993**, *54*, 477−492.
(229) Kaneda, N.; Sasaoka, T.; Kobayashi, K.; Kiuchi, K.; Nagatsu, I.; Kurosawa, Y.; Fujita, K.; Yokoyama, M.; Nomura, T.; Katsuki, M.; Nagatsu, T. *Neuron* **1991**, *6*, 583−594.
(230) During, M. J.; Naegele, J. R.; O'Malley, K. L.; Geller, A. I. *Science* **1994**, *266*, 1399−1403.
(231) Icard-Liepkalns, C.; Faucon Biguet, N.; Vyas, S.; Robert, J. J.; Sassone-Corsi, P.; Mallet, J. *J. Neurosci. Res.* **1992**, *32*, 290−298.
(232) Campbell, D. G.; Hardie, D. G.; Vulliet, P. R. *J. Biol. Chem.* **1986**, *261*, 10489−10492.
(233) Haycock, J. W.; Bennett, W. F.; George, R. J.; Waymire, J. C. *J. Biol. Chem.* **1982**, *257*, 13699−13703.
(234) Zigmond, R. E.; Schwarzchild, M. A.; Rittenhouse, A. R. *Annu. Rev. Neurosci.* **1989**, *12*, 415−461.
(235) Le Bourdellès, B.; Horellou, P.; Le Caer, J. P.; Denèfle, P.; Latta, M.; Haavik, J.; Guibert, B.; Mayaux, J. F.; Mallet, J. *J. Biol. Chem.* **1991**, *266*, 17124−17130.
(236) Ginns, E. I.; Rehavi, M.; Martin, B. M.; Weller, M.; O'Malley, K. L.; LaMarca, M. E.; McAllister, C. G.; Paul, S. M. *J. Biol. Chem.* **1988**, *263*, 7406−7410.
(237) Horellou, P.; Guibert, B.; Leviel, V.; Mallet, J. *FEBS Lett.* **1986**, *205*, 6−10.
(238) Horellou, P.; Le Bourdellès, B.; Clot-Humbert, J.; Guibert, B.; Leviel, V.; Mallet, J. *J. Neurochem.* **1988**, *51*, 652−655.
(239) Kobayashi, K.; Kiuchi, K.; Ishii, A.; Kaneda, N.; Kurosawa, Y.; Fujita, K.; Nagatsu, T. *FEBS Lett.* **1988**, *238*, 431−434.
(240) Nasrin, S.; Ichinose, H.; Hidaka, H.; Nagatsu, T. *J. Biochem. (Tokyo)* **1994**, *116*, 393−398.
(241) Haavik, J.; Le Bourdelles, B.; Martinez, A.; Flatmark, T.; Mallet, J. *Eur. J. Biochem.* **1991**, *199*, 371−378.
(242) Wu, J.; Filer, D.; Friedhoff, A. J.; Goldstein, M. *J. Biol. Chem.* **1992**, *267*, 25754−25758.
(243) Wang, Y. H.; Citron, B. A.; Ribeiro, P.; Kaufman, S. *Proc. Natl. Acad. Sci. U.S.A.* **1991**, *88*, 8779−8783.
(244) Daubner, S. C.; Lauriano, C.; Haycock, J. W.; Fitzpatrick, P. F. *J. Biol. Chem.* **1992**, *267*, 12639−12646.
(245) Fitzpatrick, P. F.; Chlumsky, L. J.; Daubner, S. C.; O'Malley, K. L. *J. Biol. Chem.* **1990**, *265*, 2042−2047.

(246) Haavik, J.; Andersson, K. K.; Petersson, L.; Flatmark, T. *Biochim. Biophys. Acta* **1988**, *953*, 142−156.
(247) Fitzpatrick, P. F. *Biochemistry* **1991**, *30*, 6386−6391.
(248) Walker, S. J.; Liu, X.; Roskoski, R.; Vrana, K. E. *Biochim. Biophys. Acta* **1994**, *1206*, 113−119.
(249) Kaufman, S. In *Chemistry and Biochemistry of Pterins*; Blakely, R. L., Benkovic, S. J., Eds.; Wiley and Sons: New York, 1985; Vol. 2.
(250) Petrack, B.; Sheppy, F.; Fetzer, V. *J. Biol. Chem.* **1968**, *243*, 743−748.
(251) Daubner, S. C.; Lohse, D. L.; Fitzpatrick, P. F. *Protein Sci.* **1993**, *2*, 1452−1460.
(252) Grenett, H. E.; Ledley, F. D.; Reed, L. L.; Woo, S. L. C. *Proc. Natl. Acad. Sci. U.S.A.* **1987**, *84*, 5530−5534.
(253) Gahn, L. G.; Roskoski, R., Jr. *Biochemistry* **1995**, *34*, 252−256.
(254) Musacchio, J. M.; Wurzburger, R. J.; D'Angelo, G. L. *Mol. Pharmacol.* **1971**, *7*, 136−146.
(255) Kuczenski, R. *J. Biol. Chem.* **1973**, *248*, 5074−5080.
(256) Vigny, A.; Henry, J.-P. *J. Neurochem.* **1981**, *36*, 483−489.
(257) Togari, A.; Ichikawa, S.; Nagatsu, T. *Biochem. Biophys. Res. Commun.* **1986**, *134*, 749−754.
(258) Abate, C.; Smith, J. A.; Joh, T. H. *Biochem. Biophys. Res. Commun.* **1988**, *151*, 1446−1453.
(259) Abate, C.; Joh, T. H. *J. Mol. Neurosci.* **1991**, *2*, 203−215.
(260) Kiuchi, K.; Kiuchi, K.; Titani, K.; Fujita, K.; Suzuki, K.; Nagatsu, T. *Biochemistry* **1991**, *30*, 10416−10419.
(261) Lohse, D. L.; Fitzpatrick, P. F. *Biochem. Biophys. Res. Commun.* **1993**, *197*, 1543−1548.
(262) Liu, X.; Vrana, K. E. *Neurochem. Int.* **1991**, *18*, 27−31.
(263) Vrana, K. E.; Walker, S. J.; Rucker, P.; Liu, X. *J. Neurochem.* **1994**, *63*, 2014−2020.
(264) Daubner, S. C.; Piper, M. M. *Protein Sci.* **1995**, *4*, 538−541.
(265) Zigmond, R. E. *J. Physiol. (Paris)* **1988**, *83*, 267−271.
(266) McGeer, P. L.; Eccles, J. C.; McGeer, E. G. *Molecular neurobiology of the mammalian brain*; Plenum Press: New York, 1987.
(267) Fujisawa, H.; Yamauchi, T.; Nakata, H.; Okuno, S. In *Enzyme Regulation by Reversible Phosphorylation*; Cohen, P., Ed.; Elsevier: New York, 1984.
(268) Weiner, N.; Rabadjija, M. *J. Pharmacol. Exp. Ther.* **1968**, *160*, 61−71.
(269) Alousi, A.; Weiner, N. *Proc. Natl. Acad. Sci. U.S.A.* **1966**, *56*, 1491−1496.
(270) Morgenroth, V. H., III; Boadle-Biber, M.; Roth, R. H. *Proc. Natl. Acad. Sci. U.S.A.* **1974**, *71*, 4283−4287.
(271) Lloyd, T.; Kaufman, S. *Biochem. Biophys. Res. Commun.* **1974**, *59*, 1262−1270.
(272) Harris, J. E.; Morgenroth, V. H., III; Roth, R. H.; Baldessarini, R. J. *Nature* **1974**, *252*, 156−158.
(273) Letendre, C. H.; MacDonnell, P. C.; Guroff, G. *Biochem. Biophys. Res. Commun.* **1976**, *76*, 615−617.
(274) Letendre, C. H.; MacDonnell, P. C.; Guroff, G. *Biochem. Biophys. Res. Commun.* **1977**, *74*, 891−897.
(275) Vulliet, P. R.; Langan, T. A.; Weiner, N. *Proc. Natl. Acad. Sci. U.S.A.* **1980**, *77*, 92−96.
(276) Meligeni, J. A.; Haycock, J. W.; Bennett, W. F.; Waymire, J. C. *J. Biol. Chem.* **1982**, *257*, 12632−12640.
(277) Vulliet, P. R.; Hall, F. L.; Mitchell, J. P.; Hardie, D. G. *J. Biol. Chem.* **1989**, *264*, 16292−16298.
(278) Haycock, J. W. *J. Biol. Chem.* **1990**, *265*, 11682−11691.
(279) Fujisawa, H.; Okuno, S. In *Adv. Enzyme Regul.*; Weber, G., Ed.; Pergamon Press: New York, 1989; Vol. 28.
(280) Yamauchi, T.; Fujisawa, H. *J. Biol. Chem.* **1979**, *254*, 503−507.
(281) Joh, T. H.; Park, D. H.; Reis, D. J. *Proc. Natl. Acad. Sci. U.S.A.* **1978**, *75*, 4744−4748.
(282) Yamauchi, T.; Nakata, H.; Fujisawa, H. *J. Biol. Chem.* **1981**, *256*, 5404−5409.
(283) Vulliet, P. R.; Woodgett, J. R.; Cohen, P. *J. Biol. Chem.* **1984**, *259*, 13680−13683.
(284) Roskoski, R., Jr.; Vulliet, P. R.; Glass, D. B. *J. Neurochem.* **1987**, *48*, 840−845.
(285) Vulliet, P. R.; Woodgett, J. R.; Ferrari, S.; Hardie, D. G. *FEBS Lett.* **1985**, *182*, 335−339.
(286) Albert, K. A.; Helmer-Matyjek, E.; Nairn, A. C.; Müller, T. H.; Haycock, J. W.; Greene, L. A.; Goldstein, M.; Greengard, P. *Proc. Natl. Acad. Sci. U.S.A.* **1984**, *81*, 7713−7717.
(287) Tachikawa, E.; Tank, A. W.; Yanagihara, N.; Mosimann, W.; Weiner, N. *Mol. Pharmacol.* **1986**, *30*, 476−485.
(288) Tachikawa, E.; Tank, A. W.; Weiner, D. H.; Mosimann, W. F.; Yanagihara, N.; Weiner, N. *J. Neurochem.* **1987**, *48*, 1366−1376.
(289) Haycock, J. W.; Ahn, N. G.; Cobb, M. H.; Krebs, E. G. *Proc. Natl. Acad. Sci. U.S.A.* **1992**, *89*, 2365−2369.
(290) Rausch, W.-D.; Hirata, Y.; Nagatsu, T.; Riederer, P.; Jellinger, K. *J. Neurochem.* **1988**, *50*, 202−208.
(291) Okuno, S.; Kanayama, Y.; Fujisawa, H. *FEBS Lett.* **1989**, *253*, 52−54.
(292) Erickson, A. K.; Payne, D. M.; Martino, P. A.; Rossomando, A. J.; Shabanowitz, J.; Weber, M. J.; Hunt, D. F.; Sturgill, T. W. *J. Biol. Chem.* **1990**, *265*, 19728−19735.
(293) Yamauchi, T.; Fujisawa, H. *Biochem. Biophys. Res. Commun.* **1979**, *90*, 28−35.
(294) Yamauchi, T.; Fujisawa, H. *Biochem. Biophys. Res. Commun.* **1981**, *100*, 807−813.
(295) Yamauchi, T.; Fujisawa, H. *Biochem. Int.* **1980**, *1*, 98−104.
(296) Ichimura, T.; Isobe, T.; Okuyama, T.; Takahashi, N.; Araki, K.; Kuwano, R.; Takahashi, Y. *Proc. Natl. Acad. Sci. U.S.A.* **1988**, *85*, 7084−7088.
(297) Sutherland, C.; Alterio, J.; Campbell, D. G.; Le Bourdellès, B.; Mallet, J.; Haavik, J.; Cohen, P. *Eur. J. Biochem.* **1993**, *217*, 715−722.
(298) Morgenroth, V. H., III; Hegstrand, L. R.; Roth, R. H.; Greengard, P. *J. Biol. Chem.* **1975**, *250*, 1946−1948.
(299) Lovenberg, W.; Bruckwick, E. A.; Hanbauer, I. *Proc. Natl. Acad. Sci. U.S.A.* **1975**, *72*, 2955−2958.
(300) Lloyd, T.; Kaufman, S. *Biochem. Biophys. Res. Commun.* **1975**, *66*, 907−917.
(301) Pollock, R. J.; Kapatos, G.; Kaufman, S. *J. Neurochem.* **1981**, *37*, 855−860.
(302) Funakoshi, H.; Okuno, S.; Fujisawa, H. *J. Biol. Chem.* **1991**, *266*, 15614−15620.
(303) Kaufman, S.; Nelson, T. J. In *Basic Aspects and Peripheral Mechanisms*; Alan R. Liss, Inc.: New York, 1988; Vol. A.
(304) Daubner, S. C.; Fitzpatrick, P. F. *Adv. Exp. Med. Biol.* **1993**, *338*, 87−92.
(305) Ribeiro, P.; Wang, Y.; Citron, B. A.; Kaufman, S. *Proc. Natl. Acad. Sci. U.S.A.* **1992**, *89*, 9593−9597.
(306) Almås, B.; Le Bourdelles, B.; Flatmark, T.; Mallet, J.; Haavik, J. *Eur. J. Biochem.* **1992**, *209*, 249−255.
(307) Andersson, K. K.; Vassort, C.; Brennan, B. A.; Que, L., Jr.; Haavik, J.; Flatmark, T.; Gros, F.; Thibault, J. *Biochem. J.* **1992**, *284*, 687−695.
(308) Yamauchi, T.; Fujisawa, H. *J. Biol. Chem.* **1979**, *254*, 6408−6413.
(309) Nelson, T. J.; Kaufman, S. *J. Biol. Chem.* **1987**, *262*, 16470−16475.
(310) Cohen, P. *Methods Enzymol.* **1991**, *201*, 389−398.
(311) Haavik, J.; Schelling, D. L.; Campbell, D. G.; Andersson, K. K.; Flatmark, T.; Cohen, P. *FEBS Lett.* **1989**, *251*, 36−42.
(312) Ribeiro, P.; Kaufman, S. *Neurochem. Res.* **1994**, *19*, 541−548.
(313) Kuczenski, R. *J. Biol. Chem.* **1973**, *248*, 2261−2265.
(314) Hamon, M.; Bourgoin, S. *J. Neurochem.* **1979**, *32*, 1837−1844.
(315) Kuczenski, R. T.; Mandell, A. J. *J. Neurochem.* **1972**, *19*, 131−137.
(316) Lloyd, T. *J. Biol. Chem.* **1979**, *254*, 7247−7254.
(317) Simon, J. R.; Roth, R. H. *Mol. Pharmacol.* **1979**, *16*, 224−233.
(318) Martell, A. M.; Smith, R. M. *Critical Stability Constants*; Plenum Press: New York, 1977.
(319) Mentasti, E.; Pelizzetti, E.; Saini, G. *J. Inorg. Nucl. Chem.* **1976**, *38*, 785−788.
(320) Haavik, J.; Martínez, A.; Flatmark, T. *FEBS Lett.* **1990**, *262*, 363−365.
(321) Morita, K.; Teraoka, K.; Hamano, S.; Oka, M.; Azuma, M. *Neurochem. Int.* **1990**, *17*, 21−26.
(322) Fitzpatrick, P. F. *J. Biol. Chem.* **1989**, *264*, 5313.
(323) Fitzpatrick, P. F. *J. Biol. Chem.* **1988**, *263*, 16058−16062.
(324) Vrana, K. E.; Roskoski, R., Jr. *J. Neurochem.* **1983**, *40*, 1692−1700.
(325) Kuhn, D. M.; Lovenberg, W. *Biochem. Biophys. Res. Commun.* **1983**, *117*, 894−900.
(326) Andersson, K. K.; Haavik, J.; Martinez, A.; Flatmark, T.; Petersson, L. *FEBS Lett.* **1989**, *258*, 9−12.
(327) Haavik, J.; Martinez, A.; Olafsdottir, S.; Mallet, J.; Flatmark, T. *Eur. J. Biochem.* **1992**, *210*, 23−31.
(328) Fitzpatrick, P. F. *Biochem. Biophys. Res. Commun.* **1989**, *161*, 211−215.
(329) Haavik, J.; Bill, E.; Lengen, M.; Martinez, A.; Flatmark, T.; Trautwein, A. X. *Adv. Exp. Med. Biol.* **1993**, *338*, 71−76.
(330) Ramsey, A. J.; Daubner, S. C.; Ehrlich, J. I.; Fitzpatrick, P. F. *Protein Sci.* **1995**, *4*, 2082−2086.
(331) Joh, T. H.; Shikimi, T.; Pickel, V. M.; Reis, D. J. *Proc. Natl. Acad. Sci. U.S.A.* **1975**, *72*, 3575−3579.
(332) Jequier, E.; Robinson, D. S.; Lovenberg, W.; Sjoerdsma, A. *Biochem. Pharmacol.* **1969**, *18*, 1071−1081.
(333) Aghajanian, G. K.; Bloom, F. E.; Sheard, M. H. *Brain Res.* **1969**, *13*, 266−273.
(334) Rusak, B.; Bina, K. G. *Annu. Rev. Neurosci.* **1990**, *13*, 387−401.
(335) Meyer, D. C.; Quay, W. B. *Endocrinology* **1976**, *98*, 1160−1165.
(336) Mason, R. *J. Physiol.* **1986**, *377*, 1−13.
(337) Bradford, H. F. *Chemical Neurobiology: An Introduction to Neurochemistry*; W. H. Freeman and Co.: New York, 1986.
(338) Crow, T. J.; Wendlandt, S. *Nature* **1976**, *259*, 42−44.
(339) Drucker-Colin, R. R.; Spanis, C. W. *Prog. Neurobiol.* **1976**, *6*, 1−22.
(340) Fuller, R. W. *Adv. Biosci.* **1992**, *85*, 255−270.
(341) Wooley, D. W.; Shaw, E. *Science* **1954**, *119*, 587−588.
(342) Lovenberg, W.; Jequier, E.; Sjoerdsma, A. *Adv. Pharmacol.* **1968**, *6*, 21−36.
(343) Hasegawa, H.; Yanagisawa, M.; Inoue, F.; Yanaihara, N.; Ichiyama, A. *Biochem. J.* **1987**, *248*, 501−509.
(344) Rodewald, H.-R.; Dessing, M.; Dvorak, A. M.; Galli, S. J. *Science* **1995**, *271*, 818−822.
(345) Galli, S. J. *N. Engl. J. Med.* **1993**, *328*, 257−265.

(346) Kuhn, D. M.; Lovenberg, W. In *Chemistry and Biochemistry of Pterins*; Blakely, R. L., Benkovic, S. J., Eds.; Wiley and Sons: New York, 1985; Vol. 2.
(347) Morrissey, J. J.; Walker, M. N.; Lovenberg, W. *Proc. Soc. Exp. Biol. Med.* **1977**, *154*, 496−499.
(348) Flanagan, J. G.; Chan, D. C.; Leder, P. *Cell* **1991**, *64*, 1025−1035.
(349) Ziegler, I.; Hultner, L.; Egger, D.; Kempkes, B.; Mailhammer, R.; Gillis, S.; Rodl, W. *J. Biol. Chem.* **1993**, *268*, 12544−12551.
(350) Lerner, A. B.; Chase, J. D.; Heinzelman, R. V. *J. Am. Chem. Soc.* **1959**, *81*, 6084−6085.
(351) Hagan, R. M.; Oakley, N. R. *Trends Pharmacol. Sci.* **1995**, *16*, 81−83.
(352) Morgan, P. J.; Mercer, J. G. *Proc. Nutr. Soc.* **1994**, *53*, 483−493.
(353) Brown, G. M. *J. Psychiatry Neurosci.* **1994**, *19*, 345−353.
(354) Webb, S. M.; Puig-Domingo, M. *Clin. Endocrinol.* **1995**, *42*, 221−234.
(355) Dawson, D.; Encel, N. *J. Pineal Res.* **1993**, *15*, 1−12.
(356) Reiter, R. J. *Experientia* **1993**, *49*, 654−664.
(357) Reiter, R. J. *Mol. Cell. Endocrinol.* **1991**, *79*, C153−158.
(358) Thomas, K. B.; Tigges, M.; Iuvone, P. M. *Brain Res.* **1993**, *601*, 303−307.
(359) Cahill, G. M.; Besharse, J. C. *J. Neurochem.* **1990**, *54*, 716−719.
(360) Redburn, D. A.; Mitchell, C. K. *Vis. Neurosci.* **1989**, *3*, 391−403.
(361) Osborne, N. N. *Brain Res.* **1980**, *184*, 283−297.
(362) Osborne, N. N.; Nesselhut, T.; Nicholas, D. A.; Patel, S.; Cuello, A. C. *J. Neurochem.* **1982**, *39*, 1519−1528.
(363) Redburn, D. A. *Neurosci. Res. Suppl.* **1988**, *8*, S127−136.
(364) Zhu, B.; Gabriel, R.; Straznicky, C. *Vis. Neurosci.* **1992**, *9*, 377−388.
(365) Wilhelm, M.; Zhu, B.; Gábriel, R.; Straznicky, C. *Exp. Eye Res.* **1993**, *56*, 231−240.
(366) Green, C. B.; Cahill, G. M.; Besharse, J. C. *Vis. Neurosci.* **1995**, *12*, 663−670.
(367) Johansen, P. A.; Wolf, W. A.; Kuhn, D. M. *Biochem. Pharmacol.* **1991**, *41*, 625−628.
(368) Baumgarten, H. G.; Victor, S. J.; Lovenberg, W. *J. Neurochem.* **1973**, *21*, 251−253.
(369) Friedman, P. A.; Kappelman, A. H.; Kaufman, S. *J. Biol. Chem.* **1972**, *247*, 4165−4173.
(370) Ichiyama, A.; Nakamura, S.; Nishizuka, Y.; Hayaishi, O. *J. Biol. Chem.* **1970**, *245*, 1699−1709.
(371) Gál, E. M.; Patterson, K. *Anal. Biochem.* **1973**, *52*, 625−629.
(372) Tong, J. H.; Kaufman, S. *J. Biol. Chem.* **1975**, *250*, 4152−4158.
(373) Nakata, H.; Fujisawa, H. *Eur. J. Biochem.* **1982**, *124*, 595−601.
(374) Nakata, H.; Fujisawa, H. *Eur. J. Biochem.* **1982**, *122*, 41−47.
(375) Kuhn, D. M.; Ruskin, B.; Lovenberg, W. *J. Biol. Chem.* **1980**, *255*, 4137−4143.
(376) Cash, C. D.; Vayer, P.; Mandel, P.; Maitre, M. *Eur. J. Biochem.* **1985**, *149*, 239−245.
(377) Kuhn, D. M.; Rosenberg, R. C.; Lovenberg, W. *J. Neurochem.* **1979**, *33*, 15−21.
(378) Darmon, M. C.; Grima, B.; Cash, C. D.; Maitre, M.; Mallet, J. *FEBS Lett.* **1986**, *206*, 43−46.
(379) Darmon, M. C.; Guibert, B.; Leviel, V.; Ehret, M.; Maitre, M.; Mallet, J. *J. Neurochem.* **1988**, *51*, 312−316.
(380) Boularand, S.; Darmon, M. C.; Ganem, Y.; Launay, J. M.; Mallet, J. *Nucleic Acids Res.* **1990**, *18*, 4257.
(381) Stoll, J.; Goldman, D. *J. Neurosci. Res.* **1991**, *28*, 457−465.
(382) Kim, K. S.; Wessel, T. C.; Stone, D. M.; Carver, C. H.; Joh, T. H.; Park, D. H. *Mol. Brain Res.* **1991**, *9*, 277−283.
(383) Tipper, J. P.; Citron, B. A.; Ribeiro, P.; Kaufman, S. *Arch. Biochem. Biophys.* **1994**, *315*, 445−453.
(384) Yang, X. J.; Kaufman, S. *Proc. Nat. Acad. Sci. U.S.A.* **1994**, *91*, 6659−6663.
(385) Park, D. H.; Stone, D. M.; Kim, K. S.; Joh, T. H. *Mol. Cell. Neurosci.* **1994**, *5*, 87−93.
(386) Hori, S. *Biochim. Biophys. Acta* **1975**, *384*, 58−68.
(387) Ledley, F. D.; Grenett, H. E.; Bartos, D. P.; van Tuinen, P.; Ledbetter, D. H.; Woo, S. L. C. *Som. Cell Mol. Genet.* **1987**, *13*, 575−580.
(388) Craig, S. P.; Boularand, S.; Darmon, M. C.; Mallet, J.; Craig, I. W. *Cytogenet. Cell Genet.* **1991**, *56*, 157−159.
(389) Nielsen, D. A.; Dean, M.; Goldman, D. *Am. J. Hum. Genet.* **1992**, *51*, 1366−1371.
(390) Shein, H. M.; Wurtman, R. J. *Life Sci. I* **1971**, *10*, 935−940.
(391) Ehret, M.; Pevet, P.; Maitre, M. *J. Neurochem.* **1991**, *57*, 1516−1521.
(392) Boularand, S.; Darmon, M. C.; Ravassard, P.; Mallet, J. *J. Biol. Chem.* **1995**, *270*, 3757−3764.
(393) Stehle, J. H.; Foulkes, N. S.; Molina, C. A.; Simonneaux, V.; Pévet, P.; Sassone-Corsi, P. *Nature* **1993**, *365*, 314−320.
(394) Borjigin, J.; Wang, M. M.; Snyder, S. H. *Nature* **1995**, *378*, 783−785.
(395) Hasegawa, H.; Kojima, M.; Oguro, K.; Nakanishi, N. *FEBS Lett.* **1995**, *368*, 151−154.
(396) Mitoma, C.; Weissbach, H.; Udenfriend, S. *Arch. Biochem. Biophys* **1956**, *63*, 122−130.
(397) Mitoma, C.; Weissbach, H.; Udenfriend, S. *Nature* **1955**, *175*, 994−995.
(398) Koe, B. K.; Weissman, A. *J. Pharmacol. Exp. Ther.* **1966**, *154*, 499−516.
(399) Gál, E. M.; Roggeveen, A. E.; Millard, S. A. *J. Neurochem.* **1970**, *17*, 1221−1235.
(400) Bagchi, S. P.; Zarycki, E. P. *Res. Commun. Chem. Pathol. Pharmacol.* **1971**, *2*, 370−381.
(401) Renson, J.; Weissbach, H.; Udenfriend, S. *J. Biol. Chem.* **1962**, *237*, 2261−2264.
(402) Boadle-Biber, M. C. *Prog. Biophys. Mol. Biol.* **1993**, *60*, 1−15.
(403) Boadle-Biber, M. C.; Johannesen, J. N.; Narasimhachari, N.; Phan, T.-H. *Neurochem. Int.* **1986**, *8*, 83−92.
(404) Elks, M. L.; Youngblood, W. W.; Kizer, J. S. *Brain Res.* **1979**, *172*, 461−469.
(405) Knowles, R. G.; Pogson, C. I. *J. Neurochem.* **1984**, *42*, 677−684.
(406) Hamon, M.; Bourgoin, S.; Artaud, F.; Glowinski, J. *J. Neurochem.* **1979**, *33*, 1031−1042.
(407) Sitaram, B. R.; Lees, G. J. *J. Neurochem.* **1978**, *31*, 1021−1026.
(408) Shibuya, H.; Toru, M.; Watanabe, S. *Brain Res.* **1978**, *138*, 364−368.
(409) Thomas, K. B.; Iuvone, P. M. *Cell. Mol. Neurobiol.* **1991**, *11*, 511−527.
(410) Boadle-Biber, M. C. *Biochem. Pharmacol.* **1980**, *29*, 669−672.
(411) Garber, S. L.; Makman, M. H. *Brain Res.* **1987**, *427*, 1−10.
(412) Hamon, M.; Bourgoin, S.; Héry, F.; Simmonet, G. *Mol. Pharmacol.* **1978**, *14*, 99−110.
(413) Kuhn, D. M.; Vogel, R. L.; Lovenberg, W. *Biochem. Biophys. Res. Commun.* **1978**, *82*, 759−766.
(414) Boadle-Biber, M. C. *Biochem. Pharmacol.* **1982**, *31*, 2203−2207.
(415) Tagliamonte, A.; Tagliamonte, P.; Forn, J.; Perez-Cruet, J.; Krishna, G.; Gessa, G. L. *J. Neurochem.* **1971**, *18*, 1191−1196.
(416) Kuhn, D. M.; O'Callaghan, J. P.; Juskevich, J.; Lovenberg, W. *Proc. Natl. Acad. Sci. U.S.A.* **1980**, *77*, 4688−4691.
(417) Hamon, M.; Bourgoin, S.; Hery, F.; Ternaux, J. P.; Glowinski, J. *Nature* **1976**, *260*, 61−63.
(418) Yamauchi, T.; Fujisawa, H. *Arch. Biochem. Biophys.* **1979**, *198*, 219−226.
(419) Ichiyama, A.; Hasegawa, H.; Tohyama, C.; Dohmoto, C.; Kataoka, T. *Adv. Exp. Med. Biol.* **1976**, *74*, 103−117.
(420) Kuhn, D. M.; Lovenberg, W. *Fed. Proc.* **1982**, *41*, 2258−2264.
(421) Lysz, T. W.; Sze, P. Y. *J. Neurosci. Res.* **1978**, *3*, 411−418.
(422) Ehret, M.; Cash, C. D.; Hamon, M.; Maitre, M. *J. Neurochem.* **1989**, *52*, 1886−1891.
(423) Vrana, K. E.; Rucker, P. J.; Kumer, S. C. *Life Sci.* **1994**, *55*, 1045−1052.
(424) Makita, Y.; Okuno, S.; Fujisawa, H. *FEBS Lett.* **1990**, *268*, 185−188.
(425) Ichimura, T.; Uchiyama, J.; Kunihiro, O.; Ito, M.; Horigome, T.; Omata, S.; Shinkai, F.; Kaji, H.; Isobe, T. *J. Biol. Chem.* **1995**, *270*, 28515−28518.
(426) Xiao, B.; Smerdon, S. J.; Jones, D. H.; Dodson, G. G.; Soneji, Y.; Aitken, A.; Gamblin, S. J. *Nature* **1995**, *376*, 188−191.
(427) Liu, D.; Bienkowska, J.; Petosa, C.; Collier, R. J.; Fu, H.; Liddington, R. *Nature* **1995**, *376*, 191−194.
(428) Johansen, P. A.; Jennings, I.; Cotton, R. G. H.; Kuhn, D. M. *J. Neurochem.* **1995**, *65*, 882−888.
(429) Kuhn, D. M.; Meyer, M. A.; Lovenberg, W. *Biochem. Pharmacol.* **1979**, *28*, 3255−3260.
(430) Hamon, M.; Bourgoin, S.; Hery, F.; Simmonet, G. *Biochem. Pharmacol.* **1978**, *27*, 915−922.
(431) Imai, Y.; Yamauchi, T.; Fujisawa, H. *J. Neurochem.* **1989**, *53*, 1293−1299.
(432) Hamon, M.; Bourgoin, S.; Artaud, F.; Héry, F. *J. Neurochem.* **1977**, *28*, 811−818.
(433) Yanagisawa, M.; Hasegawa, H.; Ichiyama, A. *J. Biochem.* **1982**, *92*, 449−456.
(434) Hori, S.; Ohotani, S. *J. Neurochem.* **1978**, *31*, 663−671.
(435) Hori, S.; Ohtani, S. *J. Neurochem.* **1981**, *36*, 551−558.
(436) Ichiyama, A.; Hori, S.; Mashimo, Y.; Nukiwa, T.; Makuuchi, H. *FEBS Lett.* **1974**, *40*, 88−91.
(437) Hamon, M.; Bourgoin, S.; Héry, F.; Simonnet, G. *Neurochem. Res.* **1978**, *3*, 585−598.
(438) Pfleger, R. C.; Piantadosi, C.; Snyder, F. *Biochim. Biophys. Acta* **1967**, *144*, 633−648.
(439) Blomstrand, R.; Ahrens, E. H., Jr. *Proc. Soc. Exptl. Biol. Med.* **1959**, *100*, 802−805.
(440) Blomstrand, R. *Proc. Soc. Exptl. Biol. Med.* **1959**, *102*, 662−665.
(441) Tietz, A.; Lindberg, M.; Kennedy, E. P. *J. Biol. Chem.* **1964**, *239*, 4081−4090.
(442) Soodsma, J. F.; Piantadosi, C.; Snyder, F. *J. Biol. Chem.* **1972**, *247*, 3923−3929.
(443) Kaufman, S.; Pollock, R. J.; Summer, G. K.; Das, A. K.; Hajra, A. K. *Biochim. Biophys. Acta* **1990**, *1040*, 19−27.
(444) Ishibashi, T.; Imai, Y. *Eur. J. Biochem.* **1983**, *132*, 23−27.
(445) Koetting, J.; Unger, C.; Eibl, H. *Lipids* **1987**, *22*, 824−830.
(446) Ishibashi, T.; Imai, Y. *J. Lipid Res.* **1985**, *26*, 393−395.
(447) Kosar-Hashemi, B.; Armarego, W. L. F. *Biol. Chem. Hoppe-Seyler* **1993**, *374*, 9−25.
(448) Taguchi, H.; Kosar-Hashemi, B.; Paal, B.; Yang, N.; Armarego, W. L. F. *Biol. Chem. Hoppe-Seyler* **1994**, *375*, 329−334.

(449) Unger, C.; Eibl, H.; von Heyden, H. W.; Nagel, G. A. *Cancer Res.* **1985**, *45*, 616−618.
(450) Kötting, J.; Unger, C.; Eibl, H. *Lipids* **1987**, *22*, 831−835.
(451) Snyder, F.; Malone, B.; Piantadosi, C. *Biochim. Biophys. Acta* **1973**, *316*, 259−265.
(452) Snyder, F. *Biochim. Biophys. Acta* **1995**, *1254*, 231−249.
(453) Snyder, F. *Biochem. J.* **1995**, *305*, 689−705.
(454) Lee, T. C.; Blank, M. L.; Fitzgerald, V.; Snyder, F. *Arch. Biochem. Biophys.* **1981**, *208*, 353−357.
(455) Snyder, F.; Wood, R. *Cancer Res.* **1969**, *29*, 251−257.
(456) Snyder, F.; Wood, R. *Cancer Res.* **1968**, *28*, 972−978.
(457) Unger, C.; Eibl, H. *Lipids* **1991**, *26*, 1412−1417.
(458) Mangold, H. K. In *Ether Lipids: Chemistry and Biology*; Snyder, F., Ed.; Academic Press: New York, 1972.
(459) Weltzien, H. U.; Munder, P. G. In *Ether Lipids: Biochemical and Biomedical Aspects*; Mangold, H. K., Paltanf, F., Eds.; Academic Press: New York, 1983.
(460) Bhat, S. G.; Vaidyanathan, C. S. *Arch. Biochem. Biophys.* **1976**, *176*, 314−323.
(461) Reddy, C. C.; Vaidyanathan, C. S. *Biochim. Biophys. Acta* **1975**, *384*, 46−57.
(462) Reddy, C. C.; Vaidyanathan, C. S. *Arch. Biochem. Biophys.* **1976**, *177*, 488−498.
(463) Sreeleela, N. S.; SubbaRao, P. V.; Premkumar, R.; Vaidyanathan, C. S. *J. Biol. Chem.* **1969**, *244*, 2293−2298.
(464) Tayeh, M. A.; Marletta, M. A. *J. Biol. Chem.* **1989**, *264*, 19654−19658.
(465) Kwon, N. S.; Nathan, C. F.; Stuehr, D. J. *J. Biol. Chem.* **1989**, *264*, 20496−20501.
(466) Marletta, M. A. *J. Biol. Chem.* **1993**, *268*, 12231−12234.
(467) Marletta, M. A. *Cell* **1994**, *78*, 927−930.
(468) Griffith, O. W.; Stuehr, D. J. *Annu. Rev. Physiol.* **1995**, *57*, 707−736.
(469) Mayer, B.; Werner, E. R. *Naunyn Schmied. Arch. Pharm.* **1995**, *351*, 453−463.
(470) Nathan, C. *J. Clin. Invest.* **1994**, *93*, 1875−1876.
(471) Giovanelli, J.; Campos, K. L.; Kaufman, S. *Proc. Natl. Acad. Sci. U.S.A.* **1991**, *88*, 7091−7095.
(472) Hevel, J. M.; Marletta, M. A. *Biochemistry* **1992**, *31*, 7160−7165.
(473) Hevel, J. M.; Marletta, M. A. *Adv. Exp. Med. Biol.* **1993**, *338*, 285−288.
(474) Stuehr, D. J.; Kwon, N. S.; Nathan, C. F.; Griffith, O. W.; Feldman, P. L.; Wiseman, J. *J. Biol. Chem.* **1991**, *266*, 6259−6263.
(475) Abu-Soud, H. M.; Loftus, M.; Stuehr, D. J. *Biochemistry* **1995**, *34*, 11167−11175.
(476) Tzeng, E.; Billiar, T. R.; Robbins, P. D.; Loftus, M.; Stuehr, D. J. *Proc. Natl. Acad. Sci. U.S.A.* **1995**, *92*, 11771−11775.
(477) Pufahl, R. A.; Marletta, M. A. *Biochem. Biophys. Res. Commun.* **1993**, *193*, 963−970.
(478) Pufahl, R. A.; Wishnok, J. S.; Marletta, M. A. *Biochemistry* **1995**, *34*, 1930−1941.
(479) Campos, K. L.; Giovanelli, J.; Kaufman, S. *J. Biol. Chem.* **1995**, *270*, 1721−1728.
(480) Witteveen, C. F. B.; Giovanelli, J.; Kaufman, S. *J. Biol. Chem.* **1996**, *271*, 4143−4147.
(481) Sawada, M.; Nagatsu, T. In *Unconjugated Pterins in Neurobiology: Basic and Clinical Aspects*; Lovenberg, W., Levine, R. A., Eds.; Taylor & Francis: Philadelphia, 1987; Vol. 1.
(482) Nichol, C. A.; Smith, G. K.; Reinhard, J. F., Jr.; Bigham, E. C.; Abou-Donia, M.; Viveros, O. H.; Duch, D. S. In *Unconjugated Pterins in Neurobiology: Basic and Clinical Aspects*; Lovenberg, W., Levine, R. A., Eds.; Taylor & Francis: Philadelphia, 1987; Vol. 1.
(483) Kaufman, S. *J. Biol. Chem.* **1967**, *242*, 3934−3943.
(484) Curtius, H.-C.; Heintel, D.; Ghisla, S.; Kuster, T.; Leimbacher, W.; Niederwieser, A. *Eur. J. Biochem.* **1985**, *148*, 413−419.
(485) Heintel, D.; Ghisla, S.; Curtius, H.-C. In *Unconjugated Pterins in Neurobiology: Basic and Clinical Aspects*; Lovenberg, W., Levine, R. A., Eds.; Taylor & Francis: Philadelphia, 1987; Vol. 1.
(486) Hatakeyama, K.; Harada, T.; Suzuki, S.; Watanabe, Y.; Kagamiyama, H. *J. Biol. Chem.* **1989**, *264*, 21660−21664.
(487) Hatakeyama, K.; Harada, T.; Kagamiyama, H. *J. Biol. Chem.* **1992**, *267*, 20734−20739.
(488) Hoshiga, M.; Hatakeyama, K.; Kagamiyama, H. *Adv. Exp. Med. Biol.* **1993**, *338*, 223−226.
(489) Davis, M. D.; Kaufman, S.; Milstien, S. *FEBS Lett.* **1992**, *302*, 73−76.
(490) Citron, B. A.; Davis, M. D.; Milstien, S.; Gutierrez, J.; Mendel, D. B.; Crabtree, G. R.; Kaufman, S. *Proc. Natl. Acad. Sci. U.S.A.* **1992**, *89*, 11891−11894.
(491) Mendel, D. B.; Khavari, P. A.; Conley, P. B.; Graves, M. K.; Hansen, L. P.; Admon, A.; Crabtree, G. R. *Science* **1991**, *254*, 1762−1767. [a] Coupled and uncoupled turnover under pterin-limiting conditions at pH 8.2, 25 °C. Data taken from and other conditions given in ref 168.
(492) Huang, C. Y.; Kaufman, S. *J. Biol. Chem.* **1973**, *248*, 4242−4251.
(493) Huang, C. Y.; Max, E. E.; Kaufman, S. *J. Biol. Chem.* **1973**, *248*, 4235−4241.
(494) Ziegler, I. *Med. Res. Rev.* **1990**, *10*, 95−114.
(495) Huber, C.; Batchelor, J. R.; Fuchs, D.; Hausen, A.; Lang, A.; Niederwieser, D.; Reibnegger, G.; Swetly, P.; Troppmair, J.; Wachter, H. *J. Exp. Med.* **1984**, *160*, 310−316.
(496) Werner, E. R.; Werner-Felmayer, G.; Fuchs, D.; Hausen, A.; Reibnegger, G.; Yim, J. J.; Pfleiderer, W.; Wachter, H. *J. Biol. Chem.* **1990**, *265*, 3189−3192.
(497) Kaufman, S. *Annu. Rev. Nutr.* **1993**, *13*, 261−286.
(498) Stuehr, D. J.; Griffith, O. W. *Adv. Enzymol. Relat. Areas Mol. Biol.* **1992**, *65*, 287−346.
(499) Werner, E. R.; Werner-Felmayer, G.; Fuchs, D.; Hausen, A.; Reibnegger, G.; Yim, J. J.; Wachter, H. *Biochem. J.* **1991**, *280*, 709−714.
(500) Fukushima, T.; Nixon, J. C. *Anal. Biochem.* **1980**, *102*, 176−188.
(501) Harada, T.; Hatakeyama, K.; Kagamiyama, H. *Adv. Exp. Med. Biol.* **1993**, *338*, 183−186.
(502) Milstien, S.; Kaufman, S. *Biochem. Biophys. Res. Commun.* **1985**, *128*, 1099−1107.
(503) Werner, E. R.; Werner-Felmayer, G.; Fuchs, D.; Hausen, A.; Reibnegger, G.; Wels, G.; Yim, J. J.; Pfleiderer, W.; Wachter, H. *J. Chromatogr.* **1991**, *570*, 43−50.
(504) Takikawa, S.; Curtius, H. C.; Redweik, U.; Leimbacher, W.; Ghisla, S. *Eur. J. Biochem.* **1986**, *161*, 295−302.
(505) Niederwieser, A.; Curtius, H.-C. *Enzyme* **1987**, *38*, 302−311.
(506) Taylor, D.; Hochstein, P. *Lancet* **1975**, *1*, 1378.
(507) Blau, N.; Dhondt, J. L. *Adv. Exp. Med. Biol.* **1993**, *338*, 255−261.
(508) Dhondt, J. L. *J. Pediatr.* **1984**, *104*, 501−508.
(509) Citron, B. A.; Kaufman, S.; Milstein, S.; Naylor, E. W.; Greene, C. L.; Davis, M. D. *Am. J. Hum. Genet.* **1993**, *53*, 768−774.
(510) Kaufman, S. *Adv. Hum. Genet.* **1983**, *13*, 217−297.
(511) Niederwieser, A.; Blau, N.; Wang, M.; Joller, P.; Atarés, M.; Cardesa-Garcia, J. *Eur. J. Pediatr.* **1984**, *141*, 208−214.
(512) Yim, J. J.; Brown, G. M. *J. Biol. Chem.* **1976**, *251*, 5087−5094.
(513) Nar, H.; Huber, R.; Meining, W.; Schmid, C.; Weinkauf, S.; Bacher, A. *Structure* **1995**, *3*, 459−466.
(514) Nar, H.; Huber, R.; Heizmann, C. W.; Thony, B.; Burgisser, D. *EMBO J.* **1994**, *13*, 1255−1262.
(515) Varughese, K. I.; Skinner, M. M.; Whiteley, J. M.; Matthews, D. A.; Xuong, N. H. *Proc. Natl. Acad. Sci. U.S.A.* **1992**, *89*, 6080−6084.
(516) Harada, T.; Kagamiyama, H.; Hatakeyama, K. *Science* **1993**, *260*, 1507−1510.
(517) Leeming, R. J.; Blair, J. A.; Green, A.; Raine, D. N. *Arch. Dis. Child.* **1976**, *51*, 771−777.
(518) Kaufman, S.; Berlow, S.; Summer, G. K.; Milstien, S.; Schulman, J. D.; Orloff, S.; Spielberg, S.; Pueschel, S. *N. Engl. J. Med.* **1978**, *299*, 673−679.
(519) McInnes, R. R.; Kaufman, S.; Warsh, J. J.; Van Loon, G. R.; Milstien, S.; Kapatos, G.; Soldin, S.; Walsh, P.; MacGregor, D.; Hanley, W. B. *J. Clin. Invest.* **1984**, *73*, 458−469.
(520) Dhondt, J. L.; Leroux, B.; Farriaux, J. P.; Largilliere, C.; Leeming, R. J. *Eur. J. Pediatr.* **1983**, *141*, 92−95.
(521) Craine, J. E.; Hall, E. S.; Kaufman, S. *J. Biol. Chem.* **1972**, *247*, 6082−6091.
(522) Nielsen, K. H.; Simonsen, V.; Lind, K. E. *Eur. J. Biochem.* **1969**, *9*, 497−502.
(523) Kaufman, S.; Citron, B. A.; Davis, M.; Milstein, S. *Adv. Exp. Med. Biol.* **1993**, *338*, 97−102.
(524) Patterson, E. L.; von Staltza, M. H.; Stokstad, E. L. R. *J. Am. Chem. Soc.* **1956**, *78*, 5871−5873.
(525) Kidder, G. W.; Nolan, L. L. *Biochem. Biophys. Res. Commun.* **1973**, *53*, 929−936.
(526) Forrest, H. S.; Mitchell, H. K. *J. Am. Chem. Soc.* **1955**, *77*, 4865−4869.
(527) Rajagopalan, K. V.; Johnson, J. L. *J. Biol. Chem.* **1992**, *267*, 10199−10202.
(528) Wang, B. Y.; Jordan, S. P.; Jorns, M. S. *Biochemistry* **1988**, *27*, 4222−4226.
(529) Johnson, J. L.; Rajagopalan, K. V. In *Chemistry and Biochemistry of Pterins*; Blakely, R. L., Benkovic, S. J., Eds.; Wiley and Sons: New York, 1985; Vol. 2.
(530) Hopkins, F. G. *Proc. R. Soc. B* **1942**, *130*, 359−379.
(531) Pfleiderer, W. *J. Heterocycl. Chem.* **1992**, *29*, 583−605.
(532) Armarego, W. L. F.; Waring, P. *J. Chem. Soc., Perkin Trans. 2* **1982**, 1227−1233.
(533) Benkovic, S. J.; Sammons, D.; Armarego, W. L. F.; Waring, P.; Inners, R. *J. Am. Chem. Soc.* **1985**, *107*, 3706−3712.
(534) Viscontini, M.; Huwyler, S. *Helv. Chim. Acta* **1965**, *48*, 764−768.
(535) Archer, M. C.; Scrimgeour, K. G. *Can. J. Biochem.* **1970**, *48*, 278−287.
(536) Armarego, W. L.; Randles, D.; Taguchi, H. *Eur. J. Biochem.* **1983**, *135*, 393−403.
(537) Bieri, J. H.; Viscontini, M. *Helv. Chim. Acta* **1977**, *60*, 447−453.
(538) Bieri, J. H.; Viscontini, M. *Helv. Chim. Acta* **1977**, *60*, 1926−1931.
(539) Fontecilla-Camps, J. C.; Bugg, C.; Temple, C., Jr.; Rose, J. D.; Montgomery, J. A.; Kisliuk, R. L. *J. Am. Chem. Soc.* **1979**, *101*, 6114−6115.
(540) Bieri, J. H. *Helv. Chim. Acta* **1977**, *60*, 2303−2308.

(541) Armarego, W. L. F.; Waring, P. *J. Chem. Res. (S)* **1980**, 318−319.
(542) Armarego, W. L. F.; Schou, H. *J. Chem. Soc., Perkin Trans. 1* **1977**, 2529−2536.
(543) Ganguly, A. N.; Sengupta, P. K.; Bieri, J. H.; Viscontini, M. *Helv. Chim. Acta* **1980**, *63*, 395−401.
(544) Weber, R.; Viscontini, M. *Helv. Chim. Acta* **1975**, *58*, 1772−1780.
(545) Storm, C. B.; Chung, H. S. *Org. Magn. Reson.* **1976**, *8*, 361−362.
(546) Benkovic, S. J. *Annu. Rev. Biochem.* **1980**, *49*, 227−251.
(547) Williams, T. C.; Storm, C. B. *Biochemistry* **1985**, *24*, 458−466.
(548) Bieri, J. H. In *Chemistry and Biology of Pteridines*; Kisliuk, R. L., Brown, G. M., Eds.; Elsevier & North-Holland: Amsterdam, 1979.
(549) Ziegler, I.; Borchert, M.; Heaney, F.; Davis, A. P.; Boyle, P. H. *Biochim. Biophys. Acta* **1992**, *1135*, 330−334.
(550) Ayling, J. E.; Dillard, S. B.; Bailey, S. W. In *Pterins and Biogenic Amines*; Blau, N., Curtius, M. C., Levine, R. A., Cotton, R. G. H., Eds.; Lakeside: Grosse Pointe, MI, 1991.
(551) Estelberger, W.; Fuchs, D.; Murr, C.; Wachter, H.; Reibnegger, G. *Biochim. Biophys. Acta* **1995**, *1249*, 23−28.
(552) Estelberger, W.; Mlekusch, W.; Reibnegger, G. *FEBS Lett.* **1995**, *357*, 37−40.
(553) Poe, M. *J. Biol. Chem.* **1973**, *248*, 7025−7032.
(554) Pfleiderer, W. In *Unconjugated pterins in neurobiology*; Lovenberg, W., Levine, R. A., Eds.; Taylor & Francis, Ltd.: Philadelphia, 1987; Vol. 2.
(555) Isay, O. *Chem. Ber.* **1906**, *39*, 250−265.
(556) Gabriel, S.; Colman, J. *Chem. Ber.* **1901**, *34*, 1234−1257.
(557) Mager, H. I. X.; Addink, R.; Berends, W. *Recl. Trav. Chim. Pays-Bas* **1967**, *86*, 833−851.
(558) Storm, C. B.; Shiman, R.; Kaufman, S. *J. Org. Chem.* **1971**, *36*, 3925−3927.
(559) Taylor, E. C.; Perlman, K. L.; Sword, I. P.; Séquin-Frey, M.; Jacobi, P. A. *J. Am. Chem. Soc.* **1973**, *95*, 6407−6412.
(560) Armarego, W. L. F.; Waring, P. *Aust. J. Chem.* **1981**, *34*, 1921−1933.
(561) Bailey, S. W.; Ayling, J. E. *Biochemistry* **1983**, *22*, 1790−1798.
(562) Bailey, S. W.; Chandrasekaran, R. Y.; Ayling, J. E. *J. Org. Chem.* **1992**, *57*, 4470−4477.
(563) Moad, G.; Luthy, C. L.; Benkovic, P. A.; Benkovic, S. J. *J. Am. Chem. Soc.* **1979**, *101*, 6068−6076.
(564) Lazarus, R. A.; Wallick, D. E.; Dietrich, R. F.; Gottschall, D. W.; Benkovic, S. J.; Gaffney, B. J.; Shiman, R. *Fed. Proc.* **1982**, *41*, 2605−2607.
(565) Moad, G.; Luthy, C. L.; Benkovic, S. J. *Tetrahedron Lett.* **1978**, *26*, 2271−2274.
(566) Moad, G.; Luthy, C. L.; Benkovic, S. J. In *Chemistry and Biology of Pteridines*; Kisliuk, R. L., Brown, G. M., Eds.; Elsevier North Holland: New York, 1979.
(567) Lazarus, R. A.; Sulewski, M. A.; Benkovic, S. J. *J. Labelled Compd. Radiopharm.* **1982**, *19*, 1189−1195.
(568) Lazarus, R. A.; DeBrosse, C. W.; Benkovic, S. J. *J. Am. Chem. Soc.* **1982**, *104*, 6869−6871.
(569) Ghisla, S.; Hastings, J. W.; Favaudon, V.; Lhoste, J. M. *Proc. Natl. Acad. Sci. U.S.A.* **1978**, *75*, 5860−5863.
(570) Wessiak, A.; Bruice, T. C. *J. Am. Chem. Soc.* **1981**, *103*, 6996−6998.
(571) Dix, T. A.; Bollag, G. E.; Domanico, P. L.; Benkovic, S. J. *Biochemistry* **1985**, *24*, 2955−2958.
(572) Dix, T. A.; Kuhn, D. M.; Benkovic, S. J. *Biochemistry* **1987**, *26*, 3354−3361.
(573) Pearson, A. J. *Chem. Ind. (London)* **1974**, 233−239.
(574) Bobst, A. *Helv. Chim. Acta* **1967**, *50*, 2222−2225.
(575) Archer, M. C.; Vonderschmitt, D. J.; Scrimgeour, K. G. *Can. J. Biochem.* **1972**, *50*, 1174−1182.
(576) Matsuura, S.; Sugimoto, T.; Murata, S. *Tetrahedron Lett.* **1985**, *26*, 4003−4004.
(577) Bobst, A. *Helv. Chim. Acta* **1967**, *50*, 1480−1491.
(578) Kiefer, P. M.; Varughese, K. I.; Su, Y.; Xuong, N.-H.; Chang, C.-F.; Gupta, P.; Bray, T.; Whiteley, J. M. *J. Biol. Chem.* **1996**, *271*, 3437−3444.
(579) Blair, J. A.; Pearson, A. J. *J. Chem. Soc., Perkin Trans. 2* **1975**.
(580) Viscontini, M.; Leidner, H.; Mattern, G.; Okada, T. *Helv. Chim. Acta* **1966**, *49*, 1911−1915.
(581) Ehrenberg, A.; Hemmerich, P.; Müller, F.; Pfleiderer, W. *Eur. J. Biochem.* **1970**, *16*, 584−591.
(582) Eberlein, G.; Bruice, T. C. *J. Am. Chem. Soc.* **1983**, *105*, 6685−6697.
(583) Lowe, H. J.; Clark, W. M. *J. Biol. Chem.* **1956**, *221*, 983−992.
(584) Mayer, J. M. *Comments Inorg. Chem.* **1988**, *8*, 123−135.
(585) Nasir, M. S.; Karlin, K. D.; Chen, Q.; Zubieta, J. *J. Am. Chem. Soc.* **1992**, *114*, 2264−2265.
(586) Kohzuma, T.; Masuda, H.; Yamauchi, O. *J. Am. Chem. Soc.* **1989**, *111*, 3431−3433.
(587) Perkinson, J.; Brodie, S.; Yoon, K.; Mosny, K.; Carroll, P. J.; Morgan, T. V.; Nieter Burgmayer, S. J. *Inorg. Chem.* **1991**, *30*, 719−727.
(588) Odani, A.; Masuda, H.; Inukai, K.; Yamauchi, O. *J. Am. Chem. Soc.* **1992**, *114*, 6294−6300.
(589) Kemal, C.; Chan, T. W.; Bruice, T. C. *J. Am. Chem. Soc.* **1977**, *99*, 7272−7286.
(590) Lazarus, R. A.; DeBrosse, C. W.; Benkovic, S. J. *J. Am. Chem. Soc.* **1982**, *104*, 6871−6872.
(591) Watson, B. M.; Armarego, W. L. F.; Schlesinger, P.; Cotton, R. G. H.; Danks, D. M. In *Chemistry and Biology of Pteridines*; Kisliuk, R. L., Brown, G. M., Eds.; Elsevier North Holland: Amsterdam, 1979.
(592) Mager, H. I. X. *Tetrahedron Lett.* **1979**, *20*, 2423−2426.
(593) Smith, S. B.; Bruice, T. C. *J. Am. Chem. Soc.* **1975**, *97*, 2875−2881.
(594) van der Plas, H. C. *Ring Transformations of Heterocycles*; Academic Press: New York, 1973.
(595) Noar, J. B.; Venkataram, U. V.; Bruice, T. C.; Bollag, G.; Whittle, R.; Sammons, D.; Henry, R.; Benkovic, S. J. *Bioorg. Chem.* **1986**, *14*, 17−27.
(596) Jongejan, J. A.; Mager, H. I. X.; Berends, W. *Tetrahedron* **1975**, *31*, 533−539.
(597) Jongegan, J. A.; Mager, H. I. X.; Berends, W. In *Chemistry and Biology of Pteridines*; Kisliuk, R. L., Brown, G. M., Eds.; Elsevier North Holland: New York, 1979; Vol. 4.
(598) van Koningsveld, H. *Tetrahedron* **1975**, *31*, 541−543.
(599) Dhondt, J. L.; Guibaud, P.; Rolland, M. O.; Dorche, C.; Andre, S.; Forzy, G.; Hayte, J. M. *Eur. J. Pediatr.* **1988**, *147*, 153−157.
(600) Curtius, H.-C.; Kuster, T.; Matasovic, A.; Blau, N.; Dhondt, J. L. *Biochem. Biophys. Res. Commun.* **1988**, *153*, 715−721.
(601) Curtius, H.-C.; Adler, C.; Rebrin, I.; Heizmann, C.; Ghisla, S. *Biochem. Biophys. Res. Commun.* **1990**, *172*, 1060−1066.
(602) Davis, M. D.; Kaufman, S.; Milstien, S. *Proc. Natl. Acad. Sci. U.S.A.* **1991**, *88*, 385−389.
(603) Bailey, S. W.; Rebrin, I.; Boerth, S. R.; Ayling, J. E. *J. Am. Chem. Soc.* **1995**, *117*, 10203−10211.
(604) Rebrin, I.; Bailey, S. W.; Boerth, S. R.; Ardell, M. D.; Ayling, J. E. *Biochemistry* **1995**, *34*, 5801−5810.
(605) Levine, R. A.; Zoephel, G. P.; Niederweiser, A.; Curtius, H.-C. *J. Pharmacol. Exp. Ther.* **1987**, *242*, 514−522.
(606) Curtius, H.-C.; Matasovic, A.; Schoedon, G.; Kuster, T.; Guibaud, P.; Giudici, T.; Blau, N. *J. Biol. Chem.* **1990**, *265*, 3923−3930.
(607) Davis, M. D.; Kaufman, S. *FEBS Lett.* **1991**, *285*, 17−20.
(608) Storm, C. B.; Kaufman, S. *Biochem. Biophys. Res. Commun.* **1968**, *32*, 788−793.
(609) Davis, M. D.; Ribeiro, P.; Tipper, J.; Kaufman, S. *Proc. Natl. Acad. Sci. U.S.A.* **1992**, *89*, 10109−10113.
(610) Bailey, S. W.; Boerth, S. R.; Dillard, S. B.; Ayling, J. E. *Adv. Exp. Med. Biol.* **1993**, *338*, 47−54.
(611) Köster, S.; Thöny, B.; Macheroux, P.; Curtius, H.-C.; Heizmann, C. W.; Pfleiderer, W.; Ghisla, S. *Eur. J. Biochem.* **1995**, *231*, 414−423.
(612) Schallreuter, K. U.; Wood, J. M.; Pittelkow, M. R.; Gütlich, M.; Lemke, K. R.; Rödl, W.; Swanson, N. N.; Hitzemann, K.; Ziegler, I. *Science* **1994**, *263*, 1444−1446.
(613) Wood, J. M.; Schallreuter-Wood, K. U.; Lindsey, N. J.; Callaghan, S.; Gardner, M. L. *Biochem. Biophys. Res. Commun.* **1995**, *206*, 480−485.
(614) Schallreuter, K. U.; Wood, J. M.; Berger, J. *J. Invest. Dermatol.* **1991**, *97*, 1081−1085.
(615) Schallreuter, K. U.; Wood, J. M.; Lemke, K. R.; Levenig, C. *Dermatology* **1995**, *190*, 223−229.
(616) Mayhew, S. G.; Ludwig, M. L. In *The Enzymes*, 3rd ed.; Boyer, P. D., Ed.; Academic Press: New York, 1975; Vol. 12.
(617) Deluca, M. *Adv. Enzymol. Relat. Areas Mol. Biol.* **1976**, *44*, 37−68.
(618) Massey, V.; Hemmerich, P. In *The Enzymes*, 3rd ed.; Boyer, P. D., Ed.; Academic Press: New York, 1975; Vol. 12.
(619) Massey, V.; Hemmerich, P. *Biochemistry* **1978**, *17*, 9−17.
(620) Massey, V.; Stankovich, M.; Hemmerich, P. *Biochemistry* **1978**, *17*, 1−8.
(621) Entsch, B.; Ballou, D. P.; Massey, V. *J. Biol. Chem.* **1976**, *251*, 2550−2563.
(622) Entsch, B.; Massey, V.; Ballou, D. P. *Biochem. Biophys. Res. Commun.* **1974**, *57*, 1018−1025.
(623) Ghisla, S.; Entsch, B.; Massey, V.; Husein, M. *Eur. J. Biochem.* **1977**, *76*, 139−148.
(624) Bruice, T. C. *Isr. J. Chem.* **1984**, *24*, 54−61.
(625) Farragi, M.; Hemmerich, P.; Pecht, I. *FEBS Lett.* **1975**, *51*, 47−51.
(626) Friedkin, M. *Adv. Enzymol. Relat. Areas Mol. Biol.* **1973**, *38*, 235−292.
(627) Sigman, D. S.; Mooser, G. *Annu. Rev. Biochem.* **1975**, *44*, 899−931.
(628) Kaufman, S. *Biochim. Biophys. Acta* **1958**, *27*, 428−429.
(629) Lloyd, T.; Mori, T.; Kaufman, S. *Biochemistry* **1971**, *10*, 2330−2336.
(630) Matthews, R. G.; Kaufman, S. *J. Biol. Chem.* **1980**, *255*, 6014−6017.
(631) Kaufman, S. *Neurochem. Res.* **1991**, *16*, 1031−1036.
(632) Randles, D.; Armarego, W. L. F. *Eur. J. Biochem.* **1985**, *146*, 467−474.
(633) Armarego, W. L. F.; Waring, P.; Paal, B. *Aust. J. Chem.* **1982**, *35*, 785−793.

(634) Matsuura, S.; Sugimoto, T.; Hasegawa, H.; Imaizumi, S.; Ichiyama, A. *J. Biochem. (Tokyo)* **1980**, *87*, 951−957.
(635) Prewo, R.; Bieri, J. H.; Ganguly, S. N.; Viscontini, M. *Helv. Chim. Acta* **1982**, *65*, 1094−1099.
(636) Armarego, W. L. F. In *Chemistry and Biology of Pteridines*; Kisliuk, R. L., Brown, G. M., Eds.; Elsevier North Holland: New York, 1979.
(637) Bailey, S. W.; Dillard, S. B.; Ayling, J. E. *Biochemistry* **1991**, *30*, 10226−10235.
(638) Numata, Y. S.; Ikuta, K.; Kato, T.; Nagatsu, T.; Sugimoto, T.; Matsuura, S. *Biochem. Pharmacol.* **1975**, *24*, 1998−2000.
(639) Numata, Y.; Kato, T.; Nagatsu, T.; Sugimoto, T.; Matsuura, S. *Biochim. Biophys. Acta* **1977**, *480*, 104−112.
(640) Davis, M. D.; Kaufman, S. *J. Biol. Chem.* **1988**, *263*, 17312−17316.
(641) Davis, M. D.; Kaufman, S. *J. Biol. Chem.* **1989**, *264*, 8585−8596.
(642) Davis, M. D.; Kaufman, S. *Neurochem. Res.* **1991**, *16*, 813−819.
(643) Curtius, H.-C.; Muldner, H.; Neiderweiser, A. In *Biochemical and Clinical Aspects of Pteridines*; Wachter, H., Curtius, H.-C., Pfleiderer, W., Eds.; W. de Gruyter: Berlin, 1982; Vol. 1.
(644) Bigham, E. C.; Smith, G. K.; Reinhard, J. F., Jr.; Mallory, W. R.; Nichol, C. A.; Morrison, R. W., Jr. *J. Med. Chem.* **1987**, *30*, 40−45.
(645) Waring, P.; Armarego, W. L. F. *Eur. J. Med. Chem.* **1987**, *22*, 83−90.
(646) Armarego, W. L. F.; Taguchi, H.; Cotton, R. G. H.; Battiston, S.; Leong, L. *Eur. J. Med. Chem.* **1987**, *22*, 283−291.
(647) Levine, R. A.; Zoephel, G. P.; Neiderwieser, A.; Curtius, H.-C. In *Biochemical and Clinical Aspects of Pteridines*; Curtius, H.-C., Pfleiderer, W., Wachter, H., Eds.; W. de Gruyter: Berlin, 1985; Vol. 4.
(648) Kapatos, G.; Kaufman, S. *Science* **1981**, *212*, 955−956.
(649) Ayling, J. E.; Bailey, S. W. In *Biochemical and Clinical Aspects of Pteridines*; Curtius, H.-C., Pfleiderer, W., Wachter, H., Eds.; W. de Gruyter: Berlin, 1983; Vol. 2.
(650) Kaufman, S. *J. Nutr. Sci. Vitaminol.* **1992**, 601−606.
(651) Kaufman, S. In *Unconjugated pterins in neurobiology*; Lovenberg, W., Levine, R. A., Eds.; Taylor & Francis, Ltd.: Philadelphia, 1987; Vol. 2.
(652) Kaufman, S.; Kapatos, G.; McInnes, R. R.; Schulman, J. D.; Rizzo, W. B. *Pediatrics* **1982**, *70*, 376−380.
(653) Snyderman, S. E.; Sansaricq, C.; Pulmones, M. T. *J. Inherit. Metab. Dis.* **1987**, *10*, 260−266.
(654) Kaufman, S. *J. Pediatr.* **1986**, *109*, 572−578.
(655) Pike, D. C.; Hora, M. T.; Bailey, S. W.; Ayling, J. E. *Biochemistry* **1986**, *25*, 4762−4771.
(656) Bailey, S. W.; Ayling, J. E. *Biochem. Biophys. Res. Commun.* **1978**, *85*, 1614−1621.
(657) Bailey, S. W.; Ayling, J. E. In *Chemistry and Biology of Pteridines*; Kisliuk, R. L., Brown, G. M., Eds.; Elsevier North Holland, Inc.: New York, 1979; Vol. 4.
(658) Kaufman, S. *J. Biol. Chem.* **1979**, *254*, 5150−5154.
(659) Lazar, M. A.; Truscott, R. J.; Raese, J. D.; Barchas, J. D. *J. Neurochem.* **1981**, *36*, 677−682.
(660) Bailey, S. W.; Ayling, J. E. *J. Biol. Chem.* **1980**, *255*, 7774−7781.
(661) Hamilton, G. A. In *Molecular Mechanisms of Oxygen Activation*; Hayaishi, O., Ed.; Academic Press: New York, 1974.
(662) Hamilton, G. A. In *Progress in Bioorganic Chemistry*; Kaiser, E. T., Kézdy, F. J., Eds.; Wiley-Interscience: New York, 1971; Vol. 1.
(663) Keay, R. E.; Hamilton, G. A. *J. Am. Chem. Soc.* **1976**, *98*, 6578−6582.
(664) Bailey, S. W.; Weintraub, S. T.; Hamilton, S. M.; Ayling, J. E. *J. Biol. Chem.* **1982**, *257*, 8253−8260.
(665) Dimitrenko, G. I.; Snieckus, V.; Viswanatha, T. *Bioorg. Chem.* **1977**, *6*, 421−429.
(666) Lai, M.; Wu, W.; Stubbe, J. *J. Am. Chem. Soc.* **1995**, *117*, 5023−5030.
(667) Prescott, A. G. *J. Exp. Bot.* **1993**, *44*, 849−861.
(668) Que, L., Jr. In *Iron Carriers and Iron Proteins*; Loehr, T. M., Ed.; VCH: New York, 1989.
(669) Blackburn, J. M.; Sutherland, J. D.; Baldwin, J. E. *Biochemistry* **1995**, *34*, 7548−7562.
(670) Baldwin, J. E.; Bradley, M. *Chem. Rev.* **1990**, *90*, 1079−1088.
(671) Nelson, M. J.; Seitz, S. P. *Curr. Opin. Struct. Biol.* **1994**, *4*, 878−84.
(672) Ohlendorf, D. H.; Orville, A. M.; Lipscomb, J. D. *J. Mol. Biol.* **1994**, *244*, 586−608.
(673) Roach, P. L.; Clifton, I. J.; Fulop, V.; Harlos, K.; Barton, G. J.; Hajdu, J.; Andersson, I.; Schofield, C. J.; Baldwin, J. E. *Nature* **1995**, *375*, 700−704.
(674) Boyington, J. C.; Gaffney, B. J.; Amzel, L. M. *Science* **1993**, *260*, 1482−1486.
(675) Feig, A.; Lippard, S. J. *Chem. Rev.* **1994**, *94*, 759−805.
(676) Rosenzweig, A. C.; Frederick, C. A.; Lippard, S. J.; Nordlund, P. *Nature* **1993**, *366*, 537−543.
(677) Lipscomb, J. D. *Annu. Rev. Microbiol.* **1994**, *48*, 371−399.
(678) Mason, H. S. *Abstracts of Papers*, 130th Meeting of the American Chemical Society, Atlantic City, NJ, Fall 1956; American Chemical Society: Washington, DC, 1956; p 55C.
(679) Holm, R. H. *Chem. Rev.* **1987**, *87*, 1401−1449.
(680) Walling, C. *Acc. Chem. Res.* **1975**, *8*, 125−131.
(681) Akhtar, M.; Wright, J. N. *Nat. Prod. Rep.* **1991**, *8*, 527−551.
(682) Ortiz de Montellano, P. R. *Cytochrome P-450: Structure, Mechanism, and Biochemistry*; Plenum Press: New York, 1986.
(683) Guengerich, F. P.; Macdonald, T. L. *Acc. Chem. Res.* **1984**, *17*, 9−16.
(684) Dawson, J. H. *Science* **1988**, *240*, 433−439.
(685) Meunier, B. *Chem. Rev.* **1992**, *92*, 1411−1456.
(686) Theorell, H. *Enzymologia* **1941**, *10*, 250−252.
(687) Penner-Hahn, J. E.; McMurry, T. J.; Renner, M.; Latos-Grazynsky, L.; Smith Eble, K.; Davis, I. M.; Balch, A. L.; Groves, J. T.; Dawson, J. H.; Hodgson, K. O. *J. Biol. Chem.* **1983**, *258*, 12761−12764.
(688) Chance, B.; Powers, L.; Ching, Y.; Poulos, T.; Schonbaum, G. R.; Yamazaki, I.; Paul, K. G. *Arch. Biochem. Biophys.* **1984**, *235*, 596−611.
(689) Penner-Hahn, J. E.; Eble, K. S.; McMurry, T. J.; Renner, M.; Balch, A. L.; Groves, J. T.; Dawson, J. H.; Hodgson, K. O. *J. Am. Chem. Soc.* **1986**, *108*, 7819−7825.
(690) Moss, T. H.; Ehrenberg, A.; Bearden, A. J. *Biochemistry* **1969**, *8*, 4159−4162.
(691) Roberts, J. E.; Hoffman, B. M.; Rutter, R.; Hager, L. P. *J. Biol. Chem.* **1981**, *256*, 2118−2121.
(692) Theorell, H.; Ehrenberg, A. *Arch. Biochem. Biophys.* **1952**, *41*, 442−461.
(693) Thurman, R. G.; Ley, H. G.; Scholz, R. *Eur. J. Biochem.* **1972**, *25*, 420−430.
(694) Gillette, J. R.; Brodie, B. B.; La Du, B. N. *J. Pharmacol. Exp. Ther.* **1957**, *119*, 532−540.
(695) Hildebrandt, A. G.; Roots, I. *Arch. Biochem. Biophys.* **1975**, *171*, 385−397.
(696) Nordblom, G. D.; Coon, M. J. *Arch. Biochem. Biophys.* **1977**, *180*, 343−437.
(697) Guroff, G.; Daly, J. W.; Jerina, D. M.; Renson, J.; Witkop, B.; Udenfriend, S. *Science* **1967**, *157*, 1524−1530.
(698) Renson, J.; Daly, J.; Weissbach, H.; Witkop, B.; Udenfriend, S. *Biochem. Biophys. Res. Commun.* **1966**, *25*, 504−513.
(699) Daly, J. W.; Witkop, B. *J. Am. Chem. Soc.* **1967**, *89*, 1032−1033.
(700) Guroff, G.; Levitt, M.; Daly, J.; Udenfriend, S. *Biochem. Biophys. Res. Commun.* **1966**, *25*, 253−259.
(701) Daly, J.; Levitt, M.; Guroff, G.; Udenfriend, S. *Arch. Biochem. Biophys.* **1968**, *126*, 593−598.
(702) Guroff, G.; Daly, J. *Arch. Biochem. Biophys.* **1967**, *122*, 212−217.
(703) Bowman, W. R.; Gretton, W. R.; Kirby, G. W. *J. Chem. Soc., Perkin Trans. 1* **1973**, *3*, 218−220.
(704) Daly, J.; Jerina, D.; Witkop, B. *Arch. Biochem. Biophys.* **1968**, *128*, 517−527.
(705) Hanzlik, R. P.; Hogberg, K.; Judson, C. M. *Biochemistry* **1984**, *23*, 3048−3055.
(706) Jerina, D. M.; Kaubisch, N.; Daly, J. W. *Proc. Natl. Acad. Sci. U.S.A.* **1971**, *68*, 2545−2548.
(707) Jerina, D. M.; Daly, J. W. *Science* **1974**, *185*, 573−582.
(708) Kaubisch, N.; Daly, J. W.; Jerina, D. M. *Biochemistry* **1972**, *11*, 3080−3088.
(709) Booth, J.; Boyland, E.; Sato, T.; Sims, P. *Biochem. J.* **1960**, *77*, 182−186.
(710) Holtzman, J.; Gillette, J. R.; Milne, G. W. A. *J. Am. Chem. Soc.* **1967**, *89*, 6341−6344.
(711) Jerina, D. M.; Daly, J. W.; Witkop, B.; Zaltzman-Nirenberg, P.; Udenfriend, S. *Biochemistry* **1970**, *9*, 147−156.
(712) Jerina, D. M.; Daly, J. W.; Witkop, B. *J. Am. Chem. Soc.* **1968**, *90*, 6523−6525.
(713) Jerina, D. M.; Daly, J. W.; Witkop, B.; Zaltzman-Nirenberg, P.; Udenfriend, S. *J. Am. Chem. Soc.* **1968**, *90*, 6525−6527.
(714) Boyd, D. R.; Daly, J. W.; Jerina, D. M. *Biochemistry* **1972**, *11*, 1961−1966.
(715) Shirwaiker, G. S.; Bhatt, M. V. *Adv. Heterocycl. Chem.* **1984**, *37*, 67−165.
(716) Yagi, H.; Jerina, D. M.; Kasperek, G. J.; Bruice, T. C. *Proc. Natl. Acad. Sci. U.S.A.* **1972**, *69*, 1985−1986.
(717) Jerina, D. M.; Witkop, B.; McIntosh, C. L.; Chapman, O. L. *J. Am. Chem. Soc.* **1974**, *96*, 5578−5580.
(718) Kasperek, G. J.; Bruice, T. C.; Yagi, H.; Jerina, D. M. *J. Chem. Soc., Chem. Commun.* **1972**, 784−785.
(719) Selander, H. G.; Jerina, D. M.; Daly, J. W. *Arch. Biochem. Biophys.* **1975**, *168*, 309−321.
(720) Selander, H. G.; Jerina, D. M.; Piccolo, D. E.; Berchtold, G. A. *J. Am. Chem. Soc.* **1975**, *97*, 4428−4430.
(721) Tomaszewski, J. E.; Jerina, D. M.; Daly, J. W. *Biochemistry* **1975**, *14*, 2024−2031.
(722) Preston, B. D.; Miller, J. A.; Miller, E. C. *J. Biol. Chem.* **1983**, *258*, 8304−8311.
(723) Ortiz de Montellano, P. R.; Kunze, K. L. *J. Am. Chem. Soc.* **1980**, *102*, 7373−7375.
(724) McMahon, R. E.; Turner, J. C.; Whitaker, G. W.; Sullivan, H. R. *Biochem. Biophys. Res. Commun.* **1981**, *99*, 662−667.
(725) Ortiz de Montellano, P. R.; Komives, E. A. *J. Biol. Chem.* **1985**, *260*, 3330−3336.
(726) Miller, R. E.; Guengerich, F. P. *Biochemistry* **1982**, *21*, 1090−1097.

(727) Henschler, D.; Hoos, W. R.; Fetz, H.; Dallmeier, E.; Metzler, M. *Biochem. Pharmacol.* **1979**, *28*, 543−548.
(728) Groves, J. T.; Kruper, W. J., Jr.; Haushalter, R. C. *J. Am. Chem. Soc.* **1980**, *102*, 6375−6377.
(729) Ortiz de Montellano, P. R. In *Cytochrome P-450*; Ortiz de Montellano, P. R., Ed.; Plenum Press: New York, 1986.
(730) Korzekwa, K.; Trager, W.; Gouterman, M.; Spangler, D.; Loew, G. H. *J. Am. Chem. Soc.* **1985**, *107*, 4273−4279.
(731) Korzekwa, K. R.; Swinney, D. C.; Trager, W. F. *Biochemistry* **1989**, *28*, 9019−9027.
(732) Rietjens, I. M. C. M.; Soffers, A. E. M. F.; Veeger, C.; Vervoort, J. *Biochemistry* **1993**, *32*, 4801−4812.
(733) Carey, F. A.; Sundberg, R. J. ; 2nd ed.; Plenum Press: New York, 1983.
(734) Groves, J. T.; McClusky, G. A. *Biochem. Biophys. Res. Commun.* **1978**, *81*, 154−60.
(735) McMurry, T. J.; Groves, J. T. In *Cytochrome P-450*; Ortiz de Montellano, P. R., Ed.; Plenum Press: New York, 1986.
(736) Ortiz de Montellano, P. R.; Stearns, R. A. *J. Am. Chem. Soc.* **1987**, *109*, 3415−3420.
(737) Newcomb, M.; Le Tadic-Biadatti, M.-H.; Chestney, D. L.; Roberts, E. S.; Hollenberg, P. F. *J. Am. Chem. Soc.* **1995**, *117*, 12085−12091.
(738) Poulos, T. L.; Finzel, B. C.; Howard, A. J. *J. Mol. Biol.* **1987**, *195*, 687−700.
(739) Li, H. Y.; Narasimhulu, S.; Havran, L. M.; Winkler, J. D.; Poulos, T. L. *J. Am. Chem. Soc.* **1995**, *117*, 6297−6299.
(740) Ostović, D.; Bruice, T. C. *J. Am. Chem. Soc.* **1988**, *110*, 6906−6908.
(741) Breslow, R.; Brown, A. B.; White, P. W.; McCullough, R. D. *J. Am. Chem. Soc.* **1989**, *111*, 4517−4518.
(742) Sharpless, K. B.; Flood, T. C. *J. Am. Chem. Soc.* **1971**, *93*, 2316−2318.
(743) Collman, J. P.; Raybuck, S. A.; Papazian, L. M.; Kodadek, T.; Brauman, J. I. *J. Am. Chem. Soc.* **1985**, *107*, 4343−4345.
(744) Sharpless, K. B.; Teranishi, A. Y.; Bäckvall, J.-E. *J. Am. Chem. Soc.* **1977**, *99*, 3120−3128.
(745) Komives, E. A.; Ortiz de Montellano, P. R. *J. Biol. Chem.* **1987**, *262*, 9793−9802.
(746) Jørgensen, K. A.; Schiøtt, B. *Chem. Rev.* **1990**, *90*, 1483−1506.
(747) Groves, J. T.; Watanabe, Y. *J. Am. Chem. Soc.* **1986**, *108*, 507−508.
(748) Hanzlik, R. P.; Ling, K.-H. J. *J. Org. Chem.* **1990**, *55*, 3992−3997.
(749) Miwa, G. T.; Lu, A. Y. H. *Bioessays* **1987**, *7*, 215−219.
(750) Ibers, J. A.; Holm, R. H. *Science* **1980**, *209*, 223−235.
(751) Mansuy, D.; Battioni, P. In *Basis and mechanisms of regulation of cytochrome P-450*; Ruckpaul, K., Horst, R., Eds.; Academic: Berlin, 1989.
(752) Gunter, M. J.; Turner, P. *Coord. Chem. Rev.* **1991**, *108*, 115−161.
(753) Groves, J. T.; Nemo, T. E.; Myers, R. S. *J. Am. Chem. Soc.* **1979**, *101*, 1032−1033.
(754) Groves, J. T.; Hanshalter, R. C.; Nakamura, M.; Nemo, T. E.; Evans, B. J. *J. Am. Chem. Soc.* **1981**, *103*, 2884−2885.
(755) Collman, J. P.; Zhang, X.; Lee, V. J.; Uffelman, E. S.; Brauman, J. I. *Science* **1993**, *261*, 1404−1411.
(756) Patzelt, H.; Woggon, W. D. *Helv. Chim. Acta* **1992**, *75*, 523−530.
(757) Coon, M. J.; Ding, X.; Pernecky, S. J.; Vaz, A. D. N. *FASEB J.* **1992**, *6*, 669−73.
(758) Hori, A.; Takamuku, S.; Sakurai, H. *J. Org. Chem.* **1977**, *42*, 2318−2321.
(759) Takamuku, S.; Matsumoto, H.; Hori, A.; Sakurai, H. *J. Am. Chem. Soc.* **1980**, *102*, 1441−1443.
(760) Haber, F.; Weiss, J. J. *Proc. R. Soc. (London)* **1934**, *A147*, 332−351.
(761) Udenfriend, S.; Zaltzman-Nirenberg, P.; Daly, J.; Guroff, G.; Chidsey, C.; Witkop, B. *Arch. Biochem. Biophys.* **1967**, *120*, 413−419.
(762) Sugimoto, H.; Sawyer, D. T. *J. Am. Chem. Soc.* **1984**, *106*, 4283−4285.
(763) Castle, L.; Lindsay-Smith, J. R. *J. Chem. Soc., Chem. Commun.* **1978**, 704−705.
(764) Kurata, T.; Watanabe, Y.; Katoh, M.; Sawaki, Y. *J. Am. Chem. Soc.* **1988**, *110*, 7472−7478.
(765) Groves, J. T.; Van Der Puy, M. *J. Am. Chem. Soc.* **1976**, *98*, 5290−5297.
(766) Sugimoto, H.; Sawyer, D. T. *J. Am. Chem. Soc.* **1985**, *107*, 5712−5716.
(767) White, R. E.; Sligar, S. G.; Coon, M. J. *J. Biol. Chem.* **1980**, *255*, 11108−11111.
(768) Jerina, D. M.; Daly, J. W.; Witkop, B. *Biochemistry* **1971**, *10*, 366−372.
(769) Foulkes, D. M. *Nature* **1969**, *221*, 582.
(770) Ullrich, V.; Jurgen, W.; Ekkehard, A.; Staudinger, H. *Hoppe-Seylers Z. Physiol. Chem.* **1968**, *349*, 85−94.
(771) Buehler, C. A.; Hart, H. *J. Am. Chem. Soc.* **1963**, *85*, 2177−2178.
(772) Traylor, P. S.; Dolphin, D.; Traylor, T. G. *J. Chem. Soc., Chem. Commun.* **1984**, 279−280.
(773) Murray, R. W. *Chem. Rev.* **1989**, *89*, 1187−1201.
(774) Adam, W.; Curci, R.; Edwards, J. O. *Acc. Chem. Res.* **1989**, *22*, 205−211.
(775) Jeyaraman, R.; Murray, R. W. *J. Am. Chem. Soc.* **1984**, *106*, 2462−2463.
(776) Murray, R. W.; Jeyaraman, R.; Mohan, L. *J. Am. Chem. Soc.* **1986**, *108*, 2470−2472.
(777) Baumstark, A. L.; Vasquez, P. C. *J. Org. Chem.* **1988**, *53*, 3437−3439.
(778) Murray, R. W.; Jeyaraman, R. *J. Org. Chem.* **1985**, *50*, 2847−2853.
(779) Appelman, E. H.; Bonnett, R.; Mateen, B. *Tetrahedron* **1977**, *33*, 2119−2122.
(780) Akhtar, M. N.; Boyd, D. R.; Jerina, D. M.; Neill, J. D. *J. Chem. Soc., Perkin Trans. 1* **1980**, 1693−1699.
(781) Lindsay Smith, J. R.; Jerina, D. M.; Kaufman, S.; Milstein, S. *J. Chem. Soc., Chem. Commun.* **1975**, 881−882.
(782) Wiberg, K. B. *Oxidation in Organic Chemistry*; Academic Press: New York, 1965.
(783) Caradonna, J. P.; Stassinopoulos, A. *Adv. Inorg. Biochem.* **1994**, *9*, 245−315.
(784) Balasubramanian, P. N.; Bruice, T. C. *Proc. Natl. Acad. Sci. U.S.A.* **1987**, *84*, 1734−1738.
(785) Fitzpatrick, P. F. *J. Am. Chem. Soc.* **1994**, *116*, 1133−1134.
(786) Gatti, D. L.; Palfey, B. A.; Lah, M. S.; Entsch, B.; Massey, V.; Ballou, D. P.; Ludwig, M. L. *Science* **1994**, *266*, 110−114.
(787) Meyer, M. M.; Fitzpatrick, P. F. *Neurochem. Int.* **1992**, *21*, 191−196.
(788) Richtand, N. M.; Inagami, T.; Misono, K.; Kuczenski, R. *J. Biol. Chem.* **1985**, *260*, 8465−8473.
(789) Chang, N.; Kaufman, S.; Milstien, S. *J. Biol. Chem.* **1979**, *25*, 2665−2668.
(790) Kaufman, S.; Fisher, D. B. In *Molecular Mechanisms of Oxygen Activation*; Hayaishi, O., Ed.; Academic Press: New York, 1974.
(791) Fisher, D. B.; Kaufman, S. *J. Neurochem.* **1972**, *19*, 1359−1365.
(792) Martínez, A.; Olafsdottir, S.; Flatmark, T. *Eur. J. Biochem.* **1993**, *211*, 259−266.
(793) Martínez, A.; Andersson, K. K.; Haavik, J.; Flatmark, T. *Eur. J. Biochem.* **1991**, *198*, 675−682.
(794) Martínez, A.; Abeygunawardana, C.; Haavik, J.; Flatmark, T.; Mildvan, A. S. *Biochemistry* **1993**, *32*, 6381−6390.
(795) Kaufman, S.; Mason, K. *J. Biol. Chem.* **1982**, *257*, 14667−14678.
(796) Kaufman, S. *Methods Enzymol.* **1962**, *5*, 809−816.
(797) Miller, R. J.; Benkovic, S. J. *Biochemistry* **1988**, *27*, 3658−3663.
(798) Carr, R. T.; Balasubramanian, S.; Hawkins, P. C.; Benkovic, S. J. *Biochemistry* **1995**, *34*, 7525−7532.
(799) Daly, J.; Guroff, G. *Arch. Biochem. Biophys.* **1968**, *125*, 136−141.
(800) Siegmund, H. U.; Kaufman, S. *J. Biol. Chem.* **1991**, *266*, 2903−2910.
(801) Tong, J. H.; D'Iorio, A.; Benoiton, N. L. *Biochem. Biophys. Res. Commun.* **1971**, *43*, 819−826.
(802) Guroff, G.; Kondo, K.; Daly, J. *Biochem. Biophys. Res. Commun.* **1966**, *25*, 622−628.
(803) Fisher, D. B.; Kaufman, S. *J. Biol. Chem.* **1973**, *248*, 4300−4304.
(804) Jequier, E.; Lovenberg, W.; Sjoerdsma, A. *Mol. Pharmacol.* **1967**, *3*, 274−278.
(805) Lipton, M. A.; Gordon, R.; Guroff, G.; Udenfriend, S. *Science* **1967**, *156*, 248−250.
(806) Gál, E. M.; Millard, S. A. *Biochim. Biophys. Acta* **1971**, *227*, 32−41.
(807) Miller, M. R.; McClure, D.; Shiman, R. *J. Biol. Chem.* **1976**, *251*, 3677−3684.
(808) Gál, E. M.; Whitacre, D. H. *Neurochem Res.* **1982**, *7*, 13−26.
(809) Koe, B. K.; Weissman, A. *J. Pharmacol. Exp. Ther.* **1967**, *157*, 565−573.
(810) Sykes, P. *A guidebook to mechanism in organic chemistry*, 4th ed.; J. Wiley & Sons: New York, 1975.
(811) Leinberger, R.; Hull, W. E.; Simon, H.; Rétey, J. *Eur. J. Biochem.* **1981**, *117*, 311−8.
(812) Kaufman, S. *Biochim. Biophys. Acta* **1961**, *51*.
(813) Davis, M. D.; Kaufman, S. *Arch. Biochem. Biophys.* **1993**, *304*, 9−16.
(814) Benkovic, S. J.; Bloom, L. M.; Bollag, G.; Dix, T. A.; Gaffney, B. J.; Pember, S. *Ann. N. Y. Acad. Sci.* **1986**, *471*, 226−232.
(815) O'Brien, P. J. *Can. J. Biochem.* **1969**, *47*, 485−492.
(816) Haavik, J.; Flatmark, T. *Eur. J. Biochem.* **1987**, *168*, 21−26.
(817) Moore, K. E.; Dominic, J. A. *Fed. Proc.* **1971**, *30*, 859−870.
(818) McGeer, E. G.; Peters, D. A. *Can. J. Biochem.* **1969**, *47*, 501−506.
(819) Wilgus, H.; Roskoski, R., Jr. *J. Neurochem.* **1988**, *51*, 1232−1239.
(820) Lerner, P.; Hartman, P.; Ames, M. M.; Lovenberg, W. *Arch. Biochem. Biophys.* **1977**, *182*, 164−170.
(821) Martinez, A.; Olafsdottir, S.; Haavik, J.; Flatmark, T. *Biochem. Biophys. Res. Commun.* **1992**, *182*, 92−98.
(822) Ribeiro, P.; Pigeon, D.; Kaufman, S. *J. Biol. Chem.* **1991**, *266*, 16207−16211.
(823) Oka, K.; Kato, T.; Sugimoto, T.; Matsuura, S.; Nagatsu, T. *Biochim. Biophys. Acta* **1981**, *661*, 45−53.

(824) Oka, K.; Ashiba, G.; Sugimoto, T.; Matsuura, S.; Nagatsu, T. *Biochim. Biophys. Acta* **1982**, *706*, 188−196.
(825) Bullard, W. P.; Capson, T. L. *Mol. Pharmacol.* **1983**, *23*, 104−111.
(826) Fitzpatrick, P. F. *Advances in Experimental Medicine & Biology* **1993**, *338*, 81−86.
(827) Segel, I. H. *Enzyme Kinetics*; Wiley: New York, 1975.
(828) Ikeda, M.; Levitt, M.; Udenfriend, S. *Biochem. Biophys. Res. Commun.* **1965**, *18*, 482−488.
(829) Tong, J. H.; D'Iorio, A.; Benoiton, N. L. *Biochem. Biophys. Res. Commun.* **1971**, *44*, 229−236.
(830) Hosoda, S. *Biochim. Biophys. Acta* **1975**, *397*, 58−68.
(831) Gál, E. M. In *Serotonin: Current Aspects of Neurochemistry and Function*; Haber, B., Gabay, S., Issidorides, M. R., Alivisatos, S. G. A., Eds.; Plenum: New York, 1981; Vol. 133.
(832) Naoi, M.; Maruyama, W.; Takahashi, T.; Ota, M.; Parvez, H. *Biochem. Pharmacol.* **1994**, *48*, 207−211.
(833) Matsubara, K.; Ota, M.; Takahashi, T.; Maruyama, W.; Naoi, M. *Brain Res.* **1994**, *655*, 121−127.
(834) Reinhard, J. F., Jr.; Shearin, M. D. *Biochem. Pharmacol.* **1990**, *39*, 1489−1491.
(835) Zhelyaskov, D. K.; Levitt, M.; Udenfriend, S. *Mol. Pharmacol.* **1968**, *4*, 445−451.
(836) Hamon, M.; Bourgoin, S.; Glowinski, J. *J. Neurochem.* **1973**, *20*, 1727−1745.
(837) Cortes, R.; Mengod, G.; Celada, P.; Artigas, F. *J. Neurochem.* **1993**, *60*, 761−764.
(838) Okabayashi, K.; Morishima, H.; Hamada, M.; Takeuchi, T.; Umezawa, H. *J. Antibiot.* **1977**, *30*, 675−677.
(839) Kowlessur, D.; Citron, B. A.; Kaufman, S. *Arch. Biochem. Biophys.* **1996**, *333*, 85−95.
(840) Døskeland, A. P.; Martinez, A.; Knappskog, P. M.; Flatmark, T. *Biochem. J.* **1996**, *313*, 409−414.
(841) Davis, M. D.; Parniak, M. A.; Kaufman, S.; Kempner, E. *Arch. Biochem. Biophys.* **1996**, *325*, 235−241.
(842) Kaufman, S. *Adv. Enzymol. Relat. Areas Mol. Biol.* **1995**, *70*, 103−220.
(843) Kumer, S. C.; Vrana, K. E. *J. Neurochem.* **1996**, *67*, 443−462.
(844) Lanièce, P.; Le Hir, P.; Bodeau-Pèan, S.; Charon, Y.; Valentin, L.; Thermes, C.; Mallet, J.; Dumas, S. *J. Neurochem.* **1996**, *66*, 1819−1825.
(845) Dumas, S.; Le Hir, H.; Bodeau-Pèan, S.; Hirsch, E.; Thermes, C.; Mallet, J. *J. Neurochem.* **1996**, *67*, 19−25.
(846) Anastasiadis, P. Z.; Kuhn, D. M.; Blitz, J.; Imerman, B. A.; Louie, M. C.; Levine, R. A. *Brain Res.* **1996**, *713*, 125−133.
(847) Hyland, K.; Gunasekera, R. S.; Engle, T.; Arnold, L. A. *J. Neurochem.* **1996**, *67*, 752−759.
(848) Martínez, A.; Haavik, J.; Flatmark, T.; Arrondo, J. L. R.; Muga, A. *J. Biol. Chem.* **1996**, *271*, 19737−19742.
(849) Öhrström, L.; Michaud-Soret, I. *J. Am. Chem. Soc.* **1996**, *118*, 3283−3284.
(850) Hillas, P. J.; Fitzpatrick, P. F. *Biochemistry* **1996**, *35*, 6968−6975.
(851) Ramsey, A. J.; Hillas, P. J.; Fitzpatrick, P. F. *J. Biol. Chem.* **1996**, *271*, 24395−24400.
(852) Florez, J. C.; Takahashi, J. S. *J. Biol. Rhythms* **1996**, *11*, 241−257.
(853) D'Sa, C. M.; Arthur, R. E., Jr.; States, J. C.; Kuhn, D. M. *J. Neurochem.* **1996**, *67*, 900−906.
(854) D'Sa, C. M.; Arthur, R. E., Jr.; Kuhn, D. M. *J. Neurochem.* **1996**, *67*, 917−926.
(855) Kuhn, D. E.; Arthur, R. E., Jr. *J. Neurochem.* **1996**, *67*, 1072−1077.

CR9402034